

- I. Total Syntheses and Biological Studies of Largazole and Brasilibactin A.
- II. Stereoselective Synthesis of 2,6-*Cis*- and 2,6-*Trans*-Piperidines through an Organocatalytic Aza-Michael Reaction.

by

Yongcheng Ying

Department of Chemistry
Duke University

Date: _____

Approved:

Jiyong Hong, Supervisor

Steven W. Baldwin

Stephen L. Craig

Richard A. MacPhail

Dissertation submitted in partial fulfillment of
the requirements for the degree of Doctor
of Philosophy in the Department of
Chemistry in the Graduate School
of Duke University

2010

ABSTRACT

- I. Total Syntheses and Biological Studies of Largazole and Brasilibactin A.
II. Stereoselective Synthesis of 2,6-*Cis*- and 2,6-*Trans*-Piperidines through an
Organocatalytic Aza-Michael Reaction.

by

Yongcheng Ying

Department of Chemistry
Duke University

Date: _____

Approved:

Jiyong Hong, Supervisor

Steven W. Baldwin

Stephen L. Craig

Richard A. MacPhail

An abstract of a dissertation submitted in partial
fulfillment of the requirements for the degree
of Doctor of Philosophy in the Department of
Chemistry in the Graduate School
of Duke University

2010

Copyright by
Yongcheng Ying
2010

Abstract

The dissertation focuses on three main projects which complement the studies towards the total syntheses of biologically active natural products as well as the development of stereoselective synthesis of 2,6-disubstituted piperidines.

The first project introduced the first total synthesis of largazole, which is a marine natural product isolated from cyanobacterium of genus *Symploca* sp. in 2008. It consists of an unusual 16-membered macrocycle incorporating a 4-methylthiazoline linearly fused to a thiazole and an ester of 3-hydroxy-7-mercaptohept-4-enoic acid unit, part of which has been identified to be essential for the potent histone deacetylase (HDAC) inhibitory and consequently antiproliferative activities. Structure-activity relationship (SAR) studies suggest that thiol group generated by hydrolysis of the thioester moiety is the warhead and is critical for its HDAC inhibitory and antiproliferative activity. The biological evaluation of the analogues focusing on macrocycle and linker chain between sulfur atom and macrocycle suggests that the four-atom linker between the macrocycle and the octanoyl group in the side chain and the (*S*)-configuration at C17-position are critical to potent HDAC inhibitory activity of largazole. In contrast, the valine residue in the macrocycle can be replaced with alanine without compromising activity to a large extent. These SAR results would provide insights into structural requirements for HDAC

inhibitory activity including the observed HDAC selectivity of largazole and help in the design of isoform-specific HDAC inhibitors based on largazole.

The second project involved the synthesis of cytotoxic mycobactin-like siderophore-brasilibactin A and its unnatural diastereomers, which are then identified to unambiguously confirm that brasilibactin A possesses the 17*S*, 18*R* absolute stereochemistry at β -hydroxy acid fragment. The convergent synthetic strategy has been applied to the synthesis of a more water-soluble analogue-Bbtan, iron-binding studies of which suggest brasilibactin A may play an important role in the iron-uptake mechanism in mycobacteria and related organisms.

The third project elucidated a convergent stereoselective synthesis of 2,6-*cis*- and 2,6-*trans*-piperidines through a *reagent-controlled* organocatalytic aza-Michael reaction promoted by the *gem*-disubstituent effect introduced by 1,3-dithiane. The reaction was applicable to a broad range of substrates and proceeded with good stereoselectivities (up to 20:1 dr) and yields. The 1,3-dithiane group allowed for rapid access to substrates, promoted the intramolecular aza-Michael reaction via the *gem*-disubstituent effect, and improved the yield of the reaction. This synthetic method should be broadly applicable to the efficient synthesis of a diverse set of bioactive natural products with 2,6-disubstituted piperidines.

For My Parents, My Wife, My Brother

Contents

Abstract.....	iv
List of Tables	x
List of Figures.....	xi
List of Abbreviations	xiii
Acknowledgements.....	xvi
1. Introduction.....	1
1.1 Organic synthesis and biological process.....	1
1.2 Natural products and chemical biology.....	3
1.2.1 Therapeutical application of natural products and drug development.....	4
1.2.2 Structure and activity relationship (SAR)	5
1.2.3 Target identification	6
1.3 Goal and outline of this dissertation.....	7
2. Total synthesis of largazole, a potent class I histone deacetylase inhibitor	8
2.1 Epigenetical control.....	8
2.1.1 Histone deacetylases (HDACs).....	10
2.1.2 Aberant HDAC relates with cancer.....	13
2.1.3 Histone deacetylase inhibitors (HDACi).....	13
2.1.3.1 Classification.....	13
2.1.3.1.1 Acyclic histone deacetylase inhibitors.....	15
2.1.3.1.2 Cyclic or bicyclic histone deacetylase inhibitors.....	16

2.1.3.2 Mechanism of action	28
2.1.3.3 Pharmaceutical application.....	26
2.2 Synthesis of largazole.....	28
2.2.1 Discovery, isolation and biological activity of largazole	28
2.2.2 Retrosynthetic strategy of largazole	30
2.2.3 Synthesis of largazole.....	31
2.2.4 Synthesis of largazole analogues.....	34
2.2.5 Biological studies of largazole and its analogues.....	36
2.2.5.1 Mode of action and pharmacophore.....	36
2.2.5.2 Structure-activity relationship (SAR).....	41
2.2.6 Other total syntheses of largazole	48
2.3 Conclusion.....	53
2.4 Experimental sections	55
3. Total synthesis of brasilibactin A and its analogues	95
3.1 Mycobactins	95
3.1.1 Iron acquisition in mycobacteria	95
3.1.2 Siderophores.....	97
3.1.3 Role of siderophores in mycobacterial iron transport	101
3.2 Biological activity of mycobactins and their analogues	104
3.3 Brasilibactin A	107
3.3.1 Isolation and biological activity	107
3.3.2 Retrosynthetic analysis.....	108
3.3.3 Total synthesis of brasilibactin A.....	109

3.3.4 Shaw's synthetic route to brasilibactin A and its HDAC inhibitory activity	117
3.3.5 Synthesis and iron-binding studies of brasilibactin A analogue.....	120
3.4 Conclusion	122
3.5 Experimental sections	122
4. Aza-Michael reaction to synthesize 2,6-disubstituted piperidines.....	147
4.1 Introduction	147
4.1.1 Importance.....	147
4.1.2 Previous studies	150
4.2 Results and discussion.....	152
4.2.1 Attempts of tandem reaction and introduction of organocatalysis	152
4.2.2 Optimization and substrate scope.....	155
4.2.3 <i>gem</i> -Disubstituent effect.....	162
4.2.4 Proposed mechanism.....	164
4.3 Conclusion.....	166
4.4 Experimental sections.....	167
References.....	194
Biography.....	203

List of Tables

Chapter 2

Table 2.1: Biological data for FK228 and redFK.	24
Table 2.2: Representative HDAC inhibitors in clinical trials (partial list)	28
Table 2.3: IC ₅₀ and GI ₅₀ Values for HDACs and growth inhibition (nM)	39
Table 2.4: IC ₅₀ Values for HDAC1 and HDAC6 inhibition (nM)	40
Table 2.5: Cancer cell growth and HDAC inhibition (GI ₅₀ and IC ₅₀ in nM)	46
Table 2.6: IC ₅₀ Values for HDAC1 and HDAC6 inhibition (nM)	48

Chapter 3

Table 3.1: Comparison of ¹ H NMR data for 3.1–3.4 with natural brasilibactin A	116
--	-----

Chapter 4

Table 4.1: Other attempts to one-pot oxidation/aza-Michael reaction by various catalysts	154
Table 4.2: Catalyst screening and optimization of reaction conditions	156
Table 4.3: Protecting group effect on the diastereoselectivity in aza-Michael reaction	159
Table 4.4: Substrate scope and stereochemical outcome	161
Table 4.5: <i>gem</i> -Disubstituent effect on stereoselectivity	164

List of Figures

Chapter 1

Figure 1.1: Relationship between organic synthesis and biology in chemical biology	3
--	---

Chapter 2

Figure 2.1: Histone acetylation and gene expression by HAT and HDAC	10
Figure 2.2: Classification of histone deacetylases	11
Figure 2.3: Mechanisms of HDAC inhibitors-induced cell death.....	13
Figure 2.4: Structure of trichostatin A (TSA) and trapoxin (TPX).....	14
Figure 2.5: Structural elements in representative HDACi	15
Figure 2.6: Selected macrocyclic peptidic HDACi's.....	17
Figure 2.7: Sulfur-containing HDACi's.....	18
Figure 2.8: Proposed mechanism of action of Zn ²⁺ -dependent HDACs and TSA binding model with zinc ion in HDAC8 active site	26
Figure 2.9: Structure of largazole	29
Figure 2.10: Retrosynthetic analysis.....	31
Figure 2.11: Structural similarity between FK228 and largazole (2.1) and modes of activation ..	37
Figure 2.12: Target identification	38
Figure 2.13: Immunoblot analysis showing various degrees of inhibition of histone H3 deacetylation by largazole analogues in HCT-116 cells upon 8 h of treatment.....	47

Chapter 3

Figure 3.1: Sources of iron for pathogenic microorganisms within a host body	96
Figure 3.2: Structures of mycobacterial siderophores.....	98

Figure 3.3: Mycobactin-iron complex with three bidentate binding moieties	99
Figure 3.4: Structures of water-insoluble mycobactins.....	100
Figure 3.5: Structures of water-soluble carboxymycobactins.....	101
Figure 3.6: Proposed iron-uptake mechanism mediated by exochelins and carboxymycobactins	103
Figure 3.7: Proposed mechanism of the reduction of ferri-mycobactins by Ratledge.....	104
Figure 3.8: Structures of Mycobactin T and S	105
Figure 3.9: Siderophores from other actinomycetes	106
Figure 3.10: Small molecules HDACi with <i>N</i> -formyl hydroxylamine or retrohydroxamate moieties	107
Figure 3.11: Structure of brasilibactin A	108
Figure 3.12: Comparison of ¹ H NMR of 3.1–3.4	116

Chapter 4

Figure 4.1: Representative naturally occurring piperdines	147
Figure 4.2: Representative examples to prepare 2,6-disubstituted piperidines.....	149
Figure 4.3: Stereoselective synthesis of 2,6- <i>cis</i> -tetrahydropyrans and piperidines via tandem allylic oxidation/Michael reactions.....	151
Figure 4.4: Molecular structure of 4.15b from X-ray crystal structure analysis.....	162
Figure 4.5: Proposed mechanism of aza-Michael reaction in “match pair” and “mismatch pair”	166

List of Abbreviations

aq.	aqueous
Asp	aspartic acid
ATP	adenosine triphosphate
brs	broad singlet
BRSM	based upon recovered starting material
<i>t</i> -Bu	<i>tert</i> -butyl
<i>n</i> -BuLi	<i>n</i> -butyllithium
<i>t</i> -BuLi	<i>t</i> -butyllithium
CH ₂ Cl ₂	methylene chloride
COD	cyclooctadiene
COSY	correlation spectroscopy
d	doublet
dd	doublet of doublets
DBU	1,8-diazabicyclo[5.4.0]undec-7-ene
DCC	dicyclohexylcarbodiimide
DEAD	diethyl azodicarboxylate
DIAD	diisopropyl azodicarboxylate
DMAP	4-(<i>N,N</i> -dimethylamino)pyridine
DMF	<i>N,N</i> -dimethylformamide
DMSO	dimethylsulfoxide
DNA	deoxyribonucleic acid
dr	diastereomeric ratio
EDC	1-[3-(dimethylamino)propyl]-3-ethylcarbodiimide hydrochloride
eq.	equivalent
Et ₂ O	diethyl ether
EtOAc	ethyl acetate
FDPP	pentafluorophenyl diphenylphosphinate
HATU	<i>O</i> -(7-azabenzotriazo-1-yl)-1,1,3,3-tetramethyluronium

	hexafluorophosphate
<i>c</i> -Hex	cyclohexane
His	histidine
HMPA	hexamethylphosphoramide
HOAt	1-hydroxy-7-azabenzotriazole
HOBt	1-hydroxy-1H-benzotriazole
HRMS	high-resolution mass spectrometry
IC ₅₀	Inhibitory concentration 50%
KHMDS	potassium bis(trimethylsilyl)amide
LAH	lithium aluminium hydride
LiHMDS	lithium bis(trimethylsilyl)amide
Lys	lysine
m	multiplet
<i>m</i> -CPBA	<i>meta</i> -chloroperbenzoic acid
MeCN	acetonitrile
MeOH	methanol
min	minute
MnO ₂	manganese dioxide
NAD ⁺	nicotinamide adenine dinucleotide
NOESY	nuclear Overhauser effect spectroscopy
NMR	nuclear magnetic resonance
NEt ₃	triethylamine
pH	negative logarithm of hydrogen ion concentration
PPh ₃	triphenylphosphine
ppm	parts per million
PPTS	pyridinium <i>p</i> -toluenesulfonate
PTSA	<i>para</i> -toluenesulfonic acid
<i>i</i> -Pr ₂ NEt	diisopropylethylamine
q	quartet
R _f	retention factor

RNA	ribonucleic acid
rt	room temperature
s	singlet
sat.	saturated
SOMO	singly-occupied molecular orbital
t	triplet
TBAF	tetra- <i>n</i> -butylammonium fluoride
TBS	<i>tert</i> -butyldimethylsilyl
TBDPS	<i>tert</i> -butyldiphenylsilyl
TBSOTf	<i>tert</i> -butyldimethylsilyl triflate
Tf	trifluoromethanesulfonyl
TFA	trifluoroacetic acid
THF	tetrahydrofuran
TLC	thin layer chromatography
Ts/Tosyl	<i>para</i> -toluenesulfonyl
Tyr	tyrosine
UV	Ultraviolet
¹ H NMR	proton nuclear magnetic resonance
¹³ C NMR	carbon 13 nuclear magnetic resonance
δ	chemical shift (ppm)
4Å MS	4Å molecular sieves

Acknowledgements

I would like to thank my graduate research advisor, Dr. Jiyong Hong, for his assistance, guidance, constant enthusiasm and intellectual support in my chemistry. I am very grateful for his continued encouragement and very fortunate to do my research under his supervision. I would also like to thank my committee members, Dr. Steven W. Baldwin, Dr. Stephen L. Craig, Dr. Richard MacPhail, Dr. Barbara R. Shaw for their excellent teaching and their time as well as the effort they have put on my research and career in chemistry.

I also thank all of the individuals at Duke who helped my research and life. Specifically, I would like to thank Dr. George Dubay for his helpful mass spectroscopy assistance and Marina Dickens for her X-ray crystallography assistance. The financial support from Duke University and National Institutes of Health are sincerely appreciated.

I also sincerely thank my former and current lab colleagues, Dr. Hyongsu Kim, Dr. Seongrim Byeon, Joseph Baker, Kyle Bolduc, Amanda Kasper, Kiyoun Lee, Heekwang Park, Ceshea Wooten for their help with all kinds of research assistance, insightful discussion and friendship.

Finally, I would like to express my deepest gratitude to my parents and my brother for their constant support and love without which I would not be here. I sincerely thank my fantastic wife, Yuting. You are always at my side, willing to share my frustrations, exciting, and joy. Your unconditional love, patience, and support are my driving force to chemistry career and our wonderful life.

Chapter 1

Introduction

1.1 Organic synthesis and biological process

Organic synthesis is a special branch of chemical synthesis dealing with the construction of complex molecules from relatively simple starting materials and reagents through the formation and breaking of covalent bonds. Traditionally, there are two main research areas associated with organic synthesis: methodology development and total synthesis. The ultimate goal of methodology is discovery, optimization, and studies of scopes and limitations of new synthetic reactions, reagents and catalysts, while total synthesis refers to complete chemical synthesis of complex organic molecules, usually natural products, from simple, commercially available or natural precursors and is to be distinguished from *partial synthesis* or *semisynthesis*.¹ Apparently, development of methodology favors the progress in the research area of total synthesis. Total synthesis of natural products appears more elegant and streamlined as the field of organic synthesis becomes more sophisticated.²

Nowadays, total synthesis of natural products is often motivated by biological activity and medicinal applications of the final product. Indeed, total synthesis contributes to a number of adjacent fields such as chemical biology, medicinal chemistry and drug discovery. Consequently, the field of total synthesis is not only associated with

natural product, but also relates with designed molecules as well. Thus, the identification of small molecules, especially biological interesting natural products which can modulate cellular functions, has been attracted a lot of interest from chemical biologists and medicinal chemists.³

There are several advantages for the use of small molecules compared to classical genetic approaches because gene depletion of a multifunctional protein may remove a specific function from the cell due to the removal of some protein-protein interaction or even cause the death of the organism, while a selective small molecule can perturb specific protein features, temporarily control or reverse the inhibition of protein function without target removal from the cell or causing death of the organism.² However, there are also some disadvantages when using small molecules such as the lack of specificity, cytotoxicity and solubility.⁴ Small molecules which lack specificity may not be suitable for drug development or can cause misinterpretation of the observed effect.⁵ Meanwhile, small molecule may induce cytotoxicity to the organism in a dose-dependent manner. Compounds with solubility issues may precipitate when treated into cell or may not penetrate through cell membrane or specific tissues to target site. It is noteworthy to mention that molecular interactions and chemical transformations as well as all biological phenomena can be tracked back to chemical processes (Figure 1.1).⁶

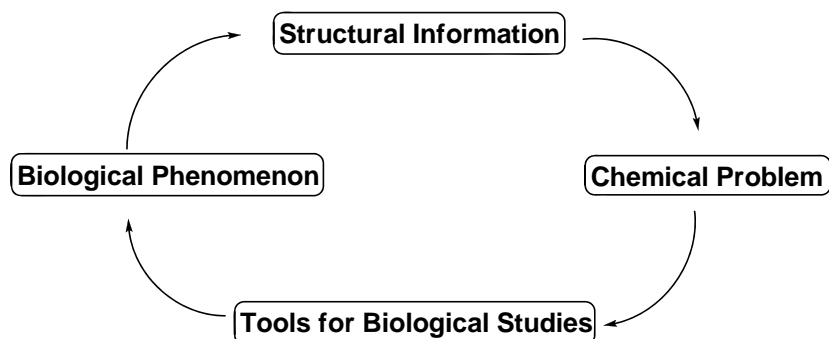


Figure 1.1 Relationship between organic synthesis and biology in chemical biology

1.2 Natural products and chemical biology

Historically, natural products chemistry and synthetic organic chemistry have been the driving force for drug discovery. Apparently, natural products have been the most productive source of leads for the development of drugs. Many natural products can modulate the function of individual protein or multifunction protein in living organisms with high potency and excellent selectivity. Those compounds are mostly discovered through phenotypic cell-based screening and are designated to be elucidated the mechanism of action at molecular level. For example, a collection of natural products which can perturb chromatin remodeling enzymes has been illustrated their signaling pathways, impacts on gene regulations and characterization of small molecule-protein interactions. New synthetic methods have been developed in parallel to accelerate the deployment of natural products and novel synthetic entities in the dissection of cellular interactions relevant to chemical biology of natural products or even human disease

treatment. More importantly, the modern tools of chemistry and biology allow scientists to discover the nature of biological effect behind the natural products on the human body as well as provide opportunities to develop new therapies against many fatal diseases including cancers.

1.2.1 Therapeutical application of natural products and drug development

Natural products has been utilized to treat disease and injuries through our evolution since our earliest ancestors chewed on some herbs to relieve pain, or wrapped certain leaves around wounds to improve healing.⁷ With the progress on molecular biology and combinatorial chemistry during the past decades, natural products have been applied in drug discovery and drug development. The use of information from natural products or compounds derived from natural products can be applied in numerous approaches to lead to novel structures with therapeutical potential.⁸ Subsequently, a large number of well known natural products have been isolated, identified, and analyzed, some of which are still widely used as drugs.

The structural analysis of natural products and the modern organic synthesis allows chemists to modify them in order to achieve great characteristics such as specificity, low cytotoxicity and solubility in human body, which are desirable for drug development. About 60% of the drugs currently used including artemisinin, camptothecin, lovastatin, maytansine, paclitaxel, penicillin, reserpine and silibinin are either directly from nature or derived from natural products.⁷ Even though many

pharmaceutical companies focus their research efforts on combinatorial chemistry and high-throughput screening to identify new drug candidates, this strategic change did not bring more drug candidates. For example, only 17 new drugs were approved in 2007, compared with 53 in 1996.⁹ Therefore, pharmaceutical community is switching back to natural products or naturally inspired products, among which FK228, a compound discovered in the 1990s by the Japanese pharmaceutical company Fujisawa, inhibits the function of a class of enzymes called histone deacetylase that are often hyperactive in cancer cells.¹⁰ FK228 (Istodax as commercial name) was approved by the US Food and Drug Administration (FDA) in November, 2009 for the treatment of cutaneous T-cell lymphoma (CTCL).

1.2.2 Structure and activity relationship (SAR)

Natural products with promising pharmacological profile are not necessarily lead compounds since complexity of the molecules may cause the difficulties of accessibility in the industrial application or have some side-effects. Therefore, modern organic synthesis is capable of achieving better properties of natural products via the preparation of a variety of analogues, which are more easily accessible and better characterized drugs for pharmaceutical process. The collection of analogues with systematic variations in different domains can determine the structure-activity relationship (SAR) of natural products, which may be useful to achieve more promising drugs possessing high potency, excellent selectivity, better solubility and little side-effect.

1.2.3 Target identification

Recent progress in bioassay-guided isolation and structure elucidation of natural products necessitates the efficiency of modern organic synthesis to provide practical access to rare and biosynthetically inaccessible natural products, which enables identification of the cellular target of those bioactive compounds and ultimate development of new therapeutic agents.¹¹ Chemical genetics is such a field that uses small molecules to probe biological systems, which contains the following three parts: natural products or small-molecule libraries, phenotypic screening and target identification, among which target identification is the biggest hurdle in chemical genetics so far.¹² Currently, the areas of affinity chromatography, yeast haploinsufficiency, complementary DNA (cDNA) overexpression, DNA microarray, small-molecule microarray and RNA interference (RNAi) technologies have undergone further optimization and have been applied increasingly to identify many cellular targets and eventually help the drug-development process.¹² Compared with traditional genetic approaches, chemical genetics appears to offer many advantages. However, there are still some drawbacks to its use. A small molecule, which lacks specificity, may interact with several structurally related target proteins to impede the feasibility to determine its mechanism of action, while natural products always possess extraordinary specificity and potency compared with artificially designed small molecules. Therefore, natural products synthesis and development of SAR profiles will ultimately lead to identification of the

cellular target responsible for biological processes we are interested in and help the development of drug and therapeutics.⁴

1.3 Goal and outline of this dissertation

The remainder of this dissertation will be focused on my studies towards total syntheses of biologically active natural products. To broad the context of each work, the biological background as well as the synthetic history will be introduced first in each chapter.

In chapter 2, the first total synthesis of largazole will be discussed and identification of molecular target as well as SAR studies will be disclosed further. Chapter 3 will be focused on total synthesis of cytotoxic siderophore-brasilibactin A and its analogues. In addition, we will report its iron-binding capability. Chapter 4 deals with the development of an asymmetric organocatalytic method to synthesize both 2,6-*cis*- and *trans*-piperidines. The practical value of this methodology should be potentially applied in the synthesis of more complex biologically active alkaloids which contain 2,6-disubstituted piperidines.

Chapter 2

Total Synthesis of Largazole, a Potent Class I Histone Deacetylase Inhibitor

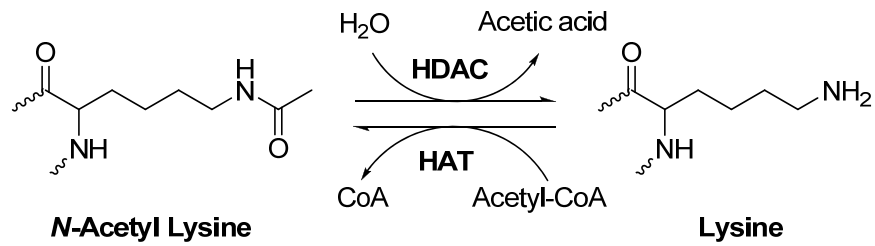
Histone deacetylases (HDACs) are zinc-dependent hydrolases that play an important role in chromatin remodeling and regulation of gene expression.¹³ HDACs associate with a number of cellular oncogenes and tumor-suppressor genes, leading to an abnormal recruitment of HDAC activity, which in turn depresses gene expression, impaired differentiation and excessive proliferation.¹⁴ Currently eighteen known HDACs have been identified on the basis of homology within the catalytic domain.¹⁵ Recent substantial progress in the studies of HDACs is achieved by the discovery of molecules that act as HDAC inhibitors (HDACi), which induce an increase in gene expression that results in their antitumor activities. Consistently, HDACi have been proposed for cancer therapeutics as well as for use as both drugs and probes of HDAC biology, due to their ability to induce growth inhibition, cell differentiation and apoptosis.¹⁴

2.1 Epigenetic Control

According to the explanation of the term “epigenetics” by Dr. Alan Wolffe in 1999,¹⁶ epigenetics refers to ‘the heritable changes in gene expression that occur without changes in DNA sequence’. Recently, studies indicated that epigenetic mechanisms include DNA methylation and histone modifications such as acetylation, methylation,

ubiquitination, and phosphorylation based on this definition. In other words, those post-translational modifications play a major role in the organization of chromatin and gene expression.¹⁷ By changing the charge of targeted amino acids followed by altering chromatin structure, histone acetylation regulates gene expression to create binding sites or platforms for specific proteins,¹⁸ including transcription factors, additional chromatin modifiers and stress-induced protein which are involved in the DNA repair process. The interaction of the histone with DNA is weakened by hyperacetylation of nuclear histones at lysine residues which leads to a relaxation of the nucleosome structure, thus providing transcription factors with access to DNA elements.¹⁹ The acetylation of histone proteins by the concerted action of histone acetyltransferases (HATs) and histone deacetylases (HDACs) is currently involved in epigenetic modulation of gene transcription (Figure 2.1a).²⁰ Histone acetyltransferase (HATs) enzyme acetylates the ϵ -nitrogen of lysine residues, disrupting the electrostatic interactions between the negatively charged DNA backbone and the positively charged amino-terminal histone. The consequent weakening of histone and DNA electrostatic interactions results in a more relaxing state, which allows transcriptional factors access to DNA, while histone deacetylases (HDACs) reverse the activity of HATs and remove acetyl groups from lysine residues in the *N*-terminal tails of histones to condense chromatin structure and silence the gene transcription (Figure 2.1b).

a) Schematic depiction of histone acetylation by HAT and HDAC



b) HAT and HDAC regulate gene expression

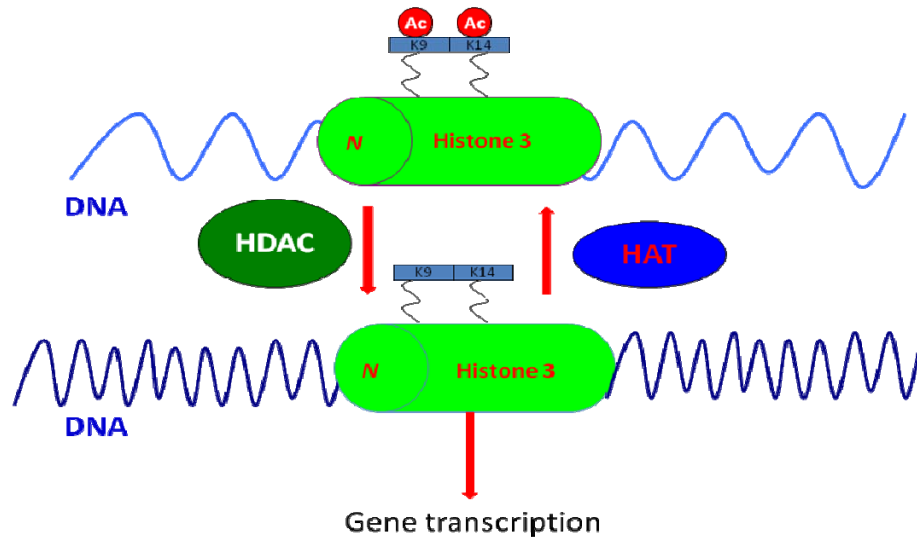


Figure 2.1 Histone acetylation and gene expression by HAT and HDAC

2.1.1 Histone deacetylases (HDACs)

In contrast with HATs, HDACs are involved in gene regulation by removing acetyl moieties from lysine residues in the *N*-terminal tails of histone and other non-histone proteins. Currently, there are eighteen known HDACs which are generally divided into four classes based on their homology to yeast counterparts (Figure 2.2).^{21,22} Class I, class II and class IV HDACs are Zn²⁺ dependent, while class III HDACs are NAD⁺ dependent. Class I HDACs include HDACs 1, 2, 3 and 8, which show high

sequence homology to the yeast protein-reduced potassium dependency protein 3 (Rpd3).²³ Class II HDACs including HDACs 4, 5, 6, 7, 9 and 10 share homologies with yeast HDA1 protein.²⁴ Class IV HDAC-HDAC 11, identified in human, controls DNA expression by modifying the core histone octamers.²⁵ In contrast, class III HDACs (SirT1-7, known as Sirtuins) require nicotinamide adenine dinucleotide (NAD⁺) for their catalytic activity and appear to be resisted to classical HDAC inhibitors like hydroxamic acid-based vorinostat (also known as SAHA and ZolinzaTM).²⁶ Therefore, only class I and class II HDACs will be discussed further in this dissertation.

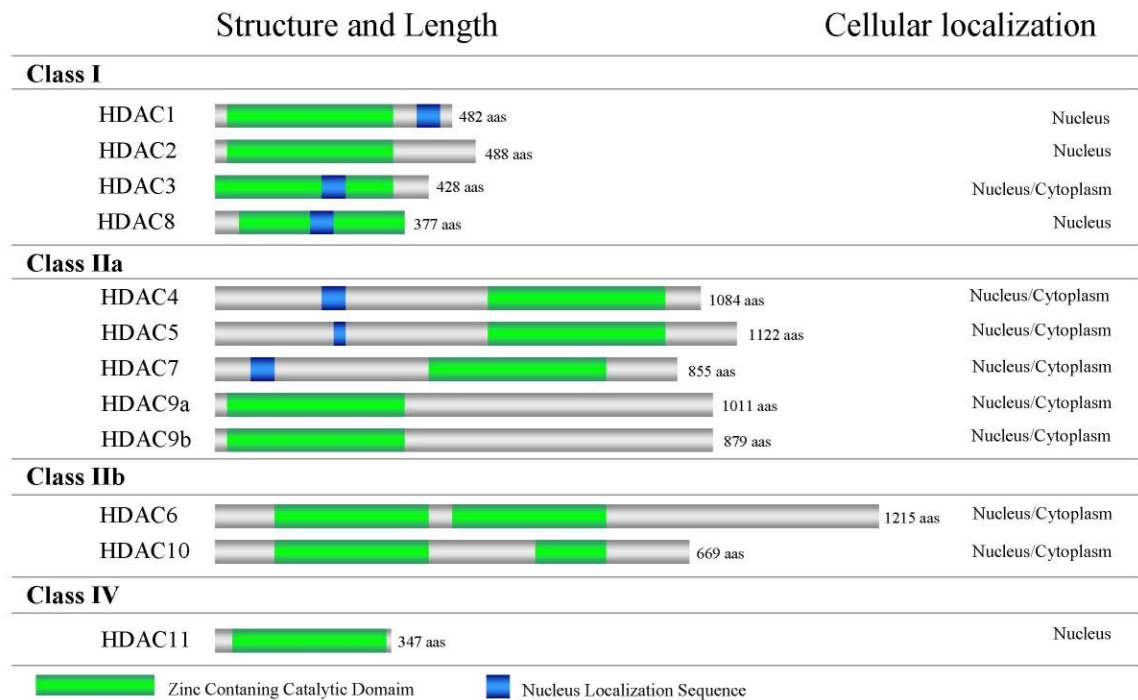


Figure 2.2 Classification of histone deacetylases*

* Original image from Lucio-Eterovic *et al. BMC Cancer* **2008**, *8*, 243.

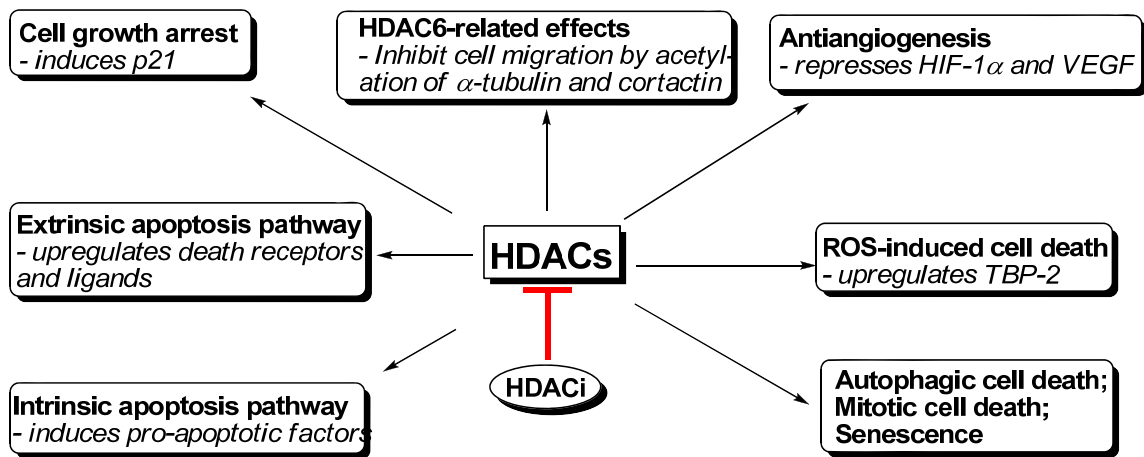
In terms of their sizes and locations within the cell, class I HDACs differ with their class II isoforms. Class I HDACs are relatively small size enzyme ranging between 42-45 kDa, mainly expressed in the nucleus, while class II HDAC tend to be large and have multidomains between 80-131 kDa, shuttling between the nucleus and the cytoplasm (Figure 2.2).²⁷ In terms of functionality, class I isoforms share sequence homology in the catalytic domain located at the *N*-terminus, while the class II HDACs have a catalytic domain at the *C*-terminus although they share a 390 amino acid region of homology in the enzyme core.²⁸ It is noteworthy that there are two catalytic sites present in HDAC6.²⁹

Recent emerging research has shown that substrates for HDACs are not only histone proteins, but also many non-histone proteins including hormone receptors, chaperone proteins, transcription factors, and cytoskeletal proteins.³⁰

2.1.2 Aberrant HDAC relates with cancer

Even though there is no direct evidence showing HDACs relate to the pathogenesis of human cancer, HDACs associate with oncogenic translocation products and tumor suppressor genes including p53, p21, and gelsolin in human carcinoma cell lines and other varieties of tumors (Figure 2.3).³¹ For example, HDAC1 tend to be upregulated in both prostate and gastric cancers. HDAC8 relates with tumorigenesis, while HDAC3 is overexpressed in lung, breast cancers and some colon cancers.³²

Generally, class I enzyme plays a significant role in survival and proliferation of cancer cells, while class II HDACs can interact with hormone receptors.^{33,34} Therefore, the molecules that inhibit HDAC activities may suppress cancerous cell growth by restoring the histone to their acetylated state in which transcription genes are activated. Apparently, HDAC inhibitors (HDACi) are potential cancer therapeutical agents.



HIF-1 α , hypoxia induced factor-1 α ; VEGF, vascular endothelial growth factor; TBP-2, thioredoxin binding protein 2; ROS, reactive oxygen species

Figure 2.3 Mechanisms of HDAC inhibitors-induced cell death

2.1.3 Histone deacetylase inhibitors (HDACi)

2.1.3.1 Classification

Recent progress on the study of HDACi facilitates the research on structure and function of HDAC enzymes. In the 1990's, trichostatin A (TSA) and other fungal antibiotics, such as trapoxin (TPX), isolated from natural source, has been shown to inhibit HDACs at nanomolar range (Figure 2.4). One of the most important developments in HDAC enzymes is using TPX, a naturally occurring HDACi, to isolate the first

HDACs by affinity chromatography.³⁵ These HDACi play important roles in inhibition and antiproliferative effect of tumors.

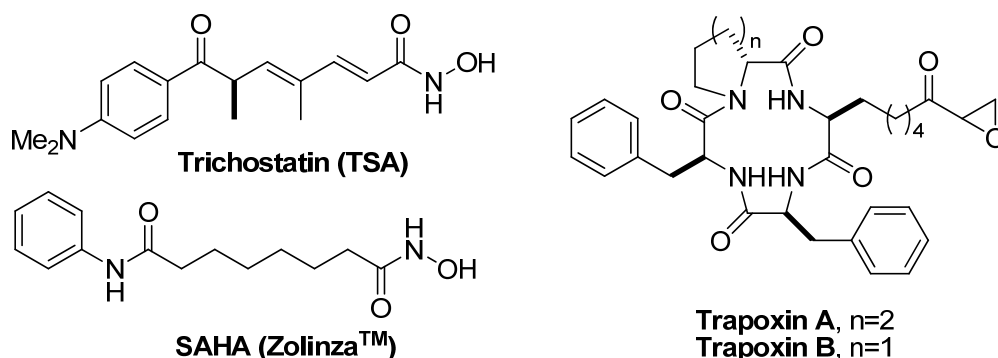


Figure 2.4 Structure of trichostatin A (TSA) and trapoxin (TPX)

Following the discovery of TSA and TPX, a variety of natural and synthetic HDACi have been described, some of which are now under clinical trials or even proved by FDA as anticancer drugs.³⁶ There are three key structural elements in all HDACi: 1) zinc binding group which coordinates the zinc ion in the active cavity – warhead; 2) a cap group which interacts with amino acids at the entrance to the active site; 3) a linker domain which interacts with amino acids at the entrance to the active site, usually five to seven carbon length (**Figure 2.5**). Based on the structure of natural occurring or synthetic HDACi, they have been divided into two classes: 1) acyclic small molecules and 2) cyclic or bicyclic depsipeptide or peptides.³⁷

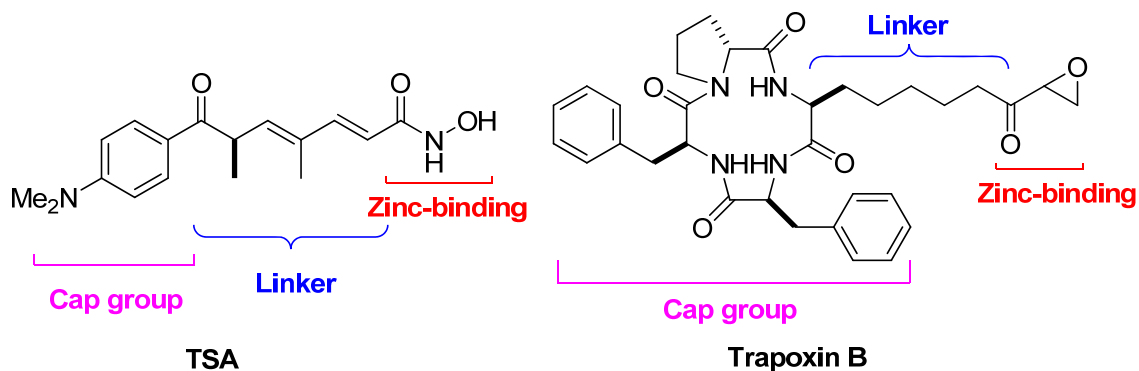


Figure 2.5 Structural elements in representative HDACi

2.1.3.1.1 Acyclic histone deacetylase inhibitors

The earliest class of HDACi and the most extensively studied HDACi are those acyclic and short chain molecules. The best known example is trichostatin A (TSA, Figure 2.4), a fungistatic antibiotic isolated from *Streptomyces hydropiscus*.³⁸ Recently, an X-ray crystal structure of TSA bound to HDLP has shown that the hydroxamic acid group tightly coordinates the Zn²⁺ in the active site, while the lone aliphatic chain reaches through a long narrow binding cavity and dimethylaniline group interacts with amino acids on the surface of the enzyme.²⁸

Even though the pharmacokinetics of this compound is poor, the discovery and related finding facilitates the development of structurally related HDACi, among which vorinostat (SAHA, Zolinza (merck)) is the most extensively studied and first FDA-approved HDACi (Figure 2.4). SAHA, not a natural product but rather from small molecules screening in 1990's, was found to induce differentiation of murine erythroleukemia cells, resulting in the increasing levels of p21, and G1 cell cycle block.³⁶

Furthermore, it has been shown to inhibit HDAC1 and 3 with $IC_{50} = 10$ nM and 20 nM respectively.³⁹ Subsequently, it was revealed that SAHA was capable to induce differentiation, cell growth arrest and apoptosis in various cell lines at low micromolar concentrations and to have antiproliferative effects against numerous cultured transformed cells. In addition, SAHA inhibits tumor growth with little toxicity in a range of animal models of solid tumors such as breast, prostate, lung and gastric cancer and hematological malignancies.²² The findings demonstrate this acyclic HDACi is a promising cancer therapeutical agent. However, even though SAHA is potent to some extent, it functions as pan-HDAC inhibitor, which lacks specificity since it tends to inhibit all isoforms in class I and class II enzymes. In order to better understand the function of individual isoforms, more specific HDACi is desired and this pan-HDAC inhibition of SAHA may be less desirable in the clinic.

2.1.3.1.2 Cyclic or bicyclic histone deacetylase inhibitors

HC-toxin was first isolated cyclic tetrapeptide HDACi from *Helminthosporium carbonum*, which possesses an α -epoxy ketone as its zinc-binding moiety (Figure 2.6).⁴⁰ The linker moiety in HC-toxin, termed (*S*)-2-amino-8-oxo-9,10-epoxydecanoic acid (AOE, marked as red), is a common structural skeleton among cyclic tetrapeptide including trapoxins A and B, chlamydocins and Cyl-2,⁴¹ which act as substrate mimics for inhibiting HDAC enzyme. HC-toxin shows modest HDAC inhibitory activity compared with TSA ($IC_{50} = 30, 3.8$ nM against HDACs, respectively),⁴² while Cyl-2 displays more potent activity as well as better selectivity ($IC_{50} = 0.75$ nM against

HDAC1, 57,000 fold preference for HDAC1 over HDAC6).⁴³ Azumamide E possesses a complete opposite absolute configuration of amino acid moieties as those shown in Figure 2.6 and the zinc-binding moiety contains carboxylic acid which is relatively weak zinc chelation motifs, resulting in less potent activity.⁴⁴

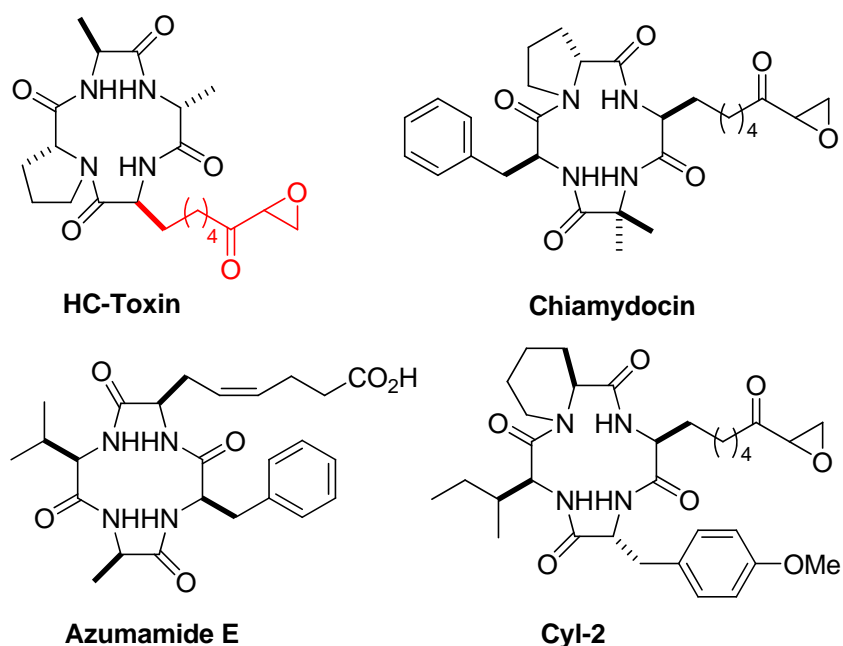


Figure 2.6 Selected macrocyclic peptidic HDACi's

Recently, the most structurally complex class of HDACi which are sulfur-containing natural products has been isolated and well studied, such as FK228, spiruchostatins, FR901375 and largazole (Figure 2.7). The common structural element among these compounds is β -hydroxy mercaptoheptenoic acid residue, however, the significant differences are located within the hybridized carbons in their macrocycles. In

FK228 and largazole, five sp^2 hybridized carbon atoms are present in the macrocycle, while spiruchostatins and FR901375 only contain four. Furthermore, investigation of binding interactions on the rim region of the HDACs with cyclic peptide HDACi helps to better understand the enzyme-inhibitor relationships and facilitates the progress on the identification of class- or isoform-selective inhibitor with high potency.

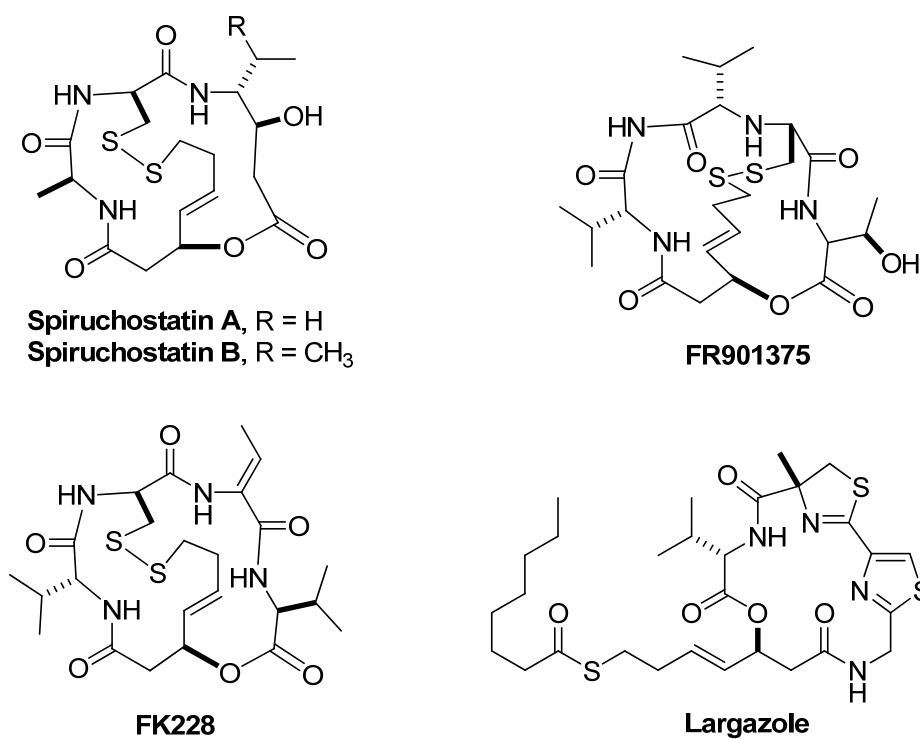


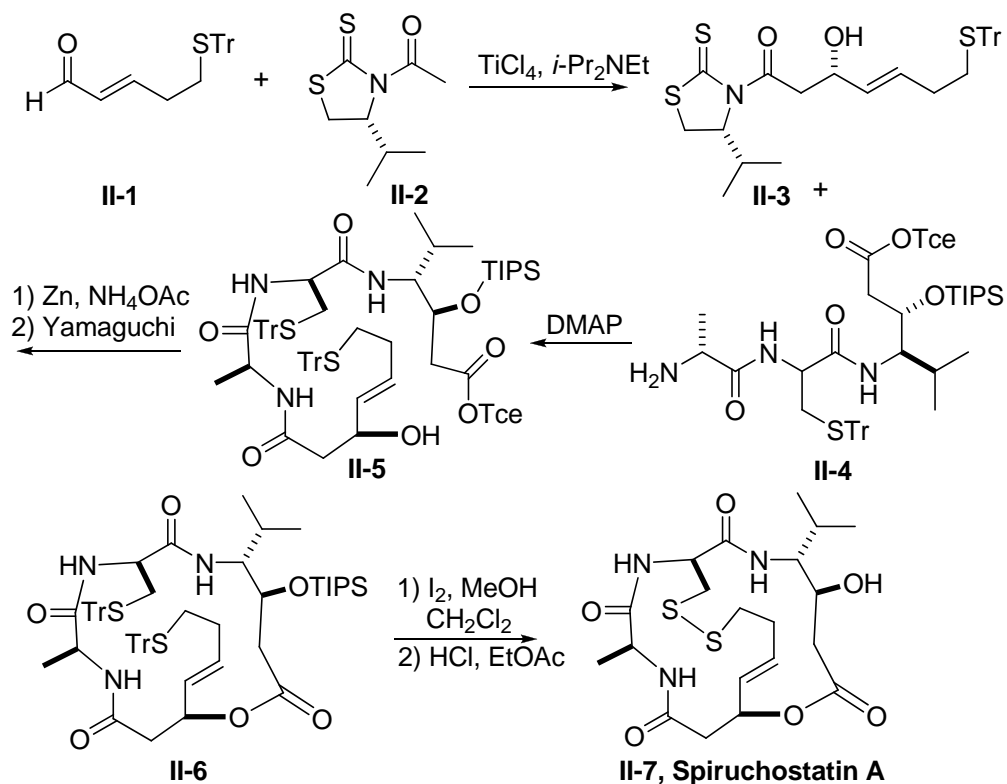
Figure 2.7 Sulfur-containing HDACi's

Spiruchostatins

The spiruchostatins A and B, isolated from a *Pseudomonas* extract in 2001, showed TGF- β -induced gene expression.⁴⁵ Although the absolute structure is not

determined, the similarity to FK228 suggested the stereochemistry of the β -hydroxy acid and statine was (*S*) and (*R*) respectively. Furthermore, HDAC inhibition of these molecules was also disclosed.

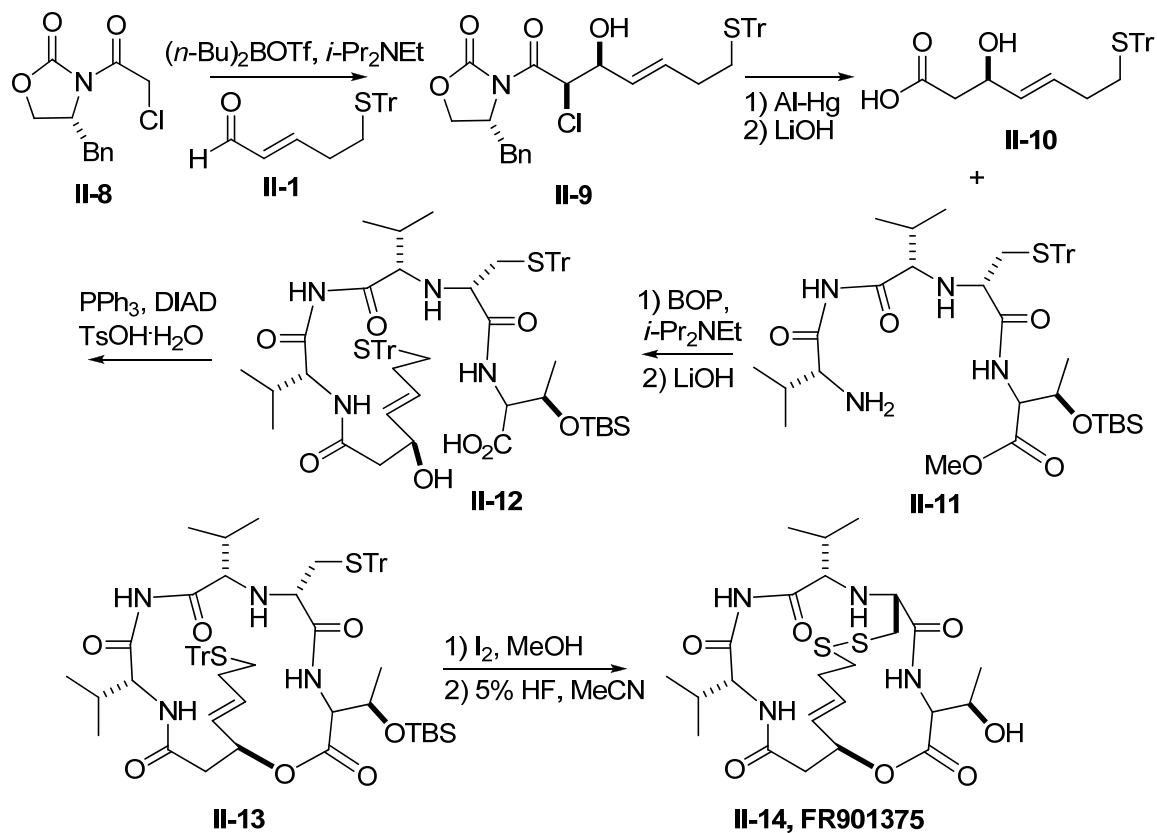
To date, there are two total syntheses of spiruchostatin A and one of spiruchostatin B, among which Ganesan's total synthesis of spiruchostatin A is worthy to mention here (Scheme 2.1). Nagao aldol reaction of **II-1** gave the β -hydroxy acid fragment **II-3**, which was then coupled to an appropriately protected peptide **II-4**. Following deprotection, Yamaguchi macrolactonization of **II-5** proceeded smoothly to give the macrocycle **II-6**. Removal of trityl group in **II-6** and subsequent disulfide bond formation followed by TIPS deprotection gave spiruchostatin A **II-7**. The biological inactivity of **II-7** with *R*-stereochemistry at the β -hydroxy acid fragment showed the stereochemistry at this position is critical for interactions with amino acids on the rim of HDAC enzymes.⁴⁶



Scheme 2.1 Ganesan's synthesis of spiruchostatin A

FR901375

FR901375 is a metabolite of *Pseudomonas chloroaphis* isolated by Fujisawa Pharmaceutical Company in 1991.⁴⁷ Janda prepared β -hydroxy acid fragment **II-9** by Evans' aldol reaction instead of utilizing Nagao's aldol reaction. Mitsunobu reaction was utilized to prepare the macrocycle **II-13** in good yield (**Scheme 2.2**).

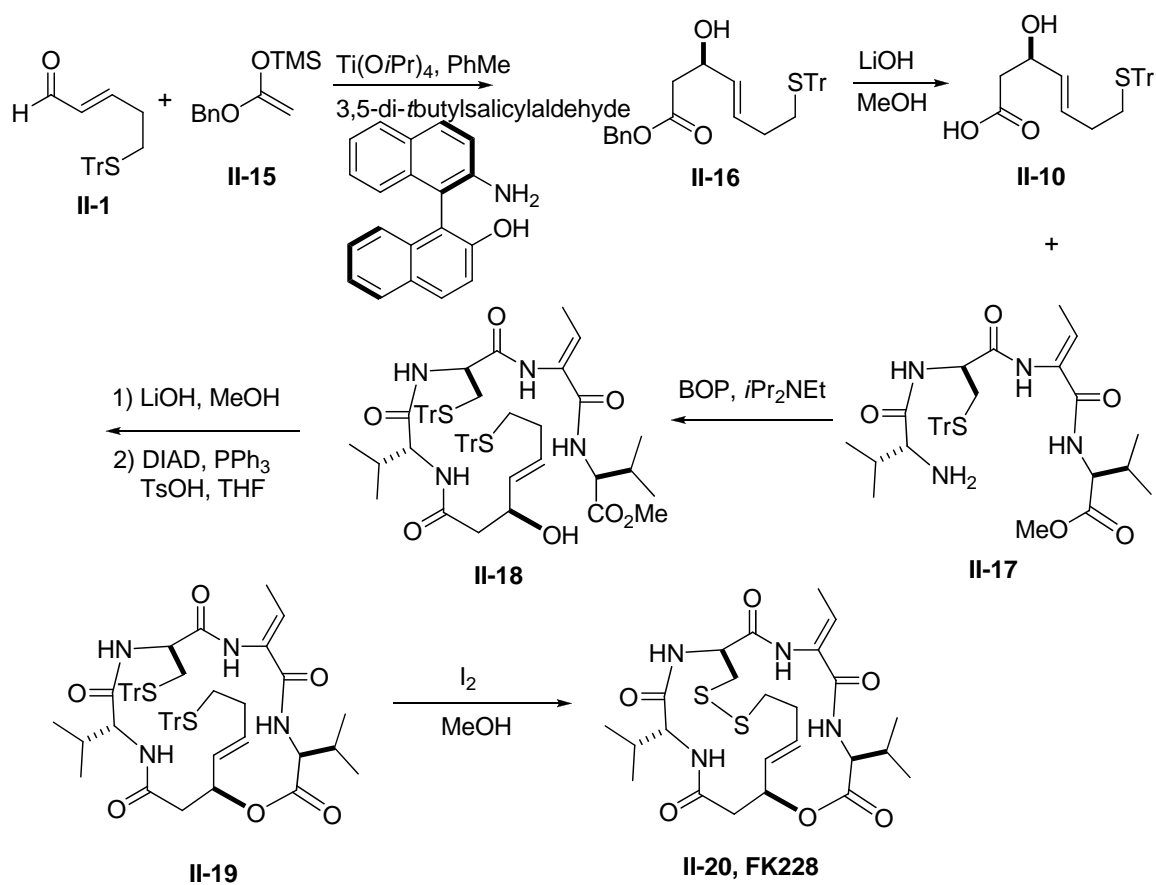


Scheme 2.2 Janda's synthesis of FR901375

FK228 (Romidepsin)

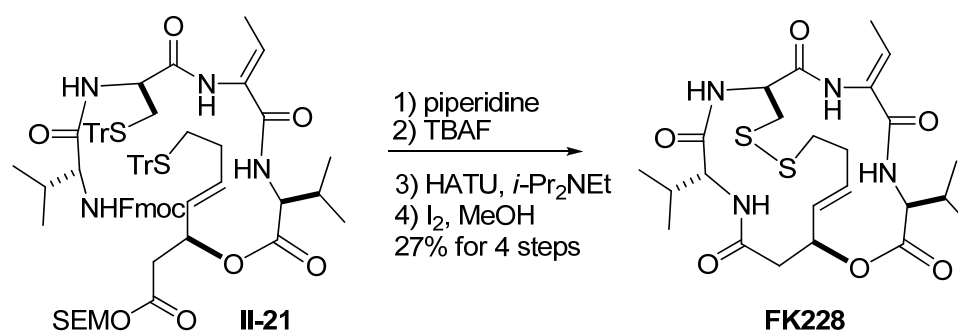
FK228 (FR901228 or Romidepsin^R), a naturally occurring depsipeptide isolated from *Chromobacterium violaceum*, is the only cyclic peptide approved by FDA (Figure 2.7).³⁶ It has progressed through clinical trials on peripheral and cutaneous T-cell lymphoma.⁴⁸ Despite the structural similarity with spiruchostatins, a bicyclic depsipeptide, FK228 features a 16-membered ring about the macrocycle and peptide backbone and a 17-membered ring about the ester and disulfide linkages, which was determined by spectroscopic and X-ray analysis as well as confirmed by numerous total

syntheses.⁴⁹ The first total synthesis was introduced by Simon, in which a titanium-mediated aldol reaction was used to prepare the enantiomer of the natural β -hydroxy acid stereoisomer, which was then mandated to inverse the stereochemistry under Mitsunobu reactions. Final trityl deprotection and disulfide bond formation gave FK228 (Scheme 2.3).⁵⁰



Scheme 2.3 Simon's synthesis of FK228

Following publication of Simon's route to FK228, Williams and Ganesan published improved syntheses based on the synthetic strategy introduced by Simon, while it is noteworthy to mention Ganesan's total synthesis of FK228 shown in [Scheme 2.4](#).^{51,52} To overcome the difficulties in terms of reproducibility of macrocyclization with Mitsunobu reaction, an alternative macrolactamization route has been reported by Ganesan (Scheme 2.4).



Scheme 2.4 Ganesan's synthesis of FK228 by macrolactamization

Analogues and peptide isostere of FK228 have also been reported to further clarify the structure-activity relationships (SAR) by Williams.⁵¹ Mechanistic studies have shown that the reduced form of FK228 (redFK) is the active form, which was generated by the reduction with glutathione after entering the cells.⁵³ 75-Fold increase in inhibitory activity against HDAC1 for redFK228 *versus* FK228 further supports FK228 acts as a pro-drug, with the disulfide bond facilitating itself penetrating through the cell walls as shown in [Table 2.1](#).

Table 2.1 Biological data for FK228 and redFK

Compound	HeLa HDACs (nM)	HDAC1 (nM)	HDAC6 (nM)
FK228	ND ^a	30	14,000
redFK228	15	0.397	787

^a ND: not determined

Largazole

The most recent sulfur-containing cyclic depsipeptide HDACi, isolated from the floridian marine cyanobacterium *Symploca* sp., is termed as largazole for its florida location (key largo) and structural feature (thiazole).⁵⁴ Largazole shares some structural similarity to FK228, FR901375 and spiruchostatins such as 3-hydroxy-7-mercaptohept-4-enoic acid moiety, while it possesses an octanoyl thioester bond instead of a disulfide linkage. Therefore, largazole is also a prodrug which must be generated by metabolic hydrolysis of the octanoyl residue. Furthermore, largazole is more potent than FK228 (0.07 nM *versus* 1.6 nM) and active form largazole thiol displays class-form selectivity in terms of HDAC1 over HDAC6.⁵⁵ The potent biological activity and selectivity of largazole attracts significant attention from synthetic chemists with eight total syntheses being published within two years, which will be introduced later in this chapter in details.

2.1.3.2 Mechanism of action

The interaction between HDACs and HDACi was studied extensively by Finnin and coworkers in 1999.²⁸ They solved the crystal structure of HDLP which is a HDAC-like protein sharing a 35% sequence identity with human HDAC1 especially located within the active site. These crystallographic studies revealed that the region interaction

between SAHA and HDLP possesses three characteristic features, which includes surface recognition region, a narrow tube-like channel $\sim 11\text{\AA}$ in depth and narrow pocket at the bottom of this channel in which a Zn^{2+} cation is coordinated with two Asp residues, one His residue and a water molecule. Importantly, all these structural features from HDLP are in excellent accord with the crystal structure of HDAC8.⁵⁶

The crystal structure of HDAC8 with bound TSA revealed a proposed catalytic mechanism explaining the function of HDACs (Figure 2.8). The proposed catalytic mechanism for the deacetylation of acetylated lysine is similar with the amide hydrolysis mechanism for zinc proteases.⁵⁷ Acetylated lysine coordinates with the zinc ion at the active site, which is also coordinated with Asp 168, His 170, Asp 258 and a water molecule. Nucleophilic attack of the water on the carbonyl carbon forms a tetrahedral intermediate which is stabilized by zinc-oxygen interaction. The intermediate collapses to release a molecule of acetic acid and lysine, which are protonated by Asp 173-His 132 (Figure 2.8).

The crystal structure of HDAC8 and TSA suggests that TSA mimics an acetylated lysine substrate, blocking access to HDACs by the acetylated lysine residues on histone tails. TSA inserts its hydroxamic acid into the pocket by the aliphatic chain which interacts with hydrophobic residues in the channel, where zinc ion at the active site is bound with hydroxamic acid in a didentate fashion (Figure 2.8).

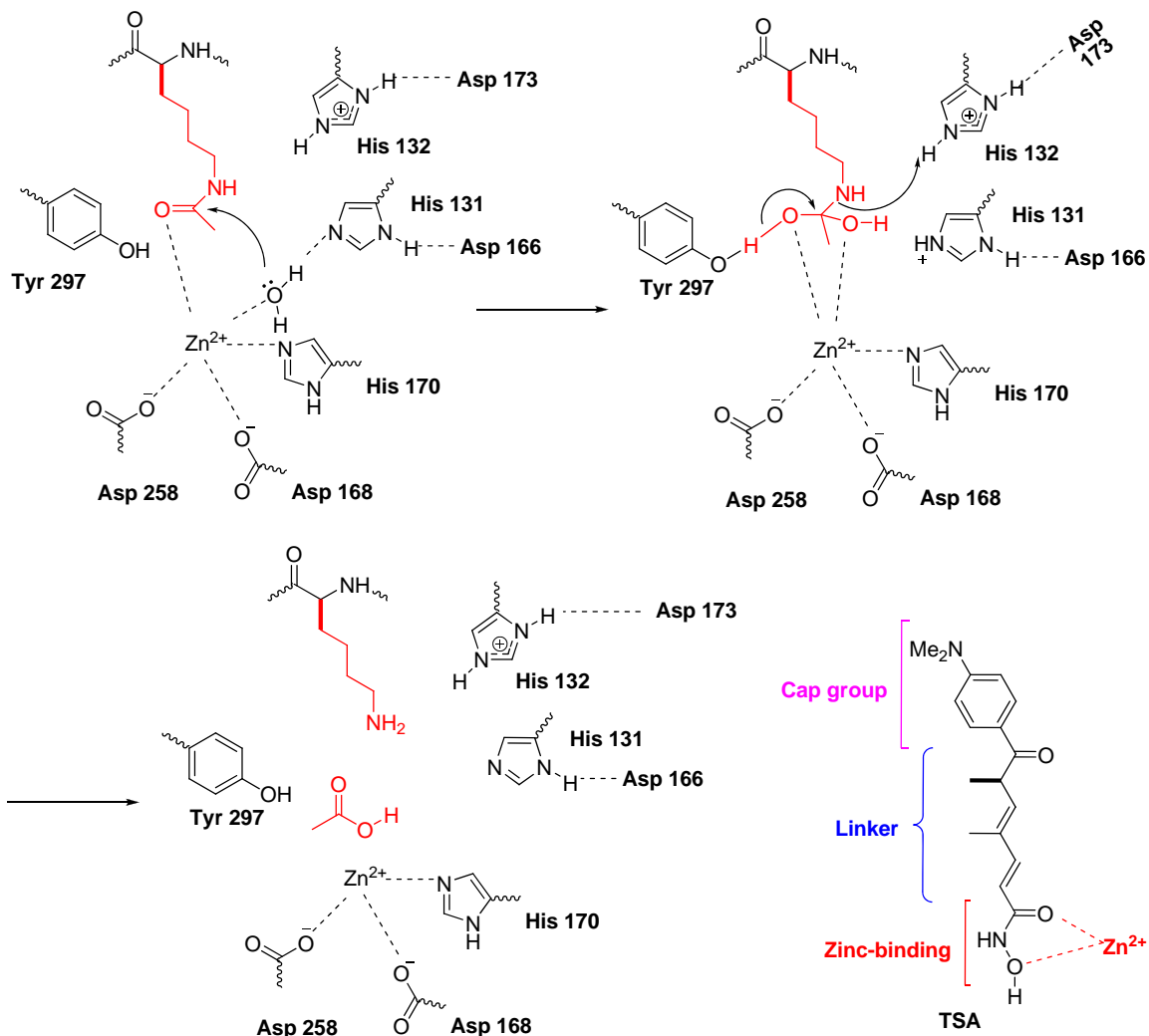


Figure 2.8 Proposed mechanism of action of Zn²⁺-dependent HDACs and TSA binding model with zinc ion in HDAC8 active site

2.1.3.3 Pharmaceutical application

There are at least 15 structurally different HDACi under clinical investigation, which acts either as monotherapy or combination therapy for hematologic and solid neoplasms (Table 2.2).⁵⁸ SAHA is the first HDACi approved by FDA for clinical use to treat cutaneous T-cell lymphoma patients.^{22,59} SAHA shows high anti-cancer activity in

numerous hematologic and solid tumors with little cytotoxicity. When patients with refractory cutaneous T cell lymphomas (CTCL) were treated with SAHA, their symptom could be relieved.⁶⁰ Furthermore, SAHA has also been used in clinical combination for synergistic or additive with a variety of chemotherapeutics.

Depsipeptide FK228, approved by FDA late in 2009, has been applied to treat patients with advanced CTCL as a single agent and it was reported that FK228 can be well tolerated with manageable toxicities including nausea, vomiting and fatigue.⁶¹ Other studies related with hormone refractory prostate cancer, multiple myeloma as well as hematological malignancies has been performed.

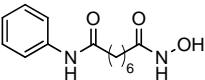
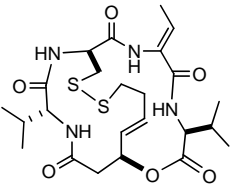
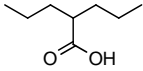
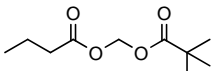
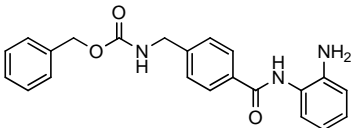
Pivanex (AN9) is in phase II clinical trials. Due to its lipophilicity, pivanex is able to penetrate through cell membranes very efficiently and has been shown to affect the growth, differentiation and apoptosis of a variety of cancerous cells at low concentration compared with its metabolite active form-butyric acid.

MS-275 is in phase II development for myeloid malignancies and melanoma and the compound was well tolerated orally at either 3 mg biweekly or 7 mg weekly based on recent clinical data.⁶²

Since the mechanisms behind HDACi regulating gene expression are still unclear, more understanding of biological role of HDACi on the molecular basis are needed to facilitate the progress on studying the functions of HDAC. Furthermore, HDACi is a promising cancer therapeutical agent and highly isoform-specific inhibitors may provide an opportunity to understand chromatin biology in cells. In order to better treatment of

human disease, the clinical development of HDACi still remains an active area of investigation.

Table 2.2 Representative HDAC inhibitors in clinical trials (partial list)

Class	Drug Name	Structure	Clinical trials
Hydroxamate	SAHA (Zolinza)		FDA approved
Cyclic depsipeptide	FK228 (Romidepsin)		FDA approved
Short-chain fatty acids	Valproic acid		Ph II-III (p.o.), Ph II (top.)
	Pivanex (AN-9)		Ph I-II (i.v.)
Benzamides	Entinostat (MS-275)		Ph I-II (p.o.)

Abbreviations: i.v.: *intravenous*; p.o.: *orally*; top.: *topical*.

2.2 Synthesis of largazole

2.2.1 Discovery, isolation and biological activity of largazole

The cytotoxic cyclic depsipeptide (**2.1**, [Figure 2.9](#)), termed largazole for its florida location (Key Largo) and one structural feature (Thiazole), was isolated from a cyanobacterium of the genus *Symploca* in early 2008 by Luesch.⁵⁴ Largazole is a marine natural product with novel chemical scaffold, which possesses a strained 16-membered macrocycle featuring a dense combination of unusual structures, including a substituted

4-methylthiazoline linearly fused to a thiazole and a 3-hydroxy-7-mercaptohept-4-enoic acid unit. It is noteworthy that thioester moiety in largazole **2.1** is rarely encountered in natural products.

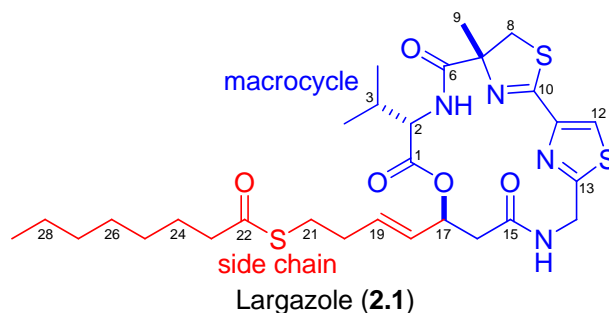


Figure 2.9 Structure of largazole

Macrocyclic natural products often exhibit unique biological properties and thus are attractive candidates for drug development in many diseases.⁶³ Largazole (**2.1**) represents such a class of compounds with highly differential growth-inhibitory activity, preferentially targeting transformed over non-transformed cells and favorably comparing to other natural products drugs such as paclitaxel (taxol) in this respect.⁵⁴ Largazole potently inhibited the growth of transformed human mammary epithelial cells (MDA-MB-231) and transformed fibroblastic osteosarcoma cells (U2OS) (GI_{50} 7.7 nM and 55 nM respectively) and induced cytotoxicity at higher concentrations (LC_{50} 117 nM and 94 nM respectively).⁵⁴ In contrast, non-transformed mammary epithelial cells (NMuMG) and non-transformed fibroblasts NIH3T3 were less susceptible to **2.1** (GI_{50} 122 nM and LC_{50} 272 nM for NMuMG; GI_{50} 480 nM and $LC_{50} > 8 \mu\text{M}$ for NIH3T3).⁵⁴

The potent biological activity and selectivity of **2.1** for cancer cells necessitates further investigation into the mode of action and potential as a cancer therapeutics. Our first total synthesis of **2.1** and its extension to preparation of key analogues will be described in details in this chapter. Furthermore, the identification of histone deacetylases (HDACs) as molecular targets and pharmacophore of **2.1** as well as the structural requirements for its HDAC inhibitory and antiproliferative activities will be disclosed further through our structure–activity relationship (SAR) studies.^{55, 64}

2.2.2 Retrosynthetic strategy of largazole

As shown in [Figure 2.10](#), introduction of the thioester moiety could be achieved by an olefin cross-metathesis of the 16-membered cyclic depsipeptide core **2.3** and the thioester **2.2**. Deliberate late-stage incorporation of the subunit bearing the thioester is amenable to a variety of analogues in search of the biological role of the thioester, the octanoyl group, and the double bond. A macrolactamization reaction of the linear precursor **2.4** would generate the requisite 16-membered cyclic depsipeptide core **2.3**. This analysis led ultimately to three key subunits (**2.5**, **2.6**, and **2.7**), which could be sequentially coupled to provide the linear precursor **2.4**.

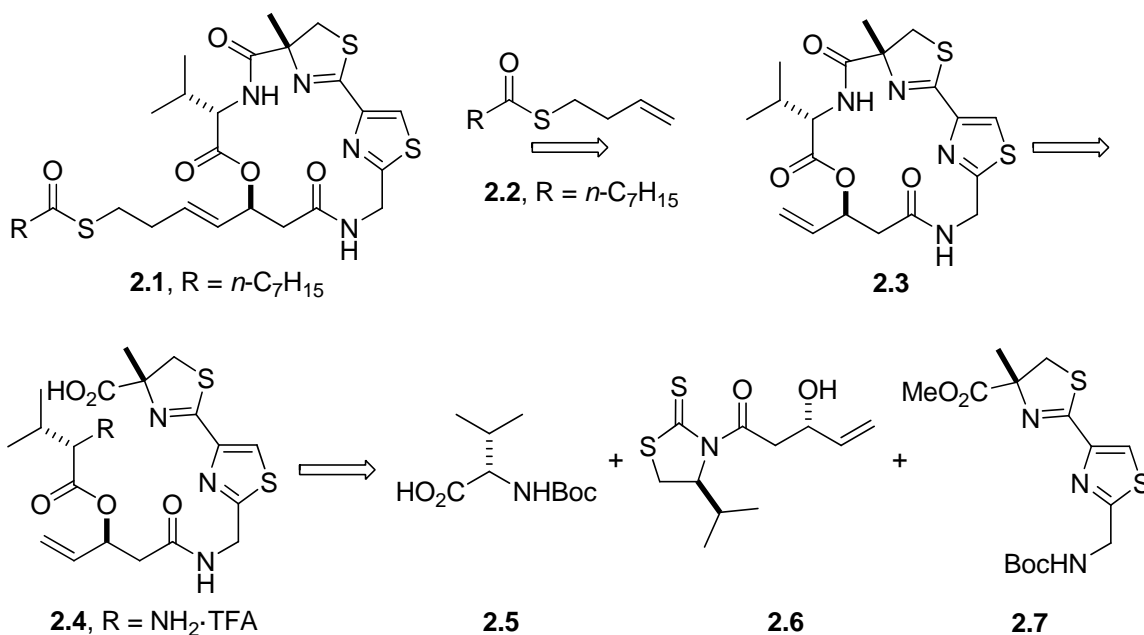
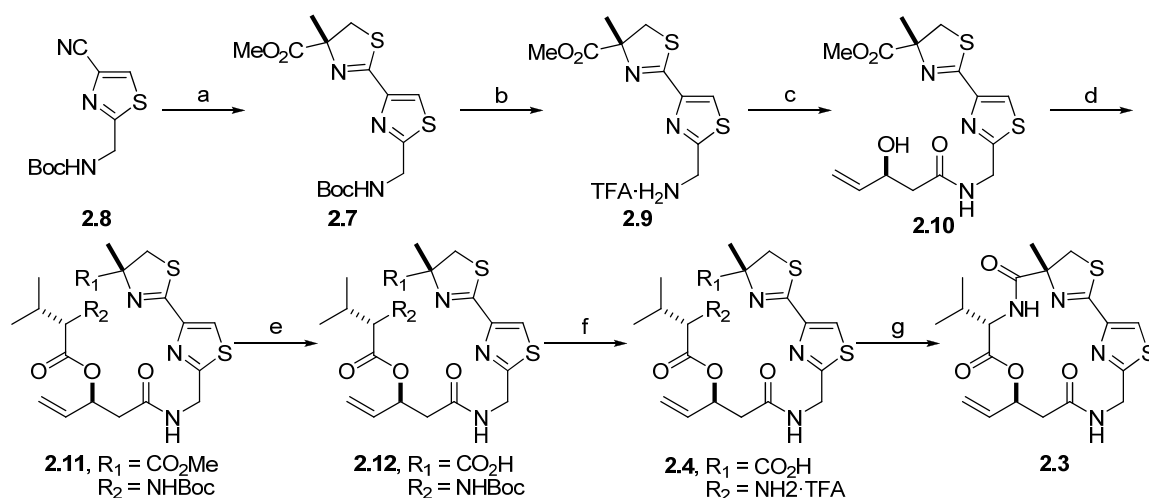


Figure 2.10 Retrosynthetic analysis

2.2.3 Synthesis of largazole

The synthesis commenced from the condensation of **2.8**⁶⁵ with (*R*)-2-methyl cysteine methyl ester hydrochloride⁶⁶ (Et₃N, EtOH, 50 °C, 72 h) to afford **2.7** in 51% (Scheme 2.5).⁶⁷ Deprotection of *N*-Boc group in **2.7** (TFA, CH₂Cl₂, 25 °C, 1 h) followed by coupling (DMAP, CH₂Cl₂, 25 °C, 1 h) of the corresponding amine **2.9** to **2.6**⁶⁸, prepared by an acetate aldol reaction of *N*-acyl thiazolidinethione and acrolein, smoothly proceeded to provide **2.10** in 94% yield (for two steps). Yamaguchi esterification reaction of **2.10** and *N*-Boc-L-valine (**2.5**) (2,4,6-trichlorobenzoyl chloride, Et₃N, THF, 0 °C, 1 h; then **5**, DMAP, 25 °C, 10 h, 99%) provided the linear depsipeptide **2.11**. Alternatively, DCC-coupling reaction of **2.10** and **2.5** (DCC, DMAP, toluene, 25 °C, 20 h) gave **2.11** in

85%. Hydrolysis of **2.11** under basic conditions using exact 1 eq. LiOH (0.5 N LiOH, THF, H₂O, 0 °C, 3 h) followed by the deprotection of *N*-Boc group in **2.12** (TFA, CH₂Cl₂, 25 °C, 2 h) provided **2.4**, a precursor to the 16-membered cyclic depsipeptide core **2.3**. Without further purification of **2.4**, we attempted to cyclize the crude **2.4** to provide the strained 16-membered cyclic depsipeptide core **2.3**. It is noteworthy that initial attempts for macrocyclization reaction⁶⁹ under EDC- (EDC, *i*-Pr₂NEt, CH₂Cl₂, 25 °C, 12 h, 12% for three steps) or FDPP-coupling conditions (FDPP, *i*-Pr₂NEt, CH₃CN, 25 °C, 36 h, 37% for three steps) afforded the desired 16-membered cyclic depsipeptide core **2.3**, but in low yields. After exploration of numerous reaction conditions, macrolactamization reaction of the crude **2.4** utilizing HATU–HOAt (HATU, HOAt, *i*-Pr₂NEt, CH₂Cl₂, 25 °C, 24 h) proceeded smoothly to provide **2.3** in 64% (for three steps).⁷⁰

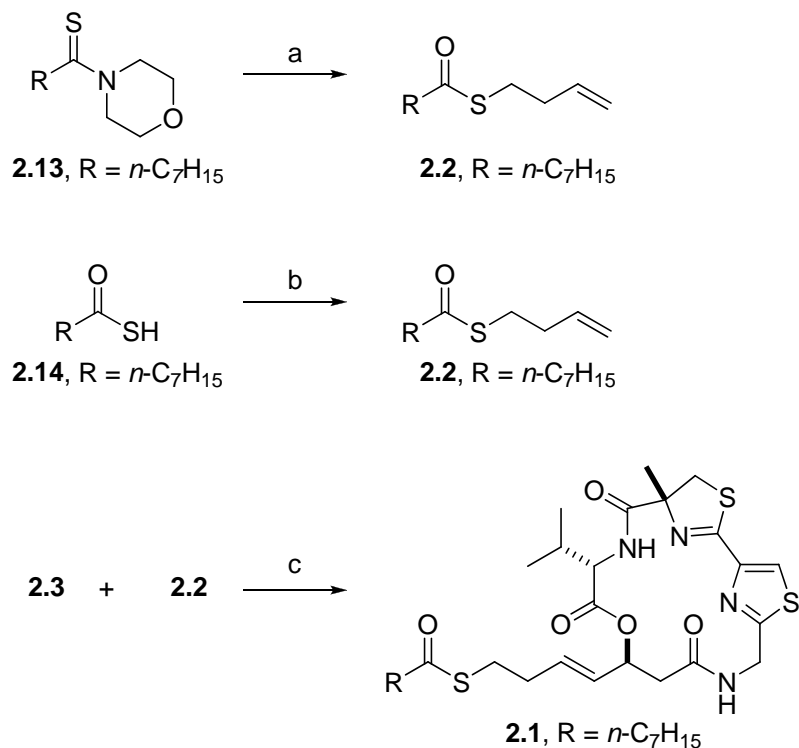


(a) (*R*)-2-methyl cysteine methyl ester hydrochloride, Et₃N, EtOH, 50 °C, 72 h, 51%; (b) TFA, CH₂Cl₂, 25 °C, 1 h; (c) **2.6**, DMAP, CH₂Cl₂, 25 °C, 1 h, 94% (two steps); (d) 2,4,6-trichlorobenzoyl chloride, Et₃N, THF, 0 °C, 1 h; then **2.5**, DMAP, 25 °C, 10 h, 99%; (e)

0.5 N LiOH, THF, H₂O, 0 °C, 3 h; (f) TFA, CH₂Cl₂, 25 °C, 2 h; (g) HATU, HOAt, *i*-Pr₂NEt, CH₂Cl₂, 25 °C, 24 h, 64% (three steps).

Scheme 2.5 Synthesis of 16-membered depsipeptide core

For synthesis of the thioester **2.2** (Scheme 2.6), initially we attempted to couple 4-(thiooctyl)-morpholine (**2.13**) with 4-bromo-1-butene (NaI, THF, H₂O, reflux, 16 h, 55%) utilizing the modified procedure developed by Harrowven and co-workers,⁷¹ but the procedure was not practical in terms of large scale preparation. Instead, the thioacid **2.14**⁷² was coupled with 4-bromo-1-butene (NaH, THF, 25 °C, 12 h) to provide the thioester **2.2** in 81%. Subjecting the 16-membered cyclic depsipeptide core **2.3** and the thioester **2.2** to a variety of olefin cross-metathesis reaction conditions⁷³ was attempted. After extensive optimization of reaction conditions, we were delighted to find that olefin cross-metathesis reaction of the macrocycle **2.3** and the thioester **2.2** in the presence of Grubbs' second-generation catalyst (50 mol%, toluene, reflux, 4 h) provided **2.1** in 41% (64% BRSM, (*E*)-isomer only) yield. The olefin cross-metathesis reaction of **2.3** and **2.2** in toluene occurred in a higher yield than in CH₂Cl₂ or benzene. Hoveyda-Grubbs catalyst was not as effective as Grubbs second-generation catalyst in the olefin cross-metathesis reaction. Synthetic largazole was indistinguishable in all respects with authentic largazole.



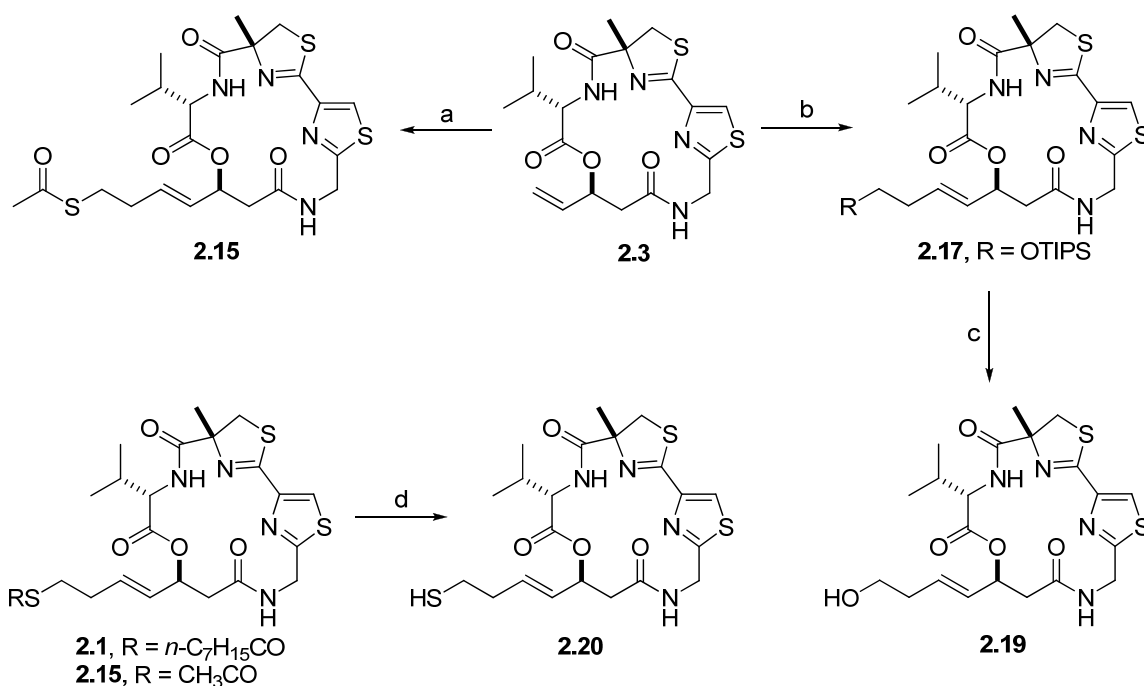
(a) 4-bromo-1-butene, NaI, THF, H₂O, reflux, 16 h, 55%; (b) NaH, 4-bromo-1-butene, THF, 25 °C, 12 h, 81%; (c) Grubbs' second-generation catalyst (50 mol%), toluene, reflux, 4 h, 41% (64% BRSM).

Scheme 2.6 Synthesis of thioester and completion of synthesis

2.2.4 Synthesis of largazole analogues

With this convergent synthetic route to largazole **2.1**, our efforts turned to the preparation and evaluation of a series of key analogues to study its origin of differential growth inhibition towards transformed *versus* nontransformed cells. To define the role of the octanoyl group in the thioester moiety (**Scheme 2.7**), we prepared the acetyl analog **2.15** of largazole by olefin cross-metathesis reaction of the macrocycle **2.3** with thioacetic acid *S*-but-3-enyl ester (**2.16**)⁷⁴ (50 mol% of Grubbs' second-generation catalyst, toluene,

reflux, 4 h, 54% (71% BRSM), (*E*)-isomer only). Similarly, the hydroxyl analog **2.19** (1-triisopropylsilyloxy-3-butene (**2.18**)⁷⁵, 30 mol% of Grubbs' second-generation catalyst, toluene, reflux, 3 h, 50%, (*E*):(*Z*) = >9:1; TBAF, THF, 25 °C, 1 h, 76%) was synthesized as shown in Scheme 2.7 to determine the role of thiol. In addition, the thiol analog **2.20** was smoothly prepared by the aminolysis of **2.1** or **2.15** (aq. NH₃, CH₃CN, 25 °C, 12–18 h) in 70–80%.



(a) thioacetic acid *S*-but-3-enyl ester (**2.16**), Grubbs' second-generation catalyst (50 mol%), toluene, reflux, 4 h, 54% (71% BRSM); (b) 1-triisopropylsilyloxy-3-butene (**2.18**), Grubbs' second-generation catalyst (30 mol%), toluene, reflux, 3 h, 50%; (c) TBAF, THF, 25 °C, 1 h, 76%; (d) aq. NH₃, CH₃CN, 25 °C, 12–18 h, 70–80%.

Scheme 2.7 Synthesis of key analogs to define the pharmacophore

2.2.5 Biological studies of largazole and its analogues

2.2.5.1 Mode of action and pharmacophore

The presence of a thioester functionality in largazole (**2.1**) is intriguing since cellular metabolism is expected to rapidly generate the corresponding thiol **2.20**, suggesting that largazole may be a prodrug. The liberated thiol **2.20** would then correspond to the mercapto unit that is generated by reduction of the disulfide bond in FK228 and the related spiruchostatins, which are potent histone deacetylase (HDAC) inhibitors (Figure 2.11).⁷⁶ Histone deacetylation is an epigenetic mechanism that regulates gene transcription, including genes that control proliferation, which can lead to silencing of tumor suppressor genes.⁷⁷ HDAC inhibition is a validated approach for cancer therapy and an active area of pharmaceutical drug discovery research.⁷⁸ The recent FDA approval of suberoylanilide hydroxamic acid (SAHA) marketed by Merck as Zolinza for the treatment of cutaneous T-cell lymphoma is the first tangible result of these efforts.²² Thus HDAC inhibition could indeed explain the largazole-induced phenotype, including selectivity for transformed cells.⁵⁴

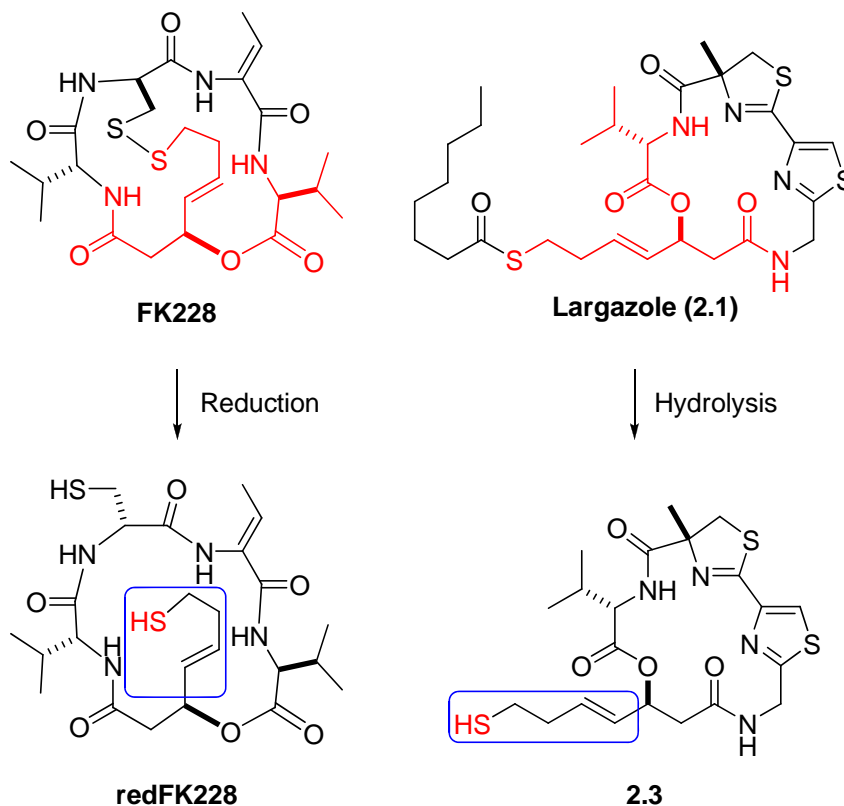
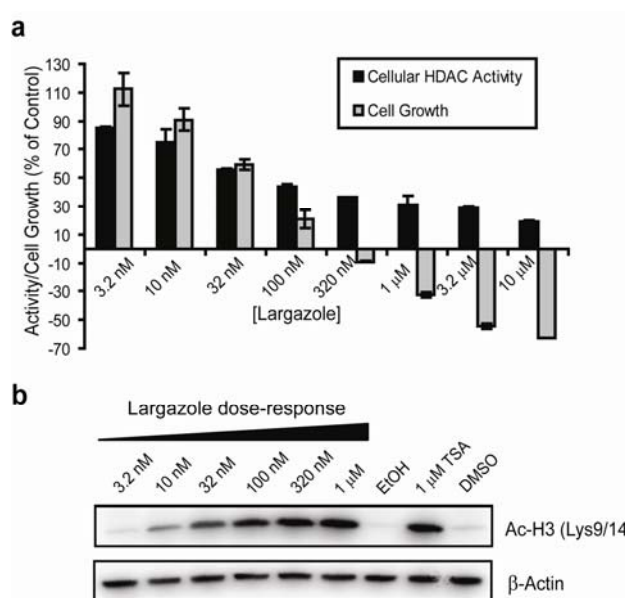


Figure 2.11 Structural similarity between FK228 and largazole (**2.1**) and modes of activation.

To test the hypothesis that largazole inhibits HDACs, we determined the cellular HDAC activity upon treatment with largazole in HCT-116 cells found to possess high intrinsic HDAC activity. We co-incubated a cell-permeable fluorogenic artificial HDAC substrate (*fluor de Lys*TM, BIOMOL) and largazole (**2.1**) and determined that largazole treatment for 8 h resulted in a decrease of HDAC activity in a dose-response manner (**Figure 2.12a**) and, importantly, the IC₅₀ for HDAC inhibition closely corresponded with the GI₅₀ of largazole in this cell line (**Figure 2.12a, Table 2.3**). This correlation suggested that HDAC is the relevant target responsible for largazole's antiproliferative effect.

Confirmatory, immunoblot analysis of an endogenous HDAC substrate, acetylated histone H3, revealed the same dose-response relationship (Figure 2.12b).*



(a) Largazole (**2.1**) inhibits cellular HDAC activity in HCT-116 cells (8 h) based on deacetylation of a fluorogenic substrate (BIOMOL). Growth-inhibitory activity (48 h) is similar. (b) Immunoblot analysis showing inhibition of endogenous histone H3 deacetylation in a dose-response fashion (8 h). Trichostatin A (TSA) was used as a positive control.

Figure 2.12 Target identification

Largazole (**2.1**) inhibited HDAC activity from a HeLa cell nuclear protein extract rich in class I HDACs 1, 2, and 3 (BIOMOL); however, it is possible that the thioester is cleaved under assay conditions. To substantiate the hypothesis that the thiol analog **2.20** is the reactive species, we liberated **2.20** from largazole (**2.1**) or the acetyl analog **2.15**

* Assay results all through this chapter from our collaborators-Kanchan Taori, Yanxia Liu and Prof. Hendrik Luesch

(Scheme 2.7) and measured enzymatic activity directly; compound **2.20** inhibited the HDACs in the nuclear extract of HeLa cells with a similar IC₅₀ value (Table 2.3). Largazole (**2.1**) and the thiol analog **2.20** exhibited similar cellular activity against HDACs derived from nuclear HeLa extracts as well as antiproliferative activity. We presume that nature engineered the biosynthesis of the protected form rather than the target-reactive metabolite itself to increase stability and avoid potential oxidation.

Table 2.3 IC₅₀ and GI₅₀ Values for HDACs and growth inhibition (nM)

	HCT-116 growth inhibition (GI ₅₀)	HCT-116 HDAC cellular assay (IC ₅₀)	HeLa nuclear extract HDACs (IC ₅₀)
2.1	44 ± 10	51 ± 3	37 ± 11
2.15	33 ± 2	50 ± 18	52 ± 27
2.20	38 ± 5	209 ± 15	42 ± 29
2.3	>10,000	>10,000	>10,000
2.19	>10,000	>10,000	>10,000

HDACs are grouped into four major classes. While class III enzymes require NAD⁺ as a cofactor, enzymes of class I, II, and of the more recently discovered class IV are Zn²⁺-dependent enzymes.⁷⁸ The activity of thiols related to largazole derivative **20** against Zn²⁺-dependent HDACs has been attributed to their ability to chelate to Zn²⁺.²²

Particularly, class I HDACs are critical in controlling proliferation in mammalian cells.⁷⁹ HDAC1 and 3 (both class I) overexpression has been observed in prostate and colon tumors, respectively,⁸⁰ while inhibition of certain class II HDACs may cause cardiac hypertrophy.⁸¹ Consequently, the selective inhibition of class I enzymes is desirable in anticancer drug discovery. To establish a preliminary selectivity profile, we tested largazole (**2.1**) and **2.20** against recombinant HDAC1 and HDAC6, representing class I and class II enzymes, respectively (Table 2.4). Compound **2.20** inhibited HDAC1 activity at low nanomolar concentrations and 150-fold less active against HDAC6. This strong class I selectivity had also been observed for FK228; conversely, the hydroxamic acids SAHA and trichostatin A are less discriminatory (Table 2.4).⁸² Furthermore, largazole (**2.1**) was 10- to 15-fold less active against both enzymes than **2.20**, indicating that hydrolysis did not as readily occur under assay conditions with the purified enzyme compared with HeLa nuclear extract, further supporting the hypothesis that largazole (**2.1**) is a prodrug and **2.20** is the reactive metabolite.

Table 2.4 IC₅₀ Values for HDAC1 and HDAC6 inhibition (nM)

Compound	HDAC1 (class I)	HDAC6 (class II)
largazole (2.1)	25 ± 11	5,700 ± 3,600
thiol 2.20	2.5 ± 1.4	380 ± 76
trichostatin A	4.9 ± 0.8	18 ± 12

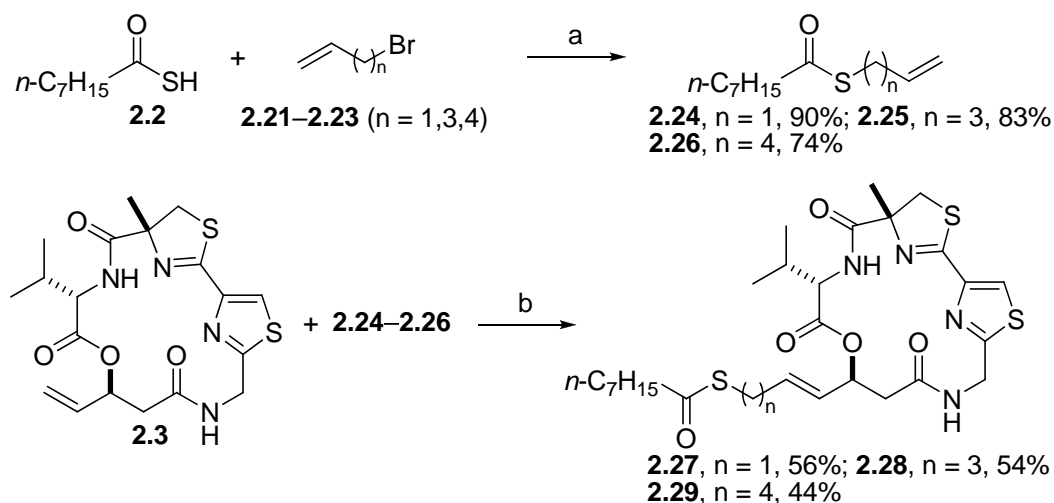
2.2.5.2 Structure–Activity relationship (SAR)

Initial SAR studies further defined the pharmacophore of largazole. The acetyl analog **2.15** showed the same activity as largazole (**2.1**) in the cellular HDAC assay and the same antiproliferative activity, underscoring that the carboxylic acid portion of the thioester merely plays a transient protective role and can be varied as long as thioester hydrolysis is achieved. To further define the pharmacophore we tested key analogues of **2.1** with modified side chain functionality. Since hydroxyl groups do not chelate to Zn^{2+} , the hydroxyl analog **2.19** was expectedly not an HDAC inhibitor, paralleling its lack of growth-inhibitory activity (Table 2.3). Additionally, the macrocycle **2.3**, which lacks the sulfur-containing aliphatic chain, also lacks any inhibitory activity in the HDAC as well as cell viability assay (Table 2.3), highlighting that the thiol group is indispensable for both activities. The correlation of HDAC inhibitory activity and antiproliferative effect for all key compounds synthesized indicates that both activities are closely related and that the growth inhibition is a functional consequence of HDAC inhibition.

In addition to define that thiol group is warhead and largazole **2.1** exhibits a pronounced selectivity for HDAC class I inhibition which is desirable for anticancer drug development, structural requirements for its HDAC inhibitory and antiproliferative activities have been characterized by structure-activity relationship (SAR) study of other analogues of **2.1**, which focuses on two areas: 1) the length of thioester side chain; 2) the modification of 16-membered macrocycle.

As shown in [Scheme 2.8](#), three-, five-, and six-atom linkers (**2.24–2.26**) were synthesized by coupling the thioacid (**2.14**)⁷² to 3-bromo-1-propene, 5-bromo-1-pentene,

and 6-bromo-1-hexene, respectively (NaH, THF, 25 °C, 5–36 h, 74–90 %). Subjecting the 16-membered macrocycle **2.3** and **2.24**, **2.25**, and **2.26** respectively to Grubbs' second-generation catalyst (50 mol %, toluene, reflux, 4 h) smoothly provided **2.27**, **2.28**, and **2.29** in 44%–56%.

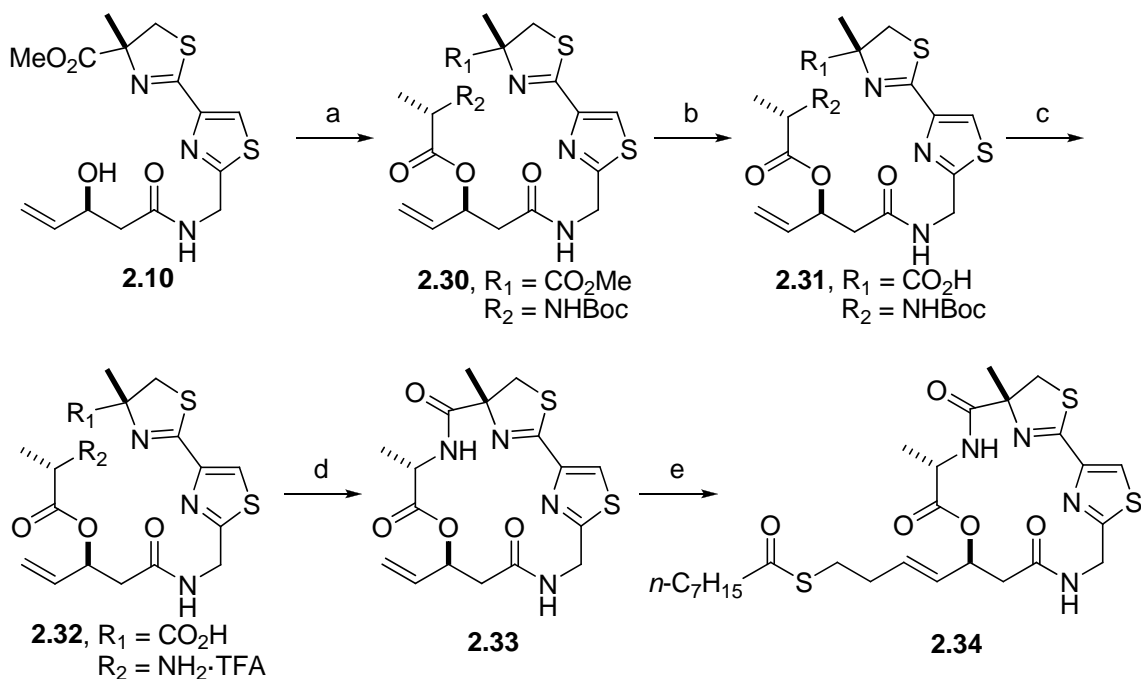


Reactions and conditions: (a) NaH, THF, 25 °C, 5–36 h, 74–90%; (b) Grubbs' 2nd-generation catalyst (50 mol %), toluene, reflux, 4 h, 44–56%.

Scheme 2.8 Synthesis of thioester and side chain analogues

To evaluate the comparative significance of side-chain functionality of valine in macrocycle, the valine residue of **2.1** was replaced with alanine (i.e., alanine scanning)⁸³ to prepare **2.34** (Scheme 2.9). Since alanine is conformationally similar with valine, we anticipated that the synthesis of **2.34** would smoothly proceed following the previously reported procedures.⁵⁵ Briefly, Yamaguchi esterification reaction of **2.10** and *N*-Boc-L-alanine (2,4,6-trichlorobenzoyl chloride, Et₃N, THF, 0 °C, 1 h; then DMAP, 25 °C, 10 h)

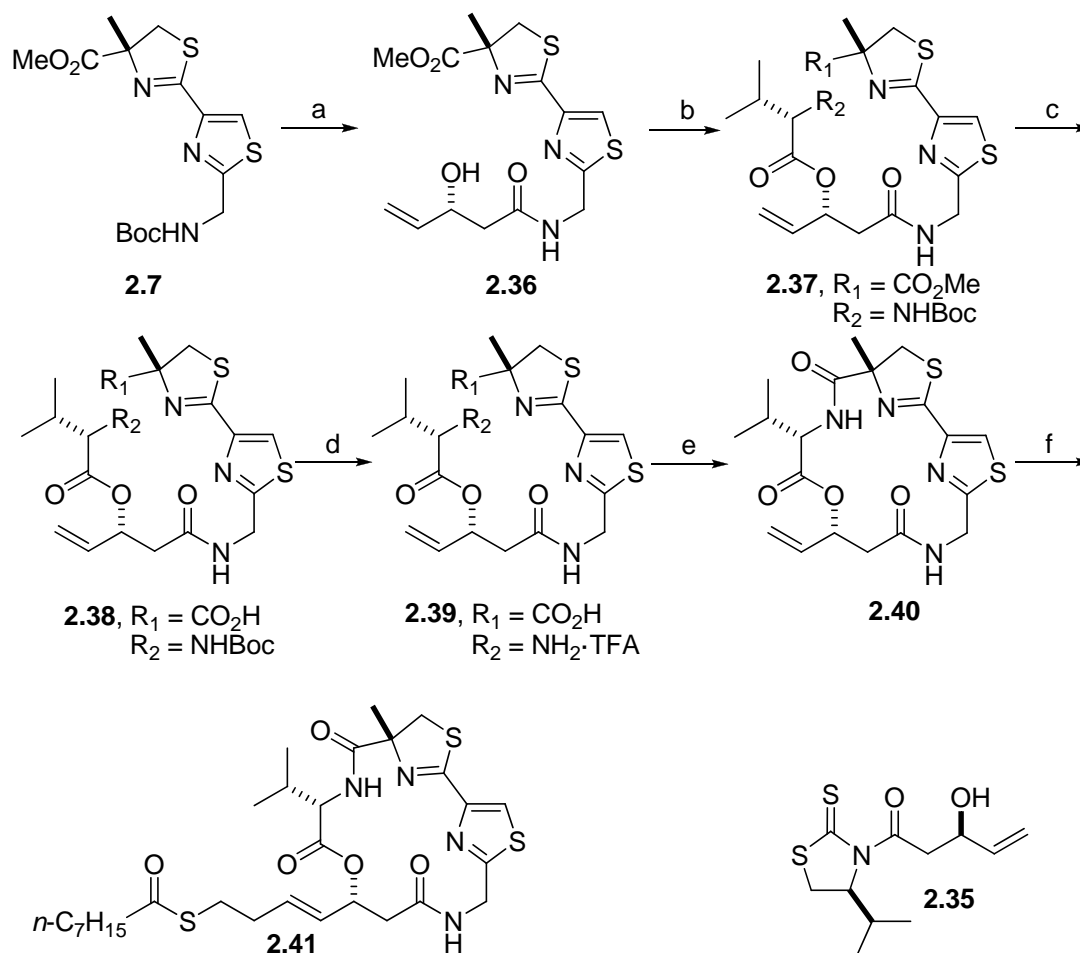
afforded the linear depsipeptide **2.30** in 99%. Hydrolysis of **2.30** under basic conditions (0.1 N LiOH, THF, H₂O, 0 °C, 1 h) to provide the carboxylic acid **2.31** and subsequent removal of *N*-Boc group in **2.31** (TFA, CH₂Cl₂, 25 °C, 2 h) provided **2.32**, a precursor to the 16-membered cyclic depsipeptide core **2.33**. Without further purification of **2.32**, macrocyclization reaction of the crude **2.32** utilizing HATU–HOAt (HATU, HOAt, *i*-Pr₂NEt, DMF, 25 °C, 24 h) proceeded smoothly to give **2.33** in 81% (for two steps).⁸⁴ Olefin cross-metathesis reaction of the macrocycle **2.33** and the thioester **2.2** in the presence of Grubbs' second-generation catalyst (50 mol %, toluene, reflux, 4 h) provided **2.34** in 61% (*E*-isomer only).



Reagents and conditions: (a) *N*-Boc-L-alanine, 2,4,6-Cl₃C₆H₂COCl, Et₃N, THF, 0 °C, 1 h; then DMAP, THF, 25 °C, 10 h, 99% for 2 steps; (b) 0.1 N LiOH, THF/H₂O (4:1), 0 °C, 1 h, 79%; (c) TFA/CH₂Cl₂ (1:5), 25 °C, 2 h; (d) HATU, *i*-Pr₂NEt, HOAt, DMF, 25 °C, 24 h, 81% for 2 steps; (e) **2.2**, Grubbs' 2nd-generation, catalyst (50 mol %), toluene, reflux, 4 h, 61%.

Scheme 2.9 Synthesis of alanine analogue

In addition to the alanine analogue **2.34**, we prepared the C17-epimer analogue **2.41** to study the effect of the configuration at C17 position on HDAC inhibitory activity. As described in our previous total synthesis of largazole,² Nagao's aldol reaction provided a 3:1 diastereomeric mixture of (3*S*)- and (3*R*)-hydroxy-carboxylic acid.¹³ We incorporated (3*R*)-hydroxy-carboxylic acid (**2.35**, the minor aldol adduct) in the macrolactone backbone to prepare the C17-epimer analogue **2.41** shown in [Scheme 2.10](#).



Reagents and conditions: (a) TFA/CH₂Cl₂ (1:5), 25 °C, 1 h; then **2.35**, DMAP, CH₂Cl₂ 25 °C, 2 h, 87% for 2 steps; (b) *N*-Boc-L-valine, 2,4,6-Cl₃C₆H₂COCl, Et₃N, THF, 0 °C, 1 h, then DMAP, THF, 25 °C, 10 h, 85%; (c) 0.5 N LiOH, THF/H₂O (4:1), 0 °C, 2 h; (d) TFA/CH₂Cl₂ (1:5), 25 °C, 2 h; (e) HATU, *i*-Pr₂NEt, HOAt, CH₂Cl₂, 25 °C, 13 h, 73% for 3 steps; (f) **2.2**, Grubbs' 2nd-generation catalyst (50 mol %), toluene, reflux, 4 h 33% (55% BRSM).

Scheme 2.10 Synthesis of C17-epimer analogue

After completing the synthesis of **2.27–2.29**, **2.34**, and **2.41**, we assessed their antiproliferative activity against HCT-116 colon cancer cells and HDAC inhibitory activity using HeLa nuclear extract as the enzyme source side-by-side with largazole (**1**).

Homologation to five-atom and six-atom linkers in **2.28** and **2.29**, respectively, reduced the cell growth and HDAC inhibitory activity by several orders of magnitude (Table 2.5), while chain shortening of the linker by one methylene group (compound **2.27**) completely abolished activity up to 20 μM . This result suggests that a four-atom chain length between the acyloxy methine (C17) and the side-chain sulfur atom, as found in **2.1**, is optimal for HDAC inhibitory activity.

The valine residue is expected to interact with the rim region of HDACs and this interaction could be a determinant of the HDAC class/isoform specificity of **2.1**. Compound **2.34** showed only approximately 2- to 3-fold decreased activity in both assays compared with **2.1**, suggesting that the valine residue is largely replaceable (Table 2.5). Largazole C17-epimer **3.41** lacked significant HDAC activity at 20 μM and only weakly inhibited HCT-116 cell growth with >500-fold reduced activity compared with **2.1** (Table 2.5). We then subjected protein extracts derived from HCT-116 cells, which had been treated for 8 h with (at least marginally active) largazole analogues, to immunoblot analysis of acetylated histone H3, an endogenous HDAC substrate (Figure 2.13). Dose–response analysis indicated that the inhibition of histone H3 deacetylation correlated with the GI_{50} values in the cell viability assay (Table 2.5).

Table 2.5 Cancer cell growth and HDAC inhibition (GI_{50} and IC_{50} in nM)

compound	HCT-116 growth inhibition (GI_{50})	HeLa nuclear extract HDACs (IC_{50}) ¹⁴
2.1	6.8 \pm 0.6	32 \pm 13

2.27	>10000	>20000
2.28	620 ± 50	7600 ± 900
2.29	2500 ± 600	4100 ± 430
2.34	21 ± 2	72 ± 21
2.41	3900 ± 450	>20000

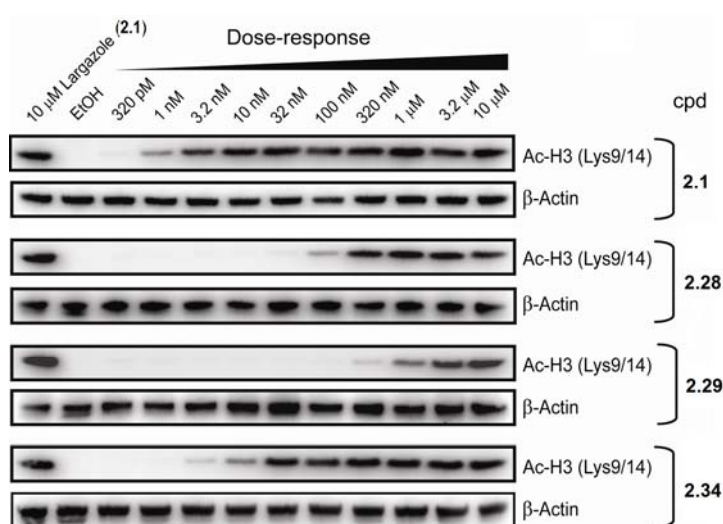


Figure 2.13 Immunoblot analysis showing various degrees of inhibition of histone H3 deacetylation by largazole analogues in HCT-116 cells upon 8 h of treatment (β -actin = control).

To determine if the structural modifications also affected the selectivity for HDAC1 versus HDAC6,⁵⁵ we profiled **2.28**, **2.29**, and **2.34** against the recombinant human HDAC1 and HDAC6 (Table 2.6). All compounds showed a similar decrease in HDAC1 inhibitory activity as in antiproliferative activity compared with **2.1**. Although the Val→Ala change reduced the discriminatory power of the macrocycle by 3-fold, **3.34** exhibited strong selectivity for HDAC1 over HDAC6.

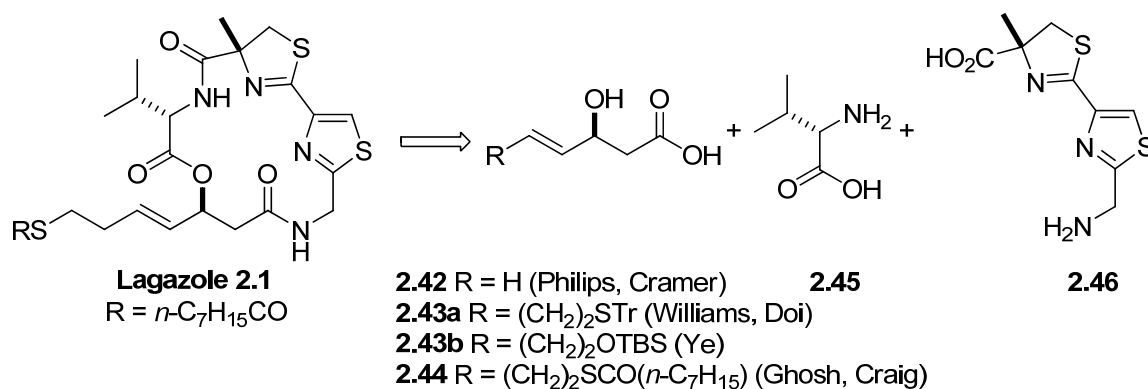
Table 2.6 IC₅₀ Values for HDAC1 and HDAC6 inhibition (nM)

compound	HDAC1 (class I)	HDAC6 (class II)
2.1 ^a	7.6	1800
2.28	690	> 10000
2.29	1900	> 10000
2.34	44	3300
trichostatin A ^b	5.2	1.8

^a Under the same assay conditions, the pure thiol analogue of largazole exhibited IC₅₀ values of 0.77 nM and 510 nM for HDAC1 and HDAC6, respectively. ^b Standard and non-selective HDAC inhibitor.

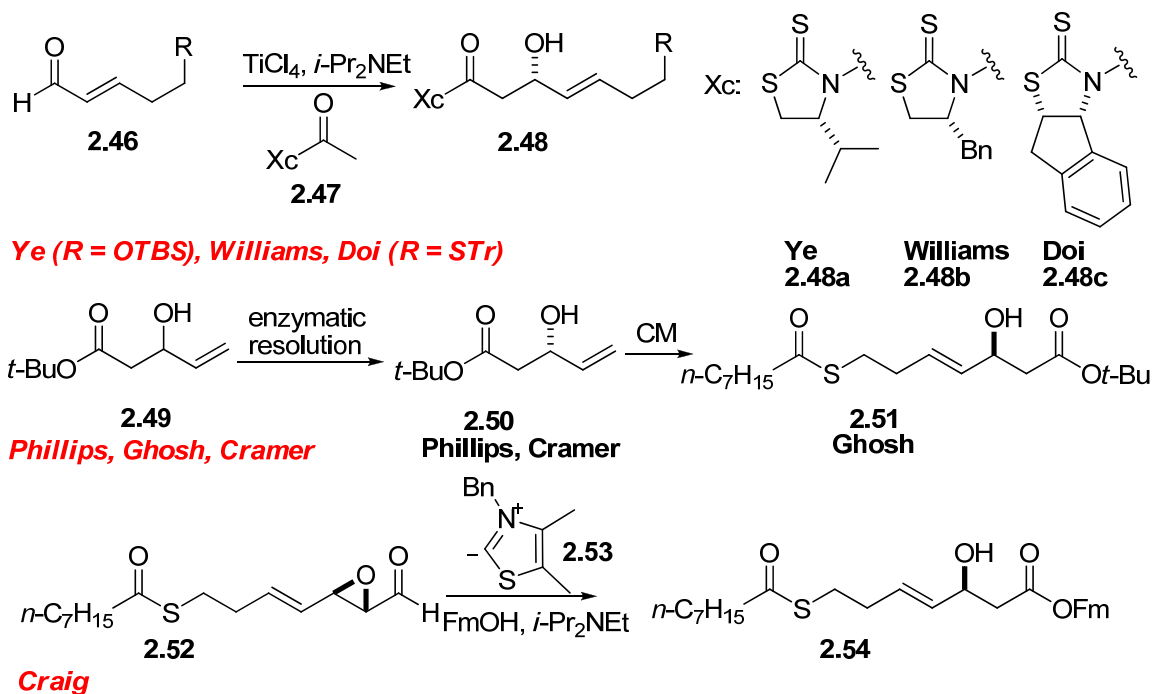
2.2.6 Other Total Syntheses of Largazole

After we finished the first total synthesis of largazole, seven total syntheses of largazole came out in less than one year due to its unprecedented biological activity and promising selectivity.⁸⁵ Distinctive features among those total syntheses involved the installation of thioester and macrocyclization steps as well as the methodology of preparing β -hydroxy acid unit. From retrosynthetic strategies they employed (**Scheme 2.11**), the first difference was how to install the thioester bond, which was assembled in the early stage or late stage. The fashion of the installation of thiol-containing zinc-binding side arm directly affected the formation of linear depsipeptides for macrocyclization.



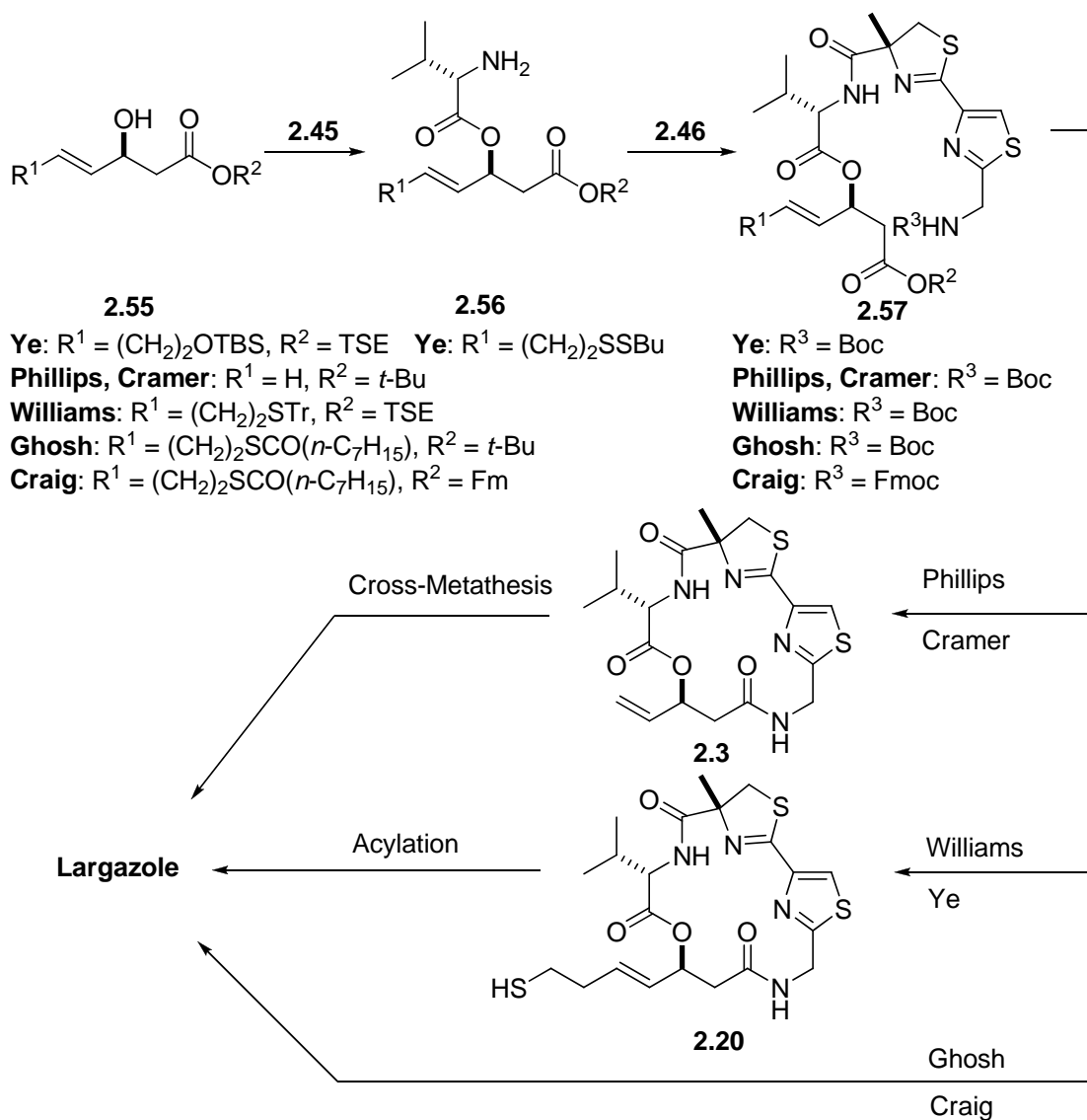
Scheme 2.11 Retrosynthetic strategies towards largazole

Initially, numerous synthetic strategies or separation approaches have been used for the formation of the β-hydroxy acid fragment (**Scheme 2.12**). Ye, Williams and Doi used asymmetric acetate aldol reactions developed by Crimmins to synthesize the β-hydroxy acid fragment that was used by Ganesan for their synthesis of spiruchostatin A even though they employed the different chiral auxiliaries, while Phillips, Ghosh and Cramer utilized an enzymatic resolution of racemic compound **2.49**. Craig employed the NHC-mediated esterification reaction using α, β-epoxy aldehyde to produce the β-hydroxy acid fragment.

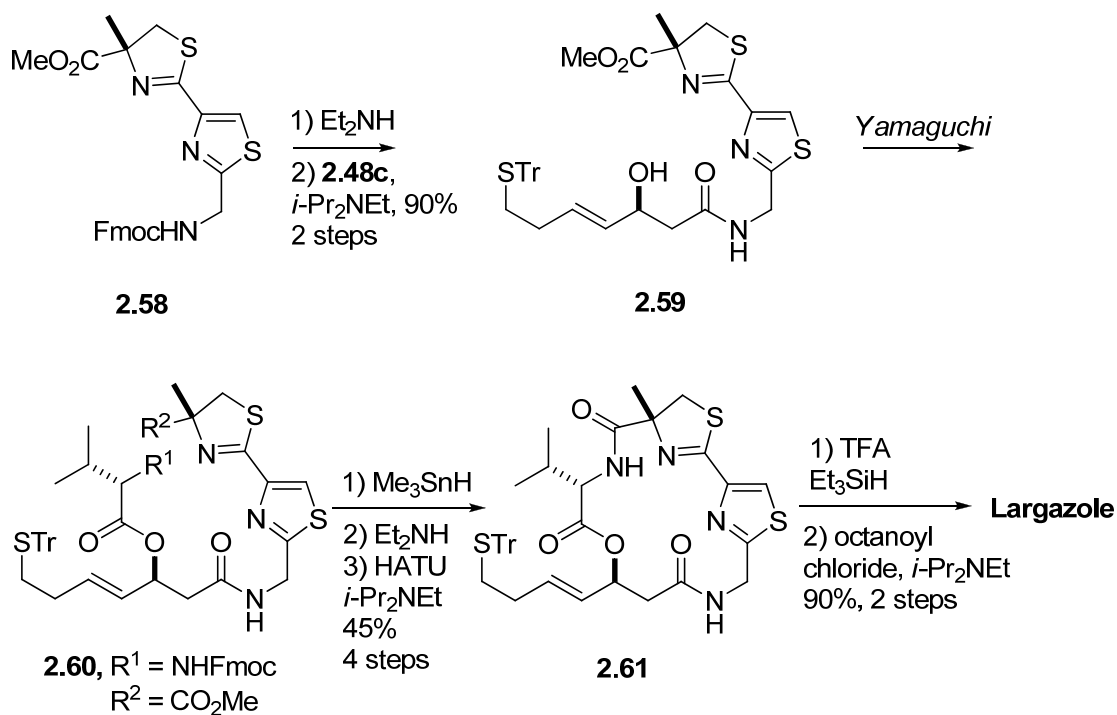


Scheme 2.12 Approaches to β -hydroxy acid unit

The most challenging part is final macrocyclization step. It is noteworthy that macrolactonization to afford the 16-membered macrocycle is not successful with all attempts by several groups including Williams, Craig and Hong group. Therefore, based on ring-closing positions in which macrolactamization step occurs, their syntheses are categorized into down-amide bond formation route which Phillips, Cramer, Williams, Ye and Craig used (Scheme 2.13) and up-amide bond formation route which Doi utilized as we did (Scheme 2.14).

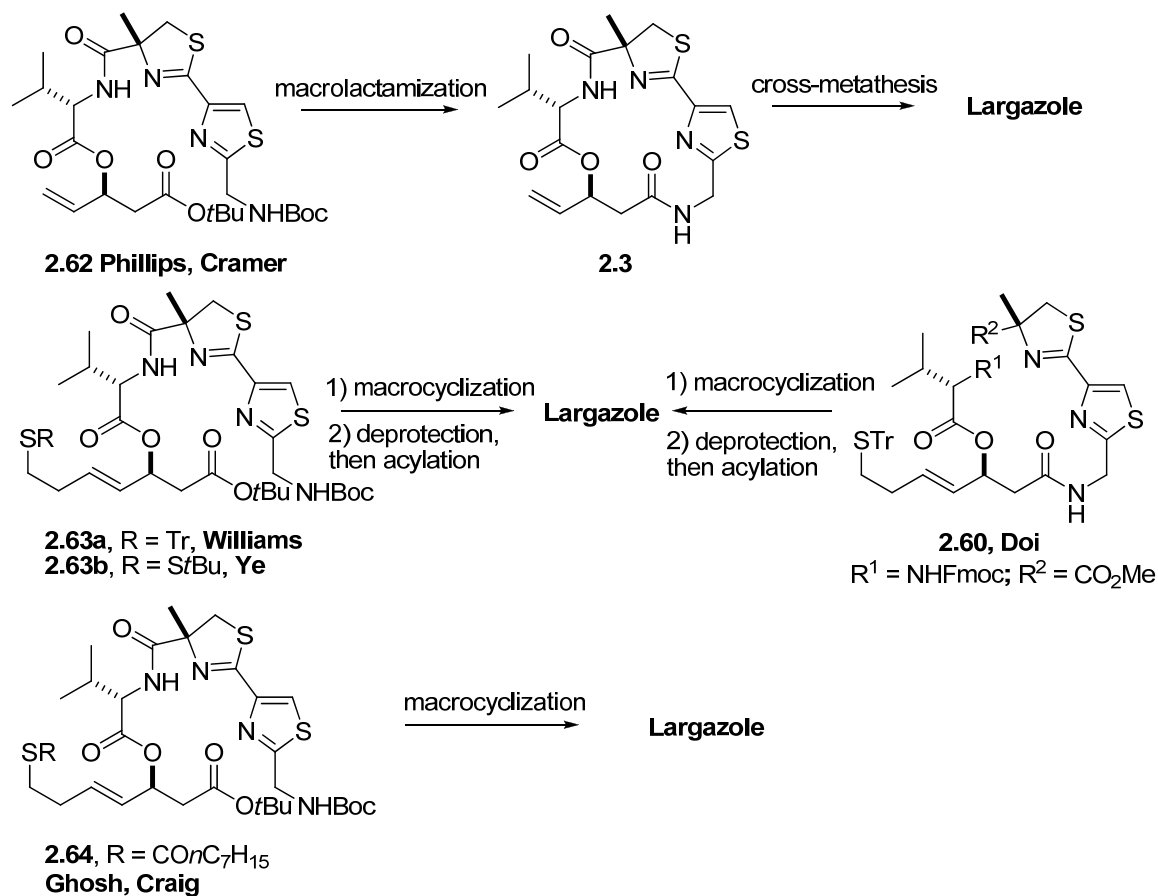


Scheme 2.13 Approaches to largazole by down-amide bond formation



Scheme 2.14 Approaches to largazole by up-amide bond formation

Several of those syntheses converge upon similar or even identical intermediates after macrocyclization. Depending on the installation of thioester bond in early or late stage, and the macrocycles they had generated, those seven total syntheses are divided into three categories as shown in **Scheme 2.15**: 1) the use of cross-metathesis to install the thioester from same macrocycle **2.3** (Phillips and Cramer); 2) the use of deprotection of Trt- or *St*Bu-thiol followed by acylation process (Ye, Williams and Doi); 3) construct of acyclic precursor with thioester fragment before macrocyclization (Ghosh and Craig).



Scheme 2.15 Summary of total syntheses of largazole

2.3 Conclusion

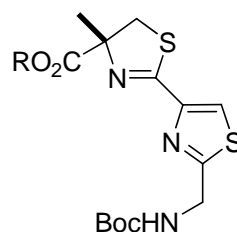
In summary, we have devised a concise and convergent synthesis of largazole that is amenable to the synthesis of key analogs. We provided evidence that HDAC is the molecular target of largazole responsible for its antiproliferative activity. HDACs are validated targets for anticancer therapy; first-in-class Zolinza (Merck) and FK228 were recently approved for the treatment of cutaneous T-cell lymphoma, and various other HDAC inhibitors are in advanced clinical trials.^{22,78} Largazole (**2.1**) is class I HDAC

selective, suggesting that it may be a valuable addition to armory against certain types of cancers. Preliminary SAR studies suggest that thiol group generated by hydrolysis of the thioester moiety is the warhead and is critical for its HDAC inhibitory and antiproliferative activity.

Furthermore, a series of largazole analogues (**2.27–2.29**, **2.34**, and **3.41**) was prepared and tested for HDAC inhibitory activity which correlated with their ability to inhibit cancer cell growth. The biological evaluation of the analogues suggested that the four-atom linker between the macrocycle and the octanoyl group in the side chain and the (*S*)-configuration at C17-position are critical to potent HDAC inhibitory activity of **2.1**. In contrast, the valine residue in the macrocycle can be replaced with alanine without compromising activity to a large extent. These SAR results would provide insights into structural requirements for HDAC inhibitory activity including the observed HDAC selectivity of largazole (**2.1**) and help in the design of isoform-specific HDAC inhibitors based on **2.1**. Further biological studies with largazole-based inhibitors are currently underway to assess the chemotherapeutic potential.

2.4 Experimental sections

Thiazole-methylthiazoline methyl ester **2.7**

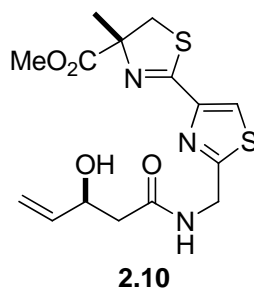


2.7, R = Me
2.65, R = Et

To a solution of cyanothiazole **2.8** (500 mg, 2.09 mmol) in EtOH (15 mL, 0.15 M) were added Et₃N (1.35 mL, 10.0 mmol) and (*R*)-2-methyl cysteine methyl ester hydrochloride (741 mg, 3.98 mmol). After being stirred at 50 °C for 72 h, the reaction mixture was concentrated and diluted with H₂O and CH₂Cl₂. The layers were separated, and the aqueous layer was extracted with CH₂Cl₂. The combined organic layers were washed with brine, dried over anhydrous Na₂SO₄, and concentrated *in vacuo*. The residue was purified by column chromatography (silica gel; hexanes/EtOAc, 2/1 to 1/1) to afford **2.7** as a pale yellow oil (394 mg, 51%) and **2.65** as a pale yellow oil (123 mg, 15%): [For methyl ester **7**]: R_f 0.45 (hexanes/EtOAc, 1/1); [α]^{25.2}_D = -10.8 (*c* 0.85, CHCl₃); ¹H NMR (400 MHz, CDCl₃) δ 7.92 (s, 1 H), 5.36 (brs, 1 H), 4.61 (d, *J* = 6.4 Hz, 2 H), 3.85 (d, *J* = 11.6 Hz, 1 H), 3.78 (s, 3 H), 3.25 (d, *J* = 11.2 Hz, 1 H), 1.62 (s, 3 H), 1.44 (s, 9 H); ¹³C NMR (100 MHz, CDCl₃) δ 173.6, 169.5, 162.8, 155.6, 148.5, 121.7, 84.5, 80.3, 52.8, 42.2, 41.4, 28.2, 23.9; IR (neat) 3336, 2976, 1712, 1603, 1515, 1453, 1366, 1278, 1246, 1161, 1118, 1019 cm⁻¹; HRMS (FAB) found 372.1051 [calcd for C₁₅H₂₂N₃O₄S₂ (M+H)⁺

372.1052]. [For ethyl ester **2.65**]: R_f 0.50 (hexanes/EtOAc, 1/1); $[\alpha]^{26.2}_D = -13.9$ (c 1.00, CHCl_3); $^1\text{H NMR}$ (400 MHz, CDCl_3) δ 7.89 (s, 1 H), 5.47 (brs, 1 H), 4.58 (d, $J = 6.0$ Hz, 2 H), 4.20 (ddd, $J = 7.2, 7.2, 7.2$ Hz, 2 H), 3.82 (d, $J = 11.6$ Hz, 1 H), 3.21 (d, $J = 11.2$ Hz, 1 H), 1.59 (s, 3 H), 1.41 (s, 9 H), 1.25 (dd, $J = 7.2, 7.2$ Hz, 1 H); $^{13}\text{C NMR}$ (100 MHz, CDCl_3) δ 172.9, 169.5, 162.5, 155.5, 148.4, 121.5, 84.4, 80.2, 61.7, 42.2, 41.3, 28.2, 23.7, 14.0; IR (neat) 3354, 2978, 2933, 1717, 1653, 1521, 1367, 1279, 1248, 1167, 1019 cm^{-1} ; HRMS (FAB) found 386.1219 [calcd for $\text{C}_{16}\text{H}_{243}\text{N}_3\text{O}_4\text{S}_2$ ($\text{M}+\text{H}$) $^+$ 386.1208].

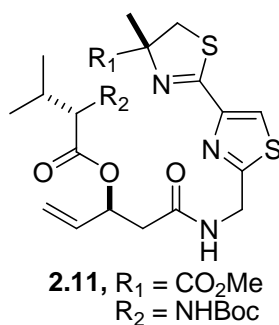
Amide **2.10**



Compound **2.7** (63 mg, 0.17 mmol) was treated with TFA/ CH_2Cl_2 (1:2, 1.0 ml) at room temperature. The resulting mixture was stirred at the same temperature for 1 h, and then purged by N_2 to remove TFA and CH_2Cl_2 . The residue was washed with Et_2O four times to remove remaining TFA. This crude TFA·amine salt **2.9** was carried to the next step without further purification. To a solution of TFA·amine salt **2.9** in CH_2Cl_2 was added DMAP (62 mg, 0.51 mmol), followed by **2.6** (44 mg, 0.17 mmol). The reaction mixture was stirred for 1 h at room temperature, quenched with 0.1 N HCl. The layers

were separated, and the aqueous layer was extracted with EtOAc. The combined organic layers were washed with brine, dried over anhydrous Na₂SO₄, and concentrated *in vacuo*. The residue was purified by column chromatography (silica gel; hexanes/EtOAc/CH₃OH, 15/15/1 to 10/10/1) to afford **2.10** as a colorless oil (59 mg, 94%): [For **2.9**]: ¹H NMR (400 MHz, CD₃OD) δ 8.34 (s, 1 H), 4.54 (s, 2 H), 3.91 (d, *J* = 11.2 Hz, 1 H), 3.80 (s, 3 H), 3.39 (d, *J* = 11.6 Hz, 1 H), 1.62 (s, 3 H); HRMS (FAB) found 272.0531 [calcd for C₁₀H₁₄N₃O₂S₂ (M+H)⁺ 272.0527]. [For **2.10**]: R_f 0.40 (hexanes/EtOAc/CH₃OH, 10/10/1); [α]^{26.3}_D = -17.3 (*c* 1.00, CHCl₃); ¹H NMR (400 MHz, CDCl₃) δ 7.88 (s, 1 H), 7.44 (dd, *J* = 6.0, 6.0 Hz, 1 H), 5.82 (ddd, *J* = 16.8, 10.8, 5.6 Hz, 1 H), 5.24 (d, *J* = 16.8 Hz, 1 H), 5.07 (d, *J* = 10.8 Hz, 1 H), 4.67 (d, *J* = 6.0 Hz, 2 H), 4.47–4.54 (m, 1 H), 3.96 (d, *J* = 4.4 Hz, 1 H), 3.82 (d, *J* = 11.6 Hz, 1 H), 3.75 (s, 3 H), 3.23 (d, *J* = 11.6 Hz, 1 H), 2.49 (dd, *J* = 15.2, 3.6 Hz, 1 H), 2.40 (dd, *J* = 15.2, 8.4 Hz, 1 H), 1.59 (s, 3 H); ¹³C NMR (100 MHz, CDCl₃) δ 173.5, 171.9, 168.0, 162.7, 148.0, 139.0, 122.2, 115.2, 84.3, 69.2, 52.8, 42.4, 41.3, 40.7, 23.8; IR (neat) 3293, 3083, 2981, 2951, 1733, 1651, 1602, 1537, 1435, 1287, 1237, 1120 cm⁻¹; HRMS (FAB) found 370.0901 [calcd for C₁₅H₂₀N₃O₄S₂ (M+H)⁺ 370.0895].

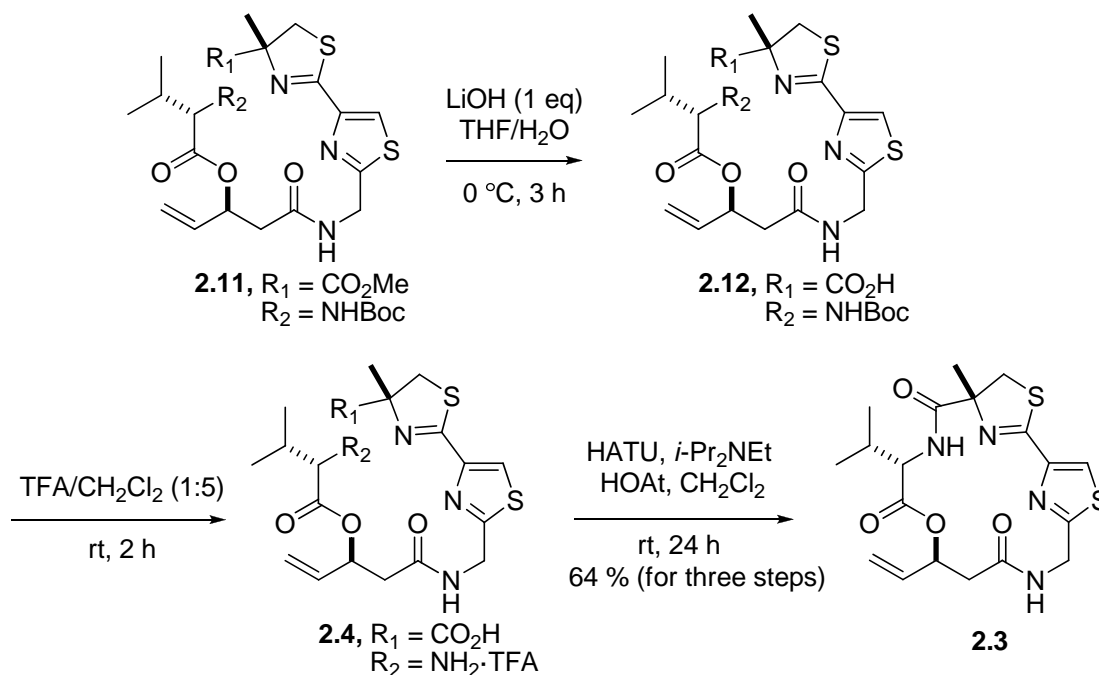
Ester **2.11**



To a stirred solution of *N*-Boc-L-valine (**2.5**) (445 mg, 2.05 mmol) and Et₃N (0.32 mL, 2.34 mmol) in THF (20.0 mL, 0.10 M) was added 2,4,6-trichlorobenzoyl chloride at 0 °C. After being stirred at the same temperature for 1 h, to the resulting mixture were added a solution of **2.10** (540 mg, 1.46 mmol) and DMAP (211 mg, 1.73 mmol). After being stirred at room temperature for 10 h, the reaction mixture was quenched with half-saturated aqueous NH₄Cl solution and diluted with EtOAc. The layers were separated, and the aqueous layer was extracted with EtOAc. The combined organic layers were washed with brine, dried over anhydrous Na₂SO₄, and concentrated *in vacuo*. The residue was purified by column chromatography (silica gel, hexanes/EtOAc/CH₃OH, 10/10/1) to afford **2.11** as a colorless oil (828 mg, 99%): R_f 0.50 (hexanes/EtOAc/CH₃OH, 10/10/1); [α]_D^{26.7} = +3.43 (*c* 1.46, CHCl₃); ¹H NMR (400 MHz, CDCl₃) δ 7.90 (s, 1 H), 7.31 (dd, *J* = 5.6, 5.6 Hz, 1 H), 5.87 (ddd, *J* = 16.8, 11.6, 6.4 Hz, 1 H), 5.63–5.67 (m, 1 H), 5.33 (d, *J* = 16.8 Hz, 1 H), 5.22 (d, *J* = 11.6 Hz, 1 H), 5.01 (d, *J* = 7.6 Hz, 1 H), 4.76 (dd, *J* = 16.4, 6.0 Hz, 1 H), 4.70 (dd, *J* = 16.0, 6.0 Hz, 1 H), 3.96 (dd, *J* = 8.0, 6.4 Hz, 1 H), 3.84 (d, *J* = 11.2 Hz, 1 H), 3.77 (s, 3 H), 3.24 (d, *J* = 11.6 Hz, 1 H), 2.67 (dd, *J* = 14.4, 5.2 Hz, 1 H), 2.61 (dd, *J* = 14.4, 6.0 Hz, 1 H), 1.96–2.06 (m, 1 H), 1.61 (s, 3 H), 1.37 (s, 9 H),

0.92 (d, $J = 6.8$ Hz, 3 H), 0.89 (d, $J = 7.2$ Hz, 3 H); ^{13}C NMR (100 MHz, CDCl_3) δ 173.6, 171.6, 169.0, 168.7, 162.8, 155.9, 148.2, 134.1, 122.0, 118.2, 118.2, 84.4, 72.1, 59.4, 52.9, 41.4, 41.1, 30.5, 28.2, 23.9, 19.0, 18.0; IR (neat) 3726, 3709, 3628, 3325, 2972, 1735, 1716, 1605, 1507, 1367, 1243, 1159, 1120 cm^{-1} ; HRMS (FAB) found 569.2108 [calcd for $\text{C}_{25}\text{H}_{37}\text{N}_4\text{O}_7\text{S}_2$ ($\text{M}+\text{H}$) $^+$ 569.2104].

Macrocycle 2.3

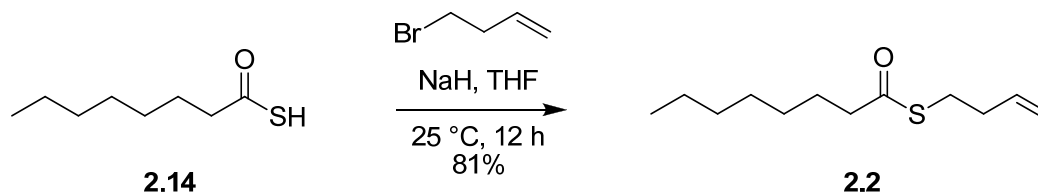


To a stirred solution of **2.11** (185 mg, 0.325 mmol) in $\text{THF}/\text{H}_2\text{O}$ (4:1, 10 mL) was added dropwise 0.5 N LiOH (0.65 mL, 0.325 mmol) at $0\text{ }^\circ\text{C}$. After being stirred at $0\text{ }^\circ\text{C}$ for 3 h, the resulting mixture was acidified with 1 M KHSO_4 solution to pH ~ 3.0 , and diluted with EtOAc . The layers were separated, and the aqueous layer was extracted with EtOAc . The combined organic layers were washed with brine, dried over anhydrous

Na₂SO₄, and concentrated *in vacuo*. This crude carboxylic acid **2.12** was carried to the next step without further purification. The carboxylic acid **2.12** was treated with TFA/CH₂Cl₂ (1:5, 5 mL). After being stirred at room temperature for 2 h, the residue was purged by N₂ to remove TFA and CH₂Cl₂, then washed with Et₂O four times to remove remaining TFA. To a solution of the crude **2.4** in CH₂Cl₂ (325 mL, 1 mM) was added HATU (247 mg, 0.65 mmol), HOAt (88 mg, 0.65 mmol), and *i*-Pr₂NEt (0.24 mL, 1.30 mmol). The reaction mixture was stirred at room temperature for 24 h and then concentrated *in vacuo*. The residue was diluted with H₂O and EtOAc. The layers were separated, and the aqueous layer was extracted with EtOAc. The combined organic layers were washed with brine, dried over anhydrous Na₂SO₄, and concentrated *in vacuo*. The residue was purified by column chromatography (silica gel, hexanes/EtOAc/CH₃OH, 10/10/1) to afford **2.3** as a white crystal. [For crude **2.12**]: NMR (400 MHz, CD₃OD) δ 8.16 (s, 1 H), 6.82 (d, *J* = 8.8 Hz, 1 H), 5.89 (ddd, *J* = 17.2, 10.8, 6.4 Hz, 1 H), 5.69 (ddd, *J* = 6.4, 6.4, 6.4 Hz, 1 H), 5.33 (d, *J* = 17.2 Hz, 1 H), 5.21 (d, *J* = 10.8 Hz, 1 H), 4.64 (d, *J* = 8.0 Hz, 2 H), 4.00–4.04 (m, 1 H), 3.85 (d, *J* = 11.6 Hz, 1 H), 3.32 (d, *J* = 12.0 Hz, 1 H), 2.69 (dd, *J* = 14.8, 8.4 Hz, 1 H), 2.63 (dd, *J* = 14.8, 5.6 Hz, 1 H), 2.03–2.10 (m, 1 H), 1.59 (s, 3 H), 1.44 (s, 9 H), 0.92 (d, *J* = 6.8 Hz, 3 H), 0.89 (d, *J* = 6.8 Hz, 3 H); HRMS (FAB) found 555.1951 [calcd for C₂₄H₃₅N₄O₇S₂ (M+H)⁺ 555.1947]. [For crude **2.4**]: ¹H NMR (400 MHz, CD₃OD) δ 8.27 (s, 1 H), 5.93 (ddd, *J* = 17.2, 10.4, 7.2 Hz, 1 H), 5.77–5.82 (m, 1 H), 5.42 (d, *J* = 17.2 Hz, 1 H), 5.32 (d, *J* = 10.4 Hz, 1 H), 4.68 (d, *J* = 3.6 Hz, 2 H), 3.92 (d, *J* = 11.6 Hz, 1 H), 3.89 (d, *J* = 4.4 Hz, 1 H), 3.42 (d, *J* = 11.6 Hz, 1 H),

2.76 (dd, $J = 14.4, 8.0$ Hz, 1 H), 2.70 (dd, $J = 14.4, 5.6$ Hz, 1 H), 2.25–2.33 (m, 1 H), 1.66 (s, 3 H), 1.047 (d, $J = 7.2$ Hz, 3 H), 1.044 (d, $J = 7.2$ Hz, 3 H); HRMS (FAB) found 455.1423 [calcd for $C_{19}H_{27}N_4O_5S_2$ (M+H) $^+$ 455.1423]. [For macrocycle **2.3**]: R_f 0.30 (hexanes/EtOAc/CH₃OH, 10/10/1); Mp: 210–211 °C . $[\alpha]^{25.8}_D = +60.2$ (c 1.00, CH₃OH); 1H NMR (400 MHz, CDCl₃) δ 7.75 (s, 1 H), 7.17 (d, $J = 9.2$ Hz, 1 H), 6.49 (dd, $J = 8.8, 2.4$ Hz, 1 H), 5.84 (ddd, $J = 17.6, 10.4, 6.0$ Hz, 1 H), 5.65–5.69 (m, 1 H), 5.34 (d, $J = 17.6$ Hz, 1 H), 5.26 (d, $J = 10.4$ Hz, 1 H), 5.25 (dd, $J = 18.0, 8.4$ Hz, 1 H), 4.60 (dd, $J = 9.6, 3.6$ Hz, 1 H), 4.24 (dd, $J = 17.6, 3.2$ Hz, 1 H), 4.02 (d, $J = 11.2$ Hz, 1 H), 3.25 (d, $J = 11.6$ Hz, 1 H), 2.83 (dd, $J = 16.4, 10.4$ Hz, 1 H), 2.70 (dd, $J = 16.4, 2.8$ Hz, 1 H), 2.05–2.13 (m, 1 H), 1.84 (s, 3 H), 0.67 (d, $J = 6.8$ Hz, 3 H), 0.50 (d, $J = 6.8$ Hz, 3 H); ^{13}C NMR (100 MHz, CDCl₃) δ 173.5, 169.2, 168.8, 167.8, 164.5, 147.4, 134.7, 124.2, 117.8, 84.3, 72.2, 57.6, 43.2, 41.0, 40.0, 34.1, 24.1, 18.8, 16.6; IR (neat) 3364, 2960, 2920, 1710, 1681, 1602, 1515, 1267, 1245 cm^{-1} ; HRMS (FAB) found 437.1308 [calcd for $C_{19}H_{25}N_4O_4S_2$ (M+H) $^+$ 437.1317].

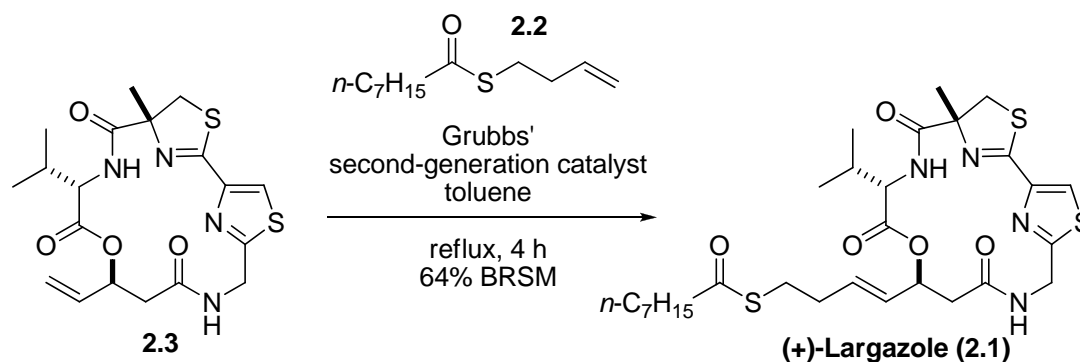
Thioester 2



To a solution of **2.14** (230 mg, 1.44 mmol) in dry THF (10.0 mL, 0.144 M) was added NaH (100 mg, 2.10 mmol) at 25 °C. After stirring at 25 °C for 10 min, 4-bromo-1-

butene (0.21 mL, 2.02 mmol) was added dropwise into the reaction mixture. After stirring at 25 °C for 12 h, the mixture was filtered and concentrated *in vacuo*. The residue was purified by column chromatography (silica gel, hexanes/EtOAc, 100/0 to 100:1) to afford thioester **2.2** (250 mg, 81%) as a colorless oil: R_f 0.50 (hexanes/EtOAc, 20/1); ^1H NMR (400 MHz, CDCl_3) δ 5.77 (dddd, $J = 17.6, 10.8, 6.4, 6.4$ Hz, 1 H), 5.07 (d, $J = 17.6$ Hz, 1 H), 5.03 (d, $J = 10.8$ Hz, 1 H), 2.93 (dd, $J = 7.2, 7.2$ Hz, 2 H), 2.53 (dd, $J = 7.2, 7.2$ Hz, 2 H), 2.31 (ddd, $J = 6.8, 6.8, 6.8$ Hz, 2 H), 1.60–1.68 (m, 2 H), 1.24–1.34 (m, 8 H), 0.87 (dd, $J = 6.4, 6.4$ Hz, 3 H); ^{13}C NMR (100 MHz, CDCl_3) δ 199.5, 136.1, 116.4, 44.1, 33.7, 31.6, 28.88, 28.87, 28.0, 25.7, 22.6, 14.0; IR (neat) 2928, 2869, 1692, 1142 cm^{-1} ; HRMS (EI) found 214.1390 [calcd for $\text{C}_{12}\text{H}_{22}\text{OS}$ (M) $^+$ 214.1391].

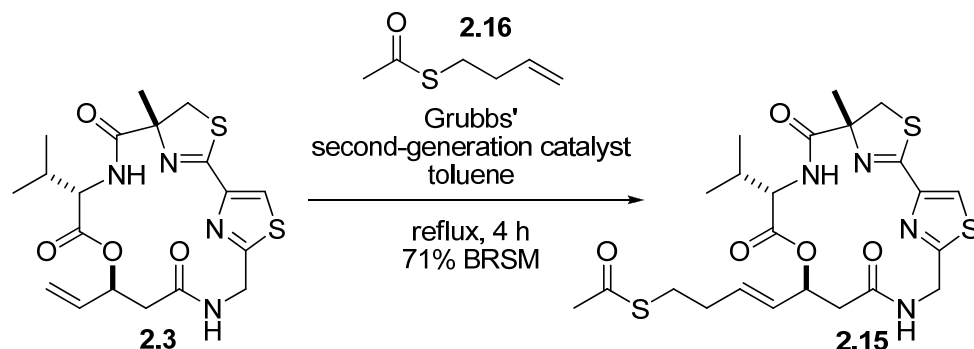
Largazole (2.1)



To a solution of macrocycle **2.3** (22.5 mg, 0.052 mmol) in dry toluene (2.0 mL, 0.026 M) were added thioester **2.2** (0.40 mL, 0.26 M in toluene, 0.10 mmol) and Grubbs' second-generation catalyst (0.20 mL, 0.052 M in toluene, 0.010 mmol). The resulting mixture was stirred at 110 °C for 1 h. An addition of thioester **2.2** (0.2 mL, 0.26 M in

toluene, 0.052 mmol) and Grubbs' second-generation catalyst (0.10 mL, 0.052 M in toluene, 0.0052 mmol) was repeated three times every 1 h. The reaction mixture was cooled to room temperature and a few drops of DMSO were added. The mixture was stirred for overnight and concentrated *in vacuo*. The residue was purified by column chromatography (silica gel, hexanes/EtOAc/CH₃OH, 15:15:1 to 10:10:1) to afford **2.1** ((*E*)-isomer only) as a white solid (13.3 mg, 41%, 64% based on recovered starting material): R_f 0.43 (hexanes/EtOAc/CH₃OH, 10/10/1); [α]^{26.6}_D = +38.9 (*c* 0.027, CH₃OH) [lit. [α]²⁰_D = +22 (*c* 0.1, CH₃OH)]; ¹H NMR (400 MHz, CDCl₃) δ 7.76 (s, 1 H), 7.16 (d, *J* = 9.6 Hz, 1 H), 6.41 (dd, *J* = 9.2, 2.8 Hz, 1 H), 5.83 (ddd, *J* = 15.6, 7.2, 7.2 Hz, 1 H), 5.66 (ddd, *J* = 10.0, 7.2, 2.4 Hz, 1 H), 5.51 (dd, *J* = 15.6, 7.2 Hz, 1 H), 5.29 (dd, *J* = 17.6, 9.6 Hz, 1 H), 4.61 (dd, *J* = 9.2, 3.2 Hz, 1 H), 4.27 (dd, *J* = 17.6, 2.8 Hz, 1 H), 4.05 (d, *J* = 11.2 Hz, 1 H), 3.28 (d, *J* = 11.6 Hz, 1 H), 2.90 (dd, *J* = 7.2, 7.2 Hz, 2 H), 2.87 (dd, *J* = 16.4, 10.4 Hz, 1 H), 2.69 (d, *J* = 16.4, 2.8 Hz, 1 H), 2.53 (dd, *J* = 7.6, 7.6 Hz, 2 H), 2.31 (ddd, *J* = 7.2, 7.2, 7.2 Hz, 2 H), 2.07–2.14 (m, 1 H), 1.87 (s, 3 H), 1.61–1.68 (m, 2 H), 1.26–1.29 (m, 8 H), 0.88 (brdd, *J* = 6.8, 6.8 Hz, 3 H), 0.69 (d, *J* = 6.8 Hz, 3 H), 0.52 (d, *J* = 7.2 Hz, 3 H); ¹³C NMR (100 MHz, CDCl₃) δ 199.4, 173.5, 169.4, 168.9, 167.9, 164.5, 147.5, 132.7, 128.4, 124.2, 84.5, 72.0, 57.7, 44.1, 43.3, 41.1, 40.5, 34.2, 32.3, 31.6, 28.9, 27.9, 25.6, 24.2, 22.6, 18.9, 16.6, 14.1; IR (neat) 3368, 2929, 2853, 1734, 1684, 1507, 1448, 1257, 1146, 1025 cm⁻¹; HRMS (FAB) found 623.2397 [calcd for C₂₉H₄₃N₄O₅S₃ (M+H)⁺ 623.2396].

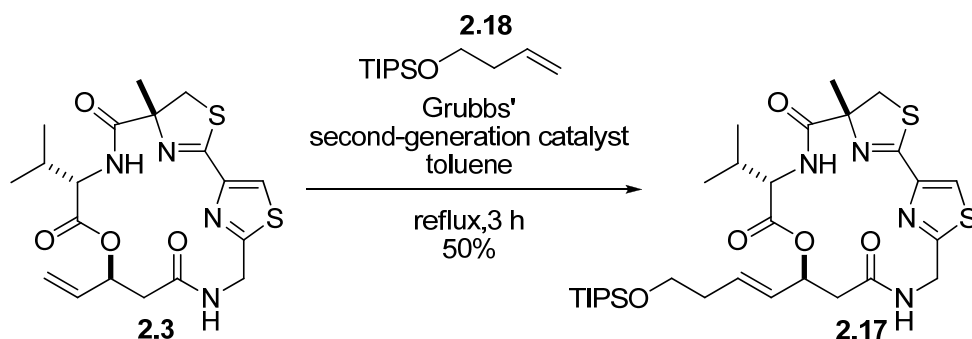
Acetyl analog 15



To a solution of macrocycle **2.3** (29.1 mg, 0.067 mmol) in dry toluene (2.0 mL, 0.034 M) were added thioester **2.16** (0.2 mL, 0.67 M in toluene, 0.134 mmol) and Grubbs' second-generation catalyst (0.20 mL, 0.067 M in toluene, 0.0134 mmol). The resulting mixture was stirred at 110 °C for 1 h. An addition of thioester **2.16** (0.10 mL, 0.67 M in toluene, 0.067 mmol) and Grubbs' second-generation catalyst (0.10 mL, 0.067 M in toluene, 0.0067 mmol) was repeated three times every 1 h. The reaction mixture was cooled to room temperature and a few drops of DMSO were added. The mixture was stirred for overnight and concentrated *in vacuo*. The residue was purified by column chromatography (silica gel, CH₂Cl₂/EtOAc, 1/1 to 1/2) to afford **2.15** (*(E)*-isomer only) as a white solid (19.2 mg, 54%, 71% based on recovered starting material): R_f 0.26 (CH₂Cl₂/EtOAc, 1/2); [α]^{25.3}_D = +37.8 (*c* 0.077, CHCl₃) ¹H NMR (400 MHz, CDCl₃) δ 7.76 (s, 1 H), 7.16 (d, *J* = 9.2 Hz, 1 H), 6.42 (dd, *J* = 9.6, 2.8 Hz, 1 H), 5.81 (ddd, *J* = 15.6, 6.8, 6.8 Hz, 1 H), 5.66 (ddd, *J* = 9.6, 6.8, 2.6 Hz, 1 H), 5.51 (dd, *J* = 15.6, 6.8 Hz, 1 H), 5.28 (dd, *J* = 17.6, 9.6 Hz, 1 H), 4.60 (dd, *J* = 9.6, 3.6 Hz, 1 H), 4.27 (dd, *J* = 17.6, 3.6 Hz, 1 H), 4.04 (d, *J* = 11.2 Hz, 1 H), 3.27 (d, *J* = 11.2 Hz, 1 H), 2.90 (dd, *J* = 7.2, 7.2 Hz, 2 H),

2.84 (dd, $J = 16.4, 10.0$ Hz, 1 H), 2.68 (dd, $J = 16.4, 2.8$ Hz, 1 H), 2.32 (s, 3 H), 2.26–2.36 (m, 2 H), 2.10 (dddd, $J = 6.8, 6.8, 6.8, 6.8, 3.2$ Hz, 1 H), 1.87 (s, 3 H), 0.68 (d, $J = 6.8$ Hz, 1 H), 0.51 (d, $J = 6.8$ Hz, 1 H), ^{13}C NMR (100 MHz, CDCl_3) δ 195.6, 173.5, 169.4, 168.9, 167.9, 164.5, 147.5, 132.5, 128.4, 124.2, 84.4, 72.0, 57.7, 43.3, 41.1, 40.4, 34.2, 32.1, 30.6, 28.2, 24.2, 18.9, 16.6; IR (neat) 3370.1, 2961.1, 2927.9, 1732.9, 1670.7, 1596.3, 1506.7, 1243.5, 1114.5, 1028.4 cm^{-1} ; HRMS (FAB) found 539.1456 [calcd for $\text{C}_{23}\text{H}_{31}\text{N}_4\text{O}_5\text{S}_3$ ($\text{M}+\text{H}$) $^+$ 539.1457].

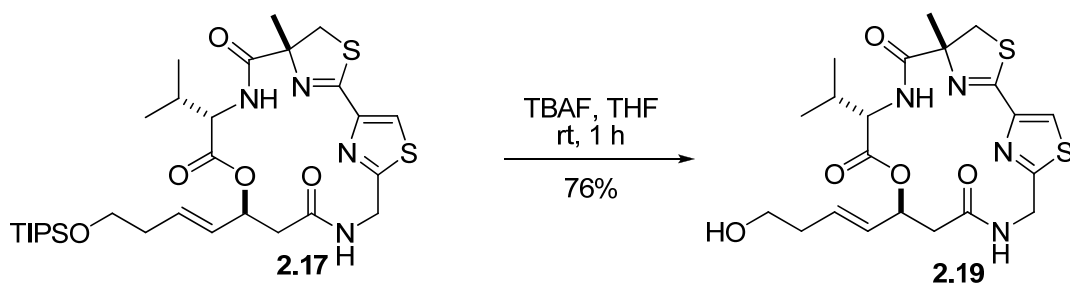
Preparation of **2.17**



To a solution of macrocycle **2.3** (29.7 mg, 0.068 mmol) in dry toluene (1.5 mL, 0.045 M) were added 1-triisopropylsilyloxy-3-butene (**2.18**) (0.136 mL, 0.5 M in toluene, 0.068 mmol) and Grubbs' second-generation catalyst (0.136 mL, 0.05 M in toluene, 0.0068 mmol). The resulting mixture was stirred at 110 °C for 1 h. An addition of 1-triisopropylsilyloxy-3-butene (**2.18**) (0.136 mL, 0.5 M in toluene, 0.068 mmol) and Grubbs' second-generation catalyst (0.136 mL, 0.05 M in toluene, 0.0068 mmol) was repeated two times every 1 h. The reaction mixture was cooled to room temperature and a

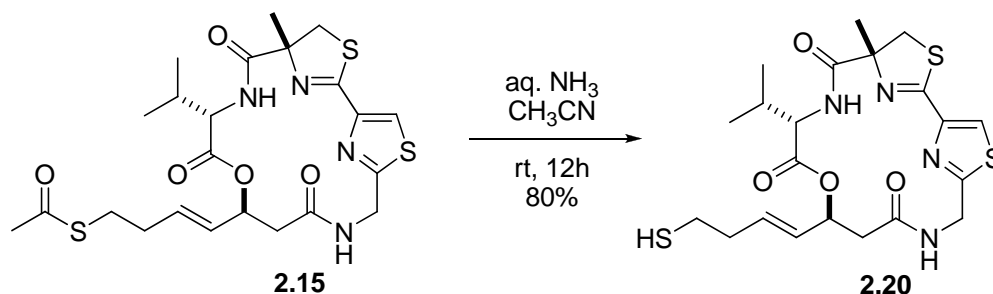
few drops of DMSO were added. The mixture was stirred for overnight and concentrated *in vacuo*. The residue was purified by column chromatography (silica gel, hexanes/EtOAc, 1/1) to afford **2.17** (*E:Z* = >9:1) as a viscous oil (21.5 mg, 50%): R_f 0.37 (hexane/EtOAc, 1/2); $[\alpha]_D^{25.7} = +18.3$ (c 0.22, CHCl_3); $^1\text{H NMR}$ (400 MHz, CDCl_3) δ 7.76 (s, 1 H), 7.16 (d, $J = 9.2$ Hz, 1 H), 6.41 (dd, $J = 9.6, 2.8$ Hz, 1 H), 5.90 (ddd, $J = 16.4, 6.4, 6.4$ Hz, 1 H), 5.68 (ddd, $J = 10.0, 7.2, 2.4$ Hz, 1 H), 5.52 (dd, $J = 15.6, 7.2$ Hz, 1 H), 5.29 (dd, $J = 17.6, 9.6$ Hz, 1 H), 4.60 (dd, $J = 9.6, 3.6$ Hz, 1 H), 4.25 (dd, $J = 17.6, 3.2$ Hz, 1 H), 4.05 (d, $J = 11.2$ Hz, 1 H), 3.70 (ddd, $J = 6.4, 6.4, 1.2$ Hz, 2 H), 3.27 (d, $J = 11.6$ Hz, 1 H), 2.85 (dd, $J = 16.4, 10.4$ Hz, 1 H), 2.69 (dd, $J = 16.4, 2.8$ Hz, 1 H), 2.23–2.33 (m, 2 H), 2.11 (dddd, $J = 6.8, 6.8, 6.8, 6.8, 3.6$ Hz, 1 H), 1.86 (s, 3 H), 1.02–1.07 (m, 21 H), 0.68 (d, $J = 6.8$ Hz, 3 H), 0.51 (d, $J = 6.8$ Hz, 3 H); $^{13}\text{C NMR}$ (100 MHz, CDCl_3) δ 173.5, 169.5, 168.8, 167.9, 164.5, 147.5, 132.3, 128.1, 124.1, 84.4, 72.2, 62.5, 57.7, 43.3, 41.0, 40.5, 36.0, 34.2, 24.2, 18.9, 18.0, 16.6, 11.9; IR (neat) 2926.8, 2864.1, 1735.0, 1670.1, 1500.4, 1257.5, 1243.7, 1109.2, 1030.3, 988.9, 970.7, 841.0, 679.8, 669.7 cm^{-1} ; HRMS (FAB) found 637.2919 [calcd for $\text{C}_{30}\text{H}_{49}\text{N}_4\text{O}_5\text{S}_2\text{Si}$ ($\text{M}+\text{H}$) $^+$ 637.2914].

Hydroxyl analog 19



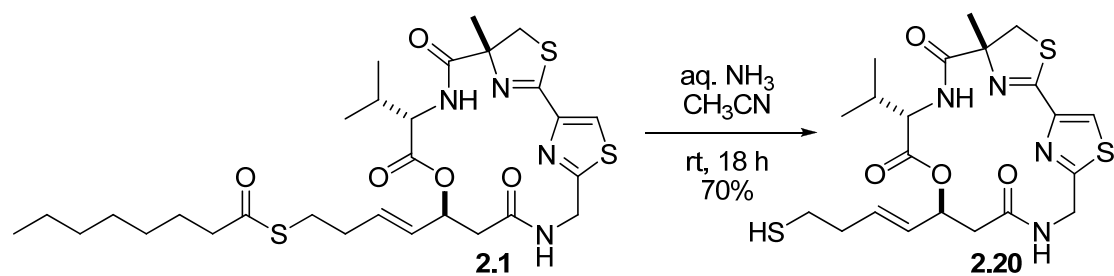
To a stirred solution of TIPS-ether **2.17** (16.1 mg, 0.025 mmol) in THF (1 mL, 0.025 M) was added TBAF (0.5 mL, 0.1 M, 0.05 mmol) at room temperature. After being stirred at the same temperature for 1 h, the reaction mixture was quenched with aqueous saturated NH₄Cl, and diluted with CH₂Cl₂ (5 mL). The layers were separated, and the aqueous layer was extracted with CH₂Cl₂ (2 × 5 mL). The combined organic layers were washed with brine, dried over anhydrous Na₂SO₄, and concentrated *in vacuo*. The residue was purified by column chromatography (silica gel; EtOAc/CH₃OH, 10/1 to 5/1) to afford **2.19** as a viscous oil (9.2 mg, 76%): R_f 0.31 (EtOAc/CH₃OH, 10/1); [α]^{27.8}_D = +15.7 (*c* 0.15, CHCl₃); ¹H NMR (400 MHz, CDCl₃) δ 7.76 (s, 1 H), 7.26 (d, *J* = 9.2 Hz, 1 H), 6.79 (dd, *J* = 8.0, 2.8 Hz, 1 H), 6.02 (ddd, *J* = 15.6, 8.4, 8.4 Hz, 1 H), 5.71–5.74 (m, 1 H), 5.62 (dd, *J* = 15.6, 5.6 Hz, 1 H), 5.18 (dd, *J* = 17.6, 8.4 Hz, 1 H), 4.58 (dd, *J* = 9.2, 4.4 Hz, 1 H), 4.33 (dd, *J* = 17.2, 3.6 Hz, 1 H), 4.02 (d, *J* = 11.2 Hz, 1 H), 3.69 (ddd, *J* = 11.2, 6.0, 6.0 Hz, 1 H), 3.58 (ddd, *J* = 11.2, 5.6, 5.6 Hz, 1 H), 3.29 (d, *J* = 11.6 Hz, 1 H), 2.83 (dd, *J* = 16.4, 7.6 Hz, 1 H), 2.73 (dd, *J* = 16.4, 4.0 Hz, 1 H), 2.33 (ddd, *J* = 6.4, 6.4, 6.4 Hz, 2 H), 2.03 (dddd, *J* = 7.2, 7.2, 7.2, 7.2, 4.4 Hz, 1 H), 1.86 (s, 3 H), 0.72 (d, *J* = 6.8 Hz, 3 H), 0.59 (d, *J* = 6.8 Hz, 3 H), ¹³C NMR (100 MHz, CDCl₃) δ 173.2, 169.1, 168.1, 168.0, 165.2, 147.4, 131.7, 128.6, 124.1, 84.3, 71.0, 61.4, 58.1, 43.2, 41.1, 40.7, 35.8, 33.7, 24.2, 18.8, 17.0; IR (neat) 3373.0, 2960.8, 2926.7, 1731.9, 1662.0, 1506.6, 1242.5, 1031.8, 971.2, 732.5 cm⁻¹; HRMS (FAB) found 481.1599 [calcd for C₂₁H₂₉N₄O₅S₂ (M+H)⁺ 481.1579].

Aminolysis of thioester **2.15**



To a solution of thioester **2.15** (2.3 mg, 0.0043 mmol) in CH₃CN (0.5 mL, 0.0086 M) was added aqueous NH₃ (28.9%, 0.05 mL). The resulting mixture was stirred at room temperature for 12 h and concentrated *in vacuo*. The residue was purified by column chromatography (silica gel, EtOAc/CH₃OH, 10/0 to 10/1) to afford thiol **2.20** as a colorless oil (1.7 mg, 80%). R_f 0.35 (EtOAc/CH₃OH, 10/1); ¹H NMR (400 MHz, CDCl₃) δ 7.79 (s, 1 H), 7.18 (d, *J* = 9.2 Hz, 1 H), 6.64 (dd, *J* = 8.8, 3.2 Hz, 1 H), 5.89 (ddd, *J* = 15.6, 6.8, 6.8 Hz, 1 H), 5.69 (dd, *J* = 6.8, 6.8 Hz, 1 H), 5.54 (dd, *J* = 15.6, 6.8 Hz, 1 H), 5.25 (dd, *J* = 17.6, 9.2 Hz, 1 H), 4.61 (dd, *J* = 9.6, 3.6 Hz, 1 H), 4.21 (dd, *J* = 17.6, 3.2 Hz, 1 H), 4.03 (d, *J* = 11.2 Hz, 1 H), 3.28 (d, *J* = 11.2 Hz, 1 H), 2.87 (dd, *J* = 16.4, 10.0 Hz, 1 H), 2.71 (dd, *J* = 6.8, 6.8 Hz, 1 H), 2.68–2.75 (m, 1 H), 2.44 (ddd, *J* = 7.2, 7.2, 7.2 Hz, 2 H), 2.07–2.13 (m, 1 H), 1.86 (s, 3 H), 0.70 (d, *J* = 6.8 Hz, 1 H), 0.53 (d, *J* = 6.8 Hz, 1 H), IR (neat) 3374.5, 3305.1, 2961.8, 2929.1, 2851.4, 1731.6, 1666.2, 1596.7, 1502.7, 1237.0, 1179.8, 1114.4, 1020.4 cm⁻¹; HRMS (FAB) found 497.1354 [calcd for C₂₁H₂₉N₄O₄S₃ (M+H)⁺ 497.1351].

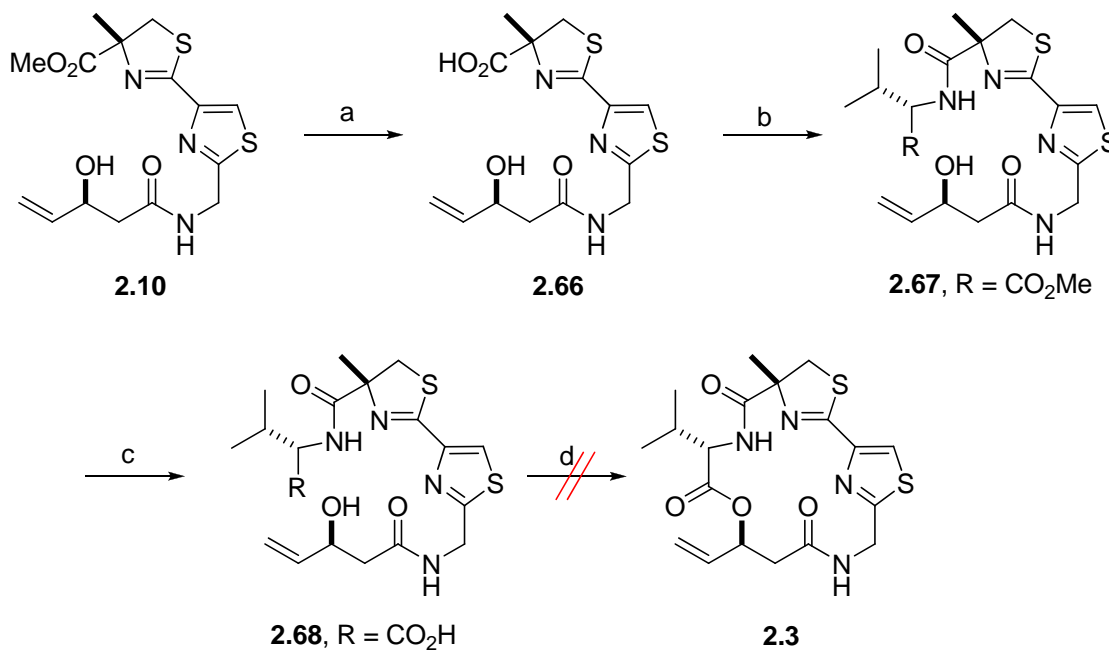
Aminolysis of Largazole (**2.1**)



To a solution of largazole (**2.1**) (2.5 mg, 0.004 mmol) in CH₃CN (0.5 mL, 0.008 M) was added aqueous NH₃ (28.9%, 0.05 mL). The resulting mixture was stirred at room temperature for 18 h and concentrated *in vacuo*. The residue was purified by column chromatography (silica gel, EtOAc/CH₃OH, 10/0 to 10/1) to afford thiol **2.20** as a colorless oil (1.4 mg, 70%).

Attempts for Macrolactonization Route

1) Yamaguchi macrolactonization



(a) 0.5 N LiOH, THF, H₂O, 0 °C, 0.5 h, then 25 °C, 1 h; (b) L-valine methyl ester hydrochloride, EDC, *i*-Pr₂NEt, CH₂Cl₂, 25 °C, 12h, 70% (two steps); (c) 0.5 N LiOH, THF, H₂O, 0 °C, 0.5 h, then 25 °C, 1 h, > 90%; (d) 2,4,6-trichlorobenzoyl chloride, Et₃N, THF, 0 °C, 1 h; then **2.68**, DMAP, 25 °C, 3 h.

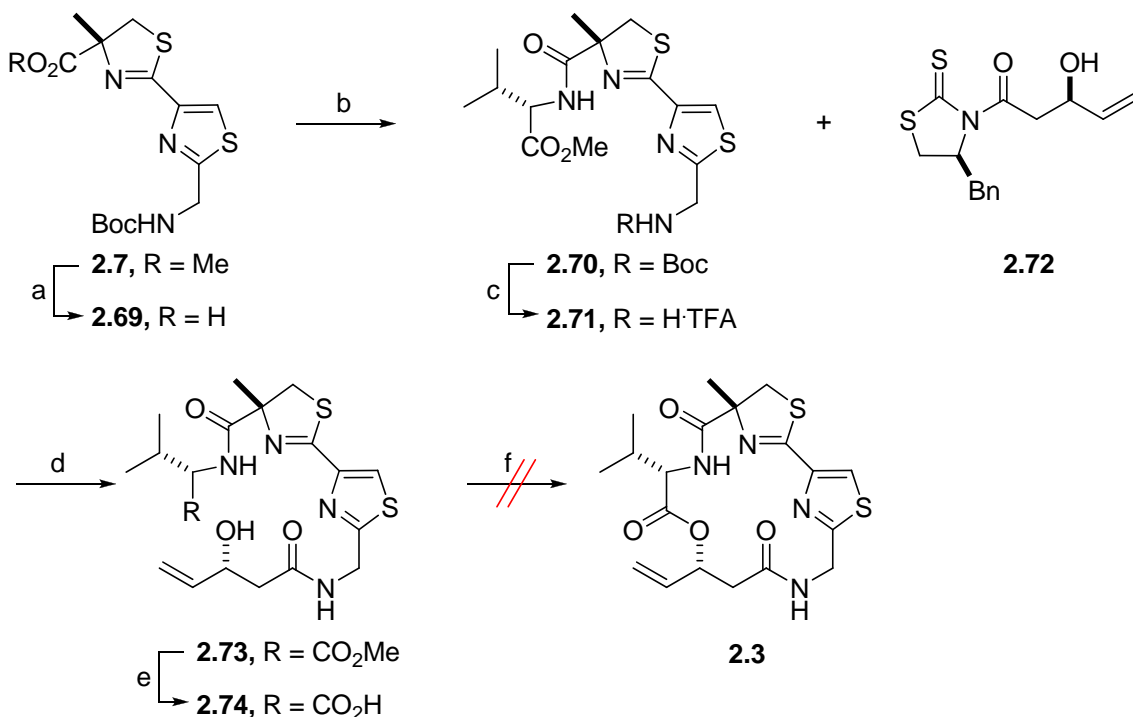
To a stirred solution of **2.10** (69 mg, 0.188 mmol) in THF/H₂O (4:1, 2.0 mL, 0.094 M) was added dropwisely 0.5 N LiOH (0.56 mL, 0.28 mmol) at 0 °C. After being stirred at 0 °C for 0.5 h and at 25 °C for 1 h, the resulting mixture was acidified with 1 M KHSO₄ solution to pH ~3.0 and diluted with EtOAc. The layers were separated and the aqueous layer was extracted with EtOAc. The combined organic layers were washed with brine, dried over anhydrous Na₂SO₄, and concentrated *in vacuo*. The crude carboxylic acid **2.66** was carried to the next step without further purification. To a stirred solution of carboxylic acid **2.66** and L-valine methyl ester hydrochloride (38 mg, 0.23 mmol) in CH₂Cl₂ (2.0 mL, 0.094 M) was added EDC (108 mg, 0.564 mmol) and *i*-Pr₂NEt (0.098

mL, 0.564 mmol). After being stirred at 25 °C for 24 h, the residue was concentrated *in vacuo* and purified by column chromatography (silica gel, EtOAc/CH₂Cl₂, 2/1) to afford **2.67** (63 mg, 70%) as a colorless oil. To a stirred solution of **2.67** (19 mg, 0.041 mmol) in THF/H₂O (4:1, 1.5 mL, 0.027 M) was added dropwise 0.5 N LiOH (0.12 mL, 0.06 mmol) at 0 °C. After being stirred at 0 °C for 0.5 h and at 25 °C for 1 h, the resulting mixture was acidified with 1 M KHSO₄ solution to pH ~3.0 and diluted with EtOAc. The layers were separated and the aqueous layer was extracted with EtOAc. The combined organic layers were washed with brine, dried over anhydrous Na₂SO₄, and concentrated *in vacuo*. The crude carboxylic acid **2.68** was carried to the next step without further purification.

[For crude carboxylic acid **2.66**]: NMR (400 MHz, CDCl₃) δ 7.85 (s, 1 H), 7.14 (dd, *J* = 6.0, 5.6 Hz, 1 H), 5.90 (ddd, *J* = 16.8, 10.4, 5.6 Hz, 1 H), 5.32 (d, *J* = 17.2 Hz, 1 H), 5.15 (d, *J* = 10.4 Hz, 1 H), 4.87 (dd, *J* = 16.8, 6.8 Hz, 1 H), 4.63 (dd, *J* = 16.4, 5.6 Hz, 1 H), 4.56–4.60 (m, 1 H), 3.93 (d, *J* = 11.6 Hz, 1 H), 3.37 (d, *J* = 11.6 Hz, 1 H), 2.57 (dd, *J* = 14.4, 3.2 Hz, 1 H), 2.46 (dd, *J* = 14.4, 9.2 Hz, 1 H), 1.67 (s, 3 H); HRMS (FAB) found 356.0731 [calcd for C₁₄H₁₈N₃O₄S₂ (M+H)⁺ 356.0739]. [For **2.67**]: R_f 0.30 (EtOAc/CH₂Cl₂, 2/1); [α]^{25.9}_D = -44.2 (*c* 0.57, CHCl₃); ¹H NMR (400 MHz, CDCl₃) δ 7.93 (s, 1 H), 7.23–7.26 (brs, 1 H), 7.23 (d, *J* = 3.2 Hz, 1 H), 5.88 (ddd, *J* = 16.8, 10.4, 5.2 Hz, 1 H), 5.29 (d, *J* = 17.2 Hz, 1 H), 5.12 (d, *J* = 10.8 Hz, 1 H), 4.75 (dddd, *J* = 16.4, 16.4, 16.4, 6.0 Hz, 2 H), 4.51–4.57 (m, 1 H), 4.49 (dd, *J* = 9.2, 5.2 Hz, 1 H), 3.76 (d, *J* = 11.6 Hz, 1 H), 3.74 (s, 3 H), 3.33 (d, *J* = 11.6 Hz, 1 H), 2.55 (dd, *J* = 15.2, 3.6 Hz, 1 H), 2.45 (dd, *J* = 15.2, 8.4 Hz, 1 H), 2.09–2.18 (m, 1 H), 1.58 (s, 3 H), 0.86 (d, *J* = 6.8 Hz, 3

H), 0.82 (d, $J = 6.8$ Hz, 3 H); ^{13}C NMR (100 MHz, CDCl_3) δ 174.5, 172.1, 171.8, 168.1, 163.0, 148.4, 139.0, 122.0, 115.4, 85.1, 69.4, 57.0, 52.1, 42.5, 41.5, 40.8, 31.0, 24.6, 19.0, 17.7; IR (neat) 3726, 3703, 3627, 3364, 2965, 1741, 1653, 1521, 1219 cm^{-1} ; HRMS (FAB) found 469.1576 [calcd for $\text{C}_{20}\text{H}_{29}\text{N}_4\text{O}_5\text{S}_2$ ($\text{M}+\text{H}$) $^+$ 469.1579]. [For crude carboxylic acid **2.68**]: NMR (400 MHz, CDCl_3) δ 7.92 (s, 1 H), 7.42 (dd, $J = 6.0, 6.0$ Hz, 1 H), 7.37 (d, $J = 8.8$ Hz, 1 H), 5.88 (ddd, $J = 17.2, 10.4, 5.6$ Hz, 1 H), 5.29 (d, $J = 17.2$ Hz, 1 H), 5.12 (d, $J = 10.4$ Hz, 1 H), 4.64 (dddd, $J = 16.0, 16.0, 16.0, 6.0$ Hz, 2 H), 4.55–4.60 (m, 1 H), 4.48 (dd, $J = 8.8, 5.6$ Hz, 1 H), 3.80 (d, $J = 11.6$ Hz, 1 H), 3.37 (d, $J = 11.6$ Hz, 1 H), 2.57 (dd, $J = 14.4, 3.2$ Hz, 1 H), 2.43 (dd, $J = 14.4, 8.8$ Hz, 1 H), 2.18–2.27 (m, 1 H), 1.60 (s, 3 H), 0.92 (d, $J = 6.8$ Hz, 3 H), 0.88 (d, $J = 6.8$ Hz, 3 H).

2) Mitsunobu macrolactonization



(a) 0.5 N LiOH, THF, H₂O, 0 °C, 0.5 h, then 25 °C, 1 h; (b) L-valine methyl ester hydrochloride, EDC, *i*-Pr₂NEt, HOAt, CH₂Cl₂, 25 °C, 12h, 89% (two steps); (c) TFA, CH₂Cl₂, 25 °C, h, 1 h; (d) DMAP, CH₂Cl₂, 25 °C, 12 h, 64% (two steps); (e) 0.5 N LiOH, THF, H₂O, 0 °C, 0.5 h, then 25 °C, 3 h, > 90%; (f) PPh₃, DIAD, TsOH·H₂O, THF, 25 °C, 30 min, then 30, 0 °C, 2h.

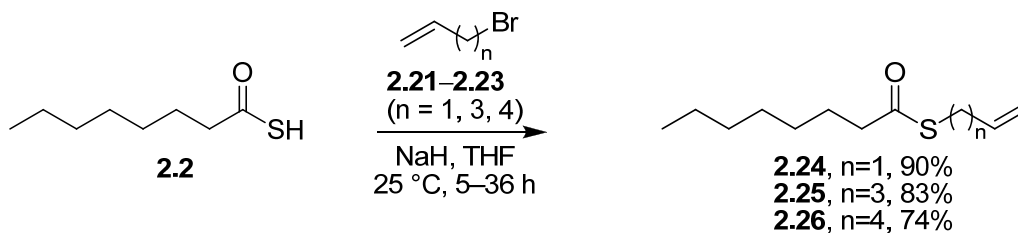
To a stirred solution of **2.7** (150 mg, 0.323 mmol) in THF/H₂O (4:1, 2.0 mL, 0.162 M) was added dropwise 0.5 N LiOH (0.97 mL, 0.485 mmol) at 0 °C. After being stirred at 0 °C for 0.5 h and at 25 °C for 1 h, the resulting mixture was acidified with 1 M KHSO₄ solution to pH ~3.0 and diluted with EtOAc. The layers were separated and the aqueous layer was extracted with EtOAc. The combined organic layers were washed with brine, dried over anhydrous Na₂SO₄, and concentrated *in vacuo*. The crude carboxylic acid **2.69** was carried to the next step without further purification. To a stirred solution of carboxylic acid **2.69** and L-valine methyl ester hydrochloride (84 mg, 0.50 mmol) in

CH₂Cl₂ (3.0 mL, 0.108 M) was added EDC (234 mg, 1.22 mmol), *i*-Pr₂NEt (0.212 mL, 1.22 mmol) and HOAt (55 mg, 0.41 mmol). After being stirred at 25 °C for 12 h, the residue was concentrated *in vacuo* and purified by column chromatography (silica gel, EtOAc/CH₂Cl₂, 2/1) to afford **2.70** (174 mg, 89%) as a colorless oil. Compound **2.70** (57 mg, 0.118 mmol) was treated with TFA/CH₂Cl₂ (1:2, 1.0 mL, 0.118 M) at 25 °C. The resulting mixture was stirred at 25 °C for 1 h, and then purged by N₂ to remove TFA and CH₂Cl₂. The residue was washed with Et₂O four times to remove remaining TFA. The crude TFA·amine salt **2.71** was carried to the next step without further purification. To a solution of TFA·amine salt **2.71** in CH₂Cl₂ (2.0 mL, 0.059 M) was added DMAP (40 mg, 0.32 mmol), followed by **2.72**⁸⁶ (33 mg, 0.107 mmol). The reaction mixture was stirred for 12 h at 25 °C, quenched with 0.1 N HCl. The layers were separated, and the aqueous layer was extracted with EtOAc. The combined organic layers were washed with brine, dried over anhydrous Na₂SO₄, and concentrated *in vacuo*. The residue was purified by column chromatography (silica gel; hexanes/EtOAc/CH₃OH, 15/15/1 to 10/10/1) to afford **2.73** as a colorless oil (33 mg, 64%). To a stirred solution of **2.73** (33 mg, 0.069 mmol) in THF/H₂O (4:1, 1.5 mL, 0.046 M) was added dropwise 0.5 N LiOH (0.21 mL, 0.103 mmol) at 0 °C. After being stirred at 0 °C for 0.5 h and at 25 °C for 3 h, the resulting mixture was acidified with 1 M KHSO₄ solution to pH ~3.0 and diluted with EtOAc. The layers were separated and the aqueous layer was extracted with EtOAc. The combined organic layers were washed with brine, dried over anhydrous Na₂SO₄, and concentrated *in vacuo*. The crude carboxylic acid **2.74** was carried to the next step

without further purification. [For carboxylic acid **2.69**]: NMR (400 MHz, CDCl₃) 9.50–9.58 (brs, 1 H), δ 7.98 (s, 1 H), 5.46–5.53 (brs, 1 H), 4.61 (d, J = 6.0 Hz, 1 H), 3.89 (d, J = 11.6 Hz, 1 H), 3.32 (d, J = 11.6 Hz, 1 H), 1.68 (s, 3 H), 1.45 (s, 9 H). [For **2.70**]: R_f 0.50 (EtOAc/hexane, 1/1); ¹H NMR (400 MHz, CDCl₃) δ 7.93 (s, 1 H), 7.17 (d, J = 8.8 Hz, 1 H), 5.42–5.48 (brs, 1 H), 4.61 (d, 6.0 Hz, 1 H), 4.49 (dd, J = 8.8, 5.2 Hz, 1 H), 3.76 (d, J = 11.6 Hz, 1 H), 3.73(s, 3H), 3.31 (d, J = 11.2 Hz, 1 H), 2.09–2.19 (m, 1 H), 1.58 (s, 3 H), 1.44(s, 9H), 0.85 (d, J = 6.4 Hz, 3 H), 0.81 (d, J = 6.8 Hz, 3 H). [For crude amine salt **2.71**]: NMR (400 MHz, CDCl₃) δ 8.48 (s, 1 H), 7.80 (d, J = 8.4 Hz, 1 H), 4.67 (s, 2 H), 4.47 (d, J = 12.0 Hz, 1 H), 4.34 (dd, J = 7.2, 6.4 Hz, 1 H), 3.70 (s, 3 H), 3.61 (d, J = 12.0 Hz, 1 H), 2.08–2.18 (m, 1 H), 1.85 (s, 3 H), 0.82 (dd, J = 6.8, 6.4 Hz, 6 H). [For **2.73**]: R_f 0.30 (EtOAc/CH₂Cl₂, 2/1); ¹H NMR (400 MHz, CDCl₃) δ 7.96 (s, 1 H), 7.23–7.27 (brs, 1 H), 7.00–7.04 (brs, 1 H), 5.90 (ddd, J = 16.4, 10.0, 5.6 Hz, 1 H), 5.32 (d, J = 17.2 Hz, 1 H), 5.16 (d, J = 10.4 Hz, 1 H), 4.75 (dddd, J = 16.4, 16.4, 16.4, 4.4 Hz, 2 H), 4.56–4.62 (m, 1 H), 4.51 (dd, J = 8.0, 4.8 Hz, 1 H), 3.81 (d, J = 11.6 Hz, 1 H), 3.76 (s, 3 H), 3.36 (d, J = 11.6 Hz, 1 H), 2.58 (d, J = 15.6 Hz, 1 H), 2.48 (dd, J = 14.8, 9.6 Hz, 1 H), 2.11–2.20 (m, 1 H), 1.61 (s, 3 H), 0.88 (d, J = 6.8 Hz, 3 H), 0.85 (d, J = 6.8 Hz, 3 H). [For crude carboxylic acid **2.74**]: NMR (400 MHz, CDCl₃) δ 7.97 (s, 1 H), 7.60 (dd, J = 6.0, 5.6 Hz, 1 H), 7.43 (d, J = 8.8 Hz, 1 H), 5.87 (ddd, J = 17.2, 10.4, 5.6 Hz, 1 H), 5.28 (d, J = 17.2 Hz, 1 H), 5.12 (d, J = 10.4 Hz, 1 H), 4.77 (dddd, J = 16.0, 16.0, 16.0, 6.0 Hz, 2 H), 4.52–4.60 (m, 1 H), 4.46 (dd, J = 8.8, 5.2 Hz, 1 H), 3.84 (d, J = 11.6 Hz, 1 H), 3.39

(d, $J = 11.6$ Hz, 1 H), 2.57 (dd, $J = 14.8, 3.2$ Hz, 1 H), 2.49 (dd, $J = 14.8, 8.4$ Hz, 1 H), 2.18–2.26 (m, 1 H), 1.61 (s, 3 H), 0.91 (d, $J = 6.8$ Hz, 3 H), 0.87 (d, $J = 6.8$ Hz, 3 H).

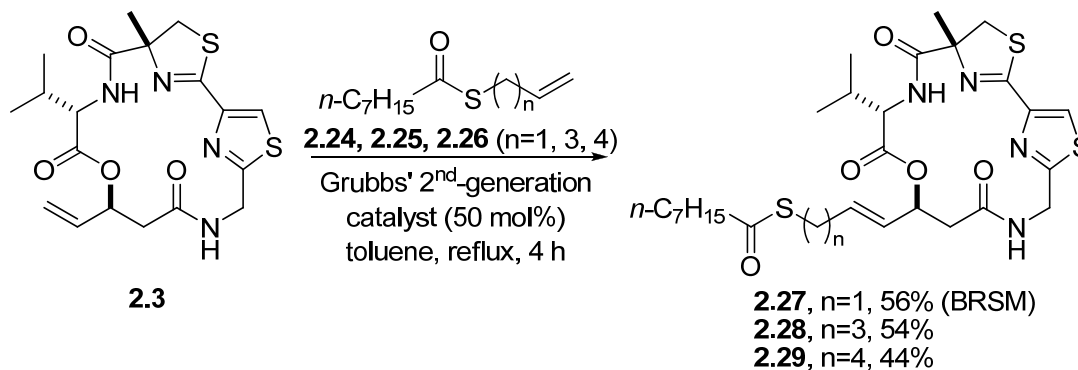
General procedure for the preparation of thioesters **2.24**–**2.26**



To a solution of **2.2** (230 mg, 1.5 mmol) in dry THF (10.0 mL, 0.15 M) was added NaH (100 mg, 2.10 mmol) at 25 °C. After stirring at 25 °C for 10 min, 3-bromo-1-propene (**2.21**) (0.18 mL, 2.10 mmol) was added dropwise into the reaction mixture. After stirring at 25 °C for 5 h, the mixture was filtered and concentrated *in vacuo*. The residue was purified by column chromatography (silica gel, hexanes/EtOAc, 100/0 to 100:1) to afford thioester **2.24** (259 mg, 90%) as a colorless oil: R_f 0.40 (hexanes/EtOAc, 20/1); $^1\text{H NMR}$ (400 MHz, CDCl_3) δ 5.78 (ddt, $J = 16.8, 10.0, 6.8$ Hz, 1 H), 5.20 (d, $J = 16.8$ Hz, 1 H), 5.06 (d, $J = 10.0$ Hz, 1 H), 3.51 (d, $J = 6.8$ Hz, 2 H), 2.53 (t, $J = 7.2$ Hz, 2 H), 1.60–1.68 (m, 2 H), 1.21–1.34 (m, 8 H), 0.86 (t, $J = 7.2$ Hz, 3 H); $^{13}\text{C NMR}$ (100 MHz, CDCl_3) δ 198.7, 133.2, 117.6, 43.9, 31.6, 31.5, 28.8, 25.5, 22.5, 14.0; IR (neat) 2954, 2925, 2856, 1691, 1638, 1465, 1421, 1378, 1232, 1123, 1040 cm^{-1} ; HRMS (EI) found 200.1233 [calcd for $\text{C}_{11}\text{H}_{20}\text{OS}$ (M) $^+$ 200.1235]; [For **2.25**, colorless oil, 83%]: R_f 0.55 (hexanes/EtOAc, 20/1); $^1\text{H NMR}$ (400 MHz, CDCl_3) δ 5.75 (ddt, $J = 16.8, 10.4, 6.8$

Hz, 1 H), 5.00 (d, $J = 16.8$ Hz, 1 H), 4.96 (d, $J = 10.0$ Hz, 1 H), 2.85 (t, $J = 7.2$ Hz, 2 H), 2.51 (t, $J = 7.2$ Hz, 2 H), 2.10 (dd, $J = 14.8, 6.8$ Hz, 2 H), 1.59–1.68 (m, 4 H), 1.20–1.34 (m, 8 H), 0.85 (t, $J = 6.8$ Hz, 3 H); ^{13}C NMR (100 MHz, CDCl_3) δ 199.4, 137.4, 115.3, 44.1, 32.7, 31.5, 28.8, 28.7, 28.1, 25.6, 22.5, 14.0; IR (neat) 3077, 2924, 2855, 1689, 1641, 1454, 1412, 1378, 1344, 1258, 1182, 1123, 1041 cm^{-1} ; HRMS (EI) found 228.1554 [calcd for $\text{C}_{13}\text{H}_{24}\text{OS}$ (M) $^+$ 228.1548]; [For **2.26**, colorless oil, 74%]: R_f 0.58 (hexanes/EtOAc, 20/1); ^1H NMR (400 MHz, CDCl_3) δ 5.76 (ddt, $J = 16.8, 10.4, 6.8$ Hz, 1 H), 4.98 (d, $J = 16.8$ Hz, 1 H), 4.92 (d, $J = 10.4$ Hz, 1 H), 2.85 (t, $J = 7.2$ Hz, 2 H), 2.51 (t, $J = 7.6$ Hz, 2 H), 2.04 (dd, $J = 14.0, 6.8$ Hz, 2 H), 1.52–1.68 (m, 4 H), 1.41–1.48 (m, 2 H), 1.20–1.31 (m, 8 H), 0.85 (t, $J = 7.2$ Hz, 3 H); ^{13}C NMR (100 MHz, CDCl_3) δ 199.5, 138.2, 114.6, 44.1, 33.1, 31.6, 29.0, 28.85, 28.83, 28.5, 27.9, 25.6, 22.5, 14.0; IR (neat) 3077, 2925, 2855, 1689, 1641, 1457, 1413, 1378, 1294, 1261, 1123, 1042 cm^{-1} ; HRMS (EI) found 242.1705 [calcd for $\text{C}_{14}\text{H}_{26}\text{OS}$ (M) $^+$ 242.1704];

General procedure for the preparation of largazole analogues 11–13

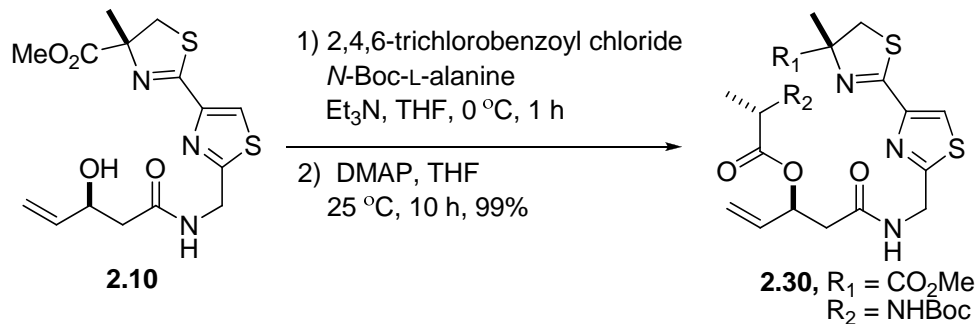


To a solution of macrocycle **2.3** (11 mg, 0.025 mmol) in dry toluene (1.0 mL, 0.025 M) were added thioester **7** (0.20 mL, 0.25 M solution in toluene) and Grubbs' second-generation catalyst (0.20 mL, 0.025 M solution in toluene). The resulting mixture was stirred at 110 °C for 1 h. An addition of thioester **2.24** (0.10 mL, 0.25 M solution in toluene) and Grubbs' second-generation catalyst (0.10 mL, 0.025 M solution in toluene) was repeated three times every 1 h. The reaction mixture was cooled to room temperature and a few drops of DMSO were added. The mixture was stirred for overnight and concentrated *in vacuo*. The residue was purified by column chromatography (silica gel, hexanes/EtOAc/CH₃OH = 10:10:1) to afford **2.27** ((*E*)-isomer only) as a colorless oil (6.3 mg, 41%, 56% based on recovered starting material): R_f 0.39 (hexanes/EtOAc/CH₃OH, 10/10/1); $[\alpha]_D^{29.7} = +11.5$ (*c* 0.080, CHCl₃); ¹H NMR (400 MHz, CDCl₃) δ 7.76 (s, 1 H), 7.16 (d, *J* = 9.6 Hz, 1 H), 6.42 (dd, *J* = 9.2, 3.2 Hz, 1 H), 5.81 (dt, *J* = 16.8, 6.8 Hz, 1 H), 5.69 (dd, *J* = 16.8, 6.8 Hz, 1 H), 5.66 (dt, *J* = 6.8, 2.8 Hz, 1 H), 5.27 (dd, *J* = 17.2, 9.2 Hz, 1 H), 4.60 (dd, *J* = 9.6, 3.6 Hz, 1 H), 4.27 (dd, *J* = 17.2, 3.2 Hz, 1 H), 4.04 (d, *J* = 11.2 Hz, 1 H), 3.50 (d, *J* = 6.8 Hz, 2 H), 3.27 (d, *J* = 11.2 Hz, 1 H), 2.82 (dd, *J* = 16.4, 10.0 Hz, 1 H), 2.68 (dd, *J* = 16.4, 2.8 Hz, 1 H), 2.52 (t, *J* = 7.2 Hz, 2 H), 2.06–2.16 (m, 1 H), 1.86 (s, 3 H), 1.60–1.68 (m, 2 H), 1.20–1.34 (m, 8 H), 0.88 (br t, *J* = 6.8 Hz, 3 H), 0.69 (d, *J* = 6.8 Hz, 3 H), 0.52 (d, *J* = 6.8 Hz, 3 H); ¹³C NMR (100 MHz, CDCl₃) δ 198.8, 173.5, 169.2, 168.8, 167.9, 164.5, 147.5, 129.6, 129.5, 124.1, 84.5, 71.5, 57.7, 44.0, 43.3, 41.1, 40.3, 34.1, 31.6, 30.3, 28.9, 25.5, 24.2, 22.6, 18.9, 16.7, 14.0; IR (neat) 3732, 3709, 3628, 3373, 2956, 2928, 1734, 1683, 1507, 1257,

1029 cm^{-1} ; HRMS (FAB) found 609.2242 [calcd for $\text{C}_{28}\text{H}_{41}\text{N}_4\text{O}_5\text{S}_3$ ($\text{M}+\text{H}$)⁺ 609.2239]; [For **2.28**, 54%]: R_f 0.42 (hexanes/EtOAc/ CH_3OH , 10/10/1); $[\alpha]_D^{29.8} = +17.4$ (c 0.092, CHCl_3); ^1H NMR (400 MHz, CDCl_3) δ 7.76 (s, 1 H), 7.16 (d, $J = 9.6$ Hz, 1 H), 6.42 (dd, $J = 9.2, 3.2$ Hz, 1 H), 5.82 (dt, $J = 15.2, 6.8$ Hz, 1 H), 5.63–5.70 (m, 1 H), 5.46 (dd, $J = 15.2, 7.2$ Hz, 1 H), 5.28 (dd, $J = 17.6, 9.2$ Hz, 1 H), 4.60 (dd, $J = 9.6, 3.6$ Hz, 1 H), 4.27 (dd, $J = 17.6, 3.2$ Hz, 1 H), 4.04 (d, $J = 11.2$ Hz, 1 H), 3.27 (d, $J = 11.2$ Hz, 1 H), 2.85 (dd, $J = 16.8, 10.4$ Hz, 1 H), 2.83 (t, $J = 7.2$ Hz, 2 H), 2.69 (dd, $J = 16.4, 2.8$ Hz, 1 H), 2.53 (t, $J = 7.6$ Hz, 2 H), 2.12 (dd, $J = 14.0, 7.2$ Hz, 2 H), 2.08–2.16 (m, 1 H), 1.87 (s, 3 H), 1.60–1.68 (m, 4 H), 1.20–1.34 (m, 8 H), 0.88 (br t, $J = 7.2$ Hz, 3 H), 0.69 (d, $J = 6.8$ Hz, 3 H), 0.51 (d, $J = 6.8$ Hz, 3 H); ^{13}C NMR (100 MHz, CDCl_3) δ 199.6, 173.5, 169.4, 168.9, 167.9, 164.4, 147.5, 134.2, 127.3, 124.1, 84.4, 72.3, 57.7, 44.1, 43.3, 41.1, 40.6, 34.2, 31.6, 31.1, 28.90, 28.88, 28.7, 28.0, 25.7, 24.2, 22.6, 18.9, 16.6, 14.0; IR (neat) 3726, 3708, 3628, 3599, 3371, 2928, 2855, 1734, 1683, 1507, 1258, 1029 cm^{-1} ; HRMS (FAB) found 637.2548 [calcd for $\text{C}_{30}\text{H}_{45}\text{N}_4\text{O}_5\text{S}_3$ ($\text{M}+\text{H}$)⁺ 637.2552]; [For **2.29**, 44%]: R_f 0.45 (hexanes/EtOAc/ CH_3OH , 10/10/1); $[\alpha]_D^{29.8} = +20.3$ (c 0.069, CHCl_3); ^1H NMR (400 MHz, CDCl_3) δ 7.76 (s, 1 H), 7.16 (d, $J = 9.2$ Hz, 1 H), 6.42 (dd, $J = 9.2, 3.2$ Hz, 1 H), 5.82 (dt, $J = 15.2, 6.8$ Hz, 1 H), 5.62–5.69 (m, 1 H), 5.43 (dd, $J = 15.2, 6.8$ Hz, 1 H), 5.28 (dd, $J = 17.6, 9.6$ Hz, 1 H), 4.60 (dd, $J = 9.6, 3.6$ Hz, 1 H), 4.27 (dd, $J = 17.6, 3.2$ Hz, 1 H), 4.04 (d, $J = 11.2$ Hz, 1 H), 3.27 (d, $J = 11.2$ Hz, 1 H), 2.84 (dd, $J = 16.0, 8.8$ Hz, 1 H), 2.83 (t, $J = 7.2$ Hz, 2 H), 2.68 (dd, $J = 16.0, 2.8$ Hz, 1 H), 2.53 (t, $J = 7.6$ Hz, 2

H), 2.04–2.15 (m, 1 H), 2.04 (dd, $J = 14.0, 6.8$ Hz, 2 H), 1.87 (s, 3 H), 1.60–1.68 (m, 2 H), 1.50–1.60 (m, 2 H), 1.39–1.48 (m, 2 H), 1.20–1.34 (m, 8 H), 0.87 (br t, $J = 6.8$ Hz, 3 H), 0.68 (d, $J = 6.8$ Hz, 3 H), 0.51 (d, $J = 6.8$ Hz, 3 H); ^{13}C NMR (100 MHz, CDCl_3) δ 199.7, 173.6, 169.5, 168.9, 167.9, 164.5, 147.5, 135.2, 126.7, 124.1, 84.4, 72.3, 57.7, 44.1, 43.3, 41.1, 40.6, 34.2, 31.6, 29.0, 28.9, 28.5, 27.9, 25.7, 24.2, 22.6, 18.9, 16.6, 14.0; IR (neat) 3726, 3709, 3627, 3600, 2927, 1734, 1683, 1507, 1259, 1219 cm^{-1} ; HRMS (FAB) found 651.2706 [calcd for $\text{C}_{31}\text{H}_{47}\text{N}_4\text{O}_5\text{S}_3$ ($\text{M}+\text{H}$) $^+$ 651.2709];

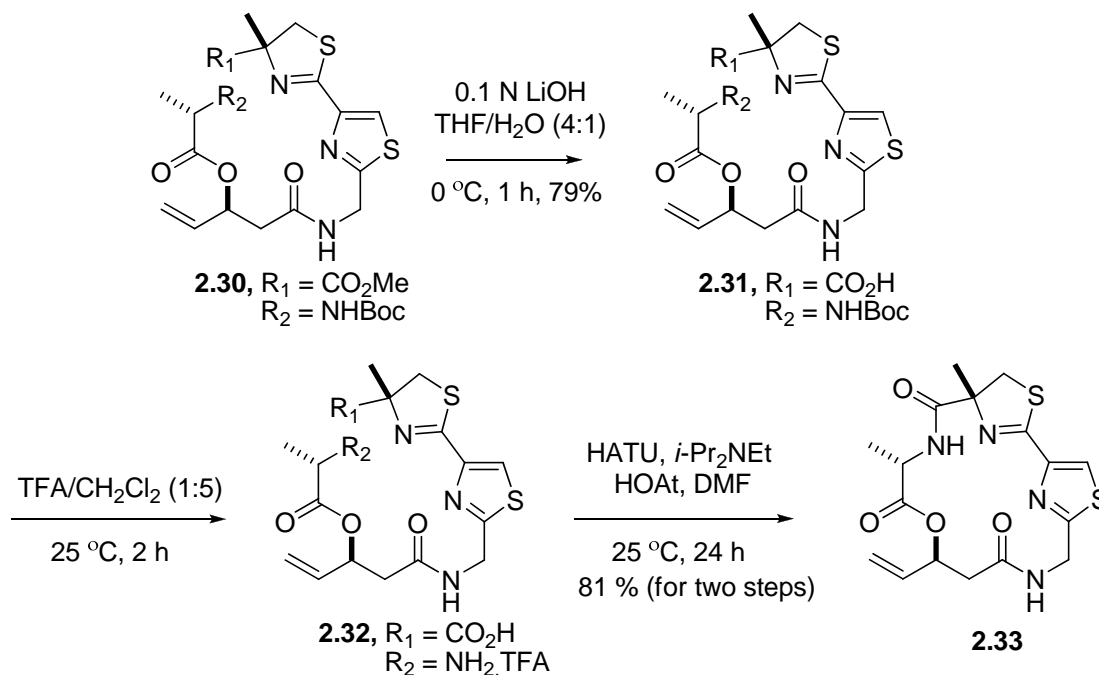
Preparation of ester **2.30**



To a stirred solution of *N*-Boc-L-alanine (22 mg, 0.114 mmol) and Et_3N (0.018 mL, 0.13 mmol) in THF (1.1 mL, 0.10 M) was added 2,4,6-trichlorobenzoyl chloride (0.018 mL, 0.122 mmol) at $0\text{ }^\circ\text{C}$. After being stirred at the same temperature for 1 h, to the resulting mixture was added a solution of **2.10** (29 mg, 0.079 mmol) and DMAP (12 mg, 0.098 mmol). After being stirred at room temperature for 10 h, the reaction mixture was quenched with half-saturated aqueous NH_4Cl solution and diluted with EtOAc. The layers were separated, and the aqueous layer was extracted with EtOAc. The combined organic layers were washed with brine, dried over anhydrous Na_2SO_4 , and concentrated

in vacuo. The residue was purified by column chromatography (silica gel, hexanes/EtOAc/CH₃OH, 10/10/1) to afford **2.30** as a colorless oil (42.2 mg, 99%): R_f 0.30 (hexanes/EtOAc/CH₃OH, 10/10/1); [α]^{29.7}_D = +2.00 (*c* 0.2, CHCl₃); ¹H NMR (400 MHz, CDCl₃) δ 7.92 (s, 1 H), 7.24 (br, 1 H), 5.89 (ddd, *J* = 16.4, 10.0, 5.6 Hz, 1 H), 5.63 (ddd, *J* = 5.6, 5.6, 5.6 Hz, 1 H), 5.32 (d, *J* = 16.8 Hz, 1 H), 5.22 (d, *J* = 10.4 Hz, 1 H), 5.08 (d, *J* = 6.4 Hz, 1 H), 4.73 (dd, *J* = 16.4, 6.4 Hz, 1 H), 4.70 (dd, *J* = 16.4, 6.0 Hz, 1 H), 4.15 (m, 1 H), 3.86 (d, *J* = 11.2 Hz, 1 H), 3.78 (s, 3 H), 3.25 (d, *J* = 11.2 Hz, 1 H), 2.69 (dd, *J* = 14.8, 4.8 Hz, 1 H), 2.60 (dd, *J* = 14.4, 6.2 Hz, 1 H), 1.63 (s, 3 H), 1.38 (s, 9 H), 1.34 (d, *J* = 6.8 Hz, 3 H); ¹³C NMR (100 MHz, CDCl₃) δ 173.8, 172.8, 169.3, 168.8, 168.1, 155.7, 148.5, 134.3, 122.2, 118.1, 84.7, 80.5, 72.4, 53.1, 49.9, 41.7, 41.3, 28.5, 28.0, 24.1, 17.8; IR (neat) 3734, 3318, 1734, 1715, 1684, 1558, 1522, 1290, 1164, 772 cm⁻¹; HRMS (FAB) found 541.1799 [calcd for C₂₃H₃₃N₄O₇S₂ (M+H)⁺ 541.1790].

Preparation of macrocycle 18

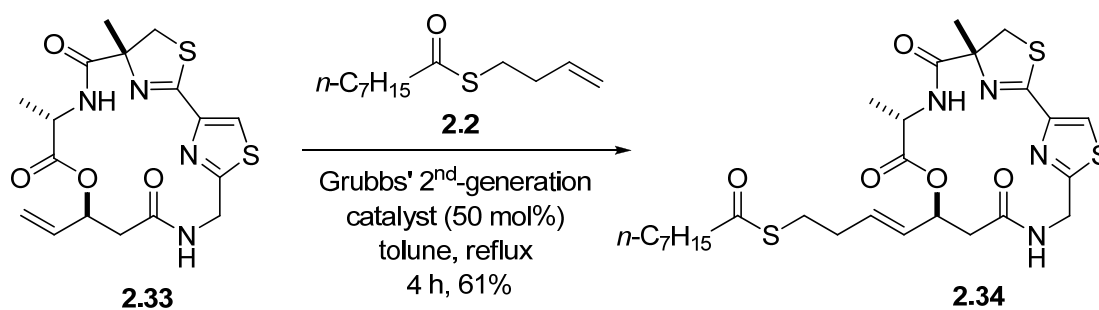


To a stirred solution of **2.30** (72.5 mg, 0.13 mmol) in THF/H₂O (4:1, 4 mL) was added dropwise 0.1 N LiOH (1.4 mL, 0.14 mmol) at 0 °C for 15 min. After being stirred at 0 °C for 1 h, the resulting mixture was acidified with 1 M KHSO₄ solution to pH ~3.0 at 0 °C, and diluted with EtOAc. The layers were separated, and the aqueous layer was extracted with EtOAc. The combined organic layers were washed with brine, dried over anhydrous Na₂SO₄, and concentrated *in vacuo*. The residue was purified by column chromatography (silica gel, CH₃OH/EtOAc, 3/7) to afford **2.31** as a colorless oil (55.6 mg, 79%). The carboxylic acid **2.31** (14.2 mg, 0.027 mmol) was treated with TFA/CH₂Cl₂ (1:5, 0.41 mL). After being stirred at 25 °C for 2 h, the residue was purged with N₂ to remove TFA and CH₂Cl₂, then washed with Et₂O four times to remove remaining TFA. To a solution of the crude **2.32** in DMF (27 mL, 1 mM) was added HATU (22 mg, 0.054 mmol), HOAt (7.3 mg, 0.054 mmol), and *i*-Pr₂NEt (0.029 mL,

0.162 mmol). The reaction mixture was stirred at room temperature for 18 h and then concentrated *in vacuo*. The residue was diluted with H₂O and EtOAc. The layers were separated, and the aqueous layer was extracted with EtOAc. The combined organic layers were washed with aqueous NaHCO₃ solution, brine, dried over anhydrous Na₂SO₄, and concentrated *in vacuo*. The residue was purified by column chromatography (silica gel, hexanes/EtOAc/CH₃OH, 10/10/1) to afford **2.33** as a white solid (8.9 mg, 81% for two steps). [For **2.31**]: NMR (400 MHz, CD₃OD) δ 8.16 (s, 1 H), 6.96 (d, $J = 7.6$ Hz, 1 H), 5.89 (ddd, $J = 17.2, 10.8, 6.0$ Hz, 1 H), 5.66 (ddd, $J = 7.6, 5.6, 5.6$ Hz, 1 H), 5.31 (d, $J = 17.6$ Hz, 1 H), 5.20 (d, $J = 10.4$ Hz, 1 H), 4.69 (d, $J = 16$ Hz, 1 H), 4.63 (d, $J = 16$ Hz, 1 H), 4.13 (m, 1 H), 3.85 (d, $J = 11.2$ Hz, 1 H), 3.32 (d, $J = 11.2$ Hz, 1 H), 2.68 (dd, $J = 14.4, 7.2$ Hz, 1 H), 2.62 (dd, $J = 14.4, 5.6$ Hz, 1 H), 1.58 (s, 3 H), 1.43 (s, 9 H), 1.31 (d, $J = 7.6$ Hz, 3 H); HRMS (FAB) found 527.1633 [calcd for C₂₂H₃₁N₄O₇S₂ (M+H)⁺ 527.1634]. [For crude **2.32**]: ¹H NMR (400 MHz, CD₃OD) δ 8.29 (s, 1 H), 5.92 (ddd, $J = 17.2, 10.8, 6.4$ Hz, 1 H), 5.78 (ddd, $J = 7.2, 6.0, 6.0$ Hz, 1 H), 5.36 (d, $J = 17.2$ Hz, 1 H), 5.28 (d, $J = 10.4$ Hz, 1 H), 4.71 (d, $J = 16$ Hz, 1 H), 4.65 (d, $J = 16$ Hz, 1 H), 4.11 (m, 1 H), 3.94 (d, $J = 11.6$ Hz, 1 H), 3.45 (d, $J = 11.6$ Hz, 1 H), 2.74 (dd, $J = 14.8, 7.6$ Hz, 1 H), 2.69 (dd, $J = 14.8, 5.6$ Hz, 1 H), 1.67 (s, 3 H), 1.53 (d, $J = 7.2$ Hz, 3 H); HRMS (FAB) found 427.1102 [calcd for C₁₇H₂₃N₄O₅S₂ (M+H)⁺ 427.1104]. [For **2.33**]: R_f 0.20 (hexanes/EtOAc/CH₃OH, 10/10/1); $[\alpha]_D^{29.7} = +64.9$ (*c* 0.13, CH₃OH); ¹H NMR (400 MHz, CDCl₃) δ 7.74 (s, 1 H), 7.28 (d, $J = 6.8$ Hz, 1 H), 6.37 (d, $J = 5.6$ Hz, 1 H), 5.85 (ddd, $J = 16.8, 10.4, 6.0$ Hz, 1 H), 5.76–5.80 (m, 1 H), 5.35 (d, $J = 17.2$ Hz, 1 H), 5.27

(d, $J = 10.4$ Hz, 1 H), 5.25 (dd, $J = 17.2, 9.2$ Hz, 1 H), 4.56 (m, 1 H), 4.28 (dd, $J = 17.6, 4.0$ Hz, 1 H), 4.05 (d, $J = 11.2$ Hz, 1 H), 3.26 (d, $J = 11.6$ Hz, 1 H), 2.91 (dd, $J = 16.8, 10.4$ Hz, 1 H), 2.73 (dd, $J = 16.4, 2.4$ Hz, 1 H), 1.84 (s, 3 H), 1.30 (d, $J = 6.8$ Hz, 3 H); ^{13}C NMR (100 MHz, CDCl_3) δ 173.7, 170.0, 169.7, 167.8, 164.4, 147.7, 134.8, 124.5, 118.3, 84.4, 72.5, 49.7, 43.2, 41.5, 40.0, 24.9, 19.4; IR (neat) 3364, 2927, 1739, 1667, 1504, 1259, 887, cm^{-1} ; HRMS (FAB) found 409.1002 [calcd for $\text{C}_{17}\text{H}_{21}\text{N}_4\text{O}_4\text{S}_2$ ($\text{M}+\text{H}$) $^+$ 409.1004].

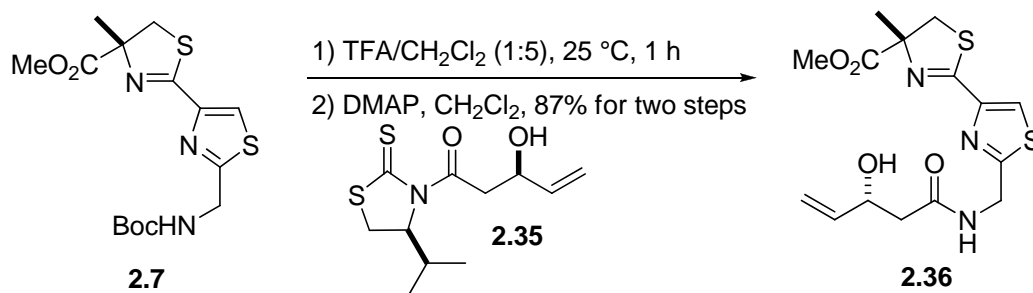
Preparation of alanine analogue **2.32**



To a solution of macrocycle **2.33** (10 mg, 0.025 mmol) in dry toluene (0.95 mL, 0.026 M) were added thioester **2.2** (0.19 mL, 0.26 M solution in toluene) and Grubbs' second-generation catalyst (0.10 mL, 0.052 M in solution toluene). The resulting mixture was stirred at 110 °C for 1 h. An addition of thioester **2.2** (0.10 mL, 0.26 M solution in toluene) and Grubbs' second-generation catalyst (0.048 mL, 0.052 M solution in toluene) was repeated three times every 1 h. The reaction mixture was cooled to 25 °C and a few drops of DMSO were added. The mixture was stirred for overnight and concentrated *in*

vacuo. The residue was purified by column chromatography (silica gel, hexanes/EtOAc/CH₃OH, 15:15:1 to 10:10:1) to afford **2.34** ((*E*)-isomer only) as a white solid (8.6 mg, 61%): R_f 0.35 (hexanes/EtOAc/CH₃OH, 10/10/1); [α]^{29.7}_D = +10.0 (*c* 0.05, CHCl₃); ¹H NMR (400 MHz, CDCl₃) δ 7.73 (s, 1 H), 7.18 (d, *J* = 8.8 Hz, 1 H), 6.35 (dd, *J* = 9.6, 4 Hz, 1 H), 5.81 (dd, *J* = 16.0, 6.8 Hz, 1 H), 5.73–5.51 (m, 1 H), 5.51 (dd, *J* = 15.6, 7.2 Hz, 1 H), 5.29 (dd, *J* = 17.6, 9.2 Hz, 1 H), 4.54 (m, 1 H), 4.28 (dd, *J* = 17.2, 3.6 Hz, 1 H), 4.05 (d, *J* = 11.2 Hz, 1 H), 3.25 (d, *J* = 11.2 Hz, 1 H), 2.90 (dd, *J* = 16.8, 10.8 Hz, 1 H), 2.89 (t, *J* = 6.8 Hz, 2 H), 2.69 (dd, *J* = 16.8, 2.4 Hz, 1 H), 2.53 (t, *J* = 7.6 Hz, 2 H), 2.30 (q, *J* = 6.8 Hz, 2 H), 1.84 (s, 3 H), 1.63–1.68 (m, 2 H), 1.29 (d, *J* = 6.8 Hz, 3 H), 1.26–1.29 (m, 8 H), 0.88 (t, *J* = 7.2 Hz, 3 H), 0.69 (d, *J* = 6.8 Hz, 3 H), 0.52 (d, *J* = 7.2 Hz, 3 H); ¹³C NMR (100 MHz, CDCl₃) δ 199.4, 173.4, 169.9, 169.6, 167.6, 163.5, 147.6, 132.9, 128.3, 124.3, 84.2, 72.1, 49.5, 44.1, 43.0, 41.3, 40.1, 35.2, 32.2, 31.6, 28.9, 27.9, 25.6, 24.7, 22.6, 19.1, 14.1; IR (neat) 3374, 2924, 2853, 1734, 1678, 1502, 1449, 1260, 1029 cm⁻¹; HRMS (FAB) found 595.2085 [calcd for C₂₇H₃₉N₄O₅S₃ (M+H)⁺ 595.2082].

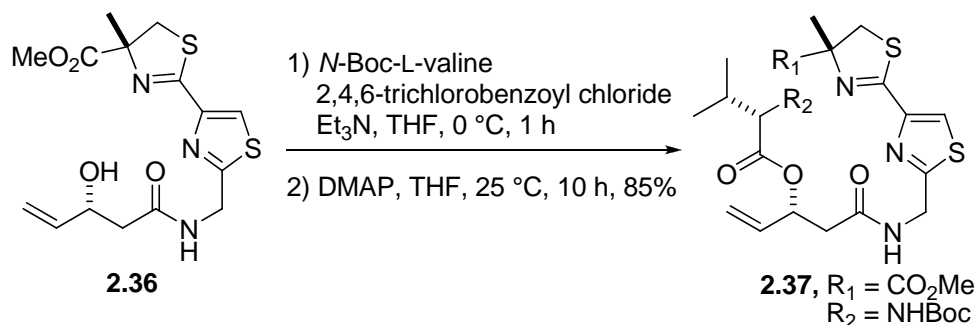
Preparation of amide **2.36**



Compound **2.7** (51 mg, 0.14 mmol) was treated with TFA/CH₂Cl₂ (1:5, 2.0 ml) at 25 °C. The resulting mixture was stirred at 25 °C for 1 h, and then purged with N₂ to remove TFA and CH₂Cl₂. The residue was washed with Et₂O four times to remove remaining TFA. This crude TFA·amine salt was carried to the next step without further purification. To a solution of TFA·amine salt in CH₂Cl₂ was added DMAP (51 mg, 0.41 mmol) and **2.35** (39 mg, 0.15 mmol). The reaction mixture was stirred for 2 h at 25 °C, quenched with 0.1 N HCl. The layers were separated, and the aqueous layer was extracted with EtOAc. The combined organic layers were washed with brine, dried over anhydrous Na₂SO₄, and concentrated *in vacuo*. The residue was purified by column chromatography (silica gel; hexanes/EtOAc/CH₃OH = 10/10/1) to afford **2.36** as a colorless oil (44 mg, 87%): R_f 0.40 (hexanes/EtOAc/CH₃OH, 10/10/1); [α]^{26.2}_D = -3.15 (*c* 0.73, CHCl₃); ¹H NMR (400 MHz, CDCl₃) δ 7.91 (s, 1 H), 7.27 (t, *J* = 6.0 Hz, 1 H), 5.85 (ddd, *J* = 17.2, 10.4, 5.6 Hz, 1 H), 5.27 (d, *J* = 17.2 Hz, 1 H), 5.10 (d, *J* = 10.4 Hz, 1 H), 4.71 (d, *J* = 6.0 Hz, 1 H), 4.70 (d, *J* = 6.0 Hz, 1 H), 4.48–4.56 (m, 1 H), 3.85 (d, *J* = 11.2 Hz, 1 H), 3.77 (s, 3 H), 3.25 (d, *J* = 11.2 Hz, 1 H), 2.51 (dd, *J* = 15.2, 3.6 Hz, 1 H), 2.42 (dd, *J* = 15.2,

8.4 Hz, 1 H), 1.61 (s, 3 H); ^{13}C NMR (100 MHz, CDCl_3) δ 173.5, 171.9, 167.9, 162.7, 148.1, 139.0, 122.3, 115.3, 84.4, 69.3, 52.9, 42.4, 41.4, 40.7, 23.9; IR (neat) 3298, 3084, 2952, 1733, 1653, 1603, 1540, 1436, 1288, 1237, 1167, 1121 cm^{-1} ; HRMS (FAB) found 370.0890 [calcd for $\text{C}_{15}\text{H}_{20}\text{N}_3\text{O}_4\text{S}_2$ ($\text{M}+\text{H}$) $^+$ 370.0895].

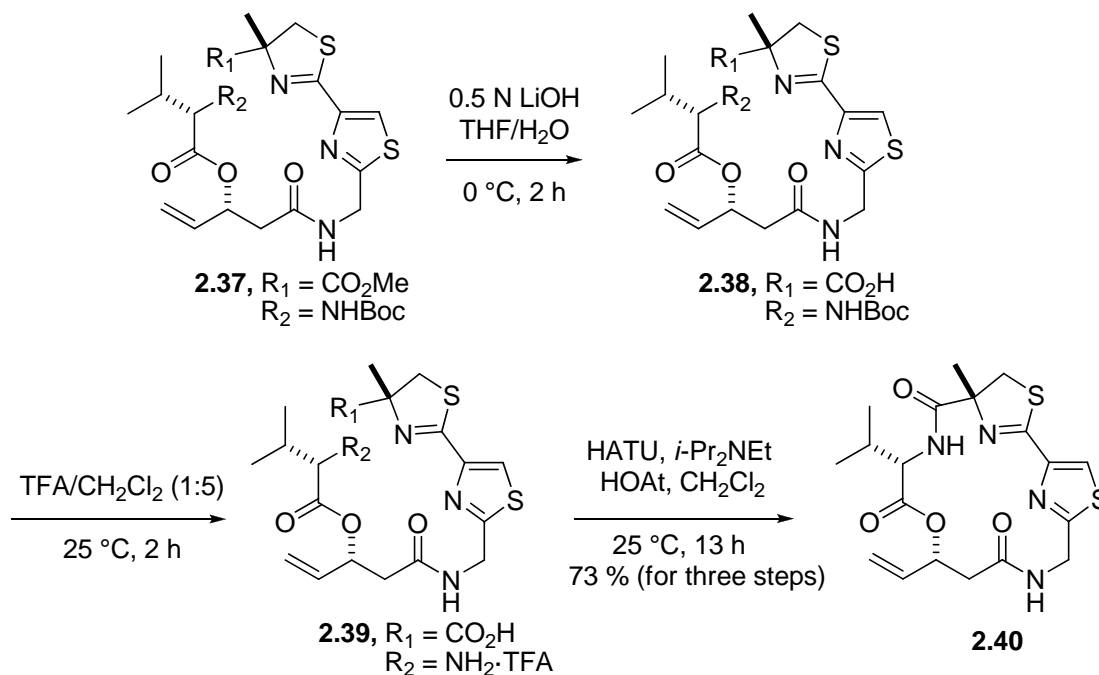
Preparation of ester 24



To a stirred solution of *N*-Boc-L-valine (39 mg, 0.18 mmol) and Et_3N (0.03 mL, 0.19 mmol) in THF (2.0 mL, 0.09 M) was added 2,4,6-trichlorobenzoyl chloride (0.03, 0.18 mmol) at $0\text{ }^\circ\text{C}$. After being stirred at $0\text{ }^\circ\text{C}$ for 1 h, to the resulting mixture were added a solution of **2.36** (44 mg, 0.12 mmol) and DMAP (18 mg, 0.14 mmol). After being stirred at $25\text{ }^\circ\text{C}$ for 10 h, the reaction mixture was quenched with half-saturated aqueous NH_4Cl solution and diluted with EtOAc. The layers were separated, and the aqueous layer was extracted with EtOAc. The combined organic layers were washed with brine, dried over anhydrous Na_2SO_4 , and concentrated *in vacuo*. The residue was purified by column chromatography (silica gel, hexanes/EtOAc/ CH_3OH , 8/8/1) to afford **2.37** as a colorless oil (58 mg, 85%): R_f 0.50 (hexanes/EtOAc/ CH_3OH , 8/8/1); $[\alpha]_D^{26.0} = -2.31$ (*c*

0.95, CHCl₃); ¹H NMR (400 MHz, CDCl₃) δ 7.91 (s, 1 H), 7.90 (t, *J* = 6.0 Hz, 1 H), 5.83 (ddd, *J* = 16.8, 10.4, 6.0 Hz, 1 H), 5.68 (dd, *J* = 12.8, 6.4 Hz, 1 H), 5.31 (d, *J* = 16.8 Hz, 1 H), 5.20 (d, *J* = 10.4 Hz, 1 H), 5.01 (d, *J* = 8.8 Hz, 1 H), 4.72 (d, *J* = 6.0 Hz, 1 H), 4.69 (d, *J* = 6.0 Hz, 1 H), 4.13 (dd, *J* = 8.8, 4.4 Hz, 1 H), 3.96 (dd, *J* = 8.0, 6.4 Hz, 1 H), 3.85 (d, *J* = 11.2 Hz, 1 H), 3.77 (s, 3 H), 3.25 (d, *J* = 11.2 Hz, 1 H), 2.63 (dd, *J* = 14.8, 8.4 Hz, 1 H), 2.56 (dd, *J* = 14.8, 5.2 Hz, 1 H), 2.04–2.12 (m, 1 H), 1.62 (s, 3 H), 1.40 (s, 9 H), 0.90 (d, *J* = 6.8 Hz, 3 H), 0.81 (d, *J* = 6.8 Hz, 3 H); ¹³C NMR (100 MHz, CDCl₃) δ 173.5, 171.1, 168.9, 167.76, 162.6, 155.8, 148.4, 134.5, 122.0, 117.9, 84.4, 79.8, 72.3, 58.6, 52.9, 41.4, 41.1, 40.9, 30.9, 28.2, 23.9, 19.0, 17.3; IR (neat) 3726, 3708, 3628, 3326, 2972, 1735, 1604, 1507, 1456, 1367, 1287, 1240, 1159, 1120 cm⁻¹; HRMS (FAB) found 569.2104 [calcd for C₂₅H₃₇N₄O₇S₂ (M+H)⁺ 569.2104].

Preparation of macrocycle 2.40

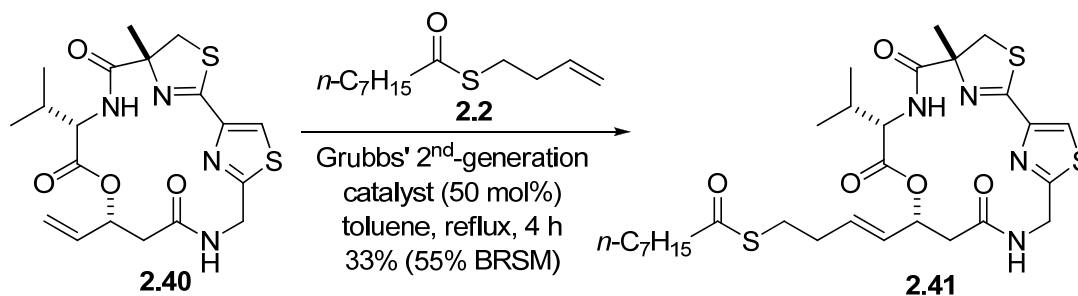


To a stirred solution of **2.37** (54 mg, 0.095 mmol) in THF/H₂O (4:1, 4.0 mL) was added dropwise 0.5 N LiOH (0.19 mL, 0.095 mmol) at 0 °C. After being stirred at 0 °C for 2 h, the resulting mixture was acidified with 1 M KHSO₄ solution to pH ~3.0, and diluted with EtOAc. The layers were separated, and the aqueous layer was extracted with EtOAc. The combined organic layers were washed with brine, dried over anhydrous Na₂SO₄, and concentrated *in vacuo*. This crude carboxylic acid **2.38** was carried to the next step without further purification. The carboxylic acid **2.38** was treated with TFA/CH₂Cl₂ (1:5, 1.5 mL). After being stirred at 25 °C for 2 h, the residue was purged with N₂ to remove TFA and CH₂Cl₂, then washed with Et₂O four times to remove remaining TFA. To a solution of the crude **2.39** in CH₂Cl₂ (100 mL, 1 mM) was added HATU (72 mg, 0.19 mmol), HOAt (26 mg, 0.19 mmol), and *i*-Pr₂NEt (0.066 mL, 0.38 mmol). The reaction mixture was stirred at 25 °C for 13 h and then concentrated *in*

vacuo. The residue was diluted with H₂O and EtOAc. The layers were separated, and the aqueous layer was extracted with EtOAc. The combined organic layers were washed with brine, dried over anhydrous Na₂SO₄, and concentrated *in vacuo*. The residue was purified by column chromatography (silica gel, hexanes/EtOAc/CH₃OH, 10/10/1) to afford **2.40** as a amorphous white solid (30 mg, 73%). [For crude **2.38**]: NMR (400 MHz, CD₃OD) δ 8.18 (s, 1 H), 5.90 (ddd, $J = 16.8, 10.8, 6.0$ Hz, 1 H), 5.66–5.76 (m, 1 H), 5.34 (d, $J = 16.8$ Hz, 1 H), 5.20 (d, $J = 10.8$ Hz, 1 H), 4.65 (d, $J = 12.4$ Hz, 2 H), 4.10 (d, $J = 6.0$ Hz, 1 H), 3.87 (d, $J = 11.6$ Hz, 1 H), 3.34 (d, $J = 11.6$ Hz, 1 H), 2.69 (dd, $J = 14.4, 8.8$ Hz, 1 H), 2.62 (dd, $J = 14.4, 5.2$ Hz, 1 H), 2.00–2.08 (m, 1 H), 1.62 (s, 3 H), 1.43 (s, 9 H), 0.89 (d, $J = 6.8$ Hz, 3 H), 0.85 (d, $J = 7.2$ Hz, 3 H); HRMS (FAB) found 555.1949 [calcd for C₂₄H₃₅N₄O₇S₂ (M+H)⁺ 555.1947]. [For crude **2.39**]: ¹H NMR (400 MHz, CD₃OD) δ 8.47 (s, 1 H), 5.92 (ddd, $J = 16.8, 10.4, 6.4$ Hz, 1 H), 5.78–5.85 (m, 1 H), 5.38 (d, $J = 16.8$ Hz, 1 H), 5.28 (d, $J = 10.4$ Hz, 1 H), 4.68 (d, $J = 9.6$ Hz, 2 H), 4.02 (d, $J = 12.0$ Hz, 1 H), 3.94 (d, $J = 4.4$ Hz, 1 H), 3.55 (d, $J = 12.0$ Hz, 1 H), 2.77 (dd, $J = 15.2, 8.4$ Hz, 1 H), 2.71 (dd, $J = 15.2, 4.8$ Hz, 1 H), 2.20–2.28 (m, 1 H), 1.73 (s, 3 H), 1.02 (d, $J = 6.8$ Hz, 3 H), 0.99 (d, $J = 7.2$ Hz, 3 H); HRMS (FAB) found 455.1424 [calcd for C₁₉H₂₇N₄O₅S₂ (M+H)⁺ 455.1423]. [For **2.40**]: R_f 0.30 (hexanes/EtOAc/CH₃OH, 8/8/1); amorphous white solid, $[\alpha]_{\text{D}}^{29.7} = +22.8$ (*c* 0.33, CH₃OH); ¹H NMR (400 MHz, CDCl₃) δ 7.74 (s, 1 H), 7.03 (d, $J = 9.6$ Hz, 1 H), 6.58 (dd, $J = 8.0, 4.0$ Hz, 1 H), 6.40 (ddd, $J = 17.2, 10.4, 8.0$ Hz, 1 H), 5.47 (ddd, $J = 8.0, 4.8, 2.8$ Hz, 1 H), 5.34 (d, $J = 17.2$ Hz, 1 H), 5.25 (d, $J = 10.4$ Hz, 1 H), 5.13 (dd, $J = 17.2, 8.0$ Hz, 1 H), 4.38 (dd, $J = 9.6, 7.2$ Hz, 1 H), 4.32

(dd, $J = 17.2, 4.0$ Hz, 1 H), 3.99 (d, $J = 11.6$ Hz, 1 H), 3.31 (d, $J = 11.2$ Hz, 1 H), 2.95 (dd, $J = 16.8, 4.8$ Hz, 1 H), 2.77 (dd, $J = 16.8, 2.8$ Hz, 1 H), 1.80–1.90 (m, 1 H), 1.80 (s, 3 H), 0.78 (d, $J = 6.8$ Hz, 3 H), 0.74 (d, $J = 6.8$ Hz, 3 H); ^{13}C NMR (100 MHz, CDCl_3) δ 173.4, 169.6, 168.1, 167.7, 164.3, 147.3, 134.9, 124.1, 119.4, 84.2, 73.7, 59.4, 43.6, 41.2, 39.7, 32.7, 24.9, 18.5, 18.1; IR (neat) 3375, 2968, 1741, 1667, 1592, 1510, 1253 cm^{-1} ; HRMS (FAB) found 437.1316 [calcd for $\text{C}_{19}\text{H}_{25}\text{N}_4\text{O}_4\text{S}_2$ ($\text{M}+\text{H}$) $^+$ 437.1317].

Preparation of C17-epimer analogue **2.41**



To a solution of macrocycle **2.40** (10 mg, 0.023 mmol) in dry toluene (1.0 mL, 0.023 M) were added thioester **2.2** (0.20 mL, 0.23 M solution in toluene) and Grubbs' second-generation catalyst (0.20 mL, 0.023 M solution in toluene). The resulting mixture was stirred at 110 °C for 1 h. An addition of thioester **2.2** (0.10 mL, 0.23 M solution in toluene) and Grubbs' second-generation catalyst (0.10 mL, 0.023 M solution in toluene) was repeated three times every 1 h. The reaction mixture was cooled to room temperature and a few drops of DMSO were added. The mixture was stirred for overnight and concentrated *in vacuo*. The residue was purified by column chromatography (silica gel,

hexanes/EtOAc/CH₃OH = 10:10:1) to afford **2.41** ((*E*)-isomer only) as a colorless oil (4.7 mg, 33%, 55% based on recovered starting material): *R*_f 0.43 (hexanes/EtOAc/CH₃OH, 10/10/1); [α]^{28.0}_D = +28.3 (*c* 0.067, CHCl₃); ¹H NMR (400 MHz, CDCl₃) δ 7.74 (s, 1 H), 7.02 (d, *J* = 9.2 Hz, 1 H), 6.52–6.58 (m, 1 H), 6.19 (dd, *J* = 15.2, 8.8 Hz, 1 H), 5.81 (dt, *J* = 15.2, 6.8 Hz, 1 H), 5.46 (ddd, *J* = 8.8, 4.4, 2.4 Hz, 1 H), 5.14 (dd, *J* = 17.2, 8.0 Hz, 1 H), 4.37 (dd, *J* = 9.6, 7.2 Hz, 1 H), 4.33 (dd, *J* = 17.2, 4.4 Hz, 1 H), 4.01 (d, *J* = 11.2 Hz, 1 H), 3.31 (d, *J* = 11.6 Hz, 1 H), 2.93 (dd, *J* = 16.4, 4.4 Hz, 1 H), 2.87 (t, *J* = 7.2 Hz, 2 H), 2.73 (d, *J* = 16.4, 2.4 Hz, 1 H), 2.50 (t, *J* = 7.6 Hz, 2 H), 2.28 (dt, *J* = 7.6, 6.8 Hz, 2 H), 1.80–1.88 (m, 1 H), 1.81 (s, 3 H), 1.58–1.66 (m, 2 H), 1.20–1.34 (m, 8 H), 0.87 (br t, *J* = 6.8 Hz, 3 H), 0.79 (d, *J* = 6.8 Hz, 3 H), 0.73 (d, *J* = 6.8 Hz, 3 H); ¹³C NMR (100 MHz, CDCl₃) δ 199.3, 173.4, 169.7, 168.0, 167.7, 164.2, 147.3, 134.5, 128.3, 124.0, 84.2, 73.3, 59.5, 44.1, 43.6, 41.3, 39.6, 32.7, 32.1, 31.6, 28.9, 27.8, 25.6, 24.9, 22.6, 18.6, 18.1, 14.0; IR (neat) 3726, 3708, 3627, 2929, 1683, 1507 cm⁻¹; HRMS (FAB) found 623.2402 [calcd for C₂₉H₄₃N₄O₅S₃ (M+H)⁺ 623.2396].

Biological Assays

Cell viability assay. HCT-116 cells were plated in 96-well plates (10,000 cells/well) with DMEM containing 10% FBS, and 24 h later treated with various concentrations of compounds or solvent control. After another 48 h of incubation, cell viability was measured using MTT according to the manufacturer's instructions (Promega).

Immunoblot analysis. HCT-116 cells (600,000 cells/well) were seeded in 6-well plates and 24 h later treated with various concentrations of compounds or solvent control. Following incubation for 8 h, whole-cell protein lysates were prepared using PhosphoSafe lysis buffer (Novagen) and protein concentration measured using the BCA Protein Assay kit (Pierce). Cell lysates containing 10 µg of protein were separated by SDS-PAGE, transferred to PVDF membranes, probed with antibodies and detected with the SuperSignal West Femto Maximum Sensitivity Substrate (Pierce). Anti-acetyl-histone H3 (Lys9/18) antibody was obtained from Millipore, anti-β-actin and anti-rabbit antibody were from Cell Signaling.

Cell-free HDAC enzymatic assay with HeLa nuclear extract. Assays were carried out according to the manufacturer's protocol (BIOMOL). Briefly, compounds or solvent control in 10 µL assay buffer were added to microtiter plate, then HDAC-enriched nuclear protein extract from HeLa cells (4 µg in 15 µL) was added. 25 µL assay buffer was used as blank. The assay plate was equilibrated at 37 °C, and then 25 µL of substrate *fluor de Lys*TM substrate was added to a final concentration of 50 µM. HDAC reaction

was allowed to proceed for 15 min and then stopped by addition of 50 μ L per well of 1X *fluor de Lys*TM Developer containing trichostatin A at 2 μ M. The plates were incubated for 15 min at 25 °C, and fluorescence was read (Ex 360 nm, Em 460 nm).

Recombinant HDAC1 and HDAC6 enzymatic assays. The assays were carried out by Reaction Biology Corp. (Malvern, PA) according to the following procedures. The full lengths of human genes of HDAC1 and HDAC6 were expressed by baculovirus expression system in Sf9 cells, with GST tags in *C* or *N*-terminal position, respectively. Enzymes stored in 50 mM Tris-HCl, pH 8.0, 138 mM NaCl, 20 mM glutathione, and 10% glycerol, and stable for >6 months at –80 °C, and the purity was checked by SDS-page. Peptide substrate, p53 residues 379–382 (RHKKAc), was conjugated with AMC (7-acetoxy-4-methyl coumarin) and used as the fluorogenic substrate at 50 μ M assay concentration. Compounds were dissolved in DMSO (1% final assay concentration). The reaction buffer contained 25 mM Tris-HCl, pH 8.0, 137 mM NaCl, 2.7 mM KCl, 1 mM MgCl₂, and 0.25 mg/mL BSA. HDAC1 and HDAC6 concentrations were 1.5 and 4 ng/ μ L. The HDAC reaction performed at 30 °C for 2 h before adding the developer reagent. The free AMC is detected with excitation of 360 nm and emission 460 nm at kinetic mode for 90 min. The initial velocity of an enzyme reaction was normalized and plotted with GraphPad Prism (GraphPad Software, Inc. La Jolla, CA, USA) to derive the IC₅₀ values.

Chapter 3

Total Synthesis of Brasilibactin A and Its Analogues

This chapter of the dissertation describes a total synthesis of brasilibactin A, a cytotoxic siderophore and its analogues. The chemistry described in total synthesis of brasilibactin A and its three diastereomeric analogues were applied in the synthesis of more hydrophilic analogue-Bbtan, iron transport studies of which will help to provide a better understanding of the biological activity demonstrated by mycobacterial siderophores.

3.1 Mycobactins

3.1.1 Iron acquisition in mycobacteria

Iron, an essential nutrient for virtually all forms of life, plays an important role in oxygen transport, electron transport and other vital biological processes ranging from respiration to DNA replication.⁸⁷ Thus, the acquisition of iron by an organism including mammals, vertebrates and microorganism like mycobacteria is essential for their survival.

Iron is elusive because it has low solubility at physiological pH. The effective concentration of Fe(III) at physiological conditions is approximately 10^{-9} M, which is far below the requirement to maintain life.⁸⁸ However, solubility of iron can be increased by 10^{-3} M per each unit pH drops, which means concentration of soluble iron is 10^{-3} M at pH = 5.⁸⁹ Therefore, bacteria and other microbes can grow at this acidic condition without any help from chelating agents. Mycobacteria are the source of a number of infectious

diseases in humans, including tuberculosis (*M. tuberculosis*) and leprosy (*M. leprae*). As with other pathogenic bacteria, mycobacteria can grow within the macrophages where the pH is between 6.1 and 6.5 at which the effective Fe(III) concentration is less than 10 ng/mL.⁹⁰

In order to grow and cause disease in a host, mycobacterial iron acquisition must compete against the host for its supply of iron. In higher organism, iron is bounded to hemeprotein, transferrin, lactoferrin and ferritin, which are iron-containing, transport and storage proteins (Figure 3.1).⁹¹ Therefore, the effective concentration of free iron is far lower than those required for pathogenic bacteria like mycobacteria.

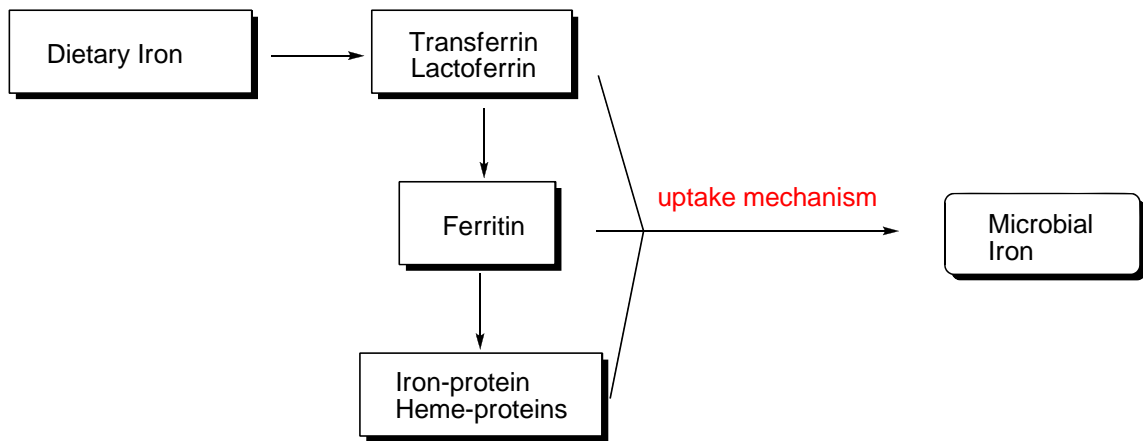


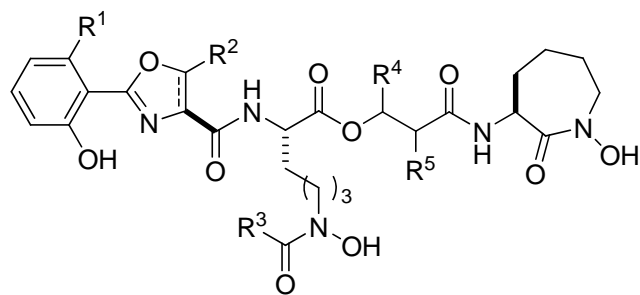
Figure 3.1 Sources of iron for pathogenic microorganisms within a host body

To circumvent the host's ability to sequester iron, mycobacteria have developed a number of iron acquisition mechanisms to fulfill their requirement of iron supply, among which mycobacteria produce iron-chelating molecules known as siderophores which can

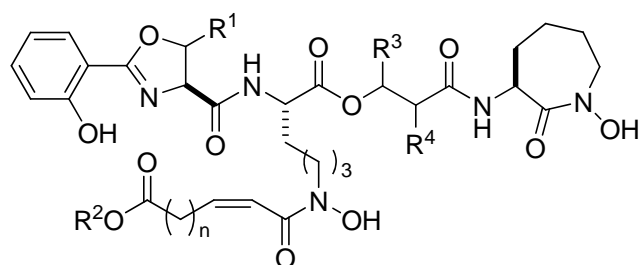
bind iron specifically and with high affinity to solubilize the metal iron and transport it to intracellular environment.⁹²

3.1.2 Siderophores

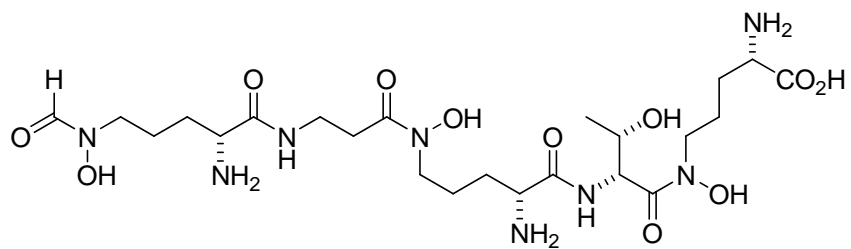
The siderophores provide a method of specific recognition and uptake by the bacteria cell through the interaction with receptor proteins on the surface of the cell. Mycobacteria can produce and utilize at least three types of siderophores which include mycobactins, carboxymycobactins, and exochelins (Figure 3.2).



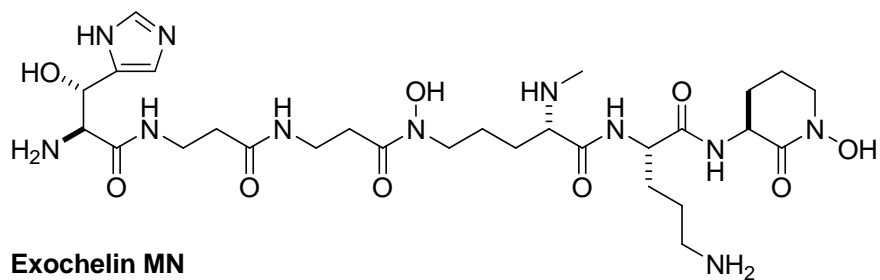
Mycobactins: $R^1, R^2, R^5 = \text{H or CH}_3$; $R_3, R_4 = \text{CH}_3, \text{CH}_2\text{CH}_3$ or long alkyl chain



Carboxymycobactins: $R^1, R^2, R^4 = \text{H or CH}_3$; $R^3 = \text{CH}_3$ or CH_2CH_3 ;



Exochelin MS



Exochelin MN

Figure 3.2 Structures of mycobacterial siderophores

Mycobactins

Mycobactin, a cell wall associated and salicylated-containing siderophore, contains four-residue depsipeptide backbone structure with a variety of side chain that acts as a tether to connect the molecule to the exterior side of the cell wall of the mycobacteria. As lipid soluble/water insoluble siderophores, mycobactins bind one atom of iron per molecule by three bidentate binding moieties with high affinity (10^{30}) as shown in [Figure 3.3](#). Due to its intracellular location, these molecules are not capable in practice to sequester iron from transferrin and ferritin, but good candidates for holding iron from other competing molecules.

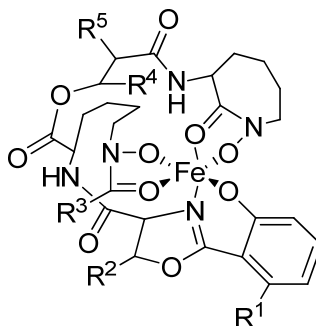
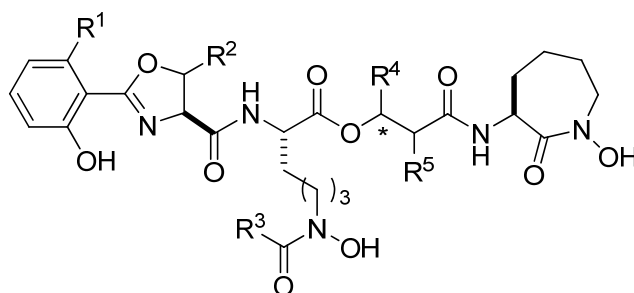


[Figure 3.3](#) Mycobactin-iron complex with three bidentate binding moieties

Generally, each mycobacterial species is corresponding with its unique mycobactin structure, which was used to identify an unknown mycobacterium.⁹³ Mycobactins can be divided into two classes, the P-type mycobactins and M-type mycobactins based on the location of the long alkyl chain. P-type mycobactins such as mycobactin P, S, T possess a long alkyl chain at the central hydroxamate ligand, while

M-type mycobactins such as mycobactin M, N contain a long alkyl chain in the central 3-hydroxy acid fragment (Figure 3.4).⁹⁴ There are a number of excellent, comprehensive reviews of mycobactins published so far.^{87, 94} Although mycobactins are structurally different from each other, they all possess common binding moieties such as a hydroxamate-modified ornithine residue, a cyclic hydroxamic acid moiety, and a 2-hydroxyphenyl oxazoline moiety.



P-Type Mycobactins

Mycobactin P: $R^1, R^5 = \text{CH}_3, R^2 = \text{H}, R^3 = \text{C}_{15-19}, R^4 = \text{CH}_2\text{CH}_3$

Mycobactin S: $R^1, R^2, R^5 = \text{H}, R^3 = \text{C}_{17-20}, R^4 = \text{CH}_3$ (S)

Mycobactin T: $R^1, R^2, R^5 = \text{H}, R^3 = \text{C}_{13-19}, R^4 = \text{CH}_3$ (R)

M-Type Mycobactins

Mycobactin M: $R^1 = \text{H}, R^2, R^3, R^5 = \text{CH}_3, R^4 = \text{C}_{15-18}$

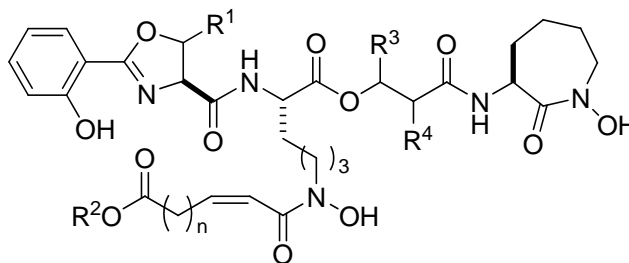
Mycobactin N: $R^1 = \text{H}, R^2, R^3, R^5 = \text{CH}_2\text{CH}_3, R^4 = \text{C}_{15-18}$

Figure 3.4 Structures of water-insoluble mycobactins

Extracellular siderophores: carboxymycobactins and exochelins

In the pathogenic mycobacteria, a water soluble siderophore, carboxymycobactin, differs from the P-type mycobactins in terms of the extended carbon chain ending with a carboxylate group or an ester group at the central hydroxamate ligand, which increases

the water solubility (Figure 3.5). Because of the presence of this group, ‘carboxymycobactins’ has been given to elucidate the structural similarity with mycobactins.



Carboxymycobactins

M. tuberculosis: $n=1-5$, $R^1, R^4 = H$, $R^2, R^3 = CH_3$

M. avium: $n=2-8$, $R^1, R^4 = CH_3$, $R^2 = H$, $R^3 = CH_2CH_3$

M. smegmatis: $n=2-9$, $R^1, R^2, R^4 = H$, $R^3 = CH_3$

Figure 3.5 Structures of water-soluble carboxymycobactins

In the nonpathogenic mycobacteria, water soluble siderophores are termed as ‘exochelins’, which are peptidic-based molecules. Besides the entirely different structures with carboxymycobactins, they possess different mechanisms in the process of mycobacterial iron transport.

3.1.3 Role of siderophores in mycobacterial iron transport

These three types of siderophores (membrane-bounded siderophores called mycobactins, and water soluble extracellular siderophores called exochelins for non-pathogenic and carboxymycobactins for pathogenic mycobacteria) play an important role

in mycobacterial iron acquisition and transport process. In most mycobacteria, extracellular siderophores are able to sequester iron from host sources such as transferrin and ferritin as well as other inorganic sources such as ferric hydroxide or ferric phosphate.⁸⁹ However, the mechanisms of uptake of iron by the two siderophores are different.

Uptake of ferri-exochelins across the cell envelope into intracellular environment requires the input of metabolic energy-ATP and involves a receptor protein (Rec),⁹⁵ while uptake of ferri-carboxymycobactins has been demonstrated to occur through an energy-independent process which possibly involves porin-mediated diffusion mechanism (Figure 3.6).⁸⁹ For both extracellular siderophores, the release of iron (Fe III) may be possibly associated with non-specific NADPH-dependent ferri-mycobactin reductase, and then Fe (II) can be incorporated into a variety of iron storage protein such as bacterioferritin.

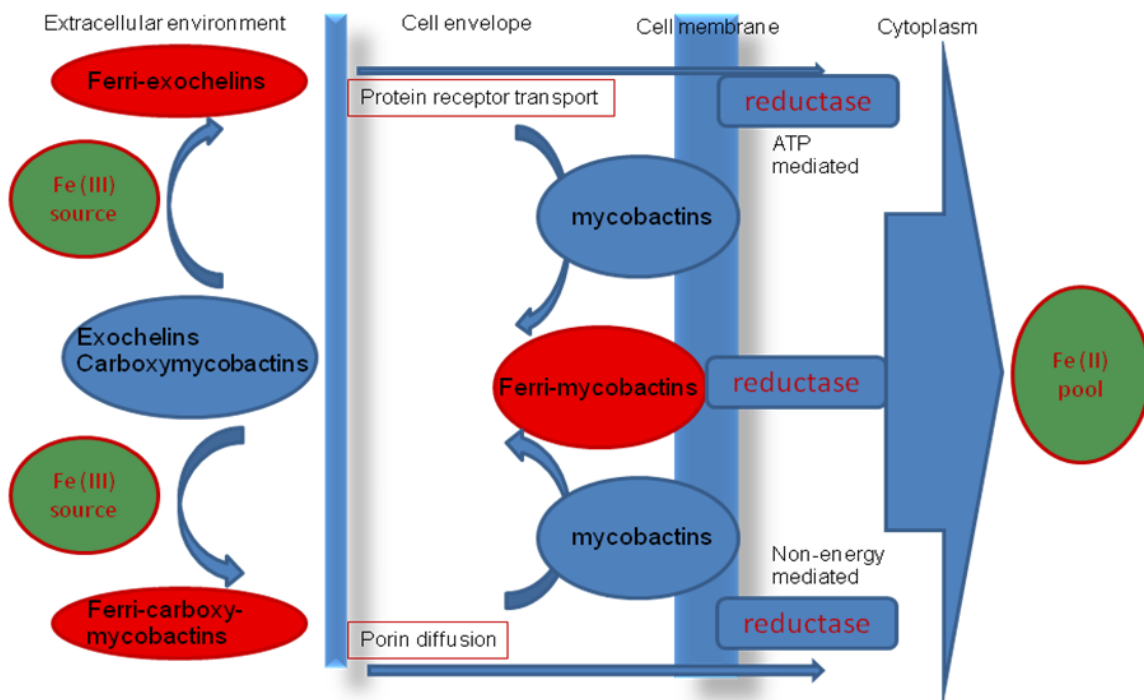


Figure 3.6 Proposed iron-uptake mechanism mediated by exochelins and carboxymycobactins

Mycobactins were proposed as a cellular membrane-bound temporary storage of Fe(III) when extracellular concentration of iron increases and cannot be uptake by extracellular siderophores, and then associate with ferri-reductase, followed by transport of the Fe(II) into the cell through some uncharacterized mechanism (Figure 3.7). It is noteworthy that iron exchange between mycobactins and carboxymycobactins may be an operative aspect of microbial iron transport even though they possess strong binding constant (10^{30}) demonstrated by Crumbliss.⁹⁶ It is also important to note that the type of mycobactin used by one species of mycobacterium can be lethal to other mycobacteria.⁹⁴

In addition, mycobactin S is the only mycobactin siderophore which Fe(III) affinity has been characterized so far.⁹⁷

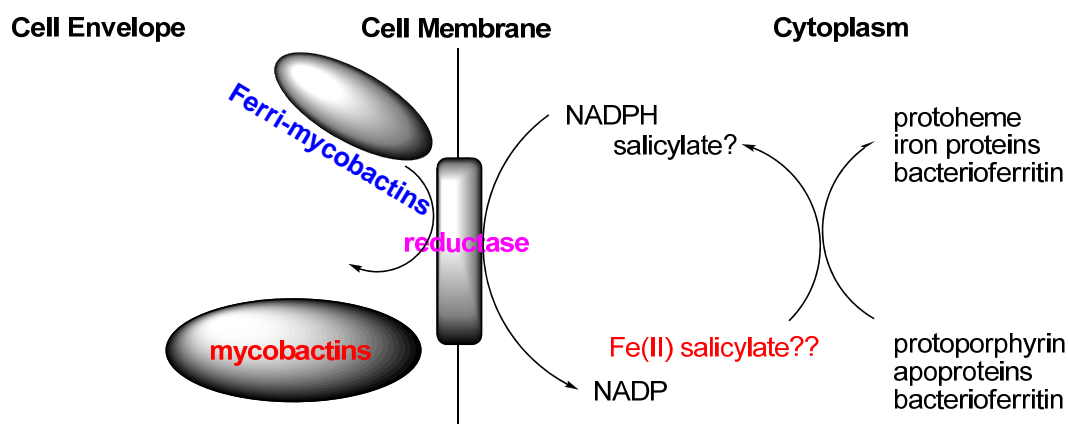
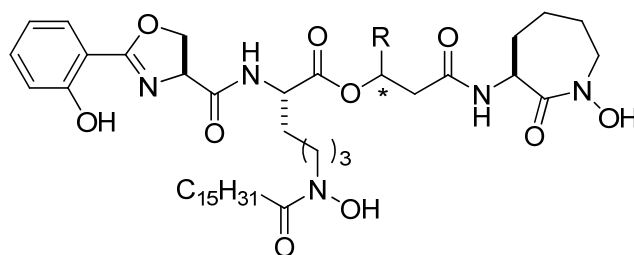


Figure 3.7 Proposed mechanism of the reduction of ferri-mycobactins by Ratledge

3.2 Biological activity of mycobactins and their analogues

Mycobactins, intracellular siderophores produced by mycobacteria, function as the acquisition, storage and transport of iron. Furthermore, some mycobactins have been demonstrated to show the potential anti-mycobacterial activity after Snow first observed that mycobactins produced by one species can inhibit the growth of another species of mycobacteria.^{94,98} Synthetic mycobactin S has been examined for its growth inhibition towards *M. tuberculosis* H37Rv with a minimum inhibitory concentration (MIC) of 3.13 $\mu\text{g/mL}$. The absolute configuration of the methyl group at 3-hydroxy acid fragment between mycobactin T and S as shown in **Figure 3.8** makes mycobactin S act as a competitor in the iron uptake process such as protein-mediated transfer of iron

sequestered by extracellular siderophores to the membrane bound mycobactins and then ferri-reductase transfer of iron from mycobactins to bacterioferritin.⁹⁸



Mycobactin T, R = CH₃, (*R*) growth promoter for *M. tuberculosis*

Mycobactin S, R = CH₃, (*S*) growth inhibitor for *M. tuberculosis* (MIC = 3.13 μg/mL)

Figure 3.8 Structures of Mycobactin T and S

Structurally similar mycobactins from other actinomycete species such as amamistatins,⁹⁹ formobactin,¹⁰⁰ nocobactin,¹⁰¹ and nocardimicins A-I¹⁰² show similar anticancer activities towards different cancer cell lines (Figure 3.9). Amamistatin A, isolated from the actinomycete *Nocardia asteroides*, exhibited antiproliferative activities against human tumor cell lines MCF-7 breast, A549 lung, and MKN45 stomach with IC₅₀ values of 0.48, 0.56, and 0.24 μM, respectively. Both amamistatin A and amamistatin B possess cytotoxicity against mouse lymphocytic leukemia cells P388 (IC₅₀ 15 and 16 ng/mL, respectively).¹⁰³ The nocardimicin series A-I were isolated from *Nocardia* sp. TP-A0674 and nova JCM6044, and inhibited the binding of tritium-labeled *N*-methylscopolamine to the muscarinic M3 receptor.¹⁰²

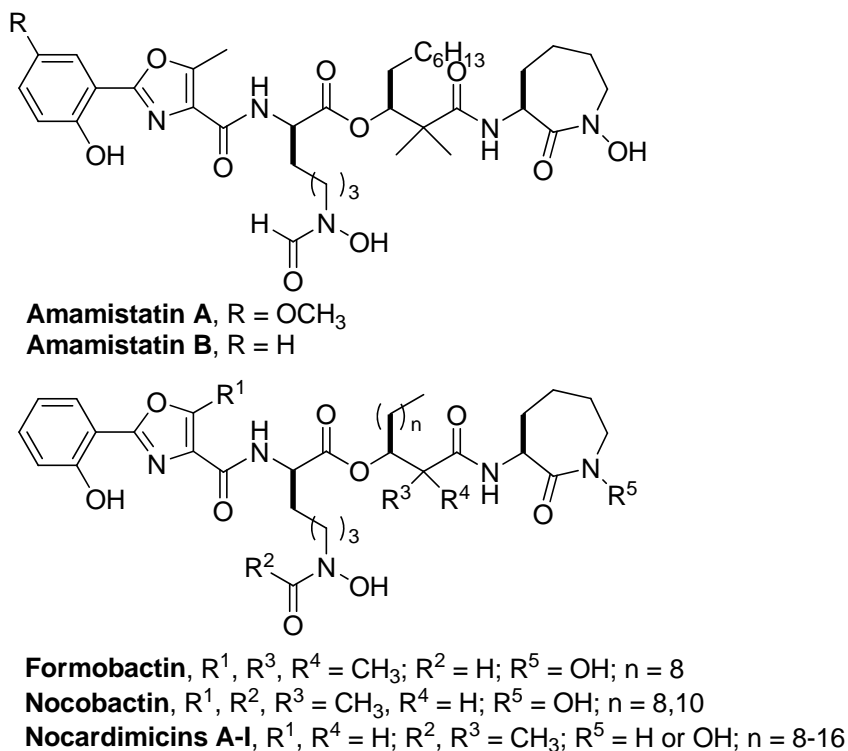


Figure 3.9 Siderophores from other actinomycetes

The recent rise in *Mycobacterium tuberculosis* infections worldwide and the emergence of drug resistance of anti-TB treatment reemphasize the need for novel antimycobacterial agents. Furthermore, some structurally similar mycobactins such as amamistatins have been proposed to be acted as histone deacetylase inhibitors (HDACi) since they possess similar *N*-formyl hydroxylamine or retrohydroxamate moieties as some small molecules HDACi (Figure 3.10).¹⁰⁴ In order to further probe the biological activities of this class of compounds, brasilibactin A was synthesized and characterized along with its analogues, which will be described in the following sections.

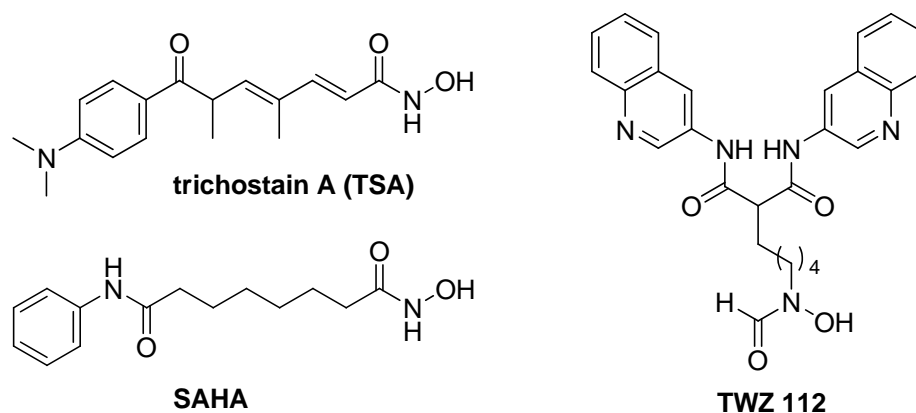


Figure 3.10 Small molecules HDACi with *N*-formyl hydroxylamine or retrohydroxamate moieties

3.3 *Brasilibactin A*

3.3.1 Isolation and biological activity

Brasilibactin A (Figure 3.11), a potent cytotoxic siderophore, was isolated from the actinomycete of *Nocardia brasiliensis* IFM 0995 by Tsuda and co-workers in 2004.¹⁰⁵ The structure and relative stereochemistry of brasilibactin A was determined by extensive spectroscopic and chemical analysis. Brasilibactin A contains a nearly identical molecular nucleus as in many mycobactin-type siderophores including a cyclic hydroxamic acid, a *N*-hydroxyformamide, and a 2-(2-hydroxyphenyl)- Δ^2 -1,3-oxazoline which serve as iron-binding moieties (Figure 3.11).^{87, 98} Brasilibactin A showed potent cytotoxicity against murine leukemia L1210 and human epidermoid carcinoma KB cells (IC₅₀, 0.02 and 0.04 $\mu\text{g/mL}$, respectively) and was reported to cause a concentration-dependent increase in the caspase-3 activity in HL60 cells,¹⁰⁶ but the absolute stereochemistry of the β -hydroxy acid moiety has not been assigned as well as the molecular mechanism of brasilibactin A has yet to be established.

Therefore, we undertook the total synthesis of brasilibactin A and its three unnatural diastereomers to determine the absolute stereochemistry of the β -hydroxy acid moiety and to study the effect of configuration of the β -hydroxy acid fragment on biological activities such as iron-binding capability and transport process.¹⁰⁶

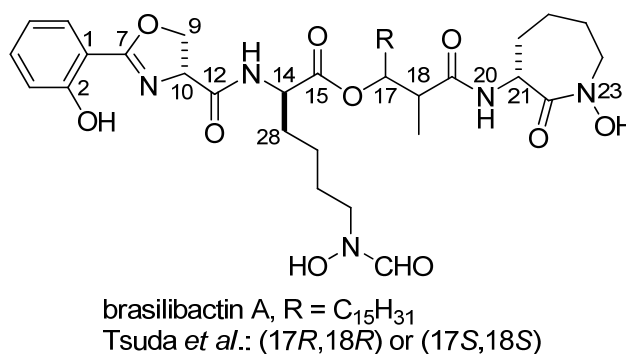
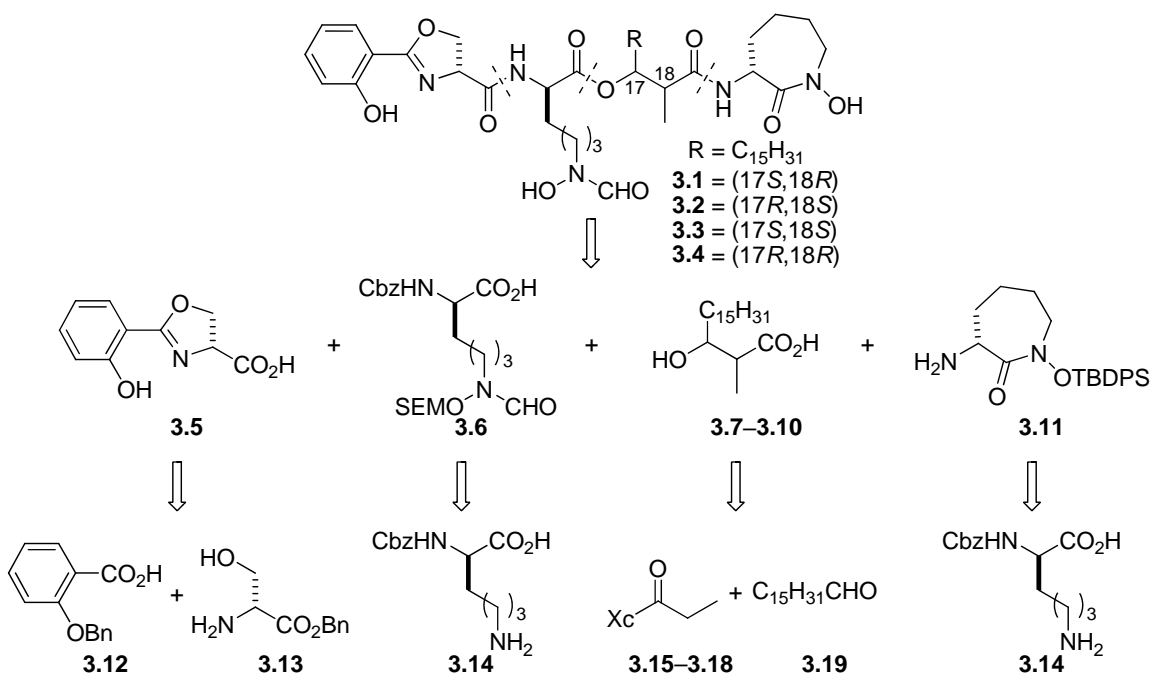


Figure 3.11 Structure of brasilibactin A

3.3.2 Retrosynthetic analysis

The retrosynthetic strategy of brasilibactin A and its diastereomers (**3.1–3.4**) is shown in scheme 3.1. Disconnection of an ester and two amide bonds of **3.1–3.4** generates four fragments (**3.5–3.11**), which include an oxazoline **3.5**, an *N*-hydroxyformamide **3.6**, a β -hydroxy acid (**3.7–3.10**), and a cyclic hydroxamic acid **3.11**. The oxazoline **3.5** could begin with a direct condensation of a derivative of salicylic acid **3.12** and serine benzyl ester (**3.13**). The *N*-hydroxyformamide **3.6** and the cyclic hydroxamic acid **3.11** could be derived from the common starting material *N* ^{α} -Cbz-D-lysine (**3.14**) via methodologies previously established by Miller and co-workers. Highly stereoselective aldol reactions of hexadecanal (**3.19**) with *N*-propanoyl-oxazolidinone and

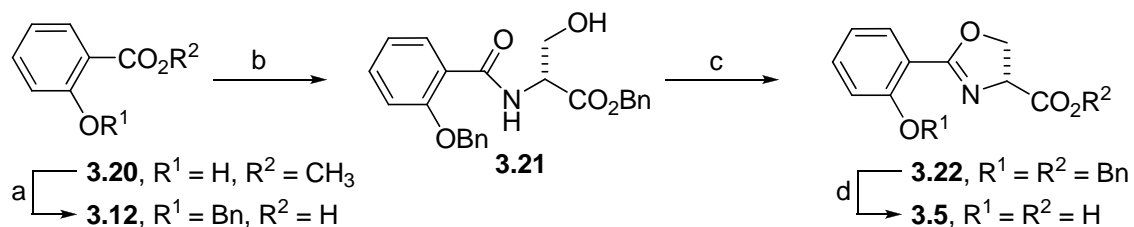
O-propanoyl-norephedrine could produce the four possible *syn*- and *anti*-diastereomers of the β -hydroxy acid (**3.7–3.10**).



Scheme 3.1 Retrosynthetic analysis of brasilbactin A

3.3.3 Total synthesis of brasilibactin A

As shown in **Scheme 3.2**, the synthesis of oxazoline **3.5** began with commercially available methyl salicylate **3.20**.⁹⁸ Benzyl Protection of **3.20** using $BnBr$ ¹⁰⁷ and subsequent hydrolysis (KOH, CH_3OH)¹⁰⁸ produced **3.12** (64% for two steps). A coupling of **3.12** to serine benzyl ester (**3.13**)¹⁰⁹ followed by treatment of **3.21** with Burgess reagent generated **3.22**.⁹⁸ Final deprotection of the Bn protecting groups in **3.22** under conventional hydrogenolysis conditions ($H_2, Pd/C$) completed the synthesis of **3.5** (90%).

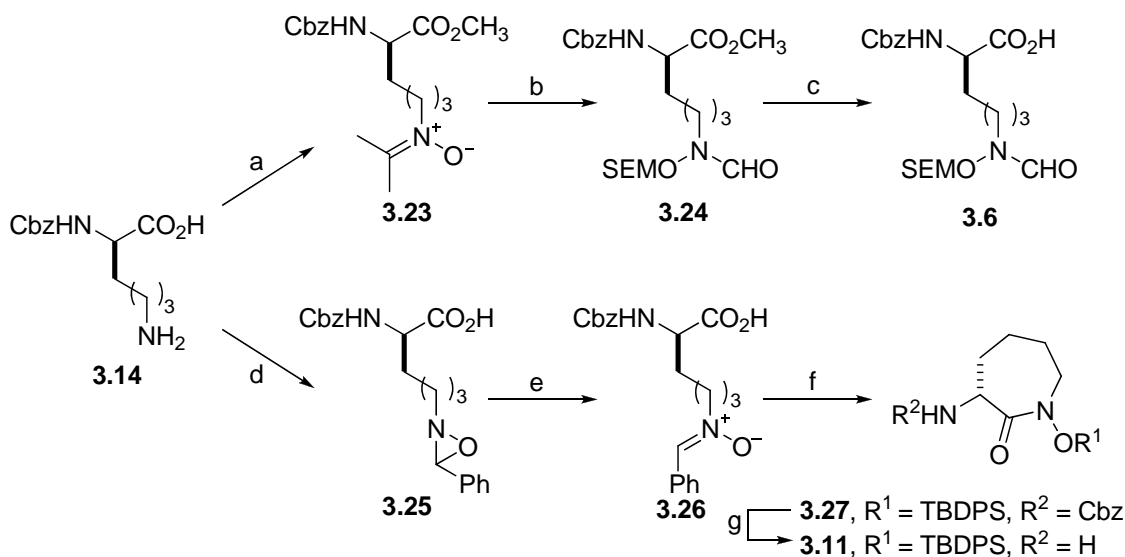


Reagents and conditions: (a) (i) BnBr, K_2CO_3 , KI, THF, rt, 24 h; (ii) KOH, CH_3OH , H_2O , 64% for two steps; (b) **3.13**, EDC, Et_3N , CH_2Cl_2 , rt, 24 h, 64%; (c) Burgess reagent, THF, reflux, 30 min, 70%; (d) 10% Pd/C, H_2 , CH_3OH , rt, 2h, 90%.

Scheme 3.2 Synthesis of oxazoline **3.5**

The *N*-hydroxyformamide **3.6** and the cyclic hydroxamic acid **3.11** were prepared from the same commercially available material *N*^α-Cbz-D-lysine (**3.14**) following the procedures demonstrated by Miller and co-workers.¹¹⁰ As shown in **Scheme 3.3**, Methyl esterification of *N*^α-Cbz-D-lysine (**3.14**) followed by oxidation with dimethyldioxirane (DMD or DMDO) in acetone gave the nitrone **3.23**.^{110a} Treatment of **3.23** with $\text{NH}_2\text{OH}\cdot\text{HCl}$, coupling with formic acid, protection with SEMCl, and hydrolysis under basic conditions completed the synthesis of the *N*-hydroxyformamide **3.6**.^{110b} Benzyl imine formation of *N*^α-Cbz-D-lysine (**3.14**) under basic conditions followed by oxidation with *m*-CPBA and TFA-promoted isomerization provided the corresponding nitrone **3.26**.^{110c, d} It is noteworthy that addition of benzaldehyde in TFA-promoted isomerization improved the yield (50% for two steps) because hydrolysis of **3.26** resulted in the formation of a hydroxylamine.^{110c} Treatment of **3.26** with $\text{NH}_2\text{OH}\cdot\text{HCl}$, cyclization of the corresponding hydroxylamine under standard conditions (EDC, HOAt, NaHCO_3), and protection of the cyclic hydroxamic acid with TBDPSCl afforded **3.27**.^{110c} Final

deprotection of the Cbz protecting group in **3.27** under conventional hydrogenolysis conditions (H_2 , Pd/C) provided **3.11** (90%).

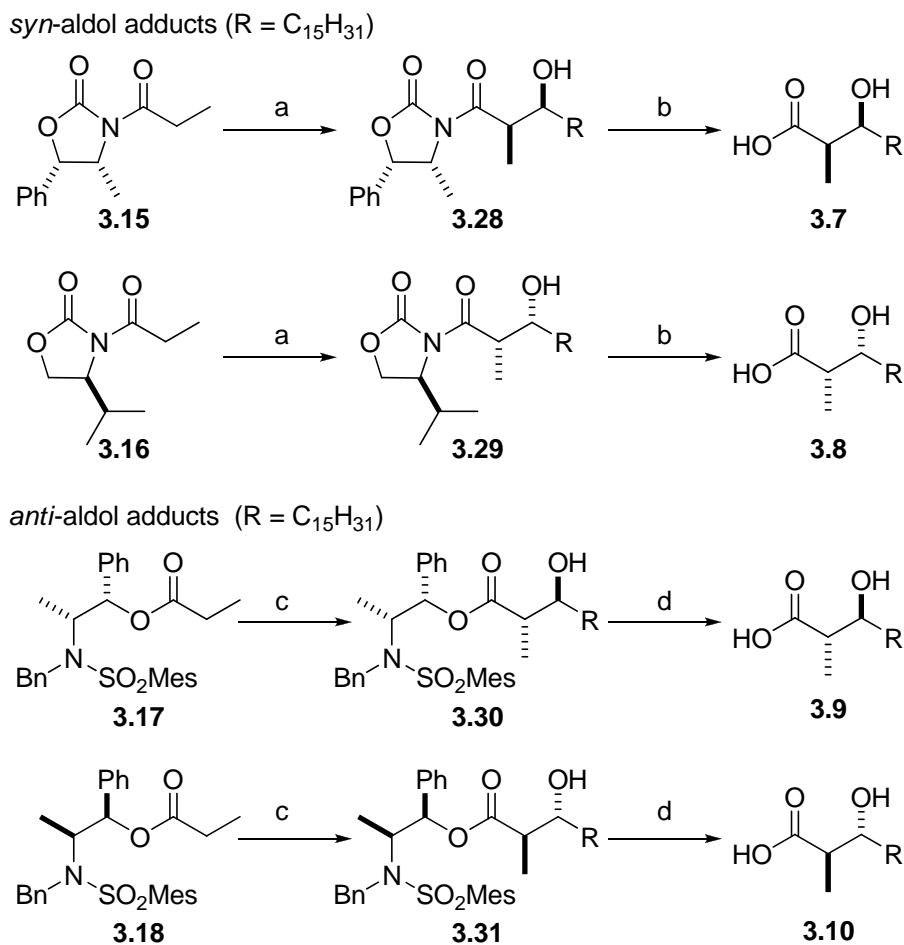


Reagents and conditions: (a) SOCl_2 , CH_3OH , rt, 24 h; then dimethyldioxirane, acetone, -78°C , 15 min, 58% for two steps; (b) (i) $\text{NH}_2\text{OH}\cdot\text{HCl}$, CH_3OH , 40°C , 12 min; (ii) HCO_2H , EDC, CH_2Cl_2 , 0°C , 2 h; then $i\text{-Pr}_2\text{NEt}$, CH_3OH , rt, 48 h, 70% for two steps; (iii) SEMCl, $i\text{-Pr}_2\text{NEt}$, DMAP, CH_2Cl_2 , rt, 24 h, 80%; (c) aq. LiOH, THF, 0°C , 30 min, rt, 1 h, 90%; (d) PhCHO, KOH, CH_3OH , 3 Å MS, rt, 24 h, then $m\text{-CPBA}$, CH_3OH , 0°C , 2 h; (e) TFA, CH_2Cl_2 , rt, 1 h; then PhCHO, rt, 24 h, 50% for two steps; (f) (i) $\text{NH}_2\text{OH}\cdot\text{HCl}$, CH_3OH , 60°C , 20 min; (ii) EDC, HOAt, NaHCO_3 , $\text{CH}_3\text{CN}/\text{DMF}$ (7:2), rt, 48 h; (iii) TBDPSCl, imidazole, DMF, 35°C , 24 h, 40% for three steps; (g) 10% Pd/C, H_2 , CH_3OH , rt, 2 h, 90%.

Scheme 3.3 Synthesis of *N*-hydroxyformamide **3.6** and cyclic hydroxamic acid **3.11**

Synthesis of four possible diastereomers of the β -hydroxy acid fragment (**3.7**–**3.10**) was achieved by employing the highly stereoselective *syn*-aldol reactions of the *N*-propanoyl-oxazolidinones (**3.15** and **3.16**) developed by Evans¹¹¹ and *anti*-aldol reactions of the *O*-propanoyl-norephedrine (**3.17** and **3.18**) demonstrated by Masamune¹¹² (Scheme 3.4). The aldol reactions of hexadecanal (**3.19**)¹⁰ with **3.15** and **3.16** in the presence of $n\text{-Bu}_2\text{BOTf}$ and $i\text{-Pr}_2\text{NEt}$ provided the desired *syn*-aldol adducts **3.28** (85%)

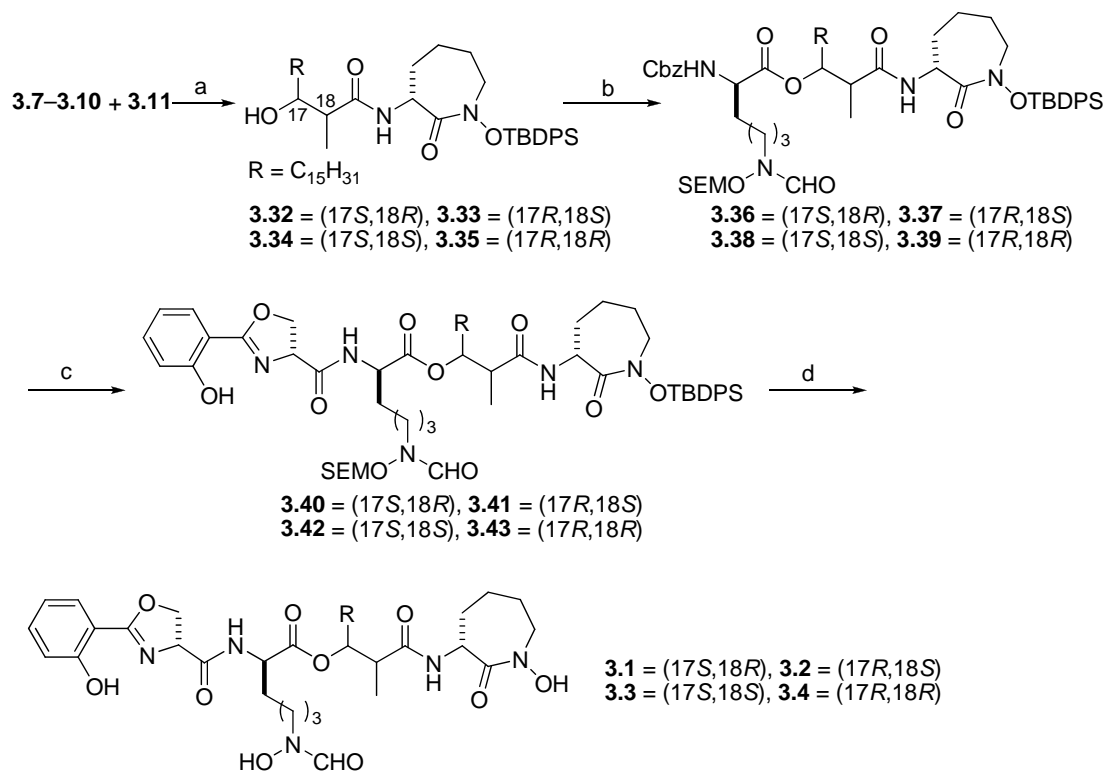
and **3.29** (85%), respectively, as a single diastereomer. Hydrolysis of the β -hydroxy amides (**3.28** and **3.29**) under conventional conditions (30% H₂O₂, LiOH) provided the corresponding β -hydroxy acids (**3.7** and **3.8**) in 90% yield, respectively. In a similar manner, the aldol reactions of hexadecanal (**3.19**) with the chiral derivatives of norephedrine (**3.17** and **3.18**) in the presence of *c*-Hex₂BOTf and Et₃N followed by hydrolysis of aldol adducts (**3.30** and **3.31**) were performed to prepare *anti*- β -hydroxy acids (**3.9** and **3.10**).



Scheme 3.4 Synthesis of β -hydroxy acid (**3.7–3.10**)

As shown in **Scheme 3.5**, the synthesis of brasilibactin A and its diastereomers (**3.1–3.4**) commenced from the coupling of **3.7–3.10** with **3.11**. EDC-coupling of **3.7** to **3.11** followed by subsequent coupling^{110b} of **3.32** to **3.6** provided **3.36**. However, alternative methods for formation of the ester bond (DEAD or DIAD, PPh₃; 2,4,6-

trichlorobenzoyl chloride, NEt_3 , then DMAP; EDC, DMAP) failed to react with this sterically hindered substrate. Deprotection of the Cbz protecting group in **3.36** followed by the coupling of the corresponding amine to **3.5** completed the synthesis of the protected depsipeptide (**3.40**). Final deprotection of the SEM and TBDPS protecting groups in **3.40** by treatment with TFA followed by HPLC purification afforded **1** in 73% yield.¹⁰⁶ The other diastereomers of brasilibactin A (**3.2–3.4**) were also prepared in the same manner. ^1H NMR data for **3.1–3.4** were carefully compared with the authentic data from natural brasilibactin A (Table 3.1, Figure 3.12). The chemical shifts and coupling patterns of **3.1**, in particular those of H-14 (δ 4.25, m), H-17 (δ 4.90, dt, $J = 8.8, 2.8$ Hz), H-18 (δ 2.62, m), and H-20 (δ 8.13, d, $J = 7.2$ Hz), were identical to those of the natural product.¹⁰⁵ The comparison unambiguously showed that brasilibactin A (**3.1**) possesses the 17*S*,18*R* absolute stereochemistry, which is also consistent with the assignment by Shaw and co-workers, who published the synthesis of the brasilibactin A when we were preparing our manuscript.¹¹³



Reagents and conditions: (a) EDC, CH_2Cl_2 , rt, 24 h, 64–68%; (b) **3.6**, DCC, DMAP, toluene, rt, 48 h, 76–89%; (c) 10% Pd/C, H_2 , CH_3OH , rt, 2 h; then **3.5**, EDC, CH_2Cl_2 , rt, 24 h, 48–60%; (d) TFA, CH_2Cl_2 , rt, 1.5 h, 68–73%.

Scheme 3.5 Synthesis of brasilibactin A (**3.1**) and other diastereomers (**3.2–3.4**)

Table 3.1: Comparison of ^1H NMR data for **3.1–3.4** with natural brasilibactin A^a

H no.	Natural 3.1	3.1 (17 <i>S</i> , 18 <i>R</i>)	3.2 (17 <i>R</i> , 18 <i>S</i>)	3.3 (17 <i>S</i> , 18 <i>S</i>)	3.4 (17 <i>R</i> , 18 <i>R</i>)	(17 <i>S</i> , 18 <i>R</i>) in ref. 113	(17 <i>R</i> , 18 <i>S</i>) in ref. 113
18	2.62	2.62	2.66	2.70	2.74	2.61	2.66
14	4.25	4.25	4.21	4.23	4.15	4.24	4.22
21	4.44	4.44	4.46	4.40	4.42	4.42	4.47
9	4.47	4.47	4.48	4.48	4.51	4.47	4.46
17	4.90	4.90	4.95	4.93	4.95	4.90	4.95
20	8.11	8.13	8.15	7.88	7.93	8.15	8.16

^a Chemical shifts (ppm) in $\text{DMSO-}d_6$

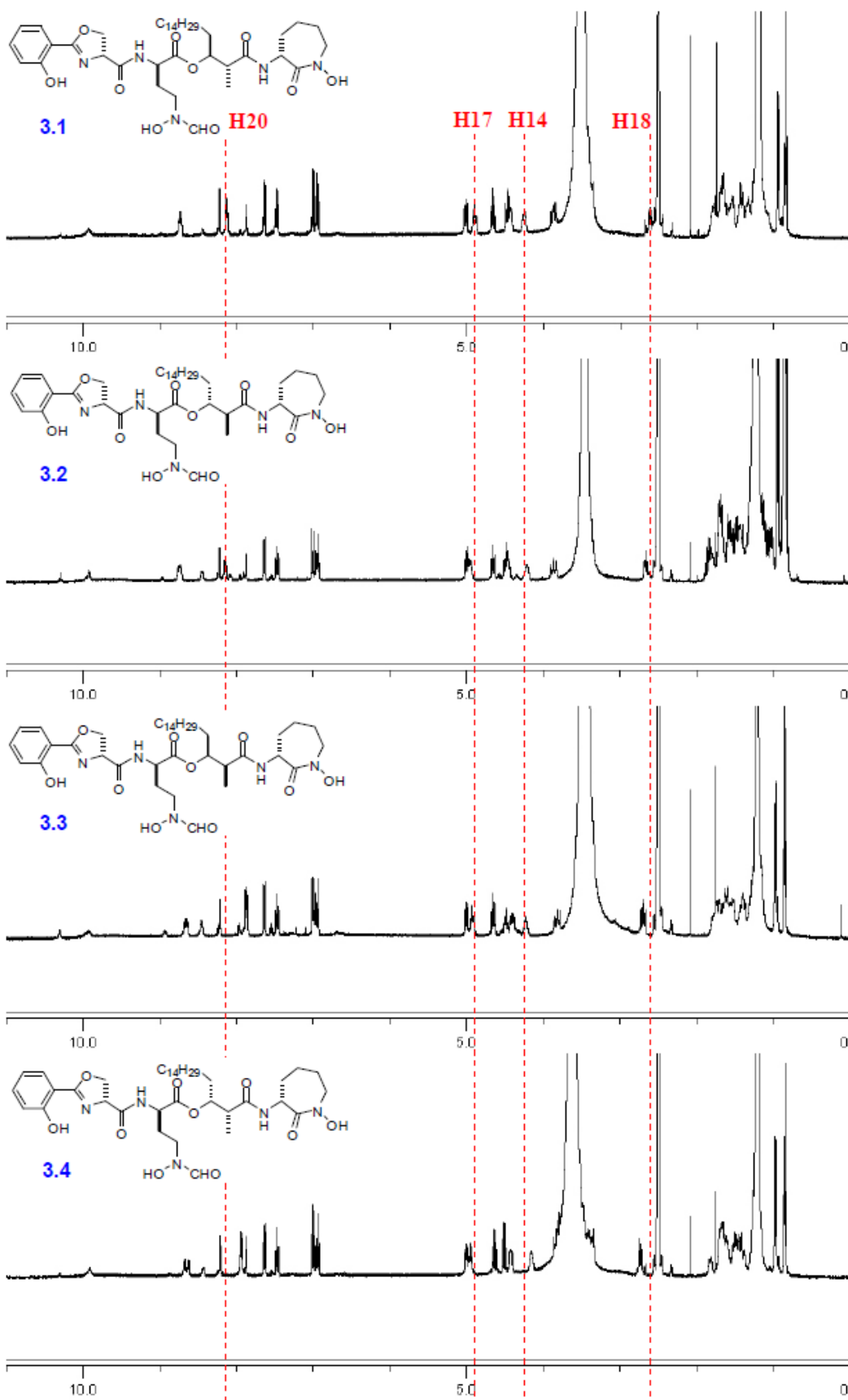
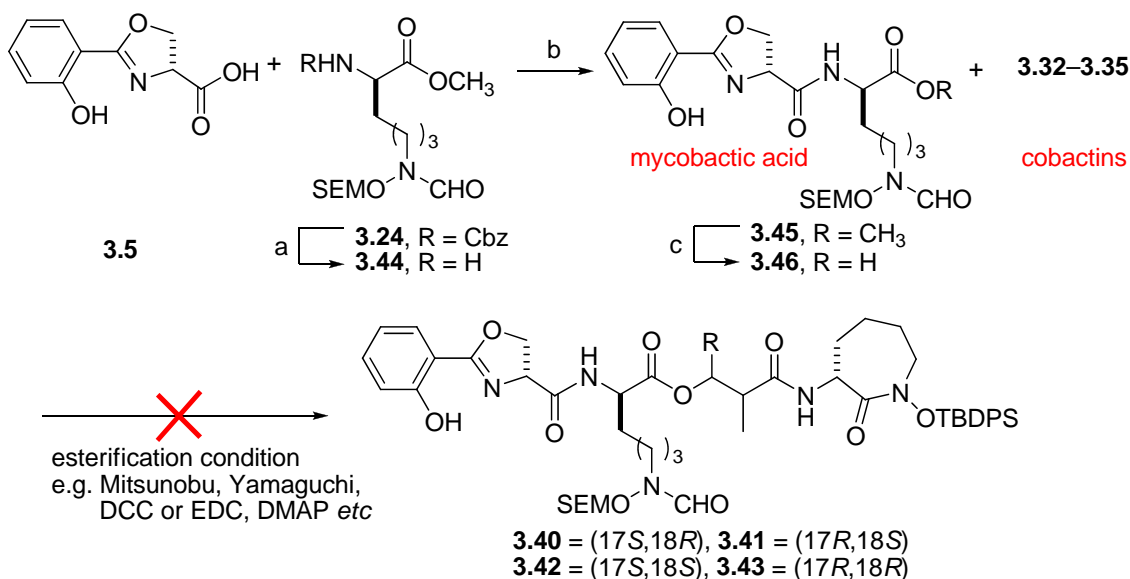


Figure 3.12 Comparison of ^1H NMR of 3.1–3.4

One point we should note is that initially we attempted to couple cobactin fragment 3.32–3.35 with mycobactic acid fragment 3.46 using several ester bond formation methods such as Mitsunobu, Yamaguchi and DCC or EDC/DMAP coupling (Scheme 3.6). However, all attempts were failed presumably because of this sterically hindered secondary alcohol.



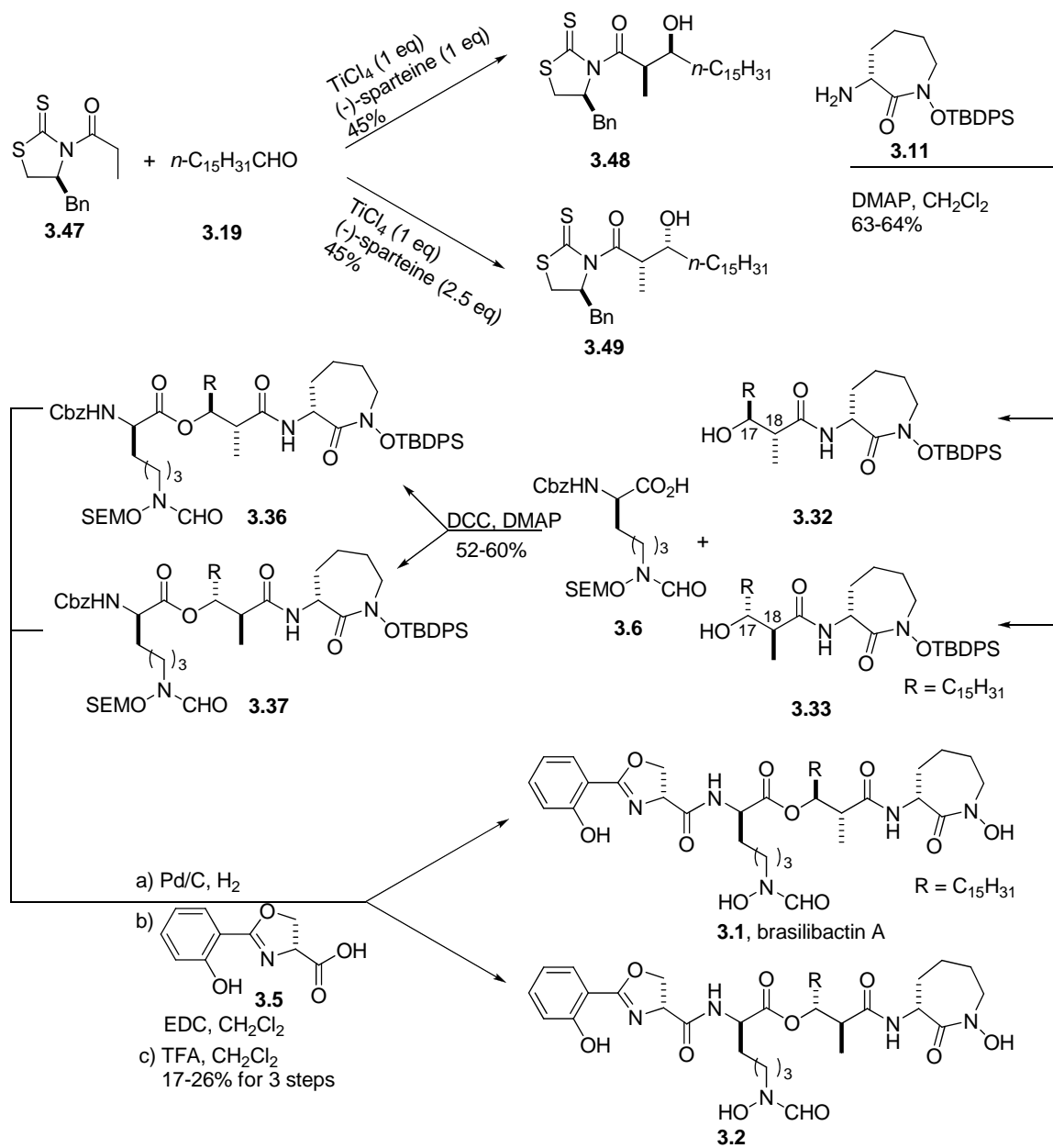
Reagents and conditions: (a) 10% Pd/C, H₂, CH₃OH, rt, 2 h; (b) EDC, CH₂Cl₂, rt, 3 h, 85% for 2 steps; (c) aq. LiOH, THF, 0 °C, 30 min, rt, 1 h, 90%;

Scheme 3.6 Attempts to couple cobactins 3.32–3.35 with mycobactic acid 3.46

3.3.4 Shaw's synthetic route to brasilibactin A and HDAC inhibitory activity of brasilibactin A

During the preparation of our manuscript, Shaw and co-workers reported the first total synthesis of brasilibactin A (Scheme 3.7).¹¹³ They examined the HDAC inhibitory effect of brasilibactin A and found that it lacked HDAC inhibitory activity using HDAC

enzymatic assay, presumably because conformation of brasilibactin structures prevents either *N*-formyl hydroxylamine or cyclic hydroxamic acid moiety from accessing the Zn ion at the active site.¹¹³ This lack of HDAC inhibition was also observed in natural products amamistatin A and B reported by Miller.¹¹⁴

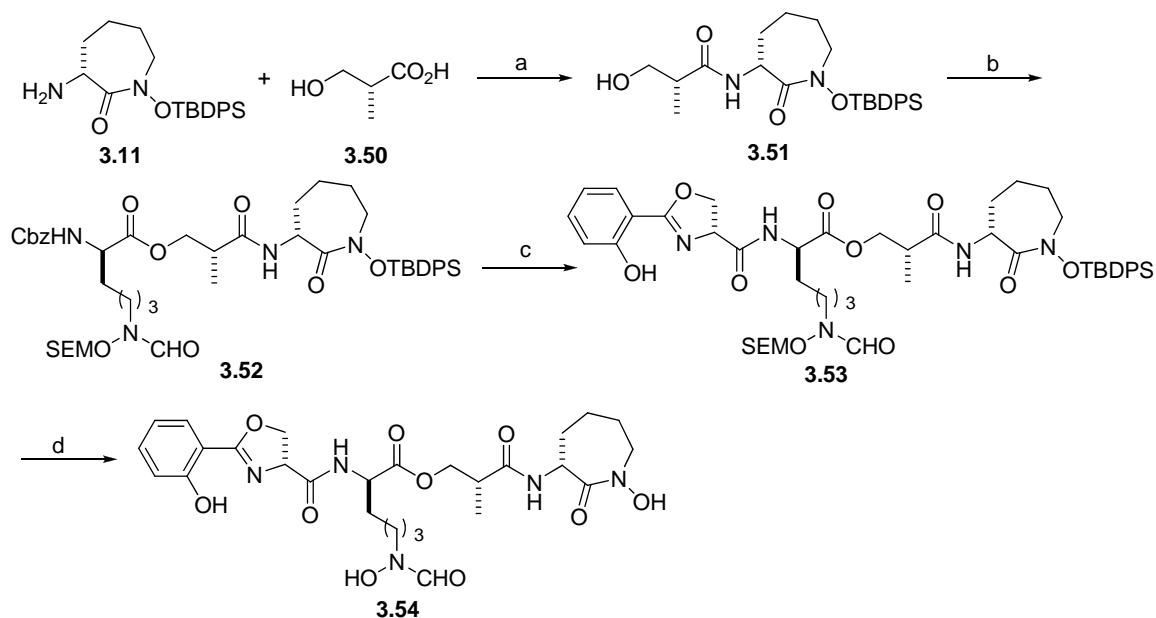


Scheme 3.7 Shaw's synthetic route to brasilibactin A

3.3.5 Synthesis and iron-binding study of brasilibactin A analogue

Due to the long alkyl chain at the β -hydroxy acid residue, brasilibactin A has a low water solubility, which prevented us from studying iron-binding capability in aqueous solution. To overcome this problem, an analogue lacking C17-alkyl chain at β -hydroxy acid fragment was designed to pursue better water solubility. Meanwhile, stereochemistry of the backbone and three iron-binding moieties was retained. The design of this brasilibactin A analogue (Bbtan) increases the water solubility presumably without affecting the iron binding properties because of three retained iron-binding moieties.

Bbtan was synthesized following the previously reported procedure (Scheme 3.8).¹⁰⁶ Briefly, EDC-coupling of **3.11** to known (*R*)-2-hydroxymethylpropanoic acid **3.50** provided **3.51** in 80% yield. Coupling of **3.51** and **3.6** using DCC and DMAP afforded **3.52** in 66% yield. Deprotection of the Cbz group in **3.52** followed by the coupling of the corresponding free amine to oxazoline **3.5** completed the synthesis of depsipeptide **3.53**. Final deprotection of the SEM and TBDPS protecting groups in **3.53** using TFA followed by HPLC purification afforded Bbtan (**3.54**) in 78 % yield.



Reagents and conditions: (a) EDC, CH₂Cl₂, rt, 24 h, 80%; (b) **3.6**, DCC, DMAP, toluene, rt, 22 h, 66%; (c) 10% Pd/C, H₂, CH₃OH, rt, 5 h; then **3.5**, EDC, CH₂Cl₂, rt, 16 h, 87%; (d) TFA, CH₂Cl₂, rt, 2 h, 78%.

Scheme 3.8 Synthesis of a water-soluble brasilibactin A analogue **3.54** (Bbtan).

A characterization of the protonation constants and iron(III) affinity of a water soluble Brasilibactin A analog (Bbtan) has been performed by our collaborator James Harrington in Dr. Crumbliss' lab at Duke University. The stability constant of the 1:1 Fe(III)-Bbtan complex was found to be $\log \beta_{110} = 26.96$ based on protonation constants and competition with EDTA. They also found that the pFe of Bbtan is 22.73, somewhat low for a proposed siderophore molecule. In addition, the redox potential of the Fe-Bbtan complex was found to be -300 mV vs NHE, which is very high for an iron-siderophore complex.*

* Iron-binding results from our collaborators-James Harrington and Prof. Alvin Crumbliss

The relative low complex stability of Bbtan and ease of iron reduction due to the high redox potential of ferri-Bbtan complex suggest brasilibactin A may play a vital role in the iron-uptake mechanism in mycobacteria and related organisms.

3.4 Conclusion

In summary, we completed a convergent synthesis of cytotoxic siderophore brasilibactin A (**3.1**), a structurally and biologically interesting linear depsipeptide, and unambiguously confirmed that **3.1** possesses the *17S*, *18R* absolute stereochemistry. The convergent synthetic strategy has been applied to the synthesis of a more water soluble analogue Bbtan (**3.54**). Characterization of iron binding property of **3.54** suggested brasilibactin A may play an important role in the iron-uptake mechanism in mycobacteria and related organisms and further studies to characterize zinc binding property are in progress.

3.5 Experimental sections

3.5.1 General Information

¹H NMR spectra were performed on a Varian (400 MHz) spectrometer. Chemical shifts are reported in ppm from residual solvent peak (CDCl₃, s, δ=7.26). Data are reported as follows: chemical shifts, multiplicity, coupling constants (Hz), integration, and assignment. Proton-decoupled ¹³C NMR spectra were performed on a Varian (100

MHz) spectrometer with complete proton decoupling. Chemical shifts are reported in ppm from tetramethylsilane with the solvent as the internal standard (CDCl_3 , t , $\delta=77.00$).

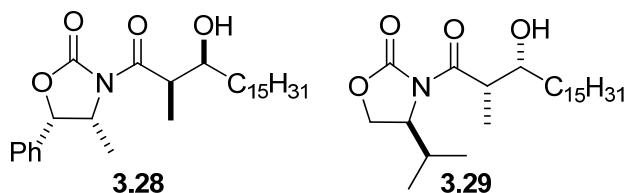
Analytical thin layer chromatography was performed on Partisil K6F, Silica Gel 60 Å with fluorescent indicator/0.25 mm thickness plates (Whatman International Ltd.). Visualization was accomplished with UV light, *p*-anisaldehyde solution, or phosphomolybdic acid followed by heating. High resolution mass spectra (HRMS) and low resolution FAB mass spectra (FAB LRMS) were done at the Analytical Facility at Chemistry Department, Duke University.

Solvents for extraction and chromatography were reagent grade. Liquid chromatography was performed with forced flow (flash chromatography of the indicated solvent mixture on silica gel *SiliaFlash* F60, 40-63 μm 60Å, SiliCycle Inc.). Anhydrous THF and acetone were commercially available from Acros, Fisher. Anhydrous CH_2Cl_2 was freshly distilled from CaH_2 before use. Toluene and *N,N*-dimethyl formamide (DMF) were dried over 4Å molecular sieves. Active 3Å molecular sieves were dried under high vacuum in the oil-bath at 250 °C for 2 h before use. Triethylamine and *N,N*-diisopropylethylamine were dried over potassium hydroxide. All other commercially obtained reagents were used as received.

DMD was generated by the method reported by Murray et al.¹¹⁵ Hexadecanal was prepared by pyridinium chlorochromate (PCC) oxidation of hexadecanol in CH_2Cl_2 .¹¹⁶ *n*-

Bu₂BOTf and *c*-Hex₂BOTf were used as commercially available solutions in CH₂Cl₂. All reactions were conducted under a nitrogen atmosphere unless otherwise indicated. Upon workup, solvents were evaporated by using a Buchi rotary evaporator, followed by high vacuum.

3.5.2 Preparation of brasilibactin A (3.1) and its diastereomers (3.2–3.4)

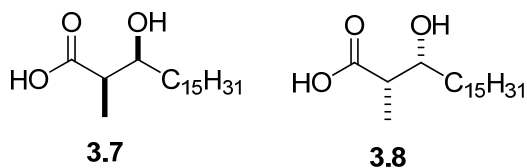


(2'*R*,3'*S*,3*R*,4*R*)-3-(3'-Hydroxy-2'-methyl-1'-octadecanoyl)-4-(methyl)-5-(phenyl)-2-oxa-zolidinone **3.28** and (2'*S*,3'*R*,4*S*)-3-(3'-Hydroxy-2'-methyl-1'-octadecanoyl)-4-(methylethyl)-2-oxazolidinone **3.29**. To a 0.2-0.5 M solution of **3.15** (or **3.16**) in anhydrous CH₂Cl₂ under nitrogen (0 °C) was added 1.1 equiv. of *n*-Bu₂BOTf followed by 1.2 equiv. of diisopropylethylamine. After allowing 30 min for complete enolization, the reaction was cooled (-78 °C) and 1.1 equiv. of freshly prepared hexadecanal was added and stirred for another 30 min at -78 °C and 1.5 h at room temperature. The boron aldol complex was quenched with pH 7 phosphate buffer and oxidized with 30% hydrogen peroxide-methanol (0 °C, 1h). The aldol adduct was then extracted 3 times by CH₂Cl₂. The combined organic extracts were dried over anhydrous Na₂SO₄, filtered, and concentrated. The residue was purified by flash chromatography

(EtOAc-Hexane=1:2) to afford the desired product **3.28** (**3.29**) as a colorless oil in 85% yield.

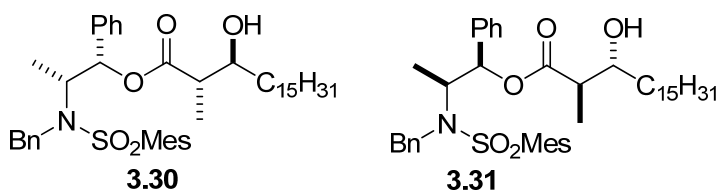
3.28. A colorless oil: $^1\text{H NMR}$ (400 MHz, CDCl_3) δ 4.42–4.46 (m, 1H), 4.19 (dd, $J = 9.2, 3.2$ Hz, 1H), 3.87–3.92 (m, 1H), 3.73 (qd, $J = 7.2, 2.8$ Hz, 1H), 2.96 (d, $J = 2.4$ Hz, 1H), 2.27–2.37 (m, 1H), 1.22 (brs, 25H), 1.21 (d, $J = 6.0$ Hz, 3H), 0.89 (d, $J = 6.8$ Hz, 3H), 0.86 (d, $J = 6.8$ Hz, 3H), 0.85 (t, $J = 7.2$ Hz, 3H).

3.29. A colorless oil: $^1\text{H NMR}$ (400 MHz, CDCl_3) δ 7.34–7.42 (m, 3H), 7.26–7.29 (m, 2H), 5.66 (d, $J = 7.2$ Hz, 1H), 4.77 (dddd, $J = 6.8, 6.8, 6.8, 6.8$ Hz, 1H), 3.81–3.92 (m, 1H), 3.75 (qd, $J = 7.2, 2.8$ Hz, 1H), 2.87 (brs, 1H), 1.34–1.56 (m, 3H), 1.23 (s, 24H), 1.21 (d, $J = 7.2$ Hz, 3H), 0.85 (t, $J = 7.6$ Hz, 3H).



(3S)-3-Hydroxy-(2R)-2-methyloctadecanoic acid (3.7) and (3R)-3-Hydroxy-(2S)-2-methyl- octadecanoic acid (3.8). To a solution of the aldol adduct **3.28** (**3.29**) (150 mg, 0.35 mmol) in 2.0 ml of 4:1 THF/ H_2O at 0°C , a 0.22 mL of 30 % H_2O_2 was added dropwise *via* syringe followed by $\text{LiOH}\cdot\text{H}_2\text{O}$ (31 mg, 0.72 mmol) in 0.9 mL of H_2O . After the solution was stirred at 0°C for 1 h, Na_2SO_3 (273 mg, 2.16 mmol) dissolved in 3.0 mL of H_2O was added to the reaction mixture. The bulk of THF was removed on a rotary evaporator and the resulting mixture was extracted 3 times with CH_2Cl_2 to remove the chiral auxiliary. The aqueous layer was cooled in an ice bath and acidified to pH 1 by the addition of an aqueous 1N HCl solution. The resulting cloudy

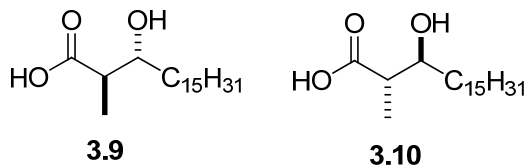
solution was then extracted 3 times with EtOAc. The combined EtOAc extracts were dried over anhydrous Na₂SO₄, filtered, and concentrated. The residue was purified by flash chromatography (EtOAc-Hexane=1:2, 1% acetic acid) to afford the desired product **3.7 (3.8)** as a white solid (99 mg, 90%). ¹H NMR (400 MHz, CDCl₃) δ 3.93 (m, 1H), 2.53 (dq, *J* = 7.2, 3.2 Hz, 1H), 1.44 (m, 3H), 1.23 (m, 29H), 0.86 (t, *J* = 7.2 Hz, 3H).



(1'S)-Phenyl-(2'R)-[(phenylethyl)[(2,4,6-trimethyl phenyl)sulfonyl]-amino]propyl-(3S)-hydroxy-(2S)-methyloctadecanoate 3.30 and (1'R)-Phenyl-(2'S)-[(phenylethyl)[(2,4,6-trimethylphenyl)sulfonyl]amino]-propyl-(3R)-hydroxy-(2R)-methyloctadecanoate 3.31. To a stirred solution of **3.17** (or **3.18**) in anhydrous CH₂Cl₂ under nitrogen (0 °C) was added triethylamine. The solution was cooled to -78 °C and to this was added *c*-Hex₂BOTf in CH₂Cl₂. The resulting solution was stirred at -78 °C for 2 h to complete enolization. Hexadecanal dissolved in CH₂Cl₂ was added dropwise to the enolate solution *via* syringe and the reaction mixture was stirred at -78 °C for 1 h and at 0 °C for 1 h. The reaction was quenched by pH 7 buffer followed by CH₃OH and 30% H₂O₂. The mixture was stirred overnight vigorously and worked up with the method Abiko described.

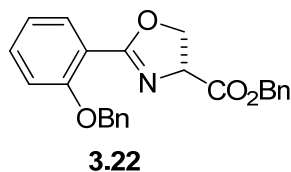
3.30. A colorless oil: ^1H NMR (400 MHz, CDCl_3) δ 7.14–7.29 (m, 8H), 6.85 (d, J = 5.6 Hz, 4H), 5.81 (d, J = 4.0 Hz, 1H), 4.63 (AB, J_{AB} = 16.4 Hz, $\Delta\nu_{\text{AB}}$ = 90.8 Hz, 2H), 4.07–4.14 (m, 1H), 3.57–3.63 (m, 1H), 2.47 (s, 6H), 2.41–2.48 (m, 2H), 2.26 (s, 3H), 1.42 (brs, 3H), 1.24 (brs, 25H), 1.16 (d, J = 6.8 Hz, 3H), 1.11 (d, J = 7.2 Hz, 3H), 0.86 (t, J = 6.8 Hz, 3H); ^{13}C NMR (100 MHz, CDCl_3) δ 174.6, 142.5, 140.2, 138.4, 138.1, 133.3, 132.1, 128.4, 128.3, 127.9, 127.6, 127.1, 125.9, 78.2, 73.1, 56.7, 48.2, 45.4, 34.4, 31.9, 29.7, 29.6, 29.3, 25.4, 22.9, 22.6, 20.8, 14.1, 13.4.

3.31. A colorless oil: ^1H NMR (400 MHz, CDCl_3) δ 7.14–7.29 (m, 8H), 6.86 (d, J = 6.4 Hz, 4H), 5.82 (d, J = 4.4 Hz, 1H), 4.63 (AB, J_{AB} = 16.8 Hz, $\Delta\nu_{\text{AB}}$ = 90.0 Hz, 2H), 4.11 (dt, J = 11.6, 7.2 Hz, 1H), 3.58–3.63 (m, 1H), 2.47 (s, 6H), 2.43–2.48 (m, 2H), 2.26 (s, 3H), 1.43 (brs, 3H), 1.24 (s, 25H), 1.16 (d, J = 7.2 Hz, 3H), 1.12 (d, J = 7.2 Hz, 3H), 0.87 (t, J = 6.8 Hz, 3H); ^{13}C NMR (100 MHz, CDCl_3) δ 174.5, 142.5, 140.1, 138.4, 138.1, 133.3, 132.0, 128.3, 128.2, 127.9, 127.6, 127.1, 125.9, 78.1, 73.1, 56.7, 48.2, 45.4, 34.3, 31.8, 29.6, 29.5, 29.3, 25.3, 22.8, 22.6, 20.8, 14.05, 13.97, 13.4.

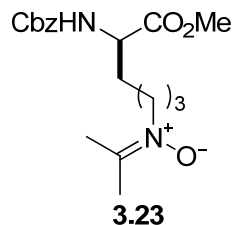


(3R)-3-Hydroxy-(2R)-2-methyloctadecanoic acid (3.9) and (3S)-3-Hydroxy-(2S)-2-methyl-octadecanoic acid (3.10). A solution of **3.30** (**3.31**) (62 mg, 0.086 mmol) and $\text{LiOH}\cdot\text{H}_2\text{O}$ (18 mg, 0.43 mmol) in $\text{THF}/\text{CH}_3\text{OH}/\text{H}_2\text{O}$ (2.1 mL, 2:3:2) was stirred at room temperature for 3 days. The mixture was poured into H_2O (10.0 mL) and extracted with ether to remove the auxiliary. The aqueous layer was acidified (pH 2~3) with 1N HCl and extracted 4 times with CH_2Cl_2 . The CH_2Cl_2 extracts were dried over anhydrous Na_2SO_4 , filtered, and concentrated. The residue was purified by flash chromatography

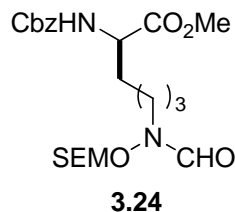
(EtOAc-Hexane=1:7, 1% acetic acid) to afford the desired product **3.9** (**3.10**) as a white solid (23 mg, 85%). ¹H NMR (400 MHz, CDCl₃) δ 3.67 (m, 1H), 2.53 (dq, *J* = 6.8, 6.8 Hz, 1H), 1.48 (m, 3H), 1.24 (m, 29H), 0.86 (t, *J* = 6.8 Hz, 3H).



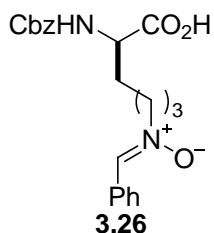
(R)-Benzyl 2-[(benzyloxy)phenyl]-Δ²-1,3-oxazoline-4-carboxylate (3.22). To a stirred solution of N-[2-(benzyloxy)benzoyl]-D-serine benzyl ester (**3.21**) (100mg, 0.248 mmol) in THF (2.0 mL) was added Burgess's reagent (50mg, 0.274 mmol). After being refluxed for 30 min under N₂, the reaction mixture was diluted with EtOAc (20.0 mL), washed with H₂O and brine. The organic layer was dried over Na₂SO₄, filtered, concentrated, and chromatographed on silica gel eluting with EtOAc/CH₂Cl₂ (1/15) to yield oxazoline **3.22** (68 mg, 71%) as a white crystalline solid. ¹H NMR (400 MHz, CDCl₃) δ 7.80 (dd, *J* = 8.0, 1.6 Hz, 1H), 7.48 (d, *J* = 7.2 Hz, 2H), 7.25–7.40 (m, 9H), 6.95–6.99 (m, 2H), 5.27 (d, *J* = 12.4 Hz, 1H), 5.19 (d, *J* = 12.4 Hz, 1H), 5.16 (s, 1H), 4.98 (dd, *J* = 10.4, 8.0 Hz, 1H), 4.64 (dd, *J* = 8.4, 8.4 Hz, 1H), 4.54 (dd, *J* = 10.4, 8.4 Hz, 1H).



Lysine nitronium (3.23). To precooled (ice-salt bath) absolute methanol (10 mL) was added slowly thionyl chloride (0.45 ml, 6.32 mmol). *N*^α-Cbz-D-lysine **3.14** (500 mg, 1.78 mmol) was added to the above mixture in one portion. The solution was allowed to warm to room temperature slowly and stirred overnight. The methanol was removed and clear oil was obtained. Part of the oil was dissolved in saturated NaHCO₃ solution (20.0 mL) and was extracted with CH₂Cl₂. The organic layer was dried over Na₂SO₄, filtered, and concentrated to give an oil (220 mg, 0.748 mmol). The oil was dissolved in acetone (10.0 mL) and stirred at 0 °C for 30 min and at -78 °C for 1 h. Enough DMD/acetone (10.0 mL) was added in one portion to the above mixture. After being stirred for 10–15 min, the reaction mixture was concentrated and chromatographed eluting with CH₃OH:EtOAc (3:8) to give 135 mg (51.4%) of nitone **3.23** as a white solid. ¹H NMR (400 MHz, CDCl₃) δ 7.27–7.32 (m, 5H), 5.60 (d, *J* = 8.0 Hz, 1H), 5.06 (s, 2H), 4.28–4.34 (m, 1H), 3.78 (t, *J* = 7.2 Hz, 2H), 3.70 (s, 3H), 2.09 (s, 3H), 2.03 (s, 1H), 1.34–1.92 (m, 6H); ¹³C NMR (100 MHz, CDCl₃) δ 172.8, 156.1, 143.6, 136.4, 128.6, 128.3, 128.2, 67.0, 58.6, 53.8, 52.5, 32.3, 26.9, 22.7, 20.5, 20.0.

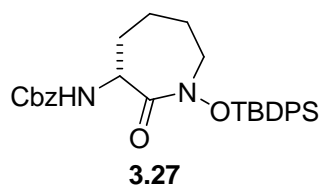


***N*^α-Cbz-*N*^ε-formyl-*N*^ε-[[2-(trimethylsilyl)ethoxy]-methoxy]-D-lysine methyl ester (3.24).** To a solution of the formate (212 mg, 0.627 mmol) in CH₂Cl₂ (5.0 mL) were added *i*-Pr₂NEt (0.55 ml, 3.135 mmol), DMAP (4 mg, 0.031 mmol) and SEMCl (0.17 ml, 0.941 mmol) at 0 °C. After being stirred at 0 °C for 30 min and then at room temperature for 17 h, the mixture was diluted with EtOAc, washed with H₂O and brine, dried over Na₂SO₄, filtered, and concentrated. The residue was purified by flash chromatography (EtOAc:Hexane=1:2) to afford the desired product **3.24** as a colorless oil (232 mg, 80%). ¹H NMR (400 MHz, CDCl₃) δ 8.27 (s, 1H), 7.28–7.34 (m, 5H), 5.34 (d, *J* = 8.0 Hz, 1H), 5.08 (s, 2H), 4.82 (s, 2H), 4.30–4.36 (m, 1H), 3.70 (m, 5H), δ 3.55 (m, 2H), 1.30–1.86 (m, 6H), 0.93 (t, *J* = 8.4 Hz, 2H), δ 0.01 (s, 9H); ¹³C NMR (100 MHz, CDCl₃) δ 172.9, 163.7, 156.1, 136.4, 128.7, 128.3, 128.3, 98.4, 67.3, 67.1, 53.8, 52.6, 44.9, 32.2, 26.4, 22.3, 18.2, -1.3.



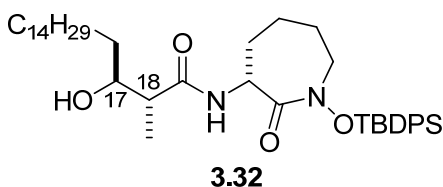
Lysine phenyl nitron (3.26). To a solution of KOH (214 mg, 3.82 mmol) and 1 g of 3 Å molecular sieves in 10 mL of CH₃OH at room temperature was added *N*^α-Cbz-

D-lysine **3.14** (1.07g, 3.58 mmol). When the stirred solution was clear, benzaldehyde (0.40 mL, 3.94 mmol) was added and the mixture was stirred for 16 h at room temperature. The mixture was filtered and the solvents were removed *in vacuo* to give a crude imine product. The residue was taken up in 40 mL of CH₃OH and cooled to 0 °C. Dry *m*-CPBA (963 mg, 4.3 mmol), dissolved in 10.0 mL of CH₃OH, was added dropwise over 4 min and the resulting solution was stirred for an additional 2 h at 0 °C. The reaction mixture was filtered and the solvents were removed *in vacuo* with no heating. Isomerization of the resulting crude oxaziridine was accomplished by the addition of 2 mL of TFA followed by 5 mL of CH₂Cl₂ to residue under a nitrogen atmosphere. The solution was stirred for 1 h at room temperature and the solvents were removed. The residue was taken up in 12 mL of EtOAc and cooled to 0 °C. PhCHO (0.2 ml) was added and the solution was stirred overnight while coming to room temperature. The solvents were removed and the residue was purified by flash chromatography on silica gel (CH₂Cl₂: acetone=1:4→ CH₃OH: CH₂Cl₂: acetone=3:13:4) to give 770 mg of nitrone as a pale yellow oil in 52% yield. ¹H NMR (400 MHz, CD₃CN) δ 9.72 (brs, 1H), 8.25 (m, 2H), 7.70 (s, 1H), 7.30–7.48 (m, 8H), 6.20 (d, *J* = 6.8 Hz, 1H), 5.04 (s, 2H), 4.17 (m, 1H), δ 3.95 (m, 2H), 1.36–1.96 (m, 6H); ¹³C NMR (100 MHz, CD₃CN) δ 174.1, 156.7, 139.2, 137.3, 131.8, 130.0, 128.9, 128.7, 128.2, 128.0, 66.5, 65.8, 54.2, 31.1, 27.0, 22.5.



TBDPS-protected azepinone hydroxamic acid (3.27). The lysine phenyl nitron **3.26** (551 mg, 1.432 mmol) and hydroxylamine hydrochloride (150 mg, 2.148 mmol) were dissolved in 10.0 mL of CH₃OH and heated in a 60 °C oil bath for 20 min and then allowed to cool. The solution was concentrated and taken up in distilled H₂O and extracted with ether until no more by-product was in the organic phase as detected by TLC. The aqueous solvent was removed *in vacuo*. Residual water was removed azeotropically *in vacuo* with benzene and methanol. The crude hydroxylamine in 45 mL of 7:2 CH₃CN:DMF was added dropwise over 2 h to a stirred solution of EDC (304 mg, 1.58 mmol), HOAt (195 mg, 1.432 mmol), and NaHCO₃ (602 mg, 7.16 mmol) in 27 mL of 7:2 CH₃CN:DMF. The solution was stirred for 48 h at room temperature. The CH₃CN was removed *in vacuo* and EtOAc and H₂O were added. The aqueous layer was acidified to approximately pH 2 with 1N HCl and extracted with EtOAc until no more product could be detected by TLC. The combined organic extracts were washed two times with 5% NaHCO₃ and one time with brine. The organic layer was dried with Na₂SO₄, filtered and concentrated to afford a crude azopine (190 mg). To a stirred solution of azepine in DMF (10.0 mL) was added TBDPSCl (0.87 mL, 3.41 mmol) and imidazole (464 mg, 6.82 mmol). After being stirred at 35 °C under N₂, the reaction was diluted with EtOAc. The EtOAc solution was washed with H₂O and brine, dried over Na₂SO₄, filtered, concentrated, and chromatographed on silica gel eluting with EtOAc:Hexane=1:6 to give azopine **3.27** (295 mg, 40%) as a clear oil. ¹H NMR (400 MHz, CDCl₃) 7.66–7.75 (m, 4H), 7.26–7.45 (m, 11H), δ 6.03 (d, *J* = 6.4 Hz, 1H), 4.94–5.10 (m, 2H), 3.99–4.05 (m, 1H), 3.36–3.50 (m, 2H), 1.05–1.89 (m, 15H); ¹³C NMR (100 MHz, CDCl₃) δ 169.8,

155.5, 136.7, 136.3, 136.2, 132.3, 131.8, 130.5, 130.4, 128.6, 128.1, 128.0, 127.8, 127.7, 66.7, 54.4, 53.3, 31.8, 27.6, 27.1, 25.5, 19.7.



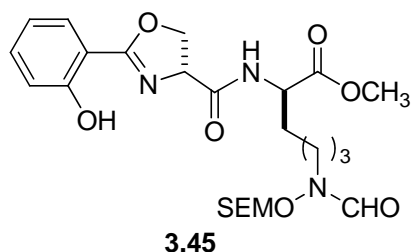
TBDPS-protected cobactin (3.32). Protected cyclic hydroxamic acid **3.27** (95 mg, 0.184 mmol) was stirred in CH₃OH (4.0 mL) in the presence of Pd/C (10%, 10 mg) under H₂ (1 atm) for 1 h. After filtration, the solvent was removed *in vacuo* to provide the corresponding free amine. The free amine was then treated with β-hydroxy acid **3.7** (77 mg, 0.245 mmol) and EDC (106 mg, 0.648 mmol) in CH₂Cl₂ (4.0 mL). After being stirred overnight, the reaction mixture was concentrated and chromatographed on silica gel eluting with EtOAc:CH₂Cl₂=1:6 to afford compound **3.32** (84 mg, 67%) as a clear oil. ¹H NMR (400 MHz, CDCl₃) δ 7.71 (t, *J* = 8.0 Hz, 4H), 7.35–7.46 (m, 6H), 6.79 (d, *J* = 6.4 Hz, 1H), 4.21 (dd, *J* = 10.4, 6.4 Hz, 1H), 3.73–3.77 (m, 1H), 3.41–3.54 (m, 2H), 2.28 (qd, *J* = 6.8, 2.8 Hz, 1H), 1.32–1.82 (m, 6H), 1.26 (brs, 26H), 1.14 (s, 9), 1.10 (d, *J* = 7.2 Hz, 3H), 0.88 (t, *J* = 6.8 Hz, 3H); ¹³C NMR (100 MHz, CDCl₃) δ 175.8, 169.4, 136.1, 136.0, 132.0, 131.5, 130.3, 130.2, 127.6, 127.5, 71.9, 54.2, 51.3, 44.2, 33.3, 31.9, 30.8, 29.67, 29.34, 27.3, 26.9, 26.0, 25.3, 22.7, 19.5, 14.1, 11.0.

3.33. a clear oil: ¹H NMR (400 MHz, CDCl₃) δ 7.71 (dd, *J* = 9.6, 7.2 Hz, 4H), 7.33–7.46 (m, 6H), 6.80 (d, *J* = 6.4 Hz, 1H), 4.13 (dd, *J* = 10.4, 5.6 Hz, 1H), 3.72–3.77

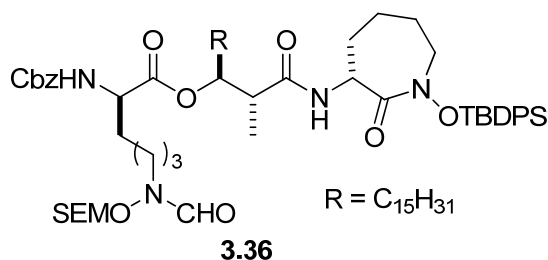
(m, 1H), 3.40–3.55 (m, 3H), 2.22 (qd, $J = 7.2, 2.4$ Hz, 1H), 1.32–1.84 (m, 6H), 1.24 (brs, 26H), 1.24 (s, 9), 1.07 (d, $J = 7.2$ Hz, 3H), 0.86 (t, $J = 6.8$ Hz, 3H); ^{13}C NMR (100 MHz, CDCl_3) δ 176.2, 169.6, 136.3, 136.2, 132.2, 131.7, 130.51, 130.47, 127.8, 127.7, 72.0, 54.4, 51.7, 44.5, 33.8, 32.1, 31.1, 29.90, 29.88, 29.87, 29.86, 29.80, 29.56, 27.5, 27.1, 26.2, 25.6, 22.9, 19.8, 14.3, 10.8.

3.34. a clear oil: ^1H NMR (400 MHz, CDCl_3) δ 7.71 (dd, $J = 10.4, 7.6$ Hz, 4H), 7.35–7.45 (m, 6H), 6.86 (d, $J = 6.4$ Hz, 1H), 4.17 (dd, $J = 11.2, 6.4$ Hz, 1H), 3.41–3.55 (m, 3H), 2.23 (dq, $J = 7.2, 6.8$ Hz, 1H), 1.32–1.86 (m, 6H), 1.25 (brs, 26H), 1.18 (d, $J = 7.2$ Hz, 3H), 1.14 (s, 9), 0.87 (t, $J = 6.8$ Hz, 3H); ^{13}C NMR (100 MHz, CDCl_3) δ 175.4, 169.6, 136.3, 136.2, 132.2, 131.7, 130.5, 127.8, 127.7, 74.2, 54.4, 51.7, 45.4, 35.9, 32.1, 31.3, 29.9, 29.8, 29.6, 27.5, 27.1, 26.0, 25.6, 22.9, 19.8, 15.7, 14.3.

3.35. a clear oil: ^1H NMR (400 MHz, CDCl_3) δ 7.73 (t, $J = 7.2$ Hz, 4H), 7.34–7.47 (m, 6H), 6.81 (d, $J = 6.4$ Hz, 1H), 4.20 (dd, $J = 11.2, 6.4$ Hz, 1H), 3.57 (d, $J = 7.2$ Hz, 1H), 3.40–3.53 (m, 3H), 2.22 (dq, $J = 7.2, 6.8$ Hz, 1H), 1.32–1.82 (m, 6H), 1.26 (brs, 26H), 1.18 (d, $J = 7.2$ Hz, 3H), 1.14 (s, 9), 0.87 (t, $J = 6.8$ Hz, 3H); ^{13}C NMR (100 MHz, CDCl_3) δ 175.8, 169.7, 136.3, 136.2, 132.2, 131.8, 130.51, 130.46, 127.8, 127.7, 74.0, 54.4, 51.6, 45.6, 35.6, 32.1, 30.8, 29.90, 29.88, 29.86, 29.6, 27.5, 27.1, 26.0, 25.6, 22.9, 19.8, 15.7, 14.3.



Mycobactic acid methyl ester analog (3.45). Protected hydroxamic acid **3.24** (208 mg, 0.414 mmol) was stirred in CH₃OH (4.0 mL) in the presence of Pd/C (10%, 20 mg) under H₂ (1 atm) for 1 h. After filtration, the solvent was removed *in vacuo* to provide the corresponding free amine. The free amine was then treated with acid **3.5** [derived from ester **3.22** (192 mg, 0.496 mmol) by hydrogenolysis] and EDC (184 mg, 0.958 mmol) in CH₂Cl₂ (5.0 mL). After being stirred overnight, the reaction mixture was concentrated and chromatographed on silica gel eluting with EtOAc:CH₂Cl₂=1:7 to afford compound **3.45** (166 mg, 63%) as a clear oil. ¹H NMR (400 MHz, CDCl₃) δ 11.36 (s, 1H), 8.21 (s, 1H), 7.67 (dd, *J* = 8.0, 1.6 Hz, 1H), 7.40 (t, *J* = 8.0 Hz, 1H), 7.00 (d, *J* = 8.0 Hz, 1H), 6.88 (t, *J* = 8.0 Hz, 1H), 6.85 (d, *J* = 8.4 Hz, 1H), 4.94 (t, *J* = 9.6 Hz, 2H), 4.78 (s, 2H), 4.60–4.68 (m, 2H), 4.51–4.58 (m, 1H), 3.74 (s, 3H), 3.67 (t, *J* = 8.0 Hz, 2H), 3.47–3.57 (m, 2H), 1.20–1.90 (m, 6H); 0.91 (t, *J* = 8.4 Hz, 2H), –0.01 (s, 9H); ¹³C NMR (100 MHz, CDCl₃) δ 172.3, 170.7, 168.0, 163.8, 160.0, 134.5, 128.8, 119.2, 117.2, 110.2, 98.4, 69.7, 68.3, 67.3, 52.8, 52.2, 44.7, 31.6, 26.3, 22.4, 18.2, –1.3.



To a solution of **3.32** (167 mg, 0.25 mmol) in toluene (4.0 mL) was added a solution of **3.6** (165 mg, 0.36 mmol) in toluene (4.0 mL) and followed by the addition of DCC (206 mg, 1.00 mmol) and DMAP (122 mg, 1.00 mmol) at 25 °C. After being stirred for 72 h at 25 °C, the reaction mixture was concentrated and purified by column chromatography (silica gel, EtOAc/hexane, 1/1) to afford cyclic hydroxamate ester **3.36** (240 mg, 88%) as a colorless oil. ¹H NMR (400 MHz, CDCl₃) δ 8.30 (s, 1H), 7.72 (d, *J* = 6.8 Hz, 4H), 7.28–7.45 (m, 11H), 6.93 (d, *J* = 4.8 Hz, 1H), 5.72 (d, *J* = 7.6 Hz, 1H), 5.10 (s, 2H), 4.95–5.03 (m, 2H), 4.84 (s, 2H), 4.32–4.38 (m, 1H), 4.13–4.20 (m, 2H), 3.72 (t, *J* = 7.6 Hz, 2H), 3.40–3.57 (m, 4H), 2.41–2.48 (m, 1H), 1.20–1.95 (m, 40H), 1.12 (s, 9H), 1.07 (d, *J* = 7.2 Hz, 3H), 0.95 (t, *J* = 8.4 Hz, 3H), 0.88 (t, *J* = 6.8 Hz, 3H), 0.02 (s, 9H); ¹³C NMR (100 MHz, CDCl₃) δ 171.7, 169.4, 163.4, 156.2, 136.5, 136.1, 136.0, 132.0, 131.5, 130.3, 130.1, 128.4, 128.0, 127.9, 127.5, 98.0, 76.2, 67.1, 66.7, 54.2, 51.6, 49.0, 44.6, 44.3, 33.9, 32.5, 31.9, 31.5, 30.8, 30.7, 29.64, 29.60, 29.50, 29.30, 27.2, 26.9, 26.3, 25.9, 25.6, 25.2, 24.9, 24.7, 22.6, 22.5, 19.5, 18.0, 14.1, -1.52.

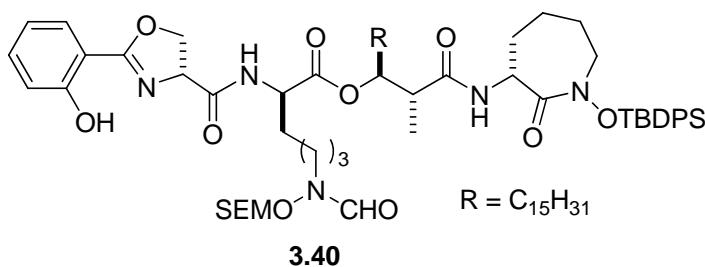
3.37. a colorless oil: ¹H NMR (400 MHz, CDCl₃) δ 8.30 (s, 1H), 7.73 (dd, *J* = 7.6, 6.8 Hz, 4H), 7.26–7.47 (m, 11H), 6.84 (d, *J* = 4.8 Hz, 1H), 5.42 (d, *J* = 8.4 Hz, 1H),

5.00–5.14 (m, 3H), 4.82 (s, 2H), 4.30–4.38 (m, 1H), 4.12–4.16 (m, 2H), 3.72 (t, $J = 8.0$ Hz, 2H), 3.40–3.58 (m, 4H), 2.30–2.38 (m, 1H), 1.20–1.95 (m, 40H), 1.14 (s, 9H), 1.04 (d, $J = 6.8$ Hz, 3H), 0.95 (dd, $J = 8.4, 7.2$ Hz, 3H), 0.87 (t, $J = 7.2$ Hz, 3H), 0.03 (s, 9H); ^{13}C NMR (100 MHz, CDCl_3) δ 172.0, 171.8, 169.6, 163.7, 156.1, 136.3, 136.2, 132.2, 131.7, 130.51, 130.46, 128.7, 128.3, 127.8, 127.7, 98.3, 76.6, 67.3, 67.1, 54.4, 54.2, 51.8, 44.7, 34.1, 32.1, 32.0, 31.0, 29.90, 29.80, 29.64, 29.55, 27.5, 27.1, 26.5, 26.1, 25.8, 25.8, 25.5, 25.1, 24.9, 22.9, 22.6, 19.8, 18.3, 14.3, 13.5, –1.26.

3.38. a colorless oil: ^1H NMR (400 MHz, CDCl_3) δ 8.30 (s, 1H), 7.72 (t, $J = 6.4$ Hz, 4H), 7.32–7.43 (m, 11H), 6.96 (d, $J = 6.0$ Hz, 1H), 5.67 (d, $J = 8.4$ Hz, 1H), 5.08 (s, 2H), 4.99–5.13 (m, 2H), 4.84 (s, 2H), 4.24–4.29 (m, 1H), 4.14 (dd, $J = 9.6, 5.6$ Hz, 1H), 3.72 (t, $J = 7.6$ Hz, 2H), 3.35–3.61 (m, 4H), 2.46–2.54 (m, 1H), 1.20–1.95 (m, 40H), 1.12 (s, 9H), 1.06 (d, $J = 7.2$ Hz, 3H), 0.95 (dd, $J = 9.6, 8.0$ Hz, 3H), 0.87 (t, $J = 7.2$ Hz, 3H), 0.02 (s, 9H); ^{13}C NMR (100 MHz, CDCl_3) δ 172.2, 171.6, 169.7, 163.7, 156.1, 136.4, 136.2, 132.2, 131.7, 130.5, 130.4, 128.7, 128.2, 127.78, 127.72, 98.2, 76.4, 67.3, 66.9, 54.5, 54.3, 51.8, 49.2, 44.8, 34.1, 32.1, 31.6, 31.2, 29.89, 29.84, 29.70, 29.55, 27.5, 27.1, 26.5, 25.8, 25.5, 25.2, 22.9, 22.6, 19.8, 18.2, 14.3, –1.26.

3.39. a colorless oil: ^1H NMR (400 MHz, CDCl_3) δ 8.30 (s, 1H), 7.72 (dd, $J = 8.0, 1.6$ Hz, 4H), 7.26–7.46 (m, 11H), 7.14 (d, $J = 6.0$ Hz, 1H), 5.78 (d, $J = 8.0$ Hz, 1H), 5.09 (s, 2H), 4.95–5.18 (m, 2H), 4.84 (s, 2H), 4.25–4.31 (m, 1H), 4.08–4.13 (m, 2H), 3.72 (t, $J = 7.6$ Hz, 2H), 3.39–3.63 (m, 4H), 2.45–2.57 (m, 1H), 1.20–1.95 (m, 40H), 1.12

(s, 9H), 1.05 (d, $J = 7.2$ Hz, 3H), 0.95 (t, $J = 10.0, 7.2$ Hz, 3H), 0.87 (t, $J = 6.8$ Hz, 3H), 0.02 (s, 9H); ^{13}C NMR (100 MHz, CDCl_3) δ 172.7, 171.5, 169.5, 163.7, 156.2, 136.4, 136.2, 132.2, 131.7, 130.6, 130.4, 128.7, 128.2, 127.8, 98.2, 76.4, 67.3, 66.9, 54.4, 52.0, 49.3, 44.6, 34.1, 32.1, 31.7, 31.0, 29.89, 29.67, 29.55, 27.5, 27.1, 26.5, 25.8, 25.4, 25.1, 22.9, 22.5, 19.8, 18.2, 14.5, 14.3, -1.26.



To a solution of Cbz protected hydroxamate ester **3.36** (116 mg, 0.092 mmol) in CH_3OH (2.0 mL) was added Pd/C (10%, 12 mg) at 25 °C. The reaction mixture was flushed with H_2 , then stirred under H_2 atmosphere for 5 h. After filtration through celite, the reaction mixture was concentrated under reduced pressure to afford the corresponding free amine. To a solution of free amine in CH_2Cl_2 (2.0 mL) was added oxazoline carboxylic acid **3.5** (89 mg, 0.43 mmol) and EDC·HCl (53 mg, 0.28 mmol) at 25 °C. After being stirred for 16 h at 25 °C, the reaction mixture was concentrated and purified by column chromatography (silica gel, EtOAc/hexane, 1/1) to afford SEM and TBDPS protected depsipeptide **3.40** (65 mg, 60%) as a colorless oil. ^1H NMR (400 MHz, CDCl_3) δ 11.40 (s, 1H), 8.25 (s, 1H), 7.68–7.74 (m, 6H), 7.32–7.45 (m, 9H), 7.13 (d, $J = 7.2$ Hz, 1H), 7.08 (d, $J = 4.0$ Hz, 1H), 7.00 (d, $J = 8.0$ Hz, 1H), 6.89 (d, $J = 7.6$ Hz, 1H), 5.01–5.05 (m, 2H), 4.96 (t, $J = 9.6$ Hz, 1H), 4.80 (s, 2H), 4.61–4.64 (m, 2H), 4.56 (q, $J = 6.4$

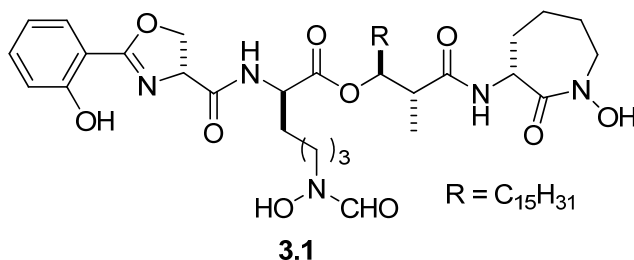
Hz, 1H), 4.23 (dd, $J = 10.4, 6.0$ Hz, 1H), 4.13 (d, $J = 7.2$ Hz, 1H), 3.70 (t, $J = 8.0$ Hz, 2H), 3.42–3.56 (m, 6H), 2.50 (t, $J = 6.0$ Hz, 1H), 1.20–1.95 (m, 40H), 1.11 (brs, 12H), 0.94 (t, $J = 8.4$ Hz, 3H), 0.87 (t, $J = 6.4$ Hz, 3H), 0.01 (s, 9H); ^{13}C NMR (100 MHz, CDCl_3) δ 171.9, 171.2, 170.6, 169.8, 167.6, 163.6, 159.8, 136.05, 135.98, 134.1, 131.9, 131.7, 130.2, 128.5, 127.52, 127.48, 118.9, 116.9, 110.1, 98.0, 76.4, 69.5, 68.1, 67.1, 54.2, 52.6, 51.6, 49.0, 44.4, 44.2, 33.9, 31.9, 30.9, 29.67, 29.61, 29.54, 29.32, 27.2, 26.8, 26.2, 25.8, 25.6, 25.3, 24.9, 22.6, 22.4, 19.6, 18.0, 14.1, -1.50.

3.41. a colorless oil: ^1H NMR (400 MHz, CDCl_3) δ 11.40 (s, 1H), 8.23 (s, 1H), 7.67–7.75 (m, 6H), 7.34–7.47 (m, 9H), 7.02 (d, $J = 8.4$ Hz, 1H), 6.94 (d, $J = 8.0$ Hz, 1H), 6.90 (t, $J = 8.0$ Hz, 1H), 6.83 (d, $J = 6.0$ Hz, 1H), 5.05–5.10 (m, 2H), 4.95 (t, $J = 9.6$ Hz, 1H), 4.80 (s, 2H), 4.62–4.65 (m, 2H), 4.52 (q, $J = 7.2$ Hz, 1H), 4.17 (dd, $J = 10.8, 6.4$ Hz, 1H), 3.70 (t, $J = 8.0$ Hz, 2H), 3.41–3.56 (m, 5H), 2.38–2.45 (m, 1H), 1.20–1.95 (m, 40H), 1.13 (brs, 12H), 1.07 (d, $J = 7.2$ Hz, 3H), 0.94 (dd, $J = 8.4, 8.4$ Hz, 3H), 0.87 (t, $J = 6.8$ Hz, 3H), 0.02 (s, 9H); ^{13}C NMR (100 MHz, CDCl_3) δ 172.0, 171.1, 170.6, 169.7, 167.9, 163.8, 160.0, 136.3, 136.2, 134.4, 132.2, 131.8, 130.5, 128.8, 127.8, 127.7, 119.2, 117.2, 110.3, 98.2, 69.7, 68.3, 67.3, 54.4, 52.7, 51.8, 44.6, 32.1, 32.0, 31.6, 31.1, 29.91, 29.65, 29.56, 27.5, 27.1, 26.4, 25.5, 22.9, 22.6, 19.8, 18.2, 14.3, 13.3, -1.26.

3.42. a colorless oil: ^1H NMR (400 MHz, CDCl_3) δ 11.40 (s, 1H), 8.23 (s, 1H), 7.66–7.75 (m, 6H), 7.33–7.47 (m, 9H), 6.97 (d, $J = 8.4$ Hz, 1H), 6.88 (d, $J = 8.0$ Hz, 1H), 6.85 (d, $J = 6.4$ Hz, 1H), 5.01–5.23 (m, 4H), 4.73 (s, 2H), 4.47 (dd, $J = 9.6, 8.4$ Hz, 1H),

4.14–4.19 (m, 1H), 3.62–3.78 (m, 2H), 3.38–3.56 (m, 5H), 2.46–2.53 (m, 1H), 1.20–1.95 (m, 40H), 1.14 (brs, 12H), 1.03 (d, $J = 6.8$ Hz, 3H), 0.94 (d, $J = 8.0$ Hz, 3H), 0.89 (t, $J = 6.8$ Hz, 3H), 0.02 (s, 9H).

3.43. a colorless oil: ^1H NMR (400 MHz, CDCl_3) δ 11.49 (s, 1H), 8.23 (s, 1H), 7.69–7.76 (m, 6H), 7.34–7.46 (m, 9H), 7.11 (d, $J = 7.6$ Hz, 1H), 7.02 (d, $J = 4.4$ Hz, 1H), 7.01 (d, $J = 8.4$ Hz, 1H), 6.90 (d, $J = 7.2$ Hz, 1H), 5.01–5.05 (m, 2H), 4.92 (dd, $J = 10.8$, 8.0 Hz, 1H), 4.80 (s, 2H), 4.58–4.70 (m, 2H), 4.44 (q, $J = 6.4$ Hz, 1H), 4.20 (dd, $J = 9.6$, 6.0 Hz, 1H), 3.69 (t, $J = 8.0$ Hz, 2H), 3.47–3.57 (m, 5H), 2.51 (dq, $J = 6.8$, 6.4 Hz, 1H), 1.20–1.95 (m, 40H), 1.12 (brs, 12H), 1.08 (d, $J = 7.2$ Hz, 3H), 0.95 (t, $J = 10.0$, 9.6 Hz, 3H), 0.87 (t, $J = 6.8$ Hz, 3H), 0.02 (s, 9H).



Depsipeptide **3.40** (30 mg, 0.026 mmol) in TFA/ CH_2Cl_2 (1.0 mL, 1:1) was stirred under N_2 atmosphere at 25 °C for 2 h. The reaction mixture was concentrated and washed with Et_2O (1.0 mL \times 3). The crude mixture was then purified by reverse phase semi-HPLC (Luna C18, Phenomenex, 250 mm \times 10 mm \times 5 μm ; eluent, $\text{CH}_3\text{CN}/\text{H}_2\text{O}$, 80:20; flow rate, 3 mL/min; UV detection, 230 nm and 254 nm) to afford iron-free brasilibactin A **3.1** (14 mg, 68%) as a white solid: ^1H NMR (400 MHz, $\text{DMSO}-d_6$) δ 11.80 (brs, 1H),

9.92 (brs, 0.7H), 8.98 (brs, 0.3H), 8.73 (brs, 1H), 8.44 (s, 0.5H), 8.22 (s, 0.5H), 8.13 (d, $J = 7.2$ Hz, 1H), 7.86 (s, 0.5H), 7.64 (dd, $J = 7.6, 1.6$ Hz, 1H), 7.47 (t, $J = 8.0$ Hz, 1H), 7.01 (d, $J = 7.6$ Hz, 1H), 6.95 (t, $J = 8.0$ Hz, 1H), 5.01 (dd, $J = 10.0, 7.6$ Hz, 1H), 4.90 (td, $J = 8.8, 2.4$ Hz, 1H), 4.67 (dd, $J = 10.0, 8.4$ Hz, 1H), 4.47 (dd, $J = 8.4, 8.0$ Hz, 1H), 4.44 (m, 1H), 4.25 (m, 1H), 3.87 (dd, $J = 15.6, 12.0$ Hz, 1H), 3.36 (m, 1H), 2.62 (m, 1H), 1.35–1.83 (m, 13H), 1.10–1.35 (m, 28H), 0.94 (d, $J = 7.2$ Hz, 3H), 0.85 (t, $J = 6.8$ Hz, 3H).
(2H between 3.42 - 3.48 are obscured by the H₂O peak in DMSO-*d*₆, but are visible in CD₃OD or acetone-*d*₆)

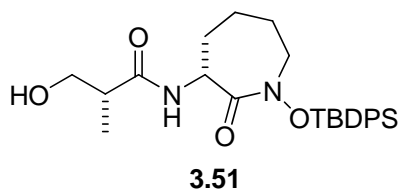
3.2. a white solid: ¹H NMR (400 MHz, DMSO-*d*₆) δ 11.79 (brs, 1H), 10.29 (s, 0.5H), 9.92 (brs, 1H), 8.96 (brs, 0.5H), 8.74 (brs, 1H), 8.45 (s, 1H), 8.22 (s, 0.5H), 8.15 (d, $J = 6.4$ Hz, 1H), 7.87 (s, 0.5H), 7.63 (dd, $J = 8.0, 1.6$ Hz, 1H), 7.47 (t, $J = 8.0$ Hz, 1H), 7.00 (d, $J = 8.4$ Hz, 1H), 6.94 (t, $J = 8.0$ Hz, 1H), 5.00 (dd, $J = 10.0, 7.6$ Hz, 1H), 4.95 (t, $J = 6.8$ Hz, 1H), 4.65 (dd, $J = 9.6, 8.4$ Hz, 1H), 4.48 (dd, $J = 8.8, 8.0$ Hz, 1H), 4.46 (m, 1H), 4.21 (m, 1H), 3.87 (dd, $J = 16.4, 11.6$ Hz, 1H), 3.48 (dd, $J = 15.2, 4.0$ Hz, 1H), 3.42 (t, $J = 6.8$ Hz, 1H), 3.37 (t, $J = 6.4$ Hz, 1H), 2.66 (m, 1H), 1.35–1.85 (m, 13H), 1.10–1.35 (m, 28H), 0.94 (d, $J = 6.8$ Hz, 3H), 0.84 (t, $J = 6.8$ Hz, 3H).

3.3. a white solid: ¹H NMR (400 MHz, DMSO-*d*₆) δ 11.80 (brs, 1H), 11.02 (s, 0.3H), 10.30 (s, 0.3H), 9.92 (brs, 0.7H), 8.94 (brs, 0.3H), 8.65 (brs, 1H), 8.45 (s, 0.5H), 8.21 (s, 0.5H), 7.88 (d, $J = 7.2$ Hz, 1H), 7.86 (s, 0.5H), 7.63 (dd, $J = 8.0, 2.0$ Hz, 1H), 7.47 (t, $J = 8.0$ Hz, 1H), 7.00 (d, $J = 8.0$ Hz, 1H), 6.95 (t, $J = 7.6$ Hz, 1H), 5.00 (dd, $J = 10.4, 7.6$ Hz, 1H), 4.95 (td, $J = 8.0, 3.2$ Hz, 1H), 4.65 (dd, $J = 10.0, 8.4$ Hz, 1H), 4.48 (dd,

$J = 7.6, 6.8$ Hz, 1H), 4.40 (dd, $J = 10.4, 6.8$ Hz, 1H), 4.23 (m, 1H), 3.81 (dd, $J = 16.0, 11.2$ Hz, 1H), 2.70 (m, 1H), 1.35–1.83 (m, 13H), 1.10–1.35 (m, 28H), 0.94 (d, $J = 7.2$ Hz, 3H), 0.85 (t, $J = 6.8$ Hz, 3H). (3H between 3.33 - 3.48 are obscured by the H_2O peak in $DMSO-d_6$, but are visible in CD_3OD or $acetone-d_6$)

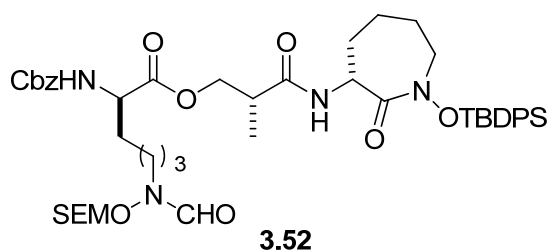
3.4. a white solid: 1H NMR (400 MHz, $DMSO-d_6$) δ 10.30 (brs, 0.5H), 9.81 (brs, 1H), 8.67 (d, $J = 7.6$ Hz, 1H), 8.63 (d, $J = 7.2$ Hz, 1H), 8.42 (brs, 0.5H), 8.21 (s, 0.5H), 7.93 (d, $J = 6.8$ Hz, 1H), 7.88 (s, 0.5H), 7.63 (dd, $J = 7.6, 1.6$ Hz, 1H), 7.47 (t, $J = 8.0$ Hz, 1H), 7.00 (d, $J = 8.4$ Hz, 1H), 6.94 (t, $J = 7.6$ Hz, 1H), 5.00 (dd, $J = 9.6, 7.6$ Hz, 1H), 4.95 (td, $J = 8.0, 2.8$ Hz, 1H), 4.64 (dd, $J = 10.0, 8.4$ Hz, 1H), 4.51 (dd, $J = 8.0, 7.6$ Hz, 1H), 4.42 (dd, $J = 10.8, 8.0$ Hz, 1H), 4.15 (m, 1H), 3.82 (dd, $J = 16.0, 11.6$ Hz, 1H), 3.38–3.43(m, 1H), 3.35 (t, $J = 6.4$ Hz, 1H), 2.74 (m, 1H), 1.36–1.85 (m, 13H), 1.12–1.32 (m, 28H), 0.97 (d, $J = 6.8$ Hz, 3H), 0.85 (t, $J = 6.8$ Hz, 3H). (1H between 3.42 - 3.48 are obscured by the H_2O peak in $DMSO-d_6$, but are visible in CD_3OD or $acetone-d_6$)

3.5.3 Preparation of brasilibactin A analogue (Bbtan, 3.54)



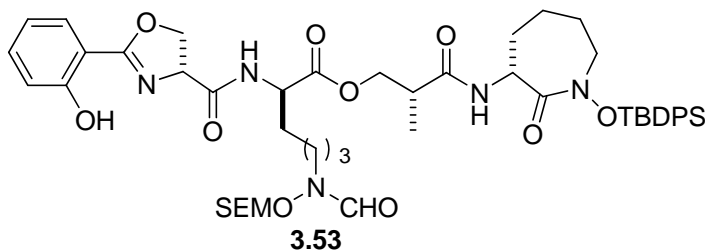
Cyclic hydroxamate alcohol (3.51). To a solution of Cbz protected hydroxamate **3.11** (255 mg, 0.49 mmol) in CH_3OH (3.0 mL) was added Pd/C (10%, 50 mg) at 25 °C.

The reaction mixture was flushed with H₂, then stirred under H₂ atmosphere for 3 h. After filtration through celite, the reaction mixture was concentrated under reduced pressure to afford the corresponding free amine. To a solution of free amine in CH₂Cl₂ (20.0 mL) was added β-hydroxy carboxylic acid **3.50** (79 mg, 0.76 mmol) and EDC·HCl (284 mg, 1.48 mmol) at 25 °C. After being stirred for 2 h at 25 °C, the reaction mixture was concentrated and purified by column chromatography (silica gel, EtOAc/hexane, 1/2) to afford cyclic hydroxamate alcohol **3.51** (168 mg, 72% for 2 steps) as a colorless oil. ¹H NMR (400 MHz, CDCl₃) δ 1.08 (d, *J* = 7.2 Hz, 3H), 1.13 (s, 9H), 1.18–1.29 (m, 1H), 1.36–1.46 (m, 1H), 1.52–1.61 (m, 2H), 1.78 (d, *J* = 10.0 Hz, 2H), 2.39–2.47 (m, 1H), 3.30 (br, s, 1H), 3.46–3.47 (m, 2H), 3.54–3.61 (m, 2H), 4.26 (dd, *J* = 6.8, 10.0 Hz, 1H), 6.73 (d, *J* = 6.8 Hz, 1H), 7.34–7.47 (m, 6H), 7.71–7.75 (m, 4H); ¹³C NMR (100 MHz, CDCl₃) δ 175.2, 170.0, 136.3, 136.2, 132.2, 131.7, 130.4, 130.3, 127.7, 127.6, 65.3, 54.3, 51.7, 42.4, 30.6, 27.4, 27.0, 25.4, 19.7, 13.7.



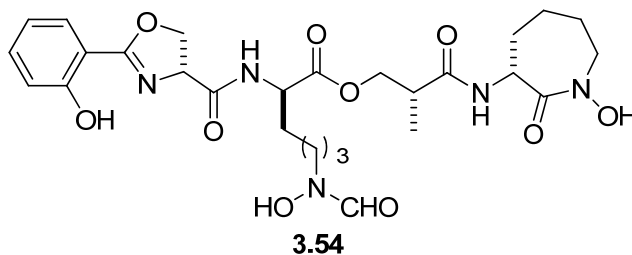
Cyclic hydroxamate ester (3.52). To a solution of **3.51** (78 mg, 0.17 mmol) in toluene (4.0 mL) was added a solution of **3.6** (96 mg, 0.21 mmol) in toluene (4.0 mL) and followed by the addition of DCC (138 mg, 0.69 mmol) and DMAP (82 mg, 0.69 mmol) at 25 °C. After being stirred for 22 h at 25 °C, the reaction mixture was concentrated and

purified by column chromatography (silica gel, EtOAc/hexane, 1/1) to afford cyclic hydroxamate ester **3.52** (100 mg, 66%) as a colorless oil. ^1H NMR (400 MHz, CDCl_3) δ 0.02 (s, 9H), 0.95 (t, $J = 8.4$ Hz, 3H), 0.97–1.91 (m, 27H), 2.53 (m, 1H), 3.42–3.57 (m, 4H), 3.72 (t, $J = 8.0$ Hz, 2H), 4.09–4.20 (m, 4H), 4.30–4.32 (m, 1H), 4.84 (s, 1H), 5.10 (s, 2H), 5.58 (d, $J = 8.0$ Hz, 1H), 6.93 (d, $J = 4.8$ Hz, 1H), 7.29–7.38 (m, 11H), 7.71–7.73 (m, 4H), 8.30 (s, 0.8H); ^{13}C NMR (100 MHz, CDCl_3) δ 172.3, 172.1, 169.6, 163.7, 156.2, 136.6, 136.3, 136.2, 132.2, 131.7, 130.5, 130.4, 128.7, 128.3, 127.7, 114.2, 98.3, 54.4, 54.0, 51.8, 44.8, 40.2, 39.0, 33.4, 32.1, 31.8, 31.2, 30.4, 30.0, 29.8, 29.5, 27.4, 27.1, 26.9, 26.5, 26.1, 25.4, 22.8, 22.4, 19.7, 18.2, 14.3, –1.3.



SEMO and TBDPS protected depsipeptide (3.53). To a solution of Cbz protected hydroxamate ester **3.52** (101 mg, 0.11 mmol) in CH_3OH (2.0 mL) was added Pd/C (10%, 15 mg) at 25 °C. The reaction mixture was flushed with H_2 , then stirred under H_2 atmosphere for 5 h. After filtration through celite, the reaction mixture was concentrated under reduced pressure to afford the corresponding free amine. To a solution of free amine in CH_2Cl_2 (10.0 mL) was added oxazoline carboxylic acid **3.5** (60 mg, 0.20 mmol) and EDC·HCl (65 mg, 0.34 mmol) at 25 °C. After being stirred for 16 h at 25 °C, the reaction mixture was concentrated and purified by column chromatography

(silica gel, acetone/hexane, 2/7) to afford SEM and TBDPS protected depsipeptide **3.53** (94 mg, 87%) as a colorless oil. ^1H NMR (400 MHz, CD_3OD) δ 0.02 (s, 9H), 0.94 (t, $J = 11.2$ Hz, 3H), 1.04 – 1.91 (m, 27H), 2.61 (dd, $J = 11.2, 17.6$ Hz, 1H), 3.49–3.57 (m, 4H), 3.70 (t, $J = 11.2$ Hz, 2H), 4.17–4.26 (m, 2H), 4.47–4.53 (m, 1H), 4.61–4.68 (m, 2H), 4.80 (s, 1H), 4.95 (dd, $J = 10.4, 14.0$ Hz, 1H), 6.91 (t, $J = 7.6$ Hz, 1H), 6.97–7.03 (m, 3H), 7.33–7.46 (m, 7H), 7.68–7.76 (m, 5H), 7.96 (s, 0.2H), 8.22 (s, 0.8H), 11.29 (br, s, 1H); ^{13}C NMR (100 MHz, CDCl_3) δ 171.2, 171.4, 170.5, 169.8, 163.7, 160.0, 136.3, 136.2, 134.3, 132.1, 131.8, 130.4, 128.7, 127.7, 119.1, 117.1, 98.2, 69.6, 68.1, 67.2, 54.4, 52.4, 51.8, 40.1, 31.0, 27.4, 27.0, 26.2, 25.4, 22.3, 19.7, 18.1, 14.4, –1.4.



Brasilibactin A analogue (Bbtan, 3.54). Depsipeptide **3.53** (50 mg, 0.052 mmol) in TFA/ CH_2Cl_2 (1.5 mL, 1:4) was stirred under N_2 atmosphere at 25 °C for 2 h. The reaction mixture was concentrated and washed with Et_2O (1.0 mL \times 3). The crude mixture was then purified by reverse phase semi-HPLC (Luna C18, Phenomenex, 250 mm \times 10 mm \times 5 μm ; eluent, $\text{CH}_3\text{CN}/\text{H}_2\text{O}$, 40:60; flow rate, 3 mL/min; UV detection, 230 nm and 254 nm) to afford iron-free brasilibactin A analogue **3.54** (24 mg, 78%) as a white solid: ^1H NMR (400 MHz, CD_3OD) δ 1.14 (d, 3H, $J = 7.2$ Hz), 1.29–1.98 (m, 12H), 2.80–2.90 (m, 1H), 3.47 (t, 1H, $J = 6.8$ Hz), 3.54 (t, 1H, $J = 6.8$ Hz), 3.67 (dd, 1H, $J =$

4.8, 16.0 Hz), 3.93 (dd, 1H, $J = 11.2, 16.0$ Hz), 4.14–4.25 (m, 2H), 4.48 (ddd, $J = 5.2, 8.6, 8.6$ Hz 1H), 4.57–4.63 (m, 3H), 5.07 (t, $J = 8.8$ Hz, 1H), 6.90 (t, $J = 7.6$ Hz, 1H), 6.96 (d, $J = 8.0$ Hz, 1H), 7.41 (t, $J = 8.0$ Hz, 1H), 7.68 (dd, $J = 2.0, 8.0$ Hz, 1H), 7.90 (br s, 0.6H), 8.22 (br s, 0.4H); ^{13}C NMR (100 MHz, CD_3OD) δ 175.6, 172.9, 170.8, 168.5, 163.9, 160.9, 159.4, 135.0, 129.5, 120.0, 117.7, 111.5, 70.4, 69.2, 67.8, 54.1, 53.8, 52.7, 51.0, 47.1, 40.9, 31.9, 28.7, 27.5, 26.9, 26.8, 23.6, 23.5, 14.4; LCMS (FAB) m/z calcd for $\text{C}_{27}\text{H}_{37}\text{N}_5\text{O}_{10}$ ($\text{M} + \text{H}$) $^+$ 592.25, found 592.21.

Chapter 4

Aza-Michael Reaction to Synthesize 2,6-Disubstituted Piperidines

4.1 Introduction

4.1.1 Importance

Structurally complex piperidines are found in a wide range of biologically interesting and naturally occurring compounds, including piperidine alkaloids (Figure 4.1).¹¹⁷ In particular, 2,6-disubstituted piperidines have attracted a considerable interest because of their therapeutical potential, such as anti-Alzheimer activity, antiangiogenic activity (solenopsin) and drug addiction treatment (lobeline).¹¹⁸

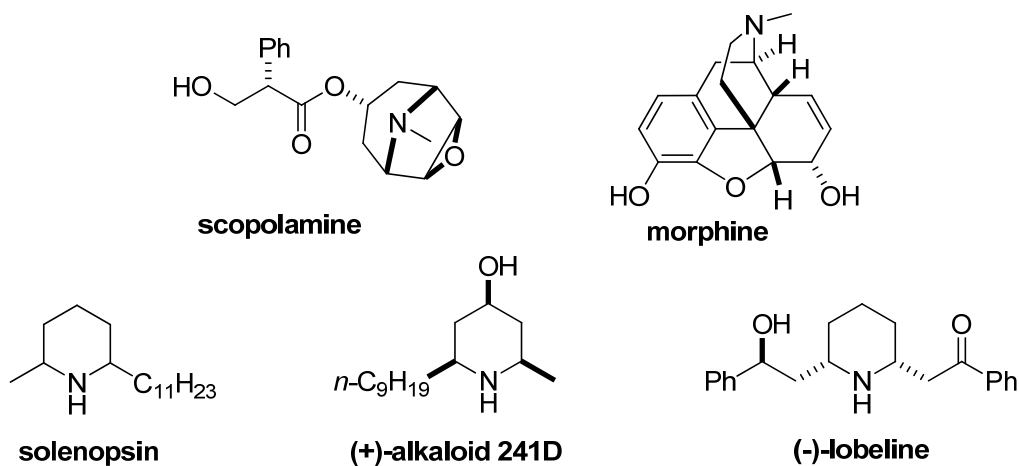
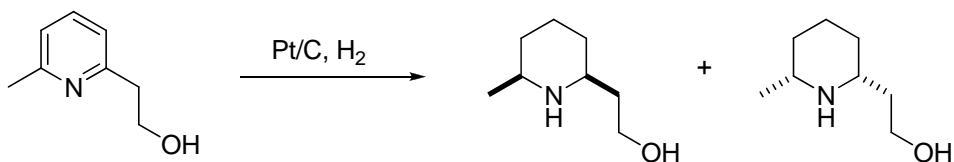


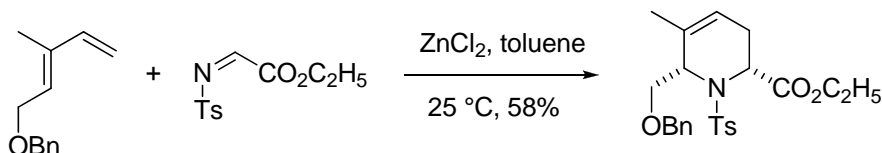
Figure 4.1 Representative naturally occurring piperidines

Due to their therapeutical potential and characteristic *cis*- or *trans*-relative stereochemistry, 2,6-disubstituted piperidines are of special synthetic significance, and many synthetic methods have been produced.¹¹⁹ One of the earliest routes to 2,6-disubstituted piperidines relied on catalytic hydrogenation of substituted pyridines using either Pd/C, Pt, PtO₂ or Rh/C.¹²⁰ Weinreb reported aza-Diels-Alder reaction of butadiene with *N*-tosyl imine to synthesize 2,6-*cis*-piperidines in the presence of lewis acid.¹²¹ More recently, Takahata and Momose reported the usefulness of nucleophilic substitution to access the 2,6-*trans*-piperidine cores.¹²² Yus and co-workers demonstrated a stereoselective synthesis of 2,6-*cis*-piperidine from *N*-tert-butylsulfinylamines with cross-metathesis reductive amination sequence.¹²³ Most recently, Helmchen and co-workers demonstrated a convergent Iridium-catalyzed allylic cyclization to both 2,6-*cis*- and *trans*-piperidines (Figure 4.2).¹²⁴

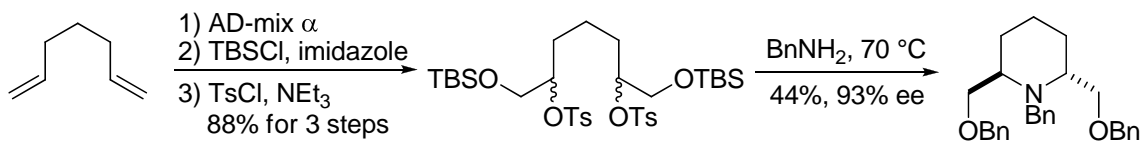
Reduction of substituted pyridines



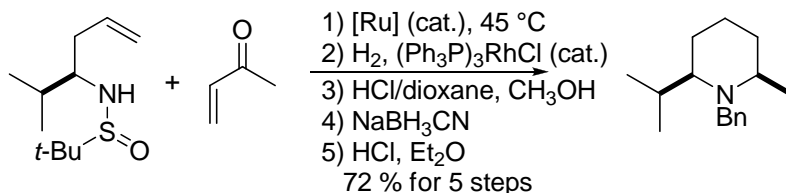
Aza-Diels-Alder Reaction



Nucleophilic substitution



Cross-metathesis and reduction cyclization



Iridium-catalyzed allylic cyclization

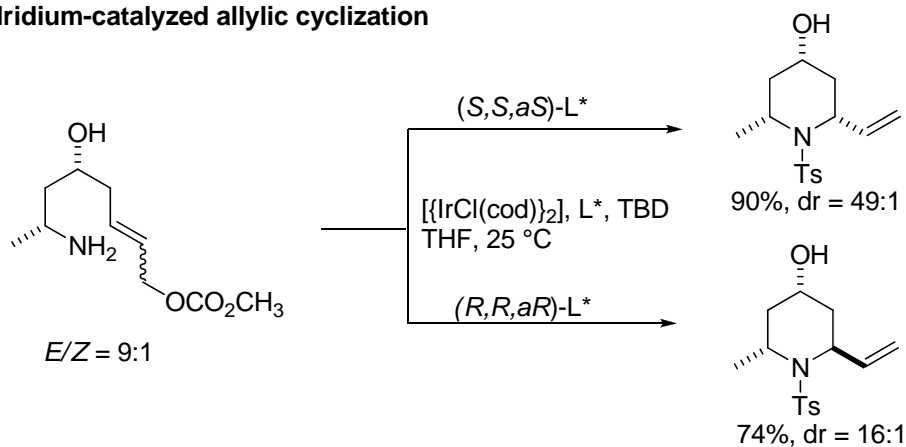


Figure 4.2 Representative examples to prepare 2,6-disubstituted piperidines

Although considerable efforts have been devoted to the development of synthetic routes for piperidines, there still exists a great need for a synthetic approach towards these classes of molecules that allows for rapid and easy access to substrates, proceeds with good stereoselectivity and yield, and requires mild reaction conditions compatible with various functional groups. However, most of the earlier synthetic methodologies have been directed towards the synthesis of either 2,6-*cis*- or *trans*-piperidines.¹²⁵ The stereoselective synthesis of both 2,6-*cis*- and *trans*-piperidines from a common intermediate still remains a substantial challenge to synthetic chemists.

4.1.2 Previous studies

While there is a wealth of methods generated to prepare this kind of piperidine alkaloids, their abundance in nature and significant biological activity led us to pursue an alternative route for their generation from a common intermediate. Recently, our group reported the feasibility of the tandem allylic oxidation/oxa-Michael reaction promoted by the *gem*-disubstituent effect for the stereoselective synthesis of 2,6-*cis*-tetrahydropyrans (THPs) (Figure 4.3).¹²⁶ The 1,3-dithiane group enabled rapid access to substrates, promoted the intramolecular oxa-Michael reaction through the *gem*-disubstituent effect, and improved the stereoselectivity of the reaction as a result of the increased 1,3-diaxial interaction. Furthermore, the 1,3-dithiane group served as a latent functional group for a carbonyl or hydroxy group. Our group applied the tandem reaction in conjunction with 1,3-dithiane coupling reaction to the stereoselective and efficient synthesis of a variety of 2,6-*cis*-tetrahydropyrans and (+)-neopeltolide macrolactone.¹²⁶

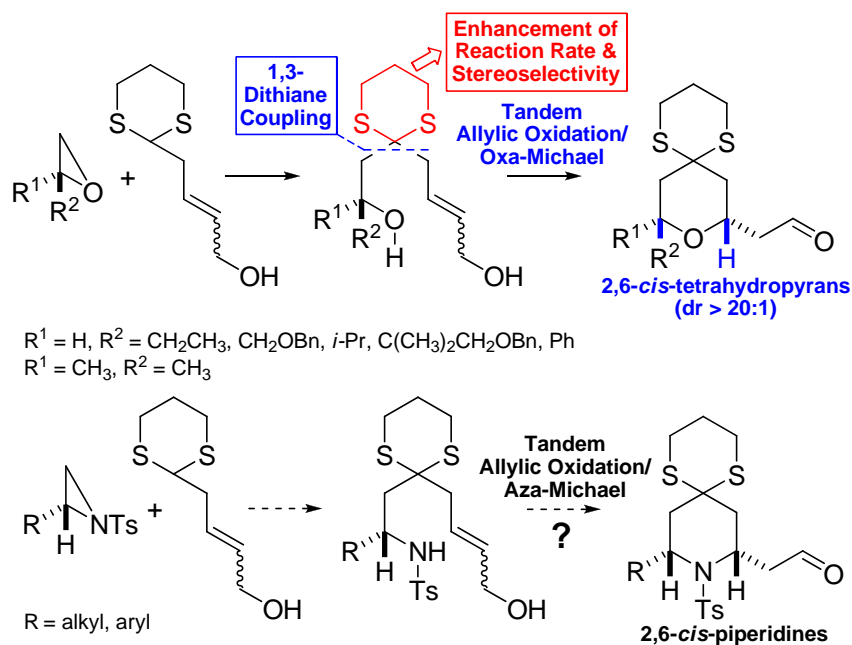


Figure 4.3 Stereoselective synthesis of 2,6-*cis*-tetrahydropyrans and piperidines via tandem allylic oxidation/ Michael reactions

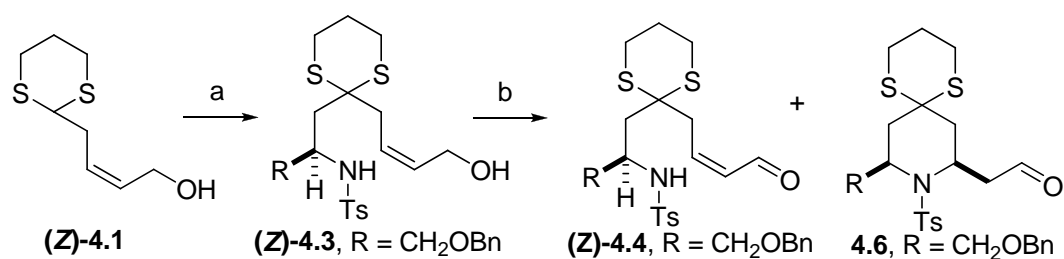
Intrigued by the potential of the tandem allylic oxidation/oxa-Michael reaction coupled with the 1,3-dithiane coupling reaction for rapid construction of substituted tetrahydropyrans, we decided to extend this methodology to the synthesis of 2,6-disubstituted piperidines, taking advantage of easy access to substrates via direct coupling of 1,3-dithiane and readily available chiral aziridines (Figure 4.3). Herein, we report the facile and efficient synthesis of both 2,6-*cis*- and 2,6-*trans*-piperidines from common substrates through a *reagent-controlled* organocatalytic aza-Michael reaction in conjunction with 1,3-dithiane coupling reaction.

4.2 Results and discussion

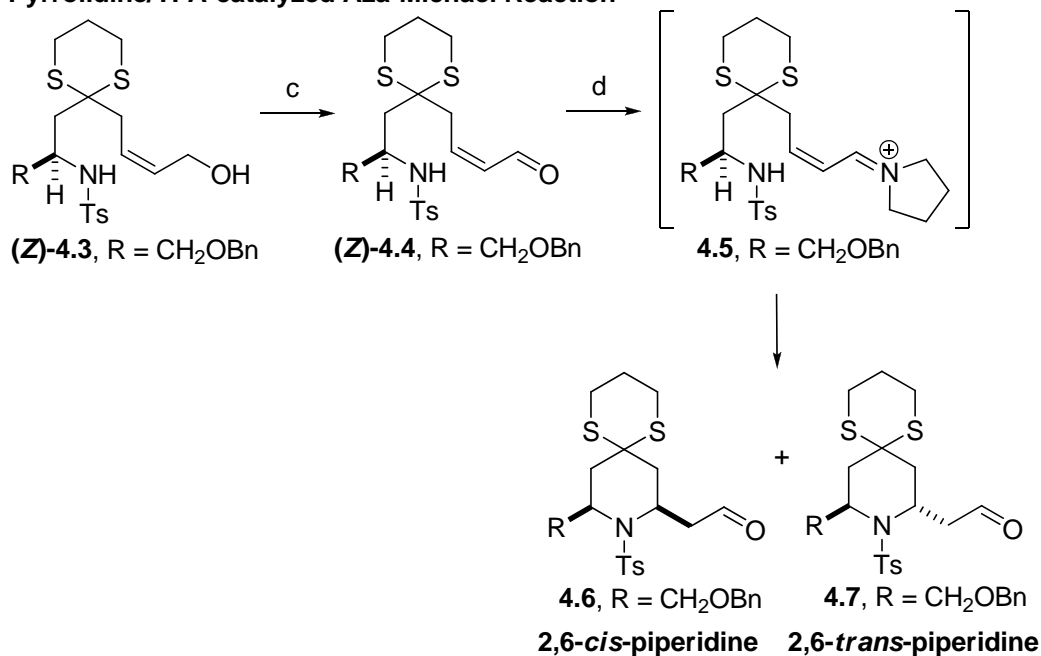
4.2.1 Attempts of tandem reaction and introduction of organocatalysis

To test the feasibility of the tandem allylic oxidation/aza-Michael reaction in the synthesis of 2,6-disubstituted piperidines, we prepared substrate **4.3** by coupling of the known dithiane allylic alcohol (**4.1**)¹²⁶ with the known 2-(phenylmethoxy)methyl-*N*-tosylaziridine (**4.2**)¹²⁷ (Scheme 4.1). The oxidation of **4.3** with MnO₂ provided the desired α,β -unsaturated aldehyde **4.4**. However, the subsequent intramolecular aza-Michael reaction of **4.4** failed to provide the desired 2,6-*cis*-piperidine **4.5**. No success of the tandem reaction was attributed to the poor nucleophilicity of the sulfonamide **4.3**.

Tandem Allylic Oxidation/Aza-Michael Reaction



Pyrrrolidine/TFA-catalyzed Aza-Michael Reaction



(a) *t*-BuLi, HMPA/THF (1:10), -78 °C, 5 min, then, 1-[4-methylphenylsulfonyl]-2-(*R*)-(phenylmethoxy)methyl]-aziridine (**4.2**), -78 °C, 30 min, 71–75%, 84–89% brsm; (b) MnO₂, CH₂Cl₂, 25 °C, 24 h, 80%; (c) MnO₂, CH₂Cl₂, 25 °C, 3 h, filtration; (d) pyrrolidine (20 mol %), TFA (20 mol %), CH₂Cl₂, 0 °C, 20 h, 70–80 % for 2 steps.

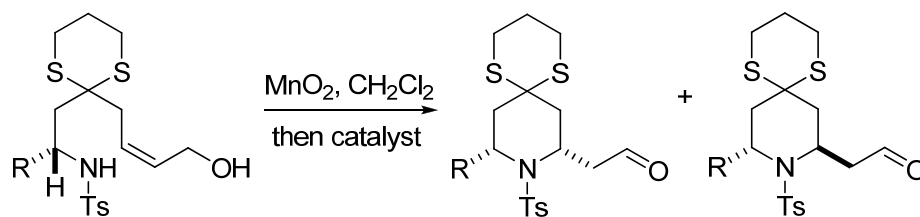
Scheme 4.1 Initial attempts for the synthesis of a 2,6-*cis*-piperidine via (a) tandem allylic oxidation/aza-Michael reaction or (b) pyrrolidine/TFA-catalyzed aza-Michael reaction

We hypothesized that the activation of conjugate acceptors would be required to overcome the poor nucleophilicity of the Ts-protected nitrogen in the aza-Michael reaction. To test the hypothesis, we oxidized **4.3** with MnO₂ to provide the intermediate

4.4. After removal of MnO₂ by filtration, the resulting aldehyde **4.4** was converted to the iminium ion intermediate **4.5** by treatment with pyrrolidine/TFA. As expected, the iminium activation of **4.5** improved the yield of the subsequent aza-Michael reaction (70–80%), but the stereoselectivity of the *substrate-controlled* aza-Michael reaction was still low (2,6-*cis*:2,6-*trans* = 3.5:1).^{*} Meanwhile, we also screened other catalysts which can facilitate Michael reaction to some extent (Table 4.1). However, diastereoselectivity issue still persisted to the same fashion even though silica worked well in Me-substrate example (dr = 9:1, ~50% yield; Table 4.1, entry 8).

Table 4.1 Other attempts to one-pot oxidation/aza-Michael reaction by various catalysts

One-pot Oxidation/Aza-Michael Reaction



entry	R	catalyst	dr (<i>cis:trans</i>) ^a
1	CH ₃	NEt ₃	5:2
2	CH ₃	<i>i</i> -Pr ₂ NH	2:1
3	CH ₃	DBU	3:1
4	CH ₃	pyrrolidine	1:1
5	CH ₃	pyrrolidine/TFA	2:1
6	<i>t</i> -Bu	pyrrolidine/TFA	n.d. ^b

^a The relative stereochemistry of the major diastereomer **4.15b** of the reaction was determined to be *cis* by 2D NMR spectroscopy and a single-crystal analysis. We attributed the low diastereoselectivity to the fact that the reaction might go through a less well-defined twist boat-like transition state as shown in the X-ray crystal (see Figure 4.4 and experimental sections for details).

7	CH ₃	PTSA	3:1
8	CH ₃	excess silica	9:1
9	CH ₃	Amberlyst-15	3:1
10	CH ₃	TFA	3:1
11	<i>i</i> -Pr	PTSA	5:1
12	<i>i</i> -Pr	PPTS	n.d. ^b
13	<i>i</i> -Pr	excess silica	4:1
14	<i>i</i> -Pr	Amberlyst-15	5:1
15	<i>t</i> -Bu	excess silica	n.d. ^b
16	<i>t</i> -Bu	Amberlyst-15	n.d. ^b

^a Diastereoselectivity was determined by ¹H NMR after simple filtration through column chromatography.

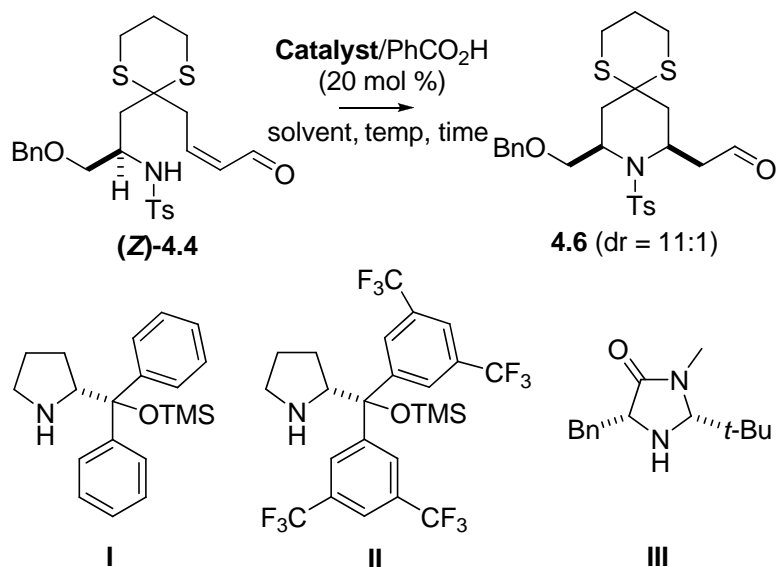
^b Allylic alcohol or reaction products were decomposed based on the TLC or crude ¹H NMR analysis.

To improve the stereoselectivity of the aza-Michael reaction, we decided to attempt an organocatalytic, *reagent-controlled* aza-Michael reaction. Asymmetric organocatalysis has been broadly established to activate carbonyl compounds by enamines, iminium ions, or the SOMO-activation strategy.¹²⁸ In addition, organocatalysis has been widely applied to asymmetric synthesis due to easy access to enantiomerically pure forms of organocatalysts, air and moisture resistance, and easy handling of reactions.¹²⁹ Organocatalysis has been broadly utilized to activate carbonyl and made a large contribution to the development of asymmetric Michael reactions.¹³⁰ During the last several years, organocatalytic asymmetric aza-Michael additions have been a very active field of research.¹³¹

4.2.3 Optimization and substrate scope

To examine if organocatalysts are compatible with our substrates with the 1,3-dithiane group, we examined organocatalysts **I**, **II**, **III** for the reaction. As shown in **Scheme 4.2**, the desired 2,6-*cis*-piperidine **4.6** was obtained with good stereoselectivity

(dr = 11:1, 92%) when **I** or **II** was employed. To further optimize the reaction conditions, a variety of solvents were tested. Among the solvents examined, CH₂Cl₂ proved to be the most effective for the reaction (Table 4.2).



Scheme 4.2 Organocatalytic aza-Michael reaction of the synthesis of a 2,6-*cis*-piperidine

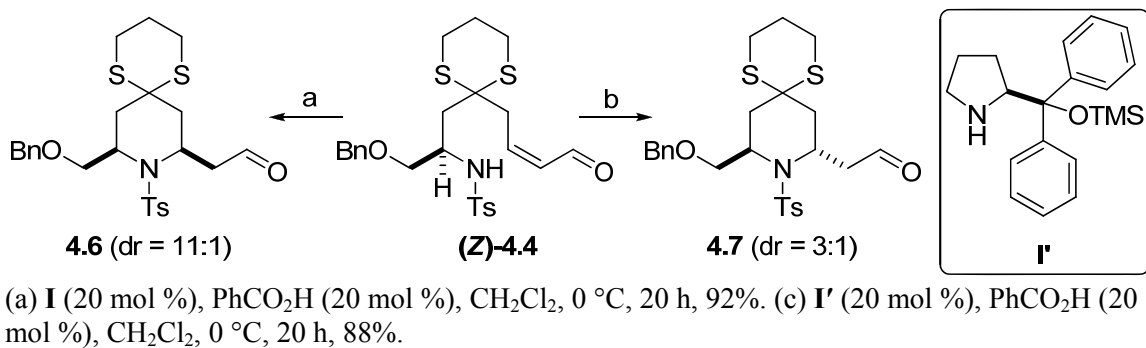
Table 4.2 Catalyst screening and optimization of reaction conditions

entry	catalyst	solvent	temp (°C)	time (h)	yield (%)	dr (<i>cis:trans</i>) ^a
1	I	CH ₂ Cl ₂	0	20	92	11:1
2	II	CH ₂ Cl ₂	0	20	92	11:1
3	III	CH ₂ Cl ₂	0	24	73	4:1
4	I	toluene	0	20	94	9:1
5	I	ether	0	48	45	4.5:1
6	I	MeOH	0	48	86	4:1
7	I	MeCN	0	48	86	4.5:1
8	I	DMF	0	72	28	4:1
9	I	THF	0	72	n.r.	n.d.
10	I	dioxane	25	72	n.r.	n.d.

^a Diastereoselectivity was determined by ¹H NMR after simple filtration through column chromatography.

n.d. = not determined

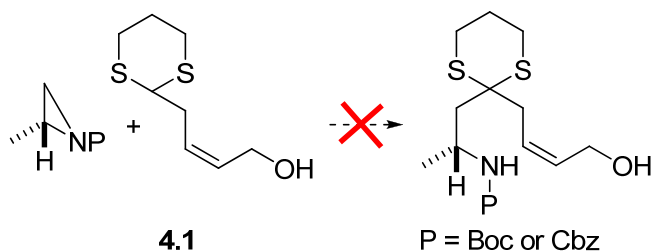
When (*R*)-(+)- α , α -diphenylprolinol trimethylsilyl ether (**I'**) was used for the aza-Michael reaction of (*Z*)-**4.4**, 2,6-*trans*-piperidine **4.6** was obtained with good stereoselectivity (dr (*trans*:*cis*) = 3:1), demonstrating that the stereoselective synthesis of both 2,6-*cis*- and 2,6-*trans*-piperidines could be achieved from common substrates through a *reagent-controlled* organocatalytic aza-Michael reaction (Scheme 4.3).¹³² To the best of our knowledge, the synthesis of both possible diastereomers from common substrates with good stereoselectivities has not been achieved for intramolecular organocatalytic aza-Michael reaction, while it has been appeared in other reactions such as Ir-catalyzed allylic substitutions.¹³²



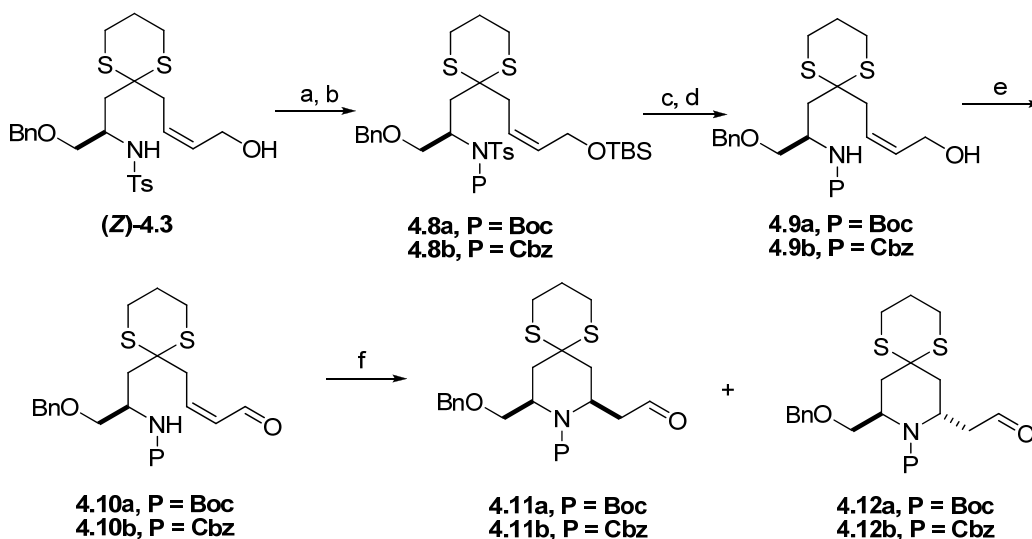
Scheme 4.3 Synthesis of both 2,6-*cis*- and 2,6-*trans*-piperidines from the common substrate through a *reagent-controlled* organocatalytic aza-Michael reaction

In addition, we examined the protecting group effect on nitrogen atom in terms of diastereoselectivity in oxidation/aza-Michael reaction. Since reacting **4.1** with either Boc-protected aziridine or Cbz-protected aziridine failed to produce allylic alcohol **4.9** (Scheme 4.4), we revised our synthetic route and started from known compound (*Z*)-**4.3**

to prepare *Boc* or *Cbz* protected allylic alcohol substrates (**4.9a** and **4.9b**) in search of protecting group effect on diastereoselectivity in aza-Michael reaction (Scheme 4.5, Table 4.2).



Scheme 4.4 Initial attempt to synthesize *Boc* or *Cbz* protected allylic alcohol

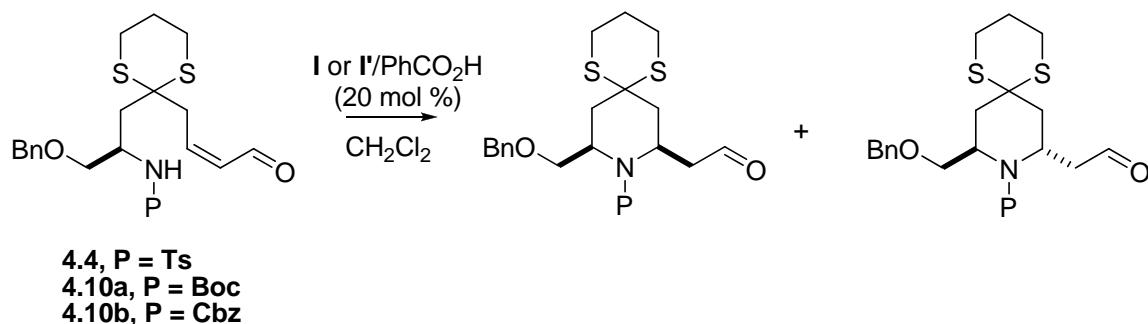


Reagents and reaction conditions: a) TBSCl, imidazole, CH₂Cl₂, 0 °C, 1 h; b) Boc₂O or Cbz₂O, cat. DMAP, MeCN, 25 °C, 17 h, 71% for 2 steps; c) Mg, MeOH, 25 °C, 24 h; d) TBAF, THF, 0 °C, 1 h, 82% for 2 steps; e) MnO₂, CH₂Cl₂, 25 °C, 4 h; f) I or I' (20 mol %), PhCO₂H (20 mol %), CH₂Cl₂, 0 °C, 20 h, 76–89% for 2 steps.

Scheme 4.5 Preparation of allylic alcohol **4.9** with *Cbz* or *Boc* protecting groups

After we prepared *Boc* and *Cbz* protected substrates as well as *Ts* protected compound **4.3** which has been already synthesized by coupling **4.1** with known aziridine **4.2**, α,β -unsaturated aldehyde **4.4**, **4.10a**, **4.10b** were subjected into organocatalytic aza-Michael reaction conditions to form 2,6-disubstituted piperidines (Table 4.3). From the results, sulfonamide substrate (**4.4**) gave either 2,6-*cis* or *trans*-piperidines as major diastereomer with better yield when **I** or **I'** was applied in the reaction respectively (Table 4.3, entries 1&2), while *Boc* and *Cbz* protected substrates (**4.10**) do not possess this *reagent-controlled* property.

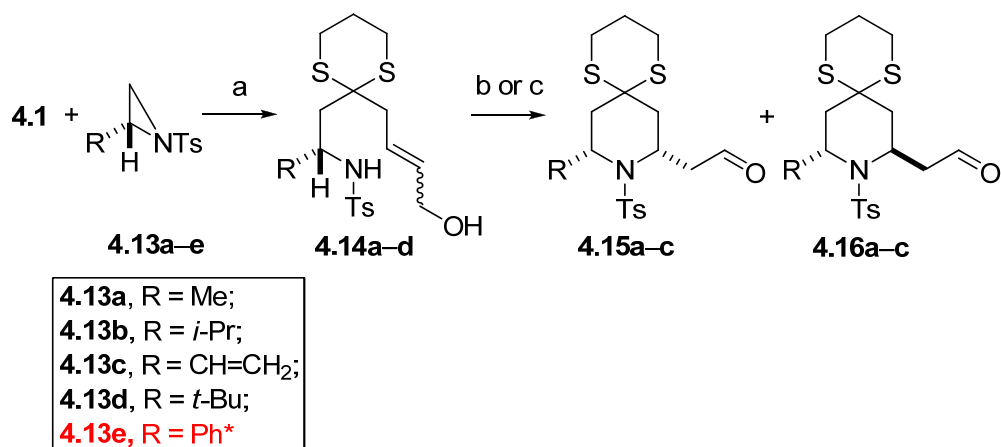
Table 4.3 Protecting group effect on the diastereoselectivity in aza-Michael reaction



entry	P	catalyst	yield (%)	dr (<i>cis:trans</i>) ^a
1	Ts	I	92	11:1
2	Ts	I'	88	1:3
3	Boc	I	80	8:1
4	Boc	I'	70	4:1
5	Cbz	I	67	20:1
6	Cbz	I'	61	2:1

^a Diastereoselectivity was determined by ¹H NMR after simple filtration through column chromatography.

To investigate the scope and stereochemical outcome of the organocatalytic aza-Michael reaction with respect to substituents at the C2 position, we prepared sulfonamides (**4.14a–d**) by coupling **4.1** with the commercially or readily available aziridines (**4.13a–e**)¹³³ and subjected them to the allylic oxidation/organocatalytic aza-Michael reaction (Scheme 4.6). We were pleased to find that the reaction of **4.14a–d** under the reaction conditions examined proceeded smoothly to provide the corresponding 2,6-*cis*-piperidine aldehydes (**4.15a–c**) with good to excellent stereoselectivities (dr > 10:1). In the presence of **I**, the aza-Michael reaction of **4.14a–d** provided the corresponding 2,6-*trans*-piperidine aldehydes **4.16a–c** with good stereoselectivities. Compounds **4.15a–c** and **4.16a–c** could be further functionalized to more complex piperidines. However, sterically hindered tertiary amine **4.14d** did not afford the desired product (Table 4.4, entry 4).



(a) *t*-BuLi, HMPA/THF (1:10), -78 °C, 5 min, then **4.8a–e**, -78 °C, 30–120 min, 14–75%, 25–90% brsm; (b) **I'** (20 mol %), PhCO₂H (20 mol %), CH₂Cl₂, 0 °C, 20–48 h; (c) **I** (20 mol %), PhCO₂H (20 mol %), CH₂Cl₂, 0 °C, 20–48 h.

Scheme 4.6 Substrate scope

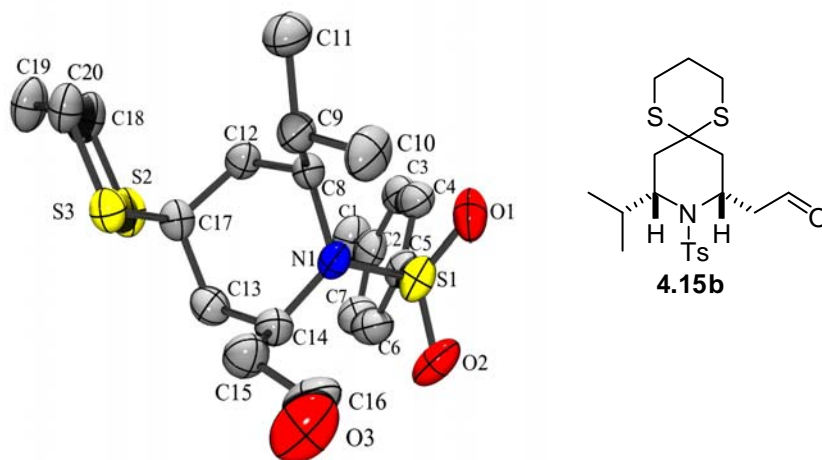
Table 4.4 Substrate scope and stereochemical outcome

entry	R	geometry	reaction conditions	product (yield)	dr (<i>cis:trans</i>) ^a
1	Me	<i>Z</i>	b	4.15a+4.16a (90%)	>15:1
			c	4.15a+4.16a (75%)	1:2
		<i>E</i>	b	4.15a+4.16a (97%)	>20:1
			c	4.15a+4.16a (80%)	1:4
2	<i>i</i> -Pr	<i>Z</i>	b	4.15b+4.16b (78%)	10:1
			c	4.15b+4.16b (78%)	1:8
		<i>E</i>	b	4.15b+4.16b (87%)	12:1
			c	4.15b+4.16b (79%)	1:10
3	CH=CH ₂	<i>Z</i>	b	4.15c+4.16c (90%)	15:1
			c	4.15c+4.16c (86%)	1:1
4	<i>t</i> -Bu	<i>Z</i>	b	no reaction	not applicable
			c	no reaction	

^a Diastereoselectivity was determined by ¹H NMR after simple filtration through column chromatography.

It is noteworthy that opening 2-phenyl-*N*-tosylaziridine (**4.13e**) by **4.1** under standard condition (*t*-BuLi, HMPA/THF (1:10), -78 °C, 5 min, then aziridine **4.13e**, -78 °C, 30–120 min) failed to provide the corresponding sulfonamide because of the acidity of α-proton in **4.13e**, which was demonstrated previously to be problematic in opening the 2-phenyl-*N*-tosylaziridine **4.13e** with 1,3-dithiane.¹³⁴

The relative stereochemistry of the major diastereomer **4.15b** of the reaction was determined to be *cis* by 2D NMR spectroscopies (See Section 4.4 for details) and a single-crystal analysis (Figure 4.4).

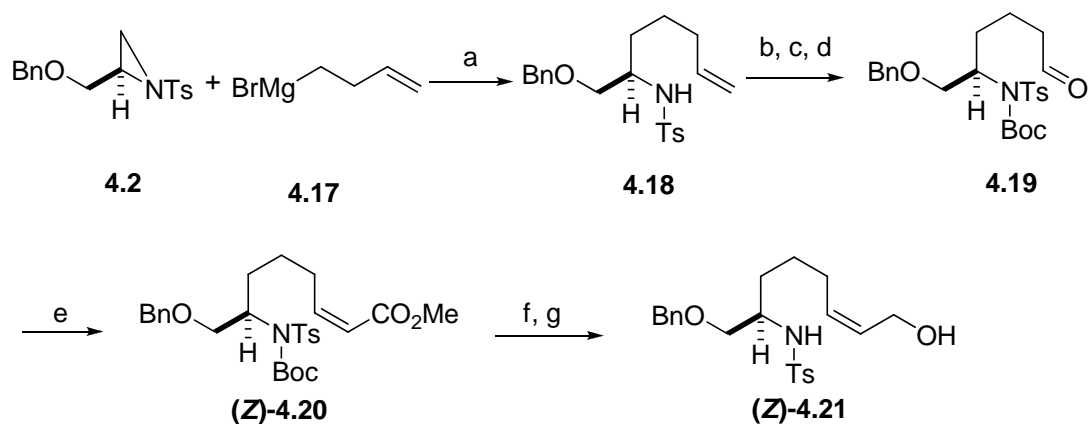


^a Grey ball represents C atom; Blue ball represents N atom; Red ball represents O atom; Yellow ball represents S atom.

Figure 4.4 Molecular structure of **4.15b** from X-ray crystal structure analysis^a

4.2.4 *gem*-Disubstituent effect

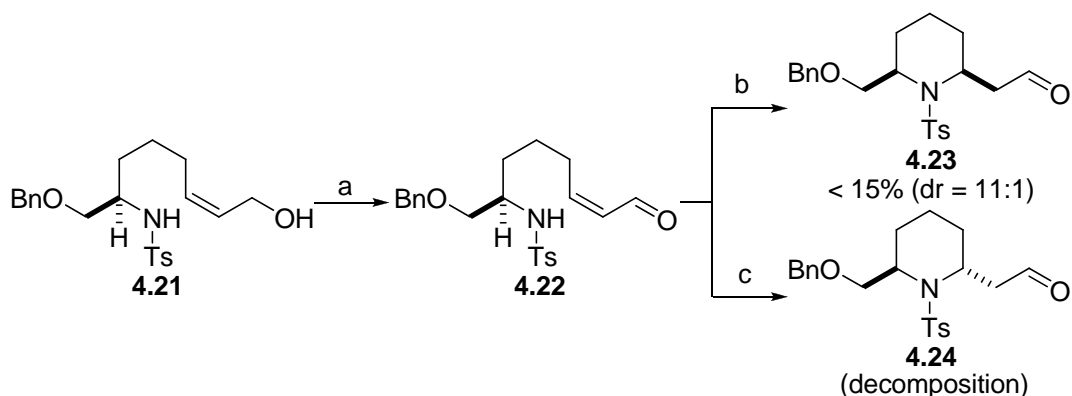
We hypothesized that the 1,3-dithiane group would be critical to overcoming the low reactivity of Ts-protected nitrogen nucleophiles by promoting an ideal conformation for cyclization through the *gem*-disubstituent effect.¹²⁶ To prove this hypothesis, we prepared substrate **4.21** with no *gem*-disubstituent effect (Scheme 4.7). We prepared alkene **4.18** by coupling known 3-butene magnesium bromide **4.17** with aziridine **4.2**.¹³⁵ Subsequent protection with Boc anhydride followed by ozonolysis provided Boc, Ts-bisprotected aldehyde **4.19** in 84%. Modified Horner-Wadsworth-Emmons reaction of **4.19** afforded methyl ester **4.20** in 85% (*Z*-isomer only).¹³⁶ Final reduction of **4.20** with DIBAL-H and subsequent deprotection of Boc group with TFA gave allylic alcohol **4.21** in 64% in 2 steps (*Z*-isomer only).



Reagents and reaction conditions: a) 10 mol % CuI, $-40\text{ }^\circ\text{C}$ to $0\text{ }^\circ\text{C}$, 1 h, 96%; b) Boc_2O , cat. DMAP, CH_3CN , $25\text{ }^\circ\text{C}$, 1 h; c) O_3 , EtOAc, $-78\text{ }^\circ\text{C}$, 10 min; d) Ph_3P , CH_2Cl_2 , $25\text{ }^\circ\text{C}$, 3 h, 84% for 3 steps; e) $(\text{CF}_3\text{CH}_2\text{O})_2\text{POCH}_2\text{CO}_2\text{Me}$, KHMDS, 18-Crown-6, $-78\text{ }^\circ\text{C}$, 1 h, 85%; f) DIBAL-H, toluene, $-78\text{ }^\circ\text{C}$, 2 h; g) TFA, CH_2Cl_2 , $0\text{ }^\circ\text{C}$, 2 h, 64% for 2 steps.

Scheme 4.7 Preparation of allylic alcohol **4.21** with *gem*-dihydrogen

We subjected **4.21** to oxidation conditions followed by organocatalytic aza-Michael reaction condition to investigate the *gem*-disubstituent effect (Scheme 4.8). Although the organocatalytic aza-Michael reaction of **4.22** in the presence of **I** provided the desired 2,6-*cis*-piperidine **4.23** (dr = 11:1; Table 4.5, entry 1), but in a poor yield (< 15%). The organocatalytic aza-Michael reaction of **4.22** in the presence of **I'** failed to provide the corresponding 2,6-*trans*-piperidine **4.24**; Instead, the decomposition of the aldehyde **4.22** was observed (Table 4.5, entry 2). This data clearly demonstrates that the *gem*-disubstituent effect by the 1,3-dithiane group is critical to the overcome of the poor nucleophilicity of the sulfonamides and the improved yield.



Scheme 4.8 *gem*-Disubstituent effect on reaction rate and stereoselectivity

Table 4.5 *gem*-Disubstituent effect on stereoselectivity

entry	reaction condition	product	Yield (%)	dr (<i>cis:trans</i>) ^a
1	b	4.23	<15	11:1
2	c	4.24	decomposed	n.d.

^a Diastereoselectivity was determined by ¹H NMR after simple filtration through column chromatography. n.d. = not determined;

4.2.5 Proposed Mechanism

The mechanism commonly invoked to rationalize the organocatalytic conjugate additions of nitrogen nucleophiles to α , β -unsaturated aldehydes involves the activation of the substrate by the catalyst through the iminium ion activation, thereby facilitating the intramolecular addition of the nucleophiles to the β -carbon. The *si* face of (*E*)-configured in the matched case and (*Z*)-configured intermediate in the mismatched case is shielded by the bulky phenyl groups introduced by the catalyst **I** and **I'**, resulting in the nitrogen nucleophile approaching from the unshielded *re* face to form *cis*-piperidine with fast

reaction rate (Figure 4.5), while the *re* face of (*E*)-configured in the mismatched case and (*Z*)-configured intermediate in the matched case is shielded by the bulky phenyl groups introduced by the catalyst **I** and **I'**, resulting in the nitrogen nucleophile approaching from the unshielded *si* face to form *trans*-piperidine with slow reaction rate. In addition, it should be noted that the diastereoselectivity with (*E*)-configured substrates were always better than those from corresponding (*Z*)-configured substrates (Table 4.4). This enhanced diastereoselectivity with (*E*)-substrates in “Match Pair” could be rationalized on the basis that while the (*Z*)-iminium ion intermediate undergoes a cyclization to provide the 2,6-*cis*-piperidine, competitive isomerization to the corresponding (*E*)-iminium ion intermediate could occur to eventually provide the 2,6-*trans*-piperidine (Figure 4.5).

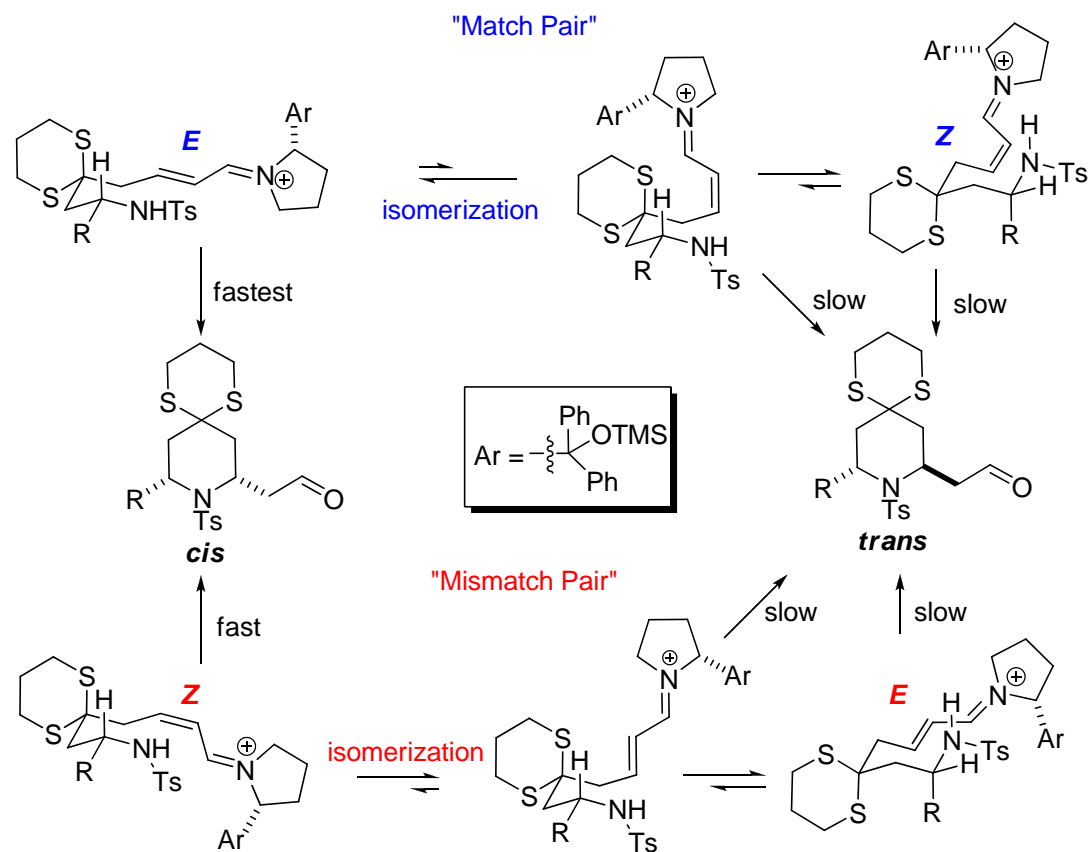


Figure 4.5 Proposed mechanism of aza-Michael reaction in “match pair” and “mismatch pair”

4.3 Conclusion

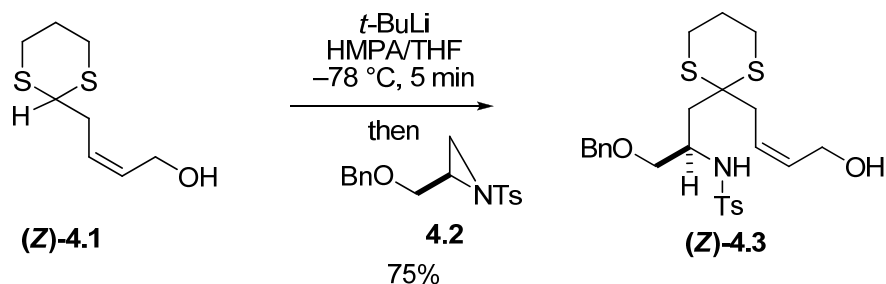
In summary, we explored the organocatalytic aza-Michael reactions for the stereoselective synthesis of 2,6-disubstituted piperidines. The reaction was applicable to a broad range of substrates and proceeded with good stereoselectivities (up to 20:1 dr) and yields. The 1,3-dithiane group allowed for rapid access to substrates, promoted the intramolecular aza-Michael reaction via the *gem*-disubstituent effect, and improved the yield of the reaction. In addition, we reported an example of *reagent-controlled* organocatalytic aza-Michael which allowed the synthesis of both 2,6-*cis*- and 2,6-*trans*-

piperidines from the common substrates. This synthetic method would be broadly applicable to the efficient synthesis of a diverse set of bioactive natural products with 2,6-disubstituted piperidines.

4.4 Experimental sections

Representative Procedure for 1,3-Dithiane Coupling with Aziridines

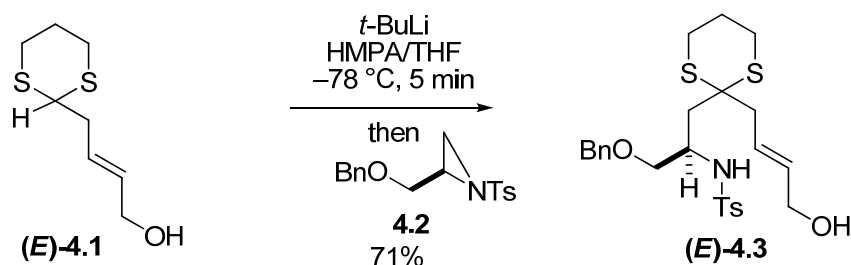
1) (Z)-Allylic Alcohol (Z)-4.3



To a cooled ($-78\text{ }^{\circ}\text{C}$) solution of (Z)-4.1 (100 mg, 0.53 mmol) in HMPA/THF (1:10, 11 mL) was added dropwise $t\text{-BuLi}$ (0.63 mL, 1.7 M in pentane, 1.07 mmol), and the resulting mixture was stirred for 5 min before aziridine **4.2** (167 mg, 0.53 mmol) was added. After stirred for 1 h at $-78\text{ }^{\circ}\text{C}$, the reaction mixture was quenched with saturated aqueous NH_4Cl and diluted with EtOAc. The layers were separated, and the aqueous layer was extracted with EtOAc. The combined organic layers were washed with brine, dried over anhydrous Na_2SO_4 , and concentrated *in vacuo*. The residue was purified by column chromatography (silica gel, hexanes/EtOAc, 2/1 to 1/1) to afford (Z)-allylic alcohol (Z)-4.3 (201 mg, 75%, 84% BRSM): $[\alpha]_D^{25} = +11.5$ (c 0.92, CHCl_3); $^1\text{H NMR}$ (400 MHz, CDCl_3) δ 7.71 (d, $J = 8.0$ Hz, 2H), 7.16–7.36 (m, 7H), 5.74 (ddd, $J = 11.2$,

7.2, 6.4 Hz, 1H), 5.60 (ddd, $J = 11.2, 7.2, 6.4$ Hz, 1H), 5.51 (d, $J = 8.0$ Hz, 1H), 4.29 (AB, $J_{AB} = 12.0$ Hz, $\Delta\nu_{AB} = 14.8$ Hz, 2H), 4.15–4.22 (m, 1H), 4.03–4.10 (m, 1H), 3.71–3.78 (m, 1H), 3.36 (dd, $J = 10.0, 3.2$ Hz, 1H), 3.15 (dd, $J = 10.0, 4.8$ Hz, 1H), 2.61–2.83 (m, 5H), 2.55 (dd, $J = 15.6, 6.8$ Hz, 1H), 2.38 (s, 3H), 2.31 (dd, $J = 15.2, 4.8$ Hz, 1H), 2.10 (dd, $J = 15.6, 6.8$ Hz, 1H), 1.77–1.93 (m, 2H) ^{13}C NMR (100 MHz, CDCl_3) δ 143.2, 137.8, 137.5, 131.8, 129.5, 128.2, 127.7, 127.6, 127.0, 125.5, 72.9, 71.8, 58.2, 51.4, 51.1, 40.0, 36.3, 26.0, 25.8, 24.6, 21.4; IR (neat) 3273, 1156, 1090, 668 cm^{-1} ;

2) (*E*)-Allylic Alcohol (*E*)-4.3

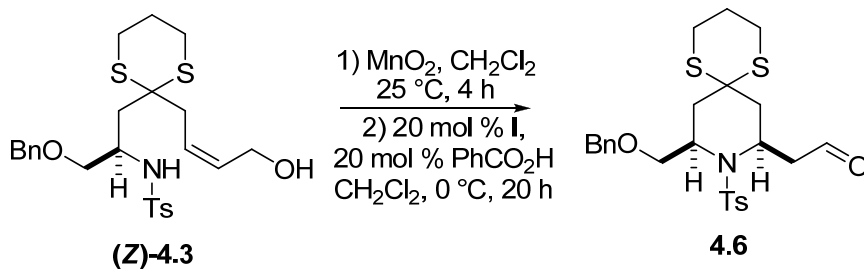


To a cooled ($-78\text{ }^\circ\text{C}$) solution of (*E*)-4.1 (150 mg, 0.79 mmol) in HMPA/THF (1:10, 11 mL) was added dropwise *t*-BuLi (0.93 mL, 1.7 M in pentane, 1.58 mmol), and the resulting mixture was stirred for 5 min before aziridine **4.2** (167 mg, 0.53 mmol) was added. After stirred for 0.5 h at $-78\text{ }^\circ\text{C}$, the reaction mixture was quenched with saturated aqueous NH_4Cl and diluted with EtOAc. The layers were separated, and the aqueous layer was extracted with EtOAc. The combined organic layers were washed with brine, dried over anhydrous Na_2SO_4 , and concentrated *in vacuo*. The residue was purified by column chromatography (silica gel, hexanes/EtOAc, 2/1 to 1/1) to afford (*E*)-allylic alcohol (*E*)-4.3 (285 mg, 71%, 89% BRSM): $[\alpha]_D^{25.9} = +22.5$ (c 2.5, CHCl_3); ^1H NMR

(400 MHz, CDCl₃) δ 7.72 (d, J = 8.4 Hz, 2H), 7.20–7.34 (m, 7H), 5.63–5.75 (m, 2H), 5.58 (d, J = 8.0 Hz, 1H), 4.29 (AB, J_{AB} = 12.0 Hz, $\Delta\nu_{AB}$ = 18.4 Hz, 2H), 4.04 (d, J = 4.4 Hz, 1H), 3.68–3.76 (m, 1H), 3.45 (dd, J = 9.6, 3.6 Hz, 1H), 3.22 (dd, J = 9.6, 5.2 Hz, 1H), 2.60–2.82 (m, 4H), 2.54 (dd, J = 15.6, 6.4 Hz, 1H), 2.43 (dd, J = 15.2, 6.4 Hz, 1H), 2.38 (s, 3H), 2.32 (dd, J = 15.2, 5.2 Hz, 1H), 2.11 (dd, J = 15.6, 6.8 Hz, 1H), 1.76–1.94 (m, 2H) ¹³C NMR (100 MHz, CDCl₃) δ 143.2, 137.8, 137.5, 133.5, 129.5, 128.2, 127.6, 127.0, 125.7, 72.9, 71.8, 63.1, 51.2, 51.0, 41.3, 39.9, 26.0, 25.8, 24.6, 21.4; IR (neat) 3289, 1597, 1326, 1092 cm⁻¹;

Representative Procedure for Allylic Oxidation/Aza-Michael Reaction by Organocatalysis

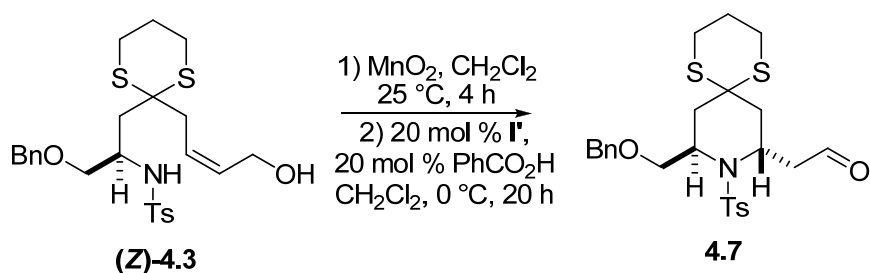
1) Matched Case with (*Z*) Allylic Alcohol **4.3**



To a stirred solution of (*Z*)-allylic alcohol (**4.3**) (13.0 mg, 0.0256 mmol) in CH₂Cl₂ (1.5 mL, 0.0171 M) was added MnO₂ (50.6mg, 0.512 mmol) at 25 °C. After stirred for 4 h at the same temperature, the reaction mixture was then filtered through celite with EtOAc and concentrated *in vacuo*. To a stirred solution of α,β -unsaturated aldehyde intermediate in CH₂Cl₂ (1.0 mL, 0.0256 M) was added **I** (1.7 mg, 0.0051 mmol) and PhCO₂H (0.6 mg, 0.0051 mmol) at 0 °C. After stirred for 20 h at the same

temperature, the reaction mixture was concentrated and purified by column chromatography (silica gel, hexanes/EtOAc, 3/1) to afford 2,6-*cis*-disubstituted piperidine aldehyde **4.6** (12.1 mg, 93%) as a colorless oil: $[\alpha]^{27.5}_D = 10.3$ (*c* 0.32, CHCl₃); ¹H NMR (400 MHz, CDCl₃) δ 9.72 (s, 1H), 7.70 (d, *J* = 8.0 Hz, 2H), 7.26–7.37 (m, 7H), 4.57 (AB, *J*_{AB} = 11.6 Hz, Δ*v*_{AB} = 20.4 Hz, 2H), 4.46–4.53 (m, 1H), 4.15–4.22 (m, 1H), 3.97 (t, *J* = 8.8 Hz, 1H), 3.72 (dd, *J* = 8.8, 4.4 Hz, 1H), 3.23 (dd, *J* = 18.0, 8.8 Hz, 1H), 3.08 (dd, *J* = 18.0, 4.4 Hz, 1H), 2.71–2.86 (m, 4H), 2.51 (dd, *J* = 15.2, 4.0 Hz, 1H), 2.41 (s, 3H), 2.19 (dd, *J* = 14.8, 3.6 Hz, 1H), 1.94 (dd, *J* = 14.8, 6.4 Hz, 1H), 1.83–1.94 (m, 2H), 1.79 (dd, *J* = 15.2, 6.8 Hz, 1H); ¹³C NMR (100 MHz, CDCl₃) δ 200.2, 143.7, 137.9, 136.7, 129.8, 128.4, 127.9, 127.7, 127.2, 73.3, 73.0, 51.6, 46.8, 44.3, 38.6, 35.3, 26.8, 26.7, 24.6, 21.5; IR (neat) 1721, 1327, 1098 cm⁻¹;

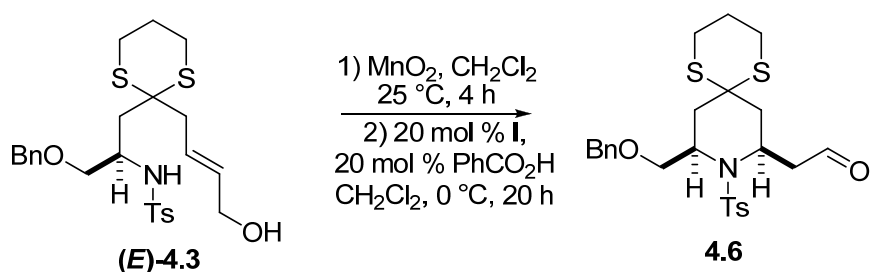
2) Mismatched Case with (*Z*)-Allylic Alcohol **4.3**



To a stirred solution of (*Z*)-allylic alcohol (**Z**)-**4.3** (13.0 mg, 0.0256 mmol) in CH₂Cl₂ (1.5 mL, 0.0171 M) was added MnO₂ (50.6mg, 0.512 mmol) at 25 °C. After stirred for 4 h at the same temperature, the reaction mixture was then filtered through celite with EtOAc and concentrated *in vacuo*. To a stirred solution of α,β-unsaturated aldehyde intermediate in CH₂Cl₂ (1.0 mL, 0.0256 M) was added **I'** (1.7 mg, 0.0051

mmol) and PhCO₂H (0.6 mg, 0.0051 mmol) at 0 °C. After stirred for 20 h at the same temperature, the reaction mixture was concentrated and purified by column chromatography (silica gel, hexanes/EtOAc, 3/1) to afford 2,6-*trans*-disubstituted piperidine aldehyde **4.7** (11.5 mg, 88%) as a colorless oil: ¹H NMR (400 MHz, CDCl₃) δ 9.50 (s, 1H), 7.73 (d, *J* = 8.4 Hz, 2H), 7.26–7.37 (m, 5H), 7.14 (d, *J* = 8.8 Hz, 2H), 4.51 (AB, *J*_{AB} = 11.6 Hz, Δ*v*_{AB} = 24.4 Hz, 2H), 4.37–4.47 (m, 2H), 4.03 (dd, *J* = 9.6, 7.2 Hz, 1H), 3.77 (dd, *J* = 10.0, 6.8 Hz, 1H), 3.12 (dd, *J* = 18.4, 6.4 Hz, 1H), 2.97 (dd, *J* = 18.4, 8.0 Hz, 1H), 2.72–2.90 (m, 4H), 2.35 (s, 3H), 2.26 (dd, *J* = 6.4, 5.6 Hz, 2H), 2.21 (d, *J* = 3.6 Hz, 1H), 2.20 (d, *J* = 6.8 Hz, 1H), 1.86–2.00 (m, 2H); ¹³C NMR (100 MHz, CDCl₃) δ 198.9, 143.3, 139.4, 138.0, 129.5, 128.3, 127.8, 127.7, 127.6, 73.0, 70.6, 54.5, 47.7, 47.5, 46.5, 40.7, 37.8, 26.33, 26.29, 24.9, 21.5; IR (neat) 1722, 1326, 1305, 1085 cm⁻¹;

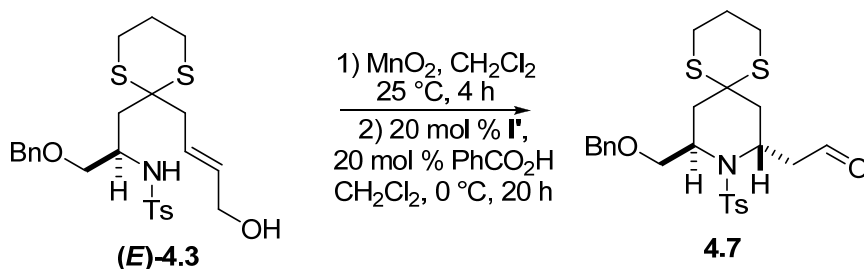
3) Matched Case with (*E*)-Allylic Alcohol **4.3**



To a stirred solution of (*E*)-allylic alcohol (*E*)-**4.3** (23.0 mg, 0.0453 mmol) in CH₂Cl₂ (1.5 mL, 0.0302 M) was added MnO₂ (89.6 mg, 0.906 mmol) at 25 °C. After stirred for 4 h at the same temperature, the reaction mixture was then filtered through celite with EtOAc and concentrated *in vacuo*. To a stirred solution of α,β-unsaturated aldehyde intermediate in CH₂Cl₂ (2.0 mL, 0.0227 M) was added **I** (2.9 mg, 0.0091 mmol)

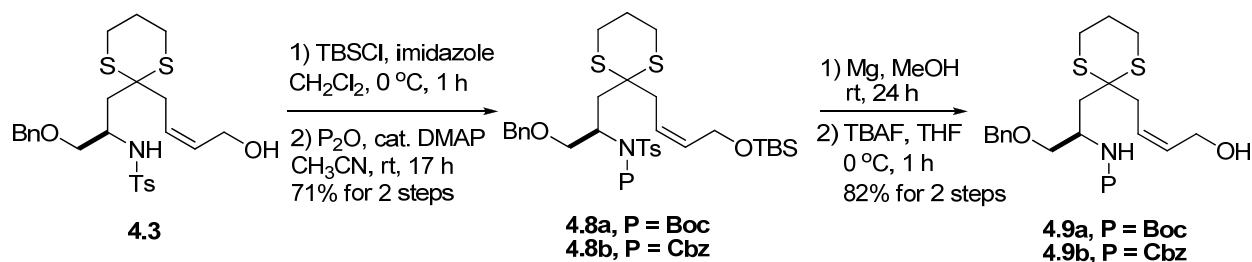
and PhCO₂H (1.1 mg, 0.0051 mmol) at 0 °C. After stirred for 20 h at the same temperature, the reaction mixture was concentrated and purified by column chromatography (silica gel, hexanes/EtOAc, 3/1) to afford 2,6-*cis*-disubstituted piperidine aldehyde **4.6** (22.0 mg, 96%) as a colorless oil.

4) Mismatched Case with (*E*)-Allylic Alcohol **4.3**



To a stirred solution of (*E*)-allylic alcohol (*E*)-**4.3** (23.0 mg, 0.0453 mmol) in CH₂Cl₂ (1.5 mL, 0.0302 M) was added MnO₂ (89.6 mg, 0.906 mmol) at 25 °C. After stirred for 4 h at the same temperature, the reaction mixture was then filtered through celite with EtOAc and concentrated *in vacuo*. To a stirred solution of α,β -unsaturated aldehyde intermediate in CH₂Cl₂ (2.0 mL, 0.0227 M) was added cat. **I'** (2.9 mg, 0.0091 mmol) and PhCO₂H (1.1 mg, 0.0051 mmol) at 0 °C. After stirred for 20 h at the same temperature, the reaction mixture was concentrated and purified by column chromatography (silica gel, hexanes/EtOAc, 3/1) to afford 2,6-*trans*-disubstituted piperidine aldehyde **4.7** (21.0 mg, 91%) as a colorless oil.

Preparation of allylic alcohol **4.9** with *Cbz* or *Boc* protecting groups



To a stirred solution of sulfonamide **4.3** (200 mg, 0.39 mmol) in CH₂Cl₂ (3 mL, 0.13 M) was added TBSCl (66 mg, 0.437 mmol) and imidazole (80 mg, 1.18 mmol) at 0 °C. After stirred at 0 °C for 1 h, the reaction mixture was concentrated and purified by purified by column chromatography (silica gel, hexanes/EtOAc, 10/1) to afford TBS-protected allylic alcohol (210 mg, 86%). To a stirred solution of TBS-protected allylic alcohol (105 mg, 0.17 mmol) in CH₃CN (6 mL, 0.03 M) was added Boc₂O (55 mg, 0.253 mmol) and DMAP (5 mg, 0.04 mmol) at 25 °C. After stirred at 25 °C for 17 h, the reaction mixture was concentrated and purified by purified by column chromatography (silica gel, hexanes/EtOAc, 10/1) to afford Boc-protected sulfonamide **4.8a** (100 mg, 82%): ¹H NMR (400 MHz, CDCl₃) δ 7.83 (d, *J* = 8.0 Hz, 2H), 7.18–7.25 (m, 5H), 7.02 (d, *J* = 7.2 Hz, 2H), 5.64 (ddd, *J* = 12.0, 6.0, 5.6 Hz, 1H), 5.55 (ddd, *J* = 12.0, 6.8, 5.6 Hz, 1H), 5.03 (brs, 1H), 4.44 (AB, *J*_{AB} = 11.6 Hz, Δ*v*_{AB} = 60.8 Hz, 2H), 4.21 (d, *J* = 6.0 Hz, 2H), 3.64 (dd, *J* = 9.6, 5.6 Hz, 1H), 2.87 (d, *J* = 11.2 Hz, 2H), 2.53–2.79 (m, 4H), 2.23–2.37 (m, 1H), 2.29 (s, 3H), 1.90–1.97 (m, 1H), 1.75–1.84 (m, 1H), 1.22 (s, 9H), 0.82 (s, 9H), 0.00 (s, 6H).

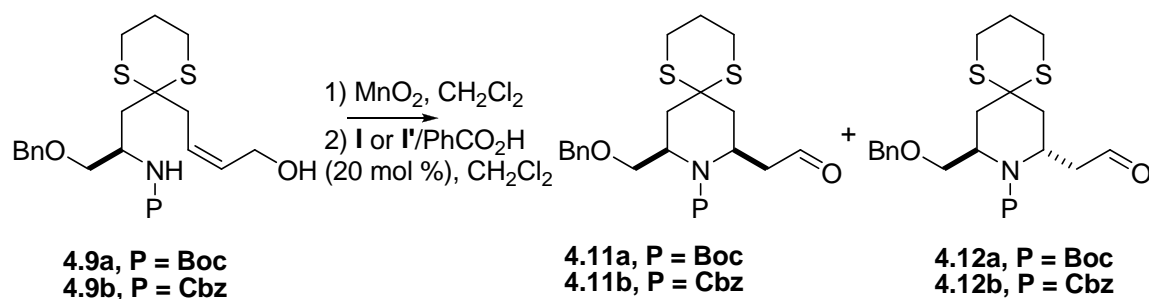
Cbz-protected sulfonamide **4.8b**: ^1H NMR (400 MHz, CDCl_3) δ 7.71 (d, $J = 8.4$ Hz, 2H), 7.17–7.26 (m, 6H), 7.11 (d, $J = 8.0$ Hz, 2H), 7.05 (d, $J = 7.2$ Hz, 2H), 6.88 (d, $J = 7.2$ Hz, 2H), 5.62 (ddd, $J = 11.6, 5.6, 5.2$ Hz, 1H), 5.50 (ddd, $J = 12.0, 6.8, 5.6$ Hz, 1H), 4.91–5.05 (m, 1H), 4.48 (d, $J = 12.0$ Hz, 1H), 4.33 (s, 1H), 4.19 (d, $J = 5.6$ Hz, 2H), 3.59 (dd, $J = 9.6, 5.2$ Hz, 1H), 2.54–2.80 (m, 7H), 2.23–2.31 (m, 1H), 2.24 (s, 3H), 1.74–1.90 (m, 2H), 0.83 (s, 9H), 0.00 (s, 6H).

To a stirred solution of Boc-protected sulfonamide **4.8a** (65mg, 0.09 mmol) in CH_3OH (3 mL, 0.03M) was added Mg powder (66mg, 2.7 mmol) and NH_4Cl (49 mg, 0.9 mmol) at room temperature. After stirring at room temperature for 24h, the reaction mixture was diluted with water and then extracted three times with EtOAc. The combined organic layers were washed with brine, dried over anhydrous Na_2SO_4 , and concentrated *in vacuo*. The residue was purified by column chromatography (silica gel, hexanes/EtOAc, 10/1) to afford Boc-protected amine (44 mg, 86%). To a stirred solution of Boc-protected amine (42mg, 0.074 mmol) in THF (3 mL, 0.025M) was added TBAF (1.0 M in THF, 0.11 mL) at 0 °C. After stirring at 0 °C for 1h, the reaction mixture was quenched with sat. NH_4Cl and then extracted three times with EtOAc. The combined organic layers were washed with brine, dried over anhydrous Na_2SO_4 , and concentrated *in vacuo*. The residue was purified by column chromatography (silica gel, hexanes/EtOAc, 2/1) to afford Boc-protected allylic alcohol **4.9a** (32 mg, 96%): ^1H NMR (400 MHz, CDCl_3) δ 7.26–7.38 (m, 5H), 5.80 (ddd, $J = 12.4, 6.8, 5.6$ Hz, 1H), 5.69 (ddd, $J = 12.4, 7.2, 5.2$ Hz, 1H), 4.95 (d, $J = 8.0$ Hz, 1H), 4.18 (brs, 2H), 4.00–4.09 (m, 1H),

3.59 (brs, 1H), 3.45 (brs, 1H), 2.68–2.88 (m, 6H), 2.50 (s, 1H), 2.36 (dd, $J = 14.8, 4.0$ Hz, 1H), 2.02 (dd, $J = 14.8, 7.2$ Hz, 1H), 1.87–1.99 (m, 2H), 1.43 (s, 9H); ^{13}C NMR (100 MHz, CDCl_3) δ 155.1, 138.0, 131.8, 128.4, 127.7, 126.0, 79.6, 73.1, 72.9, 58.3, 51.4, 47.5, 40.1, 36.0, 28.4, 26.2, 26.1, 24.9.

Cbz-protected allylic alcohol **4.9b**: $[\alpha]_D^{26.8} = 18.6$ (c 0.87, CHCl_3); ^1H NMR (400 MHz, CDCl_3) δ 7.26–7.35 (m, 9H), 5.78 (ddd, $J = 12.4, 7.2, 5.2$ Hz, 1H), 5.68 (ddd, $J = 12.4, 6.4, 5.6$ Hz, 1H), 5.28 (d, $J = 8.8$ Hz, 1H), 5.10 (brs, 2H), 4.51 (s, 2H), 4.09–4.19 (m, 3H), 3.60 (dd, $J = 8.8, 2.4$ Hz, 1H), 3.47 (dd, $J = 8.8, 4.0$ Hz, 1H), 2.72–2.85 (m, 6H), 2.42 (s, 1H), 2.34 (dd, $J = 15.2, 4.4$ Hz, 1H), 2.08 (dd, $J = 15.2, 7.6$ Hz, 1H), 1.86–1.99 (m, 2H); ^{13}C NMR (100 MHz, CDCl_3) δ 155.6, 137.8, 136.4, 131.8, 128.4, 128.3, 128.0, 127.7, 125.9, 73.1, 72.6, 66.7, 58.3, 51.3, 48.2, 40.0, 36.1, 26.2, 26.1, 24.8. IR (neat) 1699, 1520, 1268, 1238, 1052 cm^{-1} .

Aza-Michael reaction with *Boc* or *Cbz*-protected allylic alcohol (**4.9**)



entry	P	catalyst	yield (%)	dr (<i>cis:trans</i>) ^a
1	Ts	I	92	11:1
2	Ts	I'	88	1:3
3	Boc	I	80	8:1

4	Boc	I'	70	4:1
5	Cbz	I	67	20:1
6	Cbz	I'	61	2:1

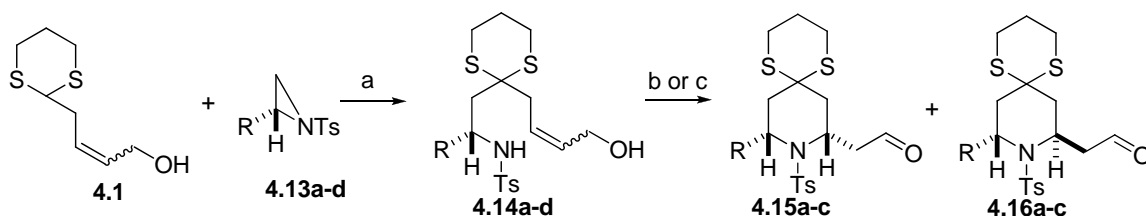
^a Diastereoselectivity was determined by ¹H NMR after simple filtration through column chromatography.

To a stirred solution of (*Z*)-allylic alcohol **4.9a** (10 mg, 0.022 mmol) in CH₂Cl₂ (1.0 mL, 0.02 M) was added MnO₂ (220 mg, 0.55 mmol) at 25 °C. After stirred for 4 h at the same temperature, the reaction mixture was then filtered through celite with EtOAc and concentrated *in vacuo*. To a stirred solution of α,β-unsaturated aldehyde intermediate (9 mg, 0.02 mmol) in CH₂Cl₂ (1.0 mL, 0.02 M) was added **I** (1.3 mg, 0.004 mmol) and PhCO₂H (0.5 mg, 0.004 mmol) at 0 °C (Entry 3). After stirred for 20 h at the same temperature, the reaction mixture was concentrated and purified by column chromatography (silica gel, hexanes/EtOAc, 3/1) to afford 2,6-*cis*-disubstituted piperidine aldehyde **4.11a** as major diastereomer (8 mg, 80%, dr = 8:1) as a colorless oil: ¹H NMR (400 MHz, CDCl₃) δ 9.70 (t, *J* = 1.6 Hz, 1H), 7.27–7.37 (m, 5H), 4.67 (ddd, *J* = 14.4, 7.6, 6.4 Hz, 1H), 4.54 (AB, *J*_{AB} = 11.6 Hz, Δ*v*_{AB} = 30.8 Hz, 2H), 4.47 (ddd, *J* = 14.0, 7.6, 5.6 Hz, 1H), 3.67 (dd, *J* = 9.6, 6.8 Hz, 1H), 3.48 (dd, *J* = 9.2, 4.8 Hz, 1H), 2.80–2.94 (m, 4H), 2.73 (dd, *J* = 16.4, 5.6 Hz, 1H), 2.56 (dd, *J* = 15.6, 7.2 Hz, 1H), 2.34 (dd, *J* = 14.4, 8.0 Hz, 1H), 2.22 (dd, *J* = 14.8, 5.2 Hz, 1H), 1.90–2.04 (m, 3H).

2,6-*cis*-disubstituted piperidine aldehyde **4.11b** (67%, dr = 20:1): ¹H NMR (400 MHz, CDCl₃) δ 9.66 (t, *J* = 1.6 Hz, 1H), 7.27–7.36 (m, 10H), 5.14 (s, 2H), 4.75 (ddd, *J* = 14.8, 7.6, 7.2 Hz, 1H), 4.51–4.58 (m, 1H), 4.51 (AB, *J*_{AB} = 12.4 Hz, Δ*v*_{AB} = 30.4 Hz,

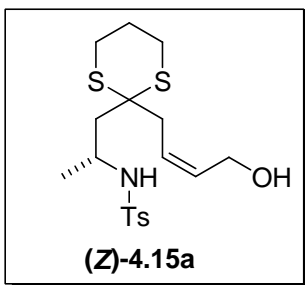
2H), 3.66 (dd, $J = 9.6, 6.4$ Hz, 1H), 3.48 (dd, $J = 9.6, 5.2$ Hz, 1H), 2.72–2.96 (m, 5H), 2.62 (ddd, $J = 14.4, 8.0, 2.0$ Hz, 1H), 2.36 (ddd, $J = 14.8, 8.4, 1.6$ Hz, 1H), 2.19 (dd, $J = 14.4, 5.6$ Hz, 1H), 1.88–2.04 (m, 3H).

Substrate Scope

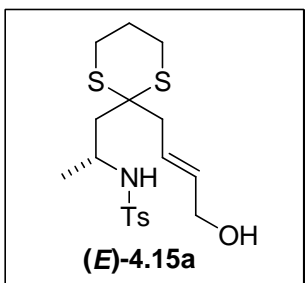


entry	R	allyl alcohol (yield)	reaction conditions ^a	product (yield)	dr ^b
1	Me	(Z) - 4.14a (60%, 73% brsm)	b	90%	>15:1
			c	75%	1:2
		(E) - 4.14a (66%, 81% brsm)	b	97%	>20:1
			c	80%	1:4
2	<i>i</i> -Pr	(Z) - 4.14b (30%, 88% brsm)	b	78%	10:1
			c	78%	1:8
		(E) - 4.14b (50%, 91% brsm)	b	87%	12:1
			c	79%	1:10
3	CH=CH ₂	(Z) - 4.14c (30%, 67% brsm)	b	90%	15:1
			c	86%	1:1
4	<i>t</i> -Bu	(Z) - 4.14d (14%, 25% brsm)	b	nr	NA
			c	nr	

^aReagents and conditions: (a) *t*-BuLi, HMPA/THF (1:10), -78 °C, 5 min, then, **4.13a-d**, -78 °C, 0.5–1 h; (b) MnO₂, CH₂Cl₂, 25 °C, 3 h; then 20 mol % **I'**, 20 mol % PhCO₂H, CH₂Cl₂, 0 °C, 7–45 h; (c) MnO₂, CH₂Cl₂, 25 °C, 3 h; then 20 mol % **I**, 20 mol % PhCO₂H, CH₂Cl₂, 0 °C, 9–67 h; ^b Diastereoselectivity was determined by ¹H NMR after simple filtration through column chromatography. n.d. = not determined;

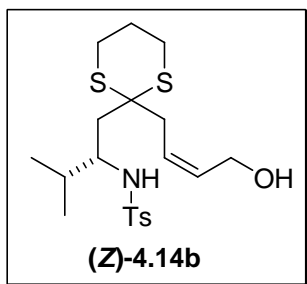


A colorless oil: $[\alpha]^{26.9}_D = -1.7$ (*c* 1.00, CHCl₃); ¹H NMR (400 MHz, CDCl₃) δ 7.72 (d, *J* = 8.0 Hz, 2H), 7.24 (d, *J* = 8.0 Hz, 2H), 5.71 (ddd, *J* = 11.2, 7.2, 6.4 Hz, 1H), 5.66 (d, *J* = 6.4 Hz, 1H), 5.53 (ddd, *J* = 10.8, 7.2, 6.4 Hz, 1H), 4.15 (dd, *J* = 12.4, 7.6 Hz, 1H), 4.03 (dd, *J* = 12.4, 6.4 Hz, 1H), 3.52–3.62 (m, 1H), 2.62–2.80 (m, 5H), 2.46–2.52 (m, 1H), 2.36 (s, 3H), 2.12 (dd, *J* = 15.2, 8.0 Hz, 1H), 1.87 (dd, *J* = 15.2, 4.0 Hz, 1H), 1.78–1.94 (m, 2H), 1.00 (d, *J* = 6.8 Hz, 3H); ¹³C NMR (100 MHz, CDCl₃) δ 143.2, 137.8, 131.8, 129.5, 127.1, 125.6, 58.2, 51.2, 47.4, 44.6, 36.2, 26.0, 24.5, 23.0, 21.4; IR (neat) 3279, 1320, 1158, 668 cm⁻¹;

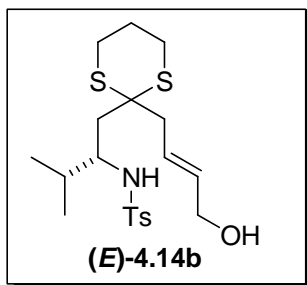


A colorless oil: $[\alpha]^{28.0}_D = -14.9$ (*c* 1.00, CHCl₃); ¹H NMR (400 MHz, CDCl₃) δ 7.75 (d, *J* = 8.8 Hz, 2H), 7.24 (d, *J* = 8.8 Hz, 2H), 5.76 (d, *J* = 6.4 Hz, 1H), 5.60–5.73 (m, 2H), 4.07 (brs, 2H), 3.51–3.61 (m, 1H), 2.68–2.82 (m, 4H), 2.54 (dd, *J* = 14.4, 6.0 Hz, 1H), 2.38–2.48 (m, 2H), 2.39 (s, 3H), 2.19 (dd, *J* = 15.2, 7.6 Hz, 1H), 1.79–1.96 (m, 3H), 1.08

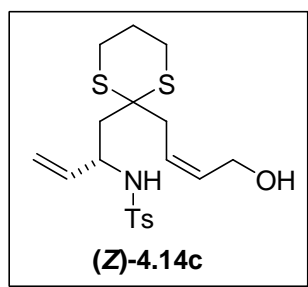
(d, $J = 6.4$ Hz, 3H); ^{13}C NMR (100 MHz, CDCl_3) δ 143.2, 137.7, 133.5, 129.5, 127.2, 125.6, 63.0, 51.0, 47.4, 44.6, 41.3, 26.0, 24.6, 23.1, 21.4; IR (neat) 3280, 1321, 1158, 1090, 668 cm^{-1} ;



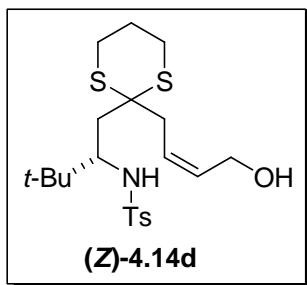
A colorless oil: $[\alpha]_{\text{D}}^{21.9} = -3.1$ (c 0.15, CHCl_3); ^1H NMR (400 MHz, CDCl_3) δ 7.75 (d, $J = 8.4$ Hz, 2H), 7.27 (d, $J = 8.0$ Hz, 2H), 5.77 (ddd, $J = 11.2, 7.2, 6.4$ Hz, 1H), 5.58 (ddd, $J = 11.2, 7.2, 6.0$ Hz, 1H), 5.32 (d, $J = 6.8$ Hz, 1H), 4.18–4.24 (m, 1H), 4.04–4.10 (m, 1H), 3.56–3.62 (m, 1H), 2.69–2.81 (m, 5H), 2.56 (dd, $J = 16.0, 5.6$ Hz, 1H), 2.40 (s, 3H), 2.28 (brs, 1H), 1.82–1.99 (m, 5H), 0.80 (d, $J = 7.2$ Hz, 3H), 0.70 (d, $J = 6.8$ Hz, 3H); ^{13}C NMR (100 MHz, CDCl_3) δ 143.2, 138.3, 131.9, 129.5, 127.1, 125.9, 58.3, 55.9, 51.3, 37.1, 36.0, 31.3, 26.2, 26.1, 24.6, 21.5, 18.2, 15.9; IR (neat) 3280, 1318, 1155, 666 cm^{-1} ;



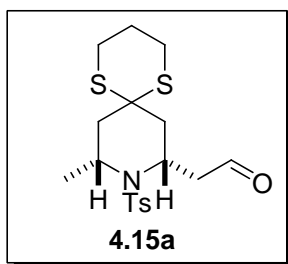
A colorless oil: $[\alpha]_{\text{D}}^{27.6} = -9.5$ (c 1.06, CHCl_3); ^1H NMR (400 MHz, CDCl_3) δ 7.74 (d, $J = 8.4$ Hz, 2H), 7.26 (d, $J = 8.0$ Hz, 2H), 5.62–5.75 (m, 2H), 5.51 (d, $J = 7.2$ Hz, 1H), 4.08 (brs, 2H), 3.50–3.56 (m, 1H), 2.67–2.82 (m, 4H), 2.56 (dd, $J = 14.4, 6.0$ Hz, 1H), 2.43 (dd, $J = 14.0, 4.8$ Hz, 1H), 2.39 (s, 3H), 1.84–2.01 (m, 5H), 0.79 (d, $J = 7.2$ Hz, 3H), 0.70 (d, $J = 7.2$ Hz, 3H); ^{13}C NMR (100 MHz, CDCl_3) δ 143.1, 138.1, 133.3, 129.4, 127.1, 126.0, 63.1, 55.8, 51.1, 40.9, 37.6, 31.4, 26.1, 26.0, 24.6, 21.4, 18.0, 16.1; IR (neat) 3288, 1320, 1157, 1092, 668 cm^{-1} ;



A colorless oil: $[\alpha]_{\text{D}}^{27.6} = +7.3$ (c 0.48, CHCl_3); ^1H NMR (400 MHz, CDCl_3) δ 7.70 (d, $J = 8.4$ Hz, 2H), 7.25 (d, $J = 8.4$ Hz, 2H), 5.78 (ddd, $J = 11.6, 7.2, 5.2$ Hz, 1H), 5.48–5.65 (m, 3H), 4.92 (d, $J = 17.6$ Hz, 1H), 4.86 (d, $J = 10.0$ Hz, 1H), 4.17–4.25 (m, 1H), 4.04–4.12 (m, 1H), 2.70–2.91 (m, 5H), 2.55 (dd, $J = 15.6, 6.4$ Hz, 1H), 2.39 (s, 3H), 2.27 (dd, $J = 15.2, 8.0$ Hz, 1H), 2.03 (dd, $J = 15.2, 4.4$ Hz, 1H), 1.94–2.02 (m, 2H), 1.82–1.92 (m, 1H); ^{13}C NMR (100 MHz, CDCl_3) δ 143.4, 138.1, 137.6, 132.0, 129.4, 127.5, 125.6, 116.3, 58.3, 54.4, 51.2, 42.7, 36.6, 26.2, 26.1, 24.7, 21.5; IR (neat) 3270, 1324, 1158, 1093, 668 cm^{-1} ;

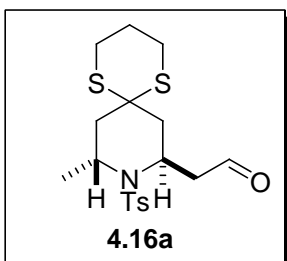


A colorless oil: $[\alpha]_D^{27.4} = -5.0$ (*c* 0.14, CHCl_3); $^1\text{H NMR}$ (400 MHz, CDCl_3) δ 7.72 (d, $J = 8.4$ Hz, 2H), 7.22 (d, $J = 8.4$ Hz, 2H), 5.77–5.83 (m, 1H), 5.67 (ddd, $J = 12.0, 6.4, 5.6$ Hz, 1H), 4.73 (d, $J = 8.4$ Hz, 1H), 4.16–4.26 (m, 1H), 4.07–4.16 (m, 1H), 3.77 (td, $J = 9.2, 1.6$ Hz, 1H), 2.93 (dd, $J = 17.2, 8.0$ Hz, 1H), 2.70–2.86 (m, 5H), 2.39 (s, 3H), 2.26 (dd, $J = 15.6, 1.6$ Hz, 1H), 2.09 (s, 1H), 1.89–1.99 (m, 2H), 1.89 (dd, $J = 15.2, 10.0$ Hz, 1H), 0.80 (s, 9H); $^{13}\text{C NMR}$ (100 MHz, CDCl_3) δ 142.7, 139.8, 131.4, 129.2, 127.0, 126.9, 60.7, 58.3, 51.8, 39.4, 36.5, 35.4, 27.0, 26.29, 26.25, 24.8, 21.5; IR (neat) 1653, 1153 cm^{-1} ;

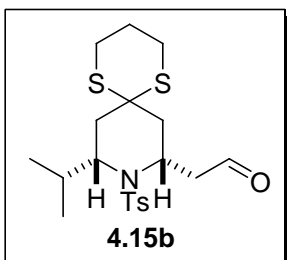


A colorless oil: $[\alpha]_D^{24.5} = 15.7$ (*c* 0.4, CHCl_3); $^1\text{H NMR}$ (400 MHz, CDCl_3) δ 9.78 (s, 1H), 7.70 (d, $J = 6.4$ Hz, 2H), 7.29 (d, $J = 8.0$ Hz, 2H), 4.47–4.53 (m, 1H), 4.06–4.17 (m, 1H), 3.41 (dd, $J = 18.0, 9.6$ Hz, 1H), 3.17 (dd, $J = 18.4, 4.8$ Hz, 1H), 2.65–2.89 (m, 4H), 2.41 (s, 3H), 2.35 (dd, $J = 15.2, 4.4$ Hz, 1H), 1.82–2.03 (m, 5H), 1.54 (d, $J = 7.2$ Hz, 3H);

^{13}C NMR (100 MHz, CDCl_3) δ 200.5, 143.5, 136.8, 129.8, 127.1, 51.3, 48.2, 47.1, 44.4, 41.3, 38.0, 26.8, 26.7, 24.8, 24.6, 21.5; IR (neat) 1720, 1160 cm^{-1} ;

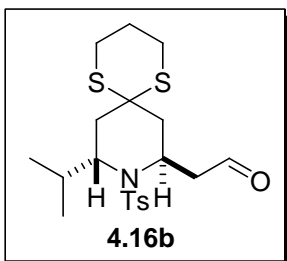


A colorless oil: ^1H NMR (400 MHz, CDCl_3) δ 9.71 (s, 1H), 7.69 (d, $J = 8.8$ Hz, 2H), 7.27 (d, $J = 8.4$ Hz, 2H), 4.74–4.81 (m, 1H), 3.98–4.08 (m, 1H), 3.13–3.27 (m, 2H), 2.68–2.95 (m, 4H), 2.41 (s, 3H), 2.36 (dd, $J = 14.8, 5.6$ Hz, 1H), 2.26 (dd, $J = 14.4, 4.4$ Hz, 1H), 2.13 (dd, $J = 14.4, 4.0$ Hz, 1H), 1.84–2.04 (m, 3H), 1.38 (d, $J = 6.8$ Hz, 3H); ^{13}C NMR (100 MHz, CDCl_3) δ 199.8, 143.3, 139.9, 129.6, 127.0, 49.1, 48.5, 47.5, 47.1, 43.2, 39.8, 26.4, 26.3, 25.0, 21.5, 20.2.

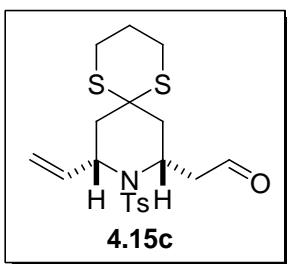


A colorless crystals: $[\alpha]_{\text{D}}^{27.4} = 69.6$ (c 0.43, CHCl_3); ^1H NMR (400 MHz, CDCl_3) δ 9.81 (s, 1H), 7.71 (d, $J = 8.4$ Hz, 2H), 7.30 (d, $J = 8.4$ Hz, 2H), 4.36–4.43 (m, 1H), 3.57–3.62 (m, 1H), 3.34 (dd, $J = 18.4, 4.4$ Hz, 1H), 3.24 (dd, $J = 18.4, 9.6$ Hz, 1H), 2.81–2.95 (m,

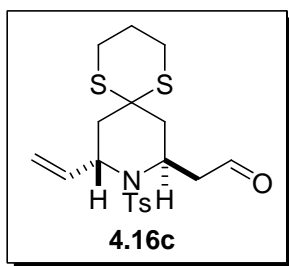
2H), 2.54–2.66 (m, 2H), 2.42 (s, 3H), 2.31 (dd, $J = 15.2, 9.6$ Hz, 2H), 1.99–2.06 (m, 3H), 1.82–1.92 (m, 1H), 0.99 (d, $J = 6.4$ Hz, 3H), 0.80 (d, $J = 6.4$ Hz, 3H); ^{13}C NMR (100 MHz, CDCl_3) δ 200.5, 143.6, 136.6, 129.8, 127.4, 59.7, 50.9, 47.3, 44.4, 37.5, 36.5, 33.0, 27.0, 26.7, 24.5, 21.5, 20.9, 20.6; IR (neat) 1720, 1598, 1338, 1326, 1095 cm^{-1} ;



A colorless crystals: ^1H NMR (400 MHz, CDCl_3) δ 9.65 (s, 1H), 7.72 (d, $J = 8.4$ Hz, 2H), 7.29 (d, $J = 8.0$ Hz, 2H), 4.18–4.24 (m, 1H), 3.65–3.70 (m, 1H), 3.41 (dd, $J = 18.4, 7.2$ Hz, 1H), 2.89–3.01 (m, 2H), 2.87 (dd, $J = 18.4, 8.0$ Hz, 1H), 2.59–2.70 (m, 2H), 2.42 (s, 3H), 2.30 (dd, $J = 14.0, 9.6$ Hz, 1H), 2.20 (dd, $J = 15.2, 2.0$ Hz, 1H), 2.07 (dd, $J = 14.8, 6.0$ Hz, 1H), 1.92–2.00 (m, 1H), 1.72–1.82 (m, 1H), 1.43 (dd, $J = 15.6, 6.4$ Hz, 1H), 1.09 (d, $J = 6.4$ Hz, 3H), 1.00 (d, $J = 6.4$ Hz, 3H); ^{13}C NMR (100 MHz, CDCl_3) δ 198.9, 143.5, 139.1, 129.6, 127.5, 63.2, 48.4, 47.5, 46.7, 40.7, 36.3, 29.6, 26.3, 25.0, 21.6, 20.7;

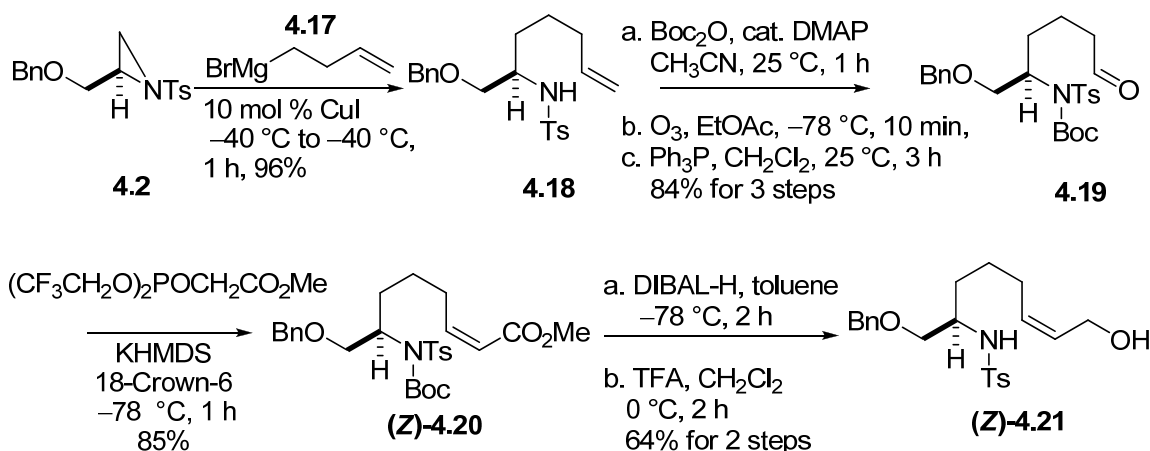


A colorless oil: $[\alpha]^{25.3}_D = 22.6$ (c 0.1, CHCl_3); ^1H NMR (400 MHz, CDCl_3) δ 9.78 (s, 1H), 7.73 (d, $J = 8.4$ Hz, 2H), 7.31 (d, $J = 8.4$ Hz, 2H), 6.07 (dddd, $J = 16.8, 10.4, 5.6, 4.8$ Hz, 1H), 5.39 (dd, $J = 16.8, 2.0$ Hz, 1H), 5.23 (dd, $J = 10.4, 2.0$ Hz, 1H), 4.44–4.57 (m, 2H), 3.35 (dd, $J = 18.4, 4.0$ Hz, 1H), 3.21 (dd, $J = 18.0, 9.6$ Hz, 1H), 2.80–2.93 (m, 2H), 2.62–2.71 (m, 2H), 2.43 (s, 3H), 2.31 (dd, $J = 14.4, 6.4$ Hz, 1H), 2.20 (d, $J = 5.2$ Hz, 1H), 2.16 (d, $J = 4.0$ Hz, 1H), 1.93–2.00 (m, 1H), 1.80–1.87 (m, 1H), 1.76 (dd, $J = 15.2, 6.4$ Hz, 1H); ^{13}C NMR (100 MHz, CDCl_3) δ 200.4, 143.8, 140.2, 136.5, 129.8, 127.4, 116.6, 53.5, 51.5, 47.7, 44.2, 40.5, 37.7, 27.0, 26.9, 24.5; IR (neat) 1721, 1325, 1162, 1094 cm^{-1} ;

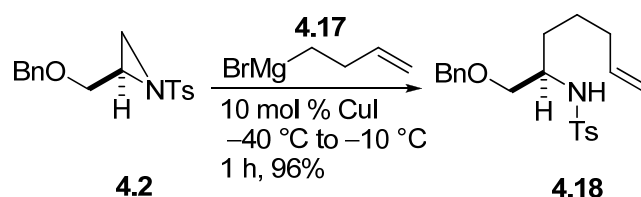


A colorless oil: ^1H NMR (400 MHz, CDCl_3) δ 9.65 (s, 1H), 7.68 (d, $J = 8.4$ Hz, 2H), 7.27 (d, $J = 8.4$ Hz, 2H), 5.96 (dddd, $J = 16.8, 10.0, 5.2, 4.8$ Hz, 1H), 5.25 (d, $J = 10.4$ Hz, 1H), 5.12 (d, $J = 10.0$ Hz, 1H), 4.58–4.64 (m, 2H), 3.27 (dd, $J = 18.0, 6.4$ Hz, 1H), 3.10 (dd, $J = 18.4, 8.0$ Hz, 1H), 2.80–2.93 (m, 2H), 2.71–2.79 (m, 2H), 2.41 (s, 3H), 2.22–2.30 (m, 2H), 2.20 (d, $J = 3.2$ Hz, 1H), 2.16 (d, $J = 3.2$ Hz, 1H), 1.95–2.04 (m, 1H), 1.78–1.88 (m, 1H).

Preparation of allylic alcohol 4.21 with *gem*-dihydrogen



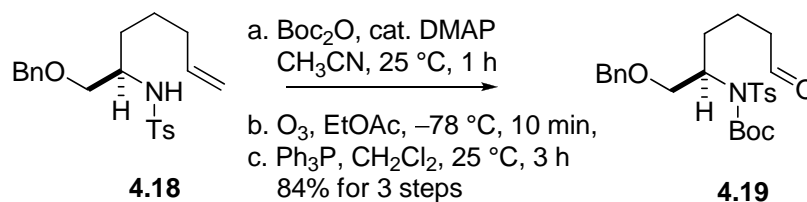
Preparation of alkene 4.18



To a cooled ($-40\text{ }^{\circ}\text{C}$) solution of the known 3-butene magnesium bromide **4.17** (0.13 M, 15 mL) in THF (15 mL, 0.13 M) was added CuI (18 mg, 0.095 mmol) and aziridine **4.2** (300 mg, 0.95 mmol). The resulting mixture was warmed to $-10\text{ }^{\circ}\text{C}$, stirred at $-10\text{ }^{\circ}\text{C}$ for 1 h and quenched with 4 mL $\text{NH}_4\text{Cl}/\text{NH}_4\text{OH}$ (3:1). After stirred at $25\text{ }^{\circ}\text{C}$ for 2 h, the reaction mixture was diluted with EtOAc. The layers were separated, and the aqueous layer was extracted with EtOAc. The combined organic layers were washed with brine, dried over anhydrous Na_2SO_4 , and concentrated *in vacuo*. The residue was purified by column chromatography (silica gel, hexanes/EtOAc, 3/1) to afford alkene **4.18** (340 mg, 96%): $[\alpha]^{25.5}_{\text{D}} = 18.1$ (c 0.68, CHCl_3); $^1\text{H NMR}$ (400 MHz, CDCl_3) δ 7.71 (d, $J = 8.8$ Hz, 2H), 7.17–7.34 (m, 7H), 5.68 (dddd, $J = 17.2, 10.4, 6.8, 2.8$ Hz, 1H), 4.97 (d, $J = 8.4$ Hz, 1H), 4.91 (d, $J = 17.2$ Hz, 1H), 4.90 (d, $J = 9.2$ Hz, 1H), 4.33 (s, 2H), 3.27–3.36 (m, 2H),

3.20 (dd, $J = 9.6, 4.8$ Hz, 1H), 2.39 (s, 3H), 1.93 (q, $J = 6.8$ Hz, 2H), 1.43–1.58 (m, 2H), 1.18–1.39 (m, 2H); ^{13}C NMR (100 MHz, CDCl_3) δ 143.0, 138.2, 138.1, 137.7, 129.5, 128.3, 127.6, 127.5, 126.9, 114.6, 73.0, 71.2, 53.4, 33.2, 31.9, 24.7, 21.4; IR (neat) 1640, 1598, 1453, 1416, 1323, 1157, 1090, 1022 cm^{-1} .

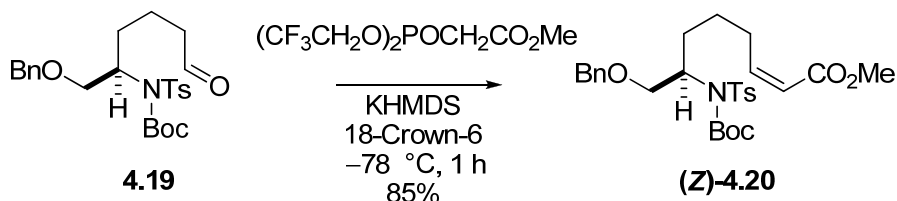
Preparation of aldehyde **4.19**



To a stirred solution of alkene **4.18** (297 mg, 0.795 mmol) in CH_3CN (15 mL, 0.053 M) was added Boc_2O (208 mg, 0.954 mmol) and DMAP (19 mg, 0.159 mmol) at 25 °C. After stirred at 25 °C for 1 h, the reaction mixture was concentrated and purified by column chromatography (silica gel, hexanes/EtOAc, 10/1) to afford Boc-protected alkene (340 mg, 96%). To a cooled (-78 °C) solution of the known Boc-protected alkene (300 mg, 0.634 mmol) in EtOAc (50 mL, 0.013 M) was bubbled O_3 until blue color was persisted (ca. 10 min). After purging the reaction with N_2 gas, EtOAc was removed and the residue was dissolved in CH_2Cl_2 (10 mL) before Ph_3P was added. The resulting mixture was stirred at 25 °C for 3 h and concentrated *in vacuo*. The residue was purified by column chromatography (silica gel, hexanes/EtOAc, 4/1) to afford aldehyde **4.19** (260 mg, 87%): ^1H NMR (400 MHz, CDCl_3) δ 9.76 (s, 1H), 7.85 (d, $J = 8.4$ Hz, 2H), 7.21–7.30 (m, 5H), 7.05 (d, $J = 8.0$ Hz, 2H), 4.75–4.82 (m, 1H), 4.49 (AB, $J_{\text{AB}} = 11.6$ Hz, $\Delta\nu_{\text{AB}} = 45.6$ Hz, 2H), 3.97 (t, $J = 9.6$ Hz, 1H), 3.58 (dd, $J = 10.0, 5.6$ Hz,

1H), 2.44–2.57 (m, 2H), 1.94–2.04 (m, 1H), 1.58–1.87 (m, 3H); ¹³C NMR (100 MHz, CDCl₃) δ 202.1, 150.5, 143.5, 137.8, 137.6, 128.7, 128.27, 128.25, 127.8, 127.5, 84.1, 73.0, 70.5, 58.1, 43.2, 29.7, 27.8, 21.5, 19.0.

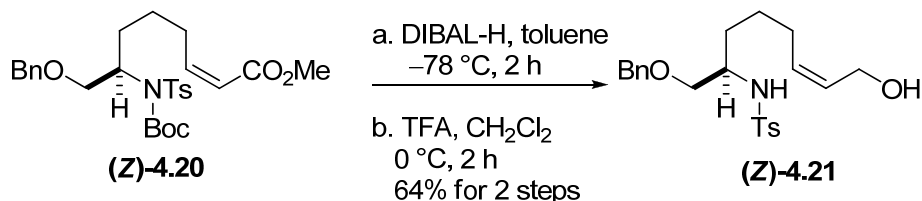
Preparation of enoates (**Z**)-4.20



To a cooled ($-78\text{ }^{\circ}\text{C}$) solution of methyl bis(2,2,2-trifluoroethyl)phosphonoacetate (0.23 mL, 1.06 mmol) and 18-crown-6 (1.4 g, 5.3 mmol) in THF (30 mL, 0.035 M) was added KHMDS (0.5 M, 2.1 mL). After stirred at the same temperature for 0.5 h, aldehyde **4.19** (250 mg, 0.53 mmol) was added to the reaction mixture. After stirred for 1 h at $-78\text{ }^{\circ}\text{C}$, the reaction mixture was quenched with saturated aqueous NH_4Cl and diluted with EtOAc. The layers were separated, and the aqueous layer was extracted with EtOAc. The combined organic layers were washed with brine, dried over anhydrous Na_2SO_4 , and concentrated *in vacuo*. The residue was purified by column chromatography (silica gel, hexanes/EtOAc, 8/1 to 4/1) to afford enoate (**Z**)-4.20 (236 mg, 85%): ¹H NMR (400 MHz, CDCl₃) δ 7.86 (d, $J = 6.4$ Hz, 2H), 7.22–7.30 (m, 5H), 7.05 (d, $J = 8.4$ Hz, 2H), 6.22 (ddd, $J = 11.2, 7.2, 4.4$ Hz, 1H), 5.78 (dt, $J = 11.2, 2.0$ Hz, 1H), 4.75–4.83 (m, 1H), 4.49 (AB, $J_{\text{AB}} = 11.6$ Hz, $\Delta\nu_{\text{AB}} = 47.6$ Hz, 2H), 3.98 (t, $J = 9.6$ Hz, 1H), 3.69 (s, 3H), 3.57 (dd, $J = 10.0, 5.6$ Hz, 1H), 2.69–2.75 (m, 2H), 2.35 (s, 3H), 1.93–2.03 (m, 1H),

1.53–1.67 (m, 3H), 1.29 (s, 9H); ^{13}C NMR (100 MHz, CDCl_3) δ 166.7, 150.5, 150.0, 143.4, 137.9, 137.7, 128.7, 128.3, 128.2, 127.8, 127.5, 119.6, 84.0, 72.9, 70.6, 58.4, 50.9, 29.9, 28.6, 27.8, 25.8, 21.5.

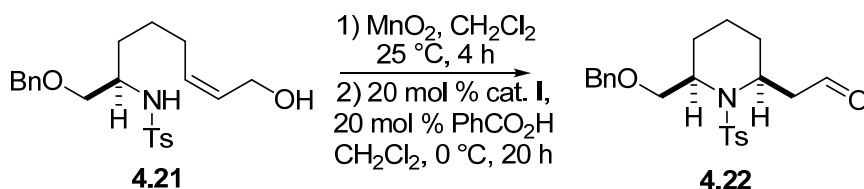
Preparation of allylic alcohol (**Z**)-4.21



[DIBAL-H Reduction] To a cooled ($-78\text{ }^\circ\text{C}$) solution of enoate (**Z**)-4.20 (230 mg, 0.433 mmol) in toluene (8 mL, 0.054 M) was added DIBAL-H (1.73 mL, 1.0 M in toluene, 1.732 mmol). After stirred at the same temperature for 2 h, the reaction mixture was quenched with MeOH, and diluted with Et_2O . The resulting mixture was stirred for 5 h at $25\text{ }^\circ\text{C}$, filtered through a pad of celite, and concentrated *in vacuo*. This crude alcohol was employed in the next step without purification. **[Boc-Deprotection]** To the crude Boc-carbamate (105 mg, 0.21 mmol) in CH_2Cl_2 (4.2 mL) was added TFA (0.8 mL) at $0\text{ }^\circ\text{C}$. After stirred at the same temperature for 2 h, the reaction mixture was concentrated *in vacuo*. and purified by column chromatography (silica gel, hexanes/ EtOAc , 1/1) to afford allylic alcohol (**Z**)-4.21 (54 mg, 64% for 2 steps) as a colorless oil: $[\alpha]^{25.6}_{\text{D}} = 8.5$ (*c* 0.20, CHCl_3); ^1H NMR (400 MHz, CDCl_3) δ 7.70 (d, $J = 8.0$ Hz, 2H), 7.18–7.35 (m, 7H), 5.58 (ddd, $J = 12.8, 6.8, 6.0$ Hz, 1H), 5.58 (ddd, $J = 15.2, 10.4, 7.2$ Hz, 1H), 5.02 (d, $J = 8.4$ Hz, 1H), 4.32 (s, 2H), 4.13 (d, $J = 6.8$ Hz, 2H), 3.28–3.38 (m, 1H), 3.28 (dd, $J = 9.2, 4.0$

Hz, 1H), 3.16 (dd, $J = 8.8, 4.4$ Hz, 1H), 2.40 (s, 3H), 2.17 (s, 1H), 1.92–2.06 (m, 2H), 1.44–1.58 (m, 2H), 1.21–1.40 (m, 2H); ^{13}C NMR (100 MHz, CDCl_3) δ 143.1, 138.0, 137.6, 132.1, 129.5, 128.8, 128.3, 127.7, 127.6, 126.9, 73.1, 71.1, 58.3, 53.3, 31.8, 26.7, 25.3, 21.4; IR (neat) 1598, 1453, 1323, 1157, 1091, 1024 cm^{-1} .

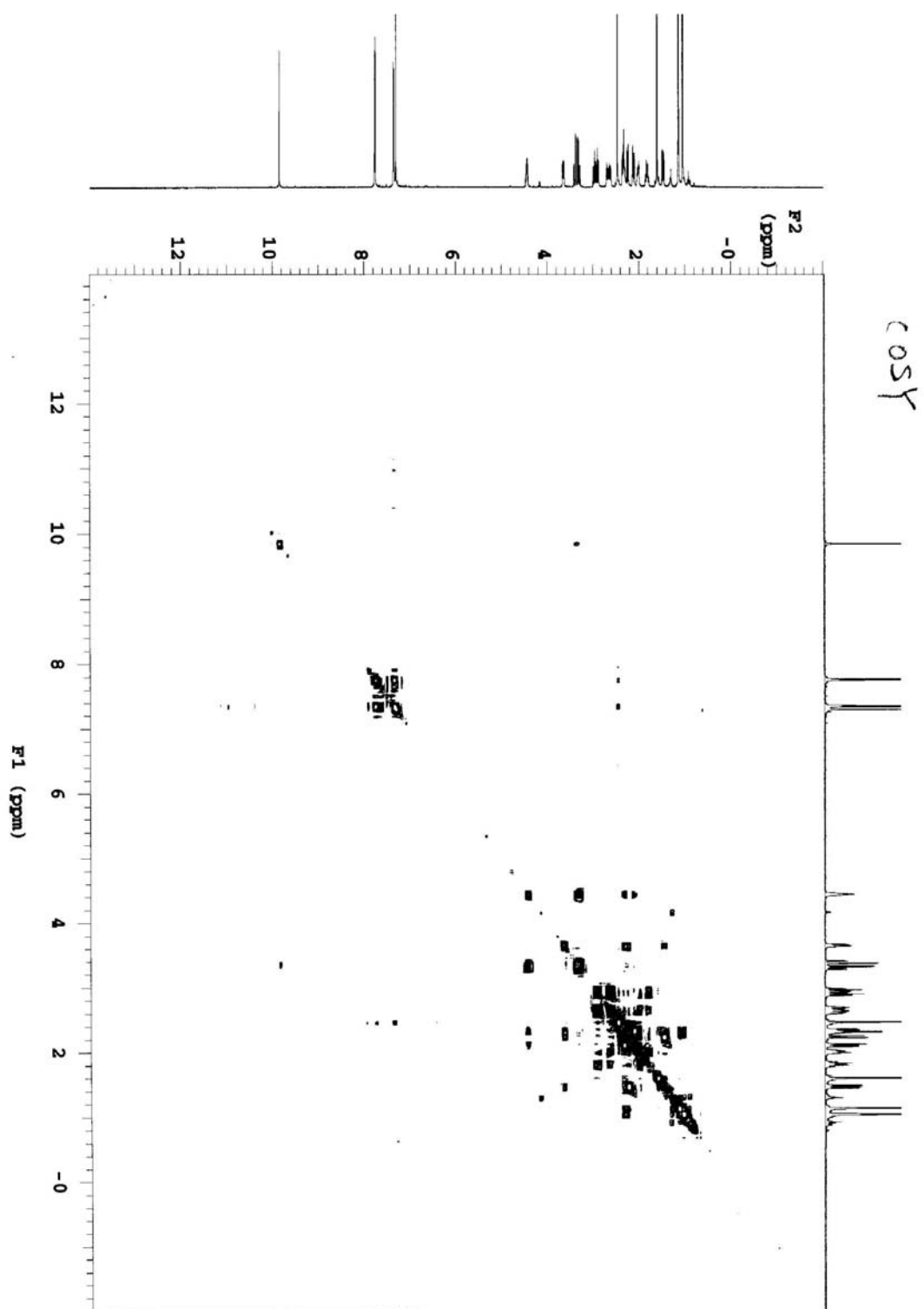
Allylic oxidation/aza-Michael reaction of (Z)-4.21



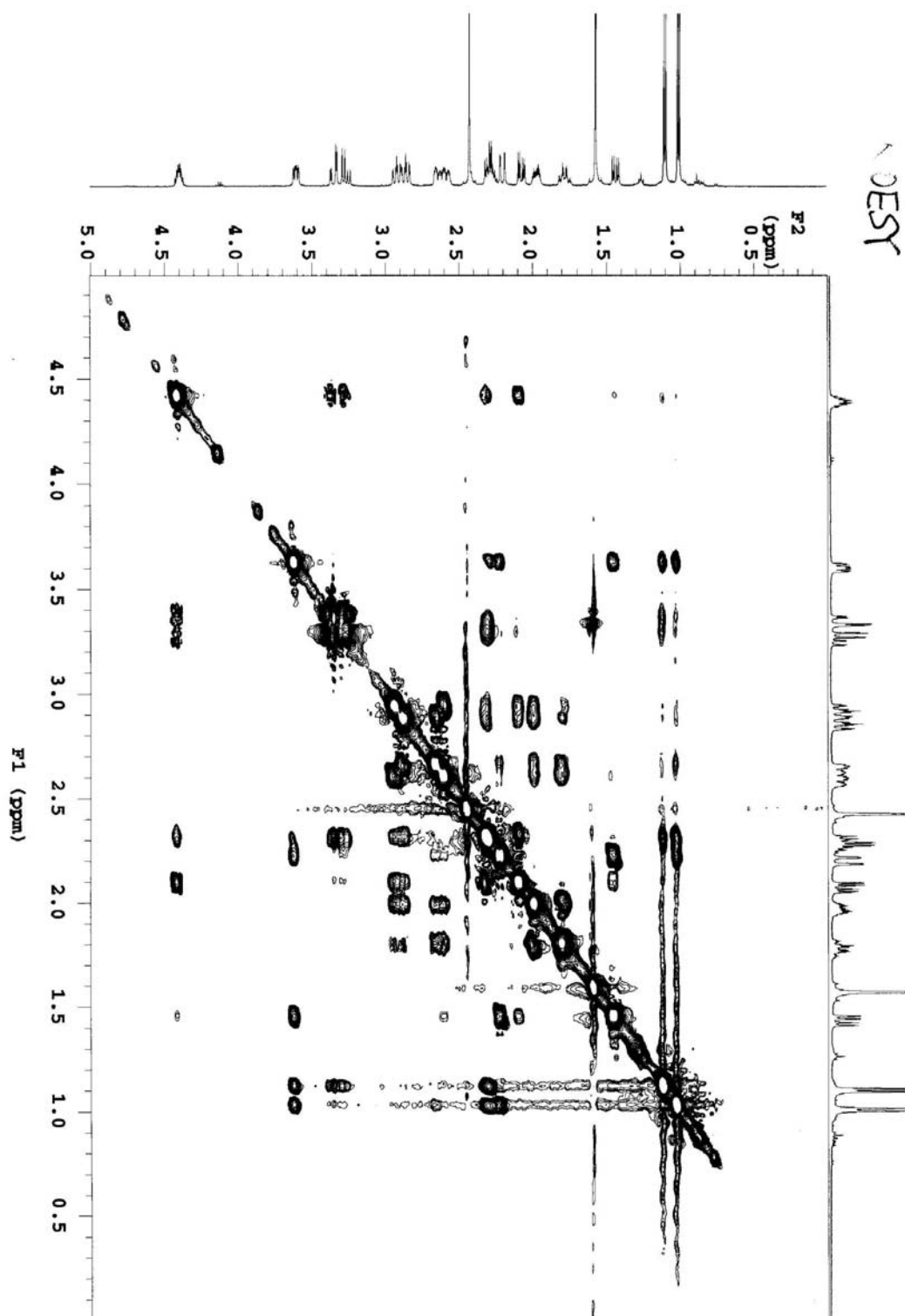
[Allylic Oxidation] To a stirred solution of (Z)-allylic alcohol **4.21** (40 mg, 0.0993 mmol) in CH_2Cl_2 (3.0 mL, 0.0331 M) was added MnO_2 (196.3 mg, 1.986 mmol) at 25 °C. After stirred for 4 h at the same temperature, the reaction mixture was then filtered through celite with EtOAc and concentrated *in vacuo*. This crude aldehyde was employed in the next step without purification. **[Aza-Michael Reaction]** To a stirred solution of α,β -unsaturated aldehyde intermediate in CH_2Cl_2 (4.0 mL, 0.0248 M) was added **I** (6.5 mg, 0.0197 mmol) and PhCO_2H (2.4 mg, 0.0197 mmol) at 0 °C. After stirred for 45 h at the same temperature, the reaction mixture was concentrated and purified by column chromatography (silica gel, hexanes/EtOAc, 3/1) to afford 2,6-*cis*-disubstituted piperidine aldehyde **4.22** (6 mg, 15%) as a colorless oil: ^1H NMR (400 MHz, CDCl_3) δ 9.71(s, 1H), 7.71 (d, $J = 8.4$ Hz, 2H), 7.26–7.38 (m, 7H), 4.56 (d, $J = 4.0$ Hz, 2H), 4.18–4.25 (m, 1H), 3.61 (d, $J = 8.0$ Hz, 1H), 3.59 (d, $J = 5.6$ Hz, 1H), 2.76 (dd, $J = 17.2, 5.6$

Hz, 1H), 2.64 (ddd, $J = 17.2, 8.8, 1.6$ Hz, 1H), 2.42 (s, 3H), 1.80 (d, $J = 12.8$ Hz, 2H),
1.17–1.56 (m, 6H).

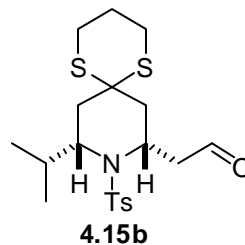
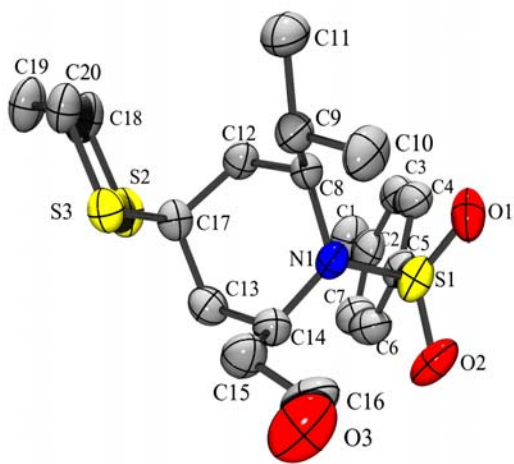
COSY of 4.15b



NOESY of 4.15b



Crystal data and structure refinement for 4.15b



Identification code	4.15b	
Empirical formula	C ₂₀ H ₂₉ N O ₃ S ₃	
Formula weight	427.62	
Temperature	296(2) K	
Wavelength	0.71073 Å	
Crystal system	Monoclinic	
Space group	P2(1)	
Unit cell dimensions	a = 10.0934(9) Å	α = 90°.
	b = 19.4755(17) Å	β = 111.576(5)°.
	c = 11.6842(11) Å	γ = 90°.
Volume	2135.9(3) Å ³	
Z	4	
Density (calculated)	1.330 Mg/m ³	
Absorption coefficient	0.367 mm ⁻¹	
F(000)	912	
Crystal size	0.18 x 0.13 x 0.06 mm ³	
Crystal color and habit	colourless prism	
Diffractometer	Bruker SMART Apex II	
Theta range for data collection	2.29 to 26.21°.	
Index ranges	-11 ≤ h ≤ 12, -24 ≤ k ≤ 24, -14 ≤ l ≤ 14	
Reflections collected	35695	
Independent reflections	8507 [R(int) = 0.0720]	
Observed reflections (I > 2σ(I))	5650	
Completeness to theta = 26.21°	99.4 %	
Absorption correction	Semi-empirical from equivalents	
Max. and min. transmission	0.9821 and 0.9368	
Solution method	SHELXS-97 (Sheldrick, 2008)	
Refinement method	SHELXL-97 (Sheldrick, 2008)	
Data / restraints / parameters	8507 / 1 / 487	
Goodness-of-fit on F ²	1.017	
Final R indices [I > 2σ(I)]	R1 = 0.0427, wR2 = 0.0812	
R indices (all data)	R1 = 0.0864, wR2 = 0.0952	
Absolute structure parameter	0.03(6)	
Largest diff. peak and hole	0.181 and -0.171 e.Å ⁻³	

References

- ¹ Nicolaou, K. C.; Sorensen, E. J. *Classics in Total Synthesis I* **1996**, VCH, New York.
- ² Davies, H. M. L.; Sorensen, E. J. *Chem. Soc. Rev.* 2009, **38**, 2981–2982.
- ³ Katja Hübel, K.; Leßmann, T.; Waldmann, H. *Chem. Soc. Rev.* **2008**, *37*, 1361–1374.
- ⁴ Stockwell, B. R. *Nature* **2004**, *432*, 846–854.
- ⁵ Guiffant, D. Tribouillard, D.; Gug, F.; Galons, H.; Meijer, L.; Blondel, M.; Bach, S. *Biotechnol. J.* **2007**, *2*, 68–75.
- ⁶ Hinterding, K.; Alonso-Diaz, D.; Waldmann, H. *Angew. Chem., Int. Ed.* **1998**, *37*, 688–749.
- ⁷ Ji, H.-F.; Li, X.-J.; Zhang, H.-Y. *EMBO rep.* **2009**, *10*, 194–200.
- ⁸ Newman, D. J. *J. Med. Chem.* **2008**, *51*, 2589–2599.
- ⁹ Hughes, B. *Nat. Rev. Drug Discov.* **2008**, *7*, 107–109.
- ¹⁰ Ueda, H.; Nakajima, H.; Hori, Y.; Goto, T.; Okuhara, M. *J. Antibiot.* **1994**, *47*, 301–310.
- ¹¹ a) Ulanovskaya, O. A.; Janjic, J.; Suzuki, M.; Sabharwal, S. S.; Schumacker, P. T.; Kron, S. J.; Kozmin, S. A. *Nat. Chem. Biol.* **2008**, *4*, 418–424; b) Paterson, I.; Anderson, E. A. *Science* **2005**, *310*, 451–453.
- ¹² Kasper, C. A.; Baker, B. J.; Kim, H.; Hong, J. *Future Med. Chem.* **2009**, *1*, 727–736.
- ¹³ Haggarty, S. J.; Koeller, K. M.; Wong, J. C.; Grozinger, C. M.; Schreiber, S. L.; *Proc. Natl. Acad. Sci. USA.* **2003**, *100*, 4389–4394.
- ¹⁴ Nielsen, T. K.; Hildmann, C.; Dickmanns, A.; Schwienhorst, A.; Ficner, R. *J. Mol. Biol.* **2005**, *354*, 107–120.
- ¹⁵ Hubbert, C.; Guardiola, A.; Shao, R.; Kawaguchi, Y.; Ito, A.; Nixon, A.; Yoshida, M.; Wang, X. F.; Yao, T. P. *Nature* **2002**, *417*, 455–458.
- ¹⁶ Wolffe, A. P.; Matzke, M. A. *Science* **1999**, *286*, 481–486.
- ¹⁷ Suzuki, T.; Miyata, N. *Curr. Med. Chem.* **2006**, *13*, 935–958.
- ¹⁸ Johnson, A. B.; Barton, M. C. *Mut. Res.* **2007**, *618*, 149–162.
- ¹⁹ Berger, S. L. *Curr. Opin. Cell Biol.* **1999**, *11*, 336–341.

- ²⁰ Kouzarides, T. *EMBO J.* **2000**, *19*, 1176–1179.
- ²¹ Minucci, S.; P. Pelicci, P. *Nat. Rev. Cancer* **2006**, *6*, 38–51.
- ²² Marks, P.; Breslow, R. *Nat. Biotechnol.* **2007**, *25*, 84–90.
- ²³ Gray, S. G.; Ekstrom, T. J. *Exp. Cell Res.* **2001**, *262*, 75–83.
- ²⁴ Verdin, E.; Dequiedt, F.; Kasler, H. G. *Trends Genet.* **2003**, *19*, 286–293.
- ²⁵ Voelter-Mahlknecht, S.; Ho, A. D.; Mahlkecht, U. *Int. J. Mol. Med.* **2005**, *16*, 589–598.
- ²⁶ Yang, X. J.; Seto, E. *Curr. Opin. Genet. Dev.* **2003**, *13*, 143–153.
- ²⁷ Monneret, C. *Eur. J. Med. Chem.* **2005**, *40*, 1–13.
- ²⁸ Finnin, M.; Donigan, J.; Cohen, A.; Richon, V.; Rifkind, R.; Marks, P.; Breslow, R.; Pavletich, N. *Nature* **1999**, *401*, 188–193.
- ²⁹ de Ruijter, A.J.; van Gennip, A.H.; Caron, H.N.; Kemp, S.; van Kuilenburg, A.B. *Biochem. J.* **2003**, *370*, 737–749.
- ³⁰ Miller, T.; Witter, D.; Belvedere, S. *J. Med. Chem.* **2003**, *46*, 5097–5116.
- ³¹ Cress, W. D.; Seto, E. *J. Cell. Physiol.* **2000**, *184*, 1–16.
- ³² Khan, N.; Jeffers, M.; Kumar, S.; Hackett, C.; Boldog, F.; Khramtsov, N.; Qian, X.; Mills, E.; Berghs, S.; Carey, N.; Finn, P.; Collins, L.; Tumber, A.; Ritchie, J.; Jensen, P.; Lichenstein, H.; Sehested, M. *Biochem. J.* **2008**, *409*, 581–589.
- ³³ Lager, G.; O’Carroll, D.; Rembold, M.; Khier, H.; Tischler, J.; Weitzer, G.; Schuettengruber, B.; Hauser, C.; Brunmeir, R.; Henuwein, T.; Seiser, C. *EMBO J.* **2002**, *21*, 2672–2681.
- ³⁴ Glaser, K.; Li, J.; Staver, M.; Wei, R.-Q.; Albert, D.; Davidsen, S. *Biochem. Biophys. Res. Comm.* **2003**, *310*, 529–536.
- ³⁵ Taunton, J.; Hassig, C.; Schreiber, S. *Science* **1996**, *272*, 408–411.
- ³⁶ (a) Richon, V. M.; Webb, Y.; Merger, R.; Sheppard, T.; Jursic, B.; Ngo, L. *Proc. Natl. Acad. Sci. USA.* **1996**, *93*, 5705–5708. (b) Ueda, H.; Nakajima, H.; Hori, Y.; Fujita, T.; Nishimura, M.; Goto, T.; Okuhara, M. *J. Antibiot.* **1994**, *47*, 301–310.
- ³⁷ Newkirk, T. L.; Bowers, A. A.; Williams, R. M. *Nat. Prod. Rep.* **2009**, *26*, 1293–1320.
- ³⁸ Tsuji, N.; Kobayashi, M.; Nagashima, K.; Wakisaka, Y.; Koizumi, K. *J. Antibiot.* **1976**, *29*, 1–6.

- ³⁹ Richon, V. M.; Emiliani, S.; Verdin, E.; Webb, Y.; Breslow, R.; Rifkind, R. A. *Proc. Natl. Acad. Sci. USA*. **1998**, *95*, 3003–3007.
- ⁴⁰ Pringle, R. B. *Plant Physiol*. **1970**, *46*, 45–49.
- ⁴¹ a) Umehara, K.; Nakahara, K.; Kiyota, S.; Iwami, M.; Okamoto, M.; Tanake, H.; Kohsaka, M.; Oaki, H.; Imanaka, H. *J. Antibiot*. **1983**, *36*, 478–483; b) Hirota, A.; Suzuki, A.; Suzuki, H.; Tamura, S. *Agric. Biol. Chem*. **1973**, *37*, 643–647.
- ⁴² Shute, R.; Dunlap, B.; Rich, D. *J. Med. Chem*. **1987**, *30*, 71–78.
- ⁴³ Furumai, R.; Komatsu, Y.; Nishino, N.; Khochbin, S.; Yoshida, M.; Horinouchi, S. *Proc. Natl. Acad. Sci. USA*. **2001**, *98*, 87–92.
- ⁴⁴ Kijima, M.; Yoshida, M.; Sugita, K.; Horinouchi, S.; Beppu, T. *J. Biol. Chem*. **1993**, *268*, 22429–22435.
- ⁴⁵ Masuoka, Y.; Nagai, A.; Shin-Ya, K.; Furihata, K.; Nagai, K.; Suzuki, K.; Hayakawa, Y.; Seto, H. *Tetrahedron Lett*. **2001**, *42*, 41–44.
- ⁴⁶ Yurek-George, A.; Habens, F.; Brimmell, M.; Pachham, G.; Ganesan, A. *J. Am. Chem. Soc*. **2004**, *126*, 1030–1031.
- ⁴⁷ a) Chen, Y.; Gambs, C.; Abe, Y.; Wentworth, P.; Janda, K. *J. Org. Chem*. **2003**, *68*, 8902–8905; b) Fujisawa Pharmaceutical Co. Ltd., Japan. Jpn. Kokai Tokkyo Koho JP, 03141296, 1991.
- ⁴⁸ Marshall, J. L.; Rizvi, N.; Kauh, J.; Dahut, W.; Figuera, M. *J. Exp. Ther. Oncol*. **2002**, *2*, 325–332.
- ⁴⁹ Shigematsu, N.; Ueda, H.; Takase, S.; Tanaka, H.; Yamamoto, K.; Tada, T. *J. Antibiot*. **1994**, *47*, 311–314.
- ⁵⁰ Khan, W.; Wu, J.; Sing, W.; Simon, J. *J. Am. Chem. Soc*. **1996**, *118*, 7237–7238.
- ⁵¹ Gresshock, T.; Johns, D.; Noguchi, Y.; Williams, R. *Org. Lett*. **2008**, *10*, 613–616.
- ⁵² Wen, S.; Packham, G.; Ganesan, A. *J. Org. Chem*. **2008**, *73*, 9353–9361.
- ⁵³ Furumai, R.; Matsuyama, A.; Kobashi, N.; Lee, K. H.; Nishiyama, M. *Cancer Res*. **2002**, *62*, 4916–4921.
- ⁵⁴ Taori, K.; Paul, V. J.; Luesch, H. *J. Am. Chem. Soc*. **2008**, *130*, 1806–1807.
- ⁵⁵ Ying, Y.; Taori, K.; Kim, H.; Hong, J.; Luesch, H. *J. Am. Chem. Soc*. **2008**, *130*, 8455–8459.

- ⁵⁶ Vannini, A.; Volpari, C.; Filocamo, G.; Casavola, E. C.; Brunetti, M.; Renzoni, D.; Chakravarty, P.; Paolini, C.; Francesco, R. D.; Steinku, P. G.; Marco, S. D. *Proc. Natl. Acad. Sci. USA*. **2004**, *201*, 15064–15069.
- ⁵⁷ Christianson, D. W.; Lipscomb, W. N. *Acc. Chem. Res.* **1989**, *22*, 62–69.
- ⁵⁸ Marks, P. A.; Xu, W.-S. *J. Cell. Biochem.* **2009**, *107*, 600–608.
- ⁵⁹ Duvic, M.; Vu, J. *Expert Opin. Invest. Drugs* **2007**, *16*, 1111–1120.
- ⁶⁰ Mei, S.; Ho, A. D.; Majlknecht, U. *Int. J. Oncol.* **2004**, *25*, 1509–1519.
- ⁶¹ Ito, T.; Ouchida, M.; Morimoto, Y.; Yoshida, A.; Jitsumori, Y.; Ozaki, T.; Sonobe, H.; Inoue, H.; Shimizu, K. *Cancer Lett.* **2005**, *224*, 311319.
- ⁶² Hooker, J. M.; Kim, S. W.; Alexoff, D.; Xu, Y.; Shea, C.; Reid, A.; Volkow, N.; Fowler, J. S. *ACS Chem. Neurosci.* **2010**, *1*, 65–73.
- ⁶³ For examples of macrocyclic natural products, see: (a) Schreiber, S. L.; Crabtree, G. R. *Immunol. Today* **1992**, *13*, 136–142. (b) Boger, D. L. *Med. Res. Rev.* **2001**, *21*, 356–381. (c) Nicolaou, K. C.; Ritzen, A.; Namoto, K. *Chem. Commun.* **2001**, 1523–1535. (d) Fürstner, A. *Angew. Chem., Int. Ed.* **2003**, *42*, 3582–3603. (e) Kobayashi, J.; Tsuda, M. *Nat. Prod. Rep.* **2004**, *21*, 77–93. (f) Yeung, K.-S.; Paterson, I. *Chem. Rev.* **2005**, *105*, 4237–4313. (g) Lachia, M.; Moody, C. J. *Nat. Prod. Rep.* **2008**, *25*, 227–253.
- ⁶⁴ Ying, Y.; Liu, Y.; Byeon, S. R.; Kim, H.; Luesch, H.; Hong, J. *Org. Lett.* **2008**, *10*, 4021–4024.
- ⁶⁵ Knopp, M.; Koser, S.; Schaefer, B. *Ger. Offen.* DE 19934066, Jan. 25, **2001**.
- ⁶⁶ Pattenden, G.; Thom, S. M.; Jones, M. F. *Tetrahedron* **1993**, *49*, 2131–2138.
- ⁶⁷ In addition to **2.7**, the reaction conditions produced the thiazole-methylthiazoline ethyl ester (15%).
- ⁶⁸ (a) Nagao, Y.; Hagiwara, Y.; Kumagai, T.; Ochiai, M.; Inoue, T.; Hashimoto, K.; Fujita, E. *J. Org. Chem.* **1986**, *51*, 2391–2393. (b) Hodge, M. B.; Olivo, H. F. *Tetrahedron* **2004**, *60*, 9397–9403.
- ⁶⁹ For examples of macrocyclization reactions in the synthesis of biologically active cyclic peptides and depsipeptides, see: (a) Hamada, Y.; Shioiri, T. *Chem. Rev.* **2005**, *105*, 4441–4482.
- (b) Li, W. R.; Ewing, W. R.; Harris, B. D.; Joullie, M. M. *J. Am. Chem. Soc.* **1990**, *112*, 7659–7672. (c) Jiang, W.; Wanner, J.; Lee, R. J.; Bounaud, P.-Y.; Boger, D. L. *J. Am. Chem. Soc.* **2002**, *124*, 5288–5290. (d) Chen, J.; Forsyth, C. J. *J. Am. Chem. Soc.* **2003**, *125*, 8734–8735.
- ⁷⁰ Attempts for macrolactonization under various conditions resulted in either no reaction or complex reaction mixtures. For details, see experimental sections.

- ⁷¹ Harrowven, D. C.; Lucas, M. C.; Howes, P. D. *Tetrahedron* **1999**, *55*, 1187–1196.
- ⁷² Toriyama, M.; Kamijo, H.; Motohashi, S.; Takido, T.; Itabashi, K. *Phosphorus Sulfur Silicon Relat. Elem.* **2003**, *178*, 1661–1665.
- ⁷³ (a) Scholl, M.; Ding, S.; Lee, C. W.; Grubbs, R. H. *Org. Lett.* **1999**, *1*, 953–956. (b) Chatterjee, A. K.; Grubbs, R. H. *Org. Lett.* **1999**, *1*, 1751–1753. (c) Chatterjee, A. K.; Grubbs, R. H. *Angew. Chem., Int. Ed.* **2002**, *41*, 3171–3174. (d) Chatterjee, A. K.; Choi, T.-L.; Sanders, D. P.; Grubbs, R. H. *J. Am. Chem. Soc.* **2003**, *125*, 11360–11370. (e) Connon, S. J.; Blechert, S. *Angew. Chem., Int. Ed.* **2003**, *42*, 1900–1923.
- ⁷⁴ Minozzi, M.; Nanni, D.; Walton, J. C. *Org. Lett.* **2003**, *5*, 901–904.
- ⁷⁵ Ćiraković, J.; Driver, T. G.; Woerpel, K. A. *J. Am. Chem. Soc.* **2002**, *124*, 9370–9371.
- ⁷⁶ (a) Li, K. W.; Wu, J.; Xing, W.; Simon, J. A. *J. Am. Chem. Soc.* **1996**, *118*, 7237–7238. (b) Yurek-George, A.; Cecil, A. R. L.; Mo, A. H. K.; Wen, S.; Rogers, H.; Habens, F.; Maeda, S.; Yoshida, M.; Packham, G.; Ganesan, A. *J. Med. Chem.* **2007**, *50*, 5720–5726. (c) Yurek-George, A.; Habens, F.; Brimmell, M.; Packham, G.; Ganesan, A. *J. Am. Chem. Soc.* **2004**, *126*, 1030–1031.
- ⁷⁷ (a) Mork, C. N.; Faller, D. V.; Spanjaard, R. A. *Curr. Pharm. Des.* **2005**, *11*, 1091–1095. (b) Yoshida, M.; Shimazu, T.; Matsuyama, A. *Prog. Cell Cycle Res.* **2003**, *5*, 269–278.
- ⁷⁸ (a) Paris, M.; Porcelloni, M.; Binaschi, M.; Fattori, D. *J. Med. Chem.* **2008**, *51*, 1505–1529. (b) Dokmanovic, M.; Clarke, C.; Marks, P. A. *Mol. Cancer Res.* **2007**, *5*, 981–989.
- ⁷⁹ Senese, S.; Zaragoza, K.; Minardi, S.; Muradore, I.; Ronzoni, S.; Passafaro, A.; Bernard, L.; Draetta, G. F.; Alcalay, M.; Seiser, C.; Chiocca, S. *Mol. Cell. Biol.* **2007**, *27*, 4784–4795.
- ⁸⁰ (a) Halkidou, K.; Gaughan, L.; Cook, S.; Leung, H. Y.; Neal, D. E.; Robson, C. N. *Prostate* **2004**, *59*, 177–189. (b) Wilson, A. J.; Byun, D.-S.; Popova, N.; Murray, L. B.; L'Italien, K.; Sowa, Y.; Arango, D.; Velcich, A.; Augenlicht, L. H.; Mariadason, J. M. *J. Biol. Chem.* **2006**, *281*, 13548–13558.
- ⁸¹ (a) Chang, S.; McKinsey, T. A.; Zhang, C. L.; Richardson, J. A.; Hill, J. A.; Olson, E. N. *Mol. Cell. Biol.* **2004**, *24*, 8467–8476. (b) Zhang, C. L.; McKinsey, T. A.; Chang, S.; Antos, C. L.; Hill, J. A.; Olson, E. N. *Cell* **2002**, *24*, 8467–8476.
- ⁸² Furumai, R.; Matsuyama, A.; Kobashi, N.; Lee, K.-H.; Nishiyama, M.; Nakajima, H.; Tanaka, A.; Komatsu, Y.; Nishino, N.; Yoshida, M.; Horinouchi, S. *Cancer Res.* **2002**, *62*, 4916–4921.
- ⁸³ (a) Cunningham, B. C.; Wells, J. A. *Science* **1989**, *244*, 1081–1085. (b) Ashkenazi, A.; Presta, L. G.; Marsters, S. A.; Camerato, T. R.; Rosenthal, K. A.; Fendly, B. M.; Capon, D. J. *Proc. Natl. Acad. Sci. USA.* **1990**, *57*, 7150–7154.

- ⁸⁴ For examples of macrocyclization reactions in the synthesis of biologically active cyclic peptides and depsipeptides, see: (a) Hamada, Y.; Shioiri, T. *Chem. Rev.* **2005**, *105*, 4441–4482. (b) Li, W. R.; Ewing, W. R.; Harris, B. D.; Joullie, M. M. *J. Am. Chem. Soc.* **1990**, *112*, 7659–7672. (c) Jiang, W.; Wanner, J.; Lee, R. J.; Bounaud, P.-Y.; Boger, D. L. *J. Am. Chem. Soc.* **2002**, *124*, 5288–5290. (d) Chen, J.; Forsyth, C. J. *J. Am. Chem. Soc.* **2003**, *125*, 8734–8735.
- ⁸⁵ (a) Bowers, A.; West, N.; Taunton, J.; Schreiber, S. L.; Bradner, J. E.; Williams, R. M. *J. Am. Chem. Soc.* **2008**, *130*, 11219–11222. (b) Seiser, T.; Kamena, F.; Cramer, N. *Angew. Chem., Int. Ed.* **2008**, *47*, 6483–6485. (c) Nasveschuk, C.; Ungermannova, D.; Liu, X.; Phillips, A. *Org. Lett.* **2008**, *10*, 3595–3598. (d) Ghosh, A.; Kulkarni, S. *Org. Lett.* **2008**, *10*, 3907–3909. (e) Ren, Q.; Dai, L.; Zhang, H.; Tan, W.; Xu, S.; Ye, T. *Synlett* **2008**, *15*, 2379–2383. (f) Numajiri, Y.; Takahashi, T.; Takagi, M.; Shin-ya, K.; Doi, T. *Synlett*, **2008**, *16*, 2483–2486. (g) Wang, B.; Craig, F. J. *Synthesis* **2009**, *17*, 2873–2880.
- ⁸⁶ Hodge, M. B.; Olivo, H. F. *Tetrahedron* **2004**, *60*, 9397–9403.
- ⁸⁷ Vergne, A. F.; Walz, A. J.; Miller, M. J. *Nat. Prod. Rep.* **2000**, *17*, 99–116.
- ⁸⁸ Dhungana, S.; Crumbliss, A. L. *Geomicrobiol. J.* **2005**, *22*, 87–98.
- ⁸⁹ Ratledge, C. *Tuberculosis* **2004**, *84*, 110–130.
- ⁹⁰ Piddington, D. L.; Kashkouli, A.; Buchmeier, N. A. *Infect. Immun.* **2000**, *68*, 4518–4522.
- ⁹¹ Hentze, M. W.; Muckenthaler, M. U.; Andrews, N. C. *Cell* **2004**, *117*, 285–297.
- ⁹² Miethke, M.; Marahiel, M. A. *Microbiol. Mol. Biol. Rev.* **2007**, *71*, 413–451.
- ⁹³ Ratledge C. Iron metabolism. In: Ratledge C, Dale J, editors. *Mycobacteria: molecular biology and virulence*. Oxford, UK: Blackwell Science; 1999. p. 206–286.
- ⁹⁴ Snow, G. A. *Bacteriol. Rev.* **1970**, *34*, 99–125.
- ⁹⁵ Rodriguez, G. M.; Smith, I. *Mol. Microbiol.* **2003**, *47*, 1485–1494.
- ⁹⁶ (a) Boukhalfa, H.; Crumbliss, A. L. *BioMetals* **2002**, *15*, 325–339. (b) Dhungana, S.; Miller, M. J.; Dong, L.; Ratledge, C.; Crumbliss, A. L. *J. Am. Chem. Soc.* **2003**, *125*, 7654–7663. (c) Ghio, A. J.; Piantadosi, C. A.; Crumbliss, A. L. *BioMetals* **1997**, *10*, 135–142.
- ⁹⁷ MacCordick, H. J.; Schleiffer, J. J.; Duplatre, G. *Radiochim. Acta* **1985**, *38*, 43–47.
- ⁹⁸ Hu, J.; Miller, M. J. *J. Am. Chem. Soc.* **1997**, *119*, 3462–3468.
- ⁹⁹ Suenaga, K.; Kokubo, S.; Shinohara, C.; Tsuji, T.; Uemura, D. *Tetrahedron Lett.* **1999**, *40*, 1945–1948.

- ¹⁰⁰ Murakami, Y.; Kato, S.; Nakajima, M.; Matsuoka, M.; Kawai, H.; Shin-Ya, K.; Seto, H. *J. Antibiot.* **1996**, *49*, 839–845.
- ¹⁰¹ Ratledge, C.; Snow, G. A. *Biochem. J.* **1974**, *139*, 407–413.
- ¹⁰² (a) Ikeda, Y.; Nonaka, H.; Furumai, T.; Onaka, H.; Igarashi, Y. *J. Nat. Prod.* **2005**, *68*, 1061–1065. (b) Ikeda, Y.; Furumai, T.; Igarashi, Y. *J. Antibiot.* **2005**, *58*, 566–572.
- ¹⁰³ Kokubo, S.; Suenaga, K.; Shinohara, C.; Tsuji, T.; Uemura, D. *Tetrahedron* **2000**, *56*, 6435–6440.
- ¹⁰⁴ Wu, T. Y. H.; Hassig, C.; Wu, Y.; Ding, S.; Schultz, P. G. *Bioorg. Med. Chem. Lett.* **2004**, *14*, 449–453.
- ¹⁰⁵ Tsuda, M.; Yamakawa, M.; Oka, S.; Tanaka, Y.; Hoshino, Y.; Mikami, Y.; Sato, A.; Fujiwara, H.; Ohizumi, Y.; Kobayashi, J. *J. Nat. Prod.* **2005**, *68*, 462–464.
- ¹⁰⁶ Ying, Y.; Hong, J. *Tetrahedron Lett.* **2007**, *48*, 8104–8107.
- ¹⁰⁷ Lin, C.-F.; Yang, J.-S.; Chang, C.-Y.; Kuo, S.-C.; Lee, M.-R.; Huang, L.-J. *Bioorg. Med. Chem.* **2005**, *13*, 1537–1544.
- ¹⁰⁸ Bremner, J. B.; Samosorn, S.; Ambrus, J. I. *Synthesis* **2004**, *16*, 2653–2658.
- ¹⁰⁹ Holden, K. G.; Mattson, M. N.; Cha, K. H.; Rapoport, H. *J. Org. Chem.* **2002**, *67*, 5913–5918.
- ¹¹⁰ (a) Hu, J.; Miller, M. J. *J. Org. Chem.* **1994**, *59*, 4858–4861. (b) Yokokawa, F.; Izumi, K.; Omata, J.; Shioiri, T. *Tetrahedron* **2000**, *56*, 3027–3034; (c) Walz, A. J.; Miller, M. J. *Org. Lett.* **2002**, *4*, 2047–2050; (d) Dong, L.; Miller, M. J. *J. Org. Chem.* **2002**, *67*, 4759–4770.
- ¹¹¹ Evans, D. A.; Bartroli, J.; Shih, T. L. *J. Am. Chem. Soc.* **1981**, *103*, 2127–2129.
- ¹¹² Abiko, A.; Liu, J.-F.; Masamune, S. *J. Am. Chem. Soc.* **1997**, *119*, 2586–2587.
- ¹¹³ Mitchell, J. M.; Shaw, J. T. *Org. Lett.* **2007**, *9*, 1679–1681.
- ¹¹⁴ (a) Fennell, K. A.; Möllmann, U.; Miller, M. J. *J. Org. Chem.* **2008**, *73*, 1018–1024. (b) Fennell, K. A.; Miller, M. J. *Org. Lett.* **2007**, *9*, 1683–1685.
- ¹¹⁵ Murray, R. W.; Jeyaraman, R. *J. Org. Chem.* **1985**, *50*, 2847–2853.
- ¹¹⁶ Corey, E. J.; Suggs, J. W. *Tetrahedron Lett.* **1975**, *31*, 2647–2650
- ¹¹⁷ (a) Putcha, L.; Cintrón, N. M.; Tsui, J.; Vanderploeg, J. M.; Kramer, W. G. *Pharm. Res.* **1989**, *6*, 481–485. (b) Crews, J. C.; Denson, D. D. *Cancer* **1990**, *66*, 2642–2644. (c) Arbiser, J. L.; Kau, T.; Konar, M.; Narra, K.; Ramchandran, R.; Summers, S. A.; Vlahos, C. J.; Ye, K.; Perry, B. N.; Matter, W.; Fischl, A.; Cook, J.; Silver, P. A.; Bain, J.; Cohen, P.; Whitmire, D.; Furness, S.;

Govindarajan, B.; Bowen, J. P. *Blood* **2007**, *109*, 560–565. (d) Ishida, N.; Kumagai, K.; Niida, T.; Tsuruoka, T.; Umoto, H. *J. Antibiot., Ser. A* **1967**, *20*, 66–71.

¹¹⁸ Reviews on the synthesis of piperidines: (a) Buffat, M. G. P. *Tetrahedron* **2004**, *60*, 1701–1729. (b) Laschat, S.; Dickner, T. *Synthesis* **2000**, *13*, 1781–1813. (c) Cossy, J. *Chem. Rev.* **2005**, *5*, 70–80. (d) Felpin, F.-X.; Lebreton, J. *Eur. J. Org. Chem.* **2003**, *19*, 3693–3712. (e) Bailey, P. D.; Millwood, P. A.; Smith, P. D. *Chem. Commun.* **1998**, 633–640.

¹¹⁹ (a) Bates, R. W.; Sa-Ei, K. *Tetrahedron* **2002**, *58*, 5957–5978. (b) Baliah, V.; Jeyraman, R.; Chandrasekaran, L. *Chem. Rev.* **1983**, *83*, 379–423.

¹²⁰ (a) Leete, E.; Carver, R. A. *J. Org. Chem.* **1975**, *40*, 2151–2153. (b) Lavagnino, E. R.; Clkuvette, R. R.; Cannon, W. N.; Kornfeld, E. C. *J. Am. Chem. Soc.* **1960**, *82*, 2609–2613.

¹²¹ Heintzelman, G. R.; Weinreb, S. M.; Parvez, M. *J. Org. Chem.* **1996**, *61*, 4594–4599.

¹²² Takahata, H.; Takahashi, S.; Kouno, S.-I.; Momose, T. *J. Org. Chem.* **1998**, *63*, 2224–2231.

¹²³ González-Gómez, J. C.; Foubelo, F.; Yus, M. *Synlett* **2008**, *18*, 2777–2780.

¹²⁴ (a) Gnamm, C.; Krauter, C. M.; Brödner, K.; Helmchen, G. *Chem. Eur. J.* **2009**, *15*, 2050–2054. (b) Gnamm, C.; Brödner, K.; Krauter, C. M.; Helmchen, G. *Chem. Eur. J.* **2009**, *15*, 10514–10532.

¹²⁵ (a) Rychman, D. M.; Stevens, R. V. *J. Org. Chem.* **1987**, *52*, 4274–4279. (b) Munchhof, M. J.; Meyers, A. I. *J. Am. Chem. Soc.* **1995**, *117*, 5399–5400. (c) Chackalamannil, S.; Wang, Y. *Tetrahedron* **1997**, *53*, 11203–11210. (d) Shu, C.; Liebeskind, L. S. *J. Am. Chem. Soc.* **2003**, *125*, 2878–2879.

¹²⁶ Kim, H.; Park, Y.; Hong, J. *Angew. Chem., Int. Ed.* **2009**, *48*, 7577–7581.

¹²⁷ Righi, P.; Scardovi, N.; Marotta, E.; Holte, P. T.; Zwanenburg, B. *Org. Lett.* **2002**, *4*, 497–500.

¹²⁸ (a) Mukherjee, S.; Yang, J. W.; Hoffmann, S.; List, B. *Chem. Rev.* **2007**, *107*, 5471–5569. (b) Barbas III, C. F. *Angew. Chem., Int. Ed.* **2008**, *47*, 42–47. (c) Melchiorre, P.; Marigo, M.; Carlone, A.; Bartoli, G. *Angew. Chem., Int. Ed.* **2008**, *47*, 6138–6171.

¹²⁹ (a) Dalko, P. I.; Moisan, L. *Angew. Chem., Int. Ed.* **2001**, *40*, 3726–3748. (b) Berkessel, A.; Groeger, H. (2005). *Asymmetric Organocatalysis*. Weinheim: Wiley-VCH. ISBN 3-527-30517-3. (c) Benjamin, L. *Chem. Rev.* **2007**, *107*, 5413–5883.

¹³⁰ (a) Enders, D.; Wang, C.; Liebich, J. X. *Chem. Eur. J.* **2009**, *15*, 11058–11076. (b) Fustero, S.; Jimenez, D.; Moscardo, J.; Catalan, S.; del Pozo, C. *Org. Lett.* **2007**, *9*, 5283–5286.

¹³¹ (a) Yujiro, H.; Hiroaki, G.; Takaaki, H.; Mitsuru, S. *Angew. Chem., Int. Ed.* **2005**, *44*, 4212–4215. (b) Vicario, J. L.; Badía, D.; Carrillo, L. *Synthesis* **2007**, *14*, 2065–2092.

¹³² (a) Gnamm, C.; Krauter, C. M.; Brödner, K.; Helmchen, G. *Chem. Eur. J.* **2009**, *15*, 2050–2054. (b) Gnamm, C.; Brödner, K.; Krauter, C. M.; Helmchen, G. *Chem. Eur. J.* **2009**, *15*, 10514–10532. (c) Unthank, M. G.; Tavassoli, B.; Aggarwal, W. K. *Org. Lett.* **2008**, *10*, 1501–1504.

¹³³ (a) Vicario, J. L.; Badia, D.; Carrillo, L. *ARKIVOC*, **2007**, 304–311. (b) Lapinsky, D. J.; Bergmeier, S. C. *Tetrahedron Lett.* **2001**, *42*, 8583–8586.

¹³⁴ Osborn, H. M. I.; Sweeney, J. B.; Howson, B. *Synlett* **1993**, *9*, 675–676.

¹³⁵ Akio, T.; Hideyuki, A.; Chitaru, H.; Kohei, T. *J. Chem. Soc., Perkin Trans. I* **1994**, *23*, 3465–3471.

¹³⁶ Still, W. C.; Gennari, C. *Tetrahedron Lett.* **1983**, *24*, 4405–4408.

Biography

Yongcheng Ying was born on August 10, 1980 in Jiande, Zhejiang, China. He received his Bachelor of Science degree in Applied Chemistry and a minor in Computer Science and Technology from University of Science and Technology of China (USTC), Hefei, Anhui, China in July of 2004, and received his Doctor of Philosophy in Chemistry from Duke University, Durham, NC in May of 2010.